An Ecological Study of Hunting Creek

2017

FINAL REPORT

March 21, 2018

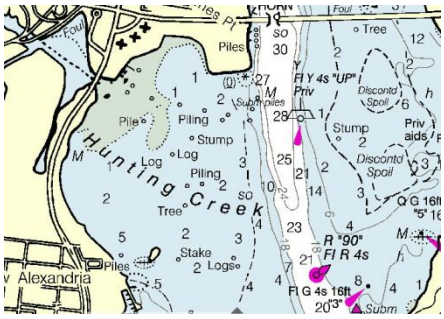

by

R. Christian Jones
Professor, Project Director

Kim de Mutsert
Assistant Professor, Co-Principal Investigator

Robert Jonas
Associate Professor, Co-Principal Investigator

Gregory Foster
Professor, Co-Principal Investigator

Thomas Huff
Co-Principal Investigator

Amy Fowler
Assistant Professor, Co-Principal Investigator

Potomac Environmental Research and Education Center
Department of Environmental Science and Policy
Department of Chemistry and Biochemistry
George Mason University

to

Alexandria Renew Enterprises
Alexandria, VA

This page intentionally blank.

Table of Contents

An Ecological Study of Hunting Creek - 2017

Executive Summary

Hunting Creek is an embayment of the tidal Potomac River located just downstream of the City of Alexandria and the I-95/I-495 Woodrow Wilson bridge. This embayment receives treated wastewater from the Alexandria Renew Enterprises wastewater treatment plant and inflow from Cameron Run which drains most of the Cities of Alexandria and Falls Church and much of eastern Fairfax County. Hunting Creek is bordered on the north by the City of Alexandria and on the west and south by the George Washington Memorial Parkway and associated park land. Due to its tidal nature and shallowness, the embayment does not seasonally stratify vertically, and its water is flushed by rainstorms and may mix readily with the adjacent tidal Potomac River mainstem. Beginning in 2013 the Potomac Environmental Research and Education (PEREC) in collaboration with Alexandria Renew Enterprises (AlexRenew) initiated a program to monitor water quality and biological communities in the Hunting Creek area including stations in the embayment itself, its tributaries, and the adjacent river mainstem. This document presents study findings from 2017 and compares them with that from the previous three years. In addition special studies were continued on anadromous fish usage of Hunting Creek and Cameron Run, *Escherichia coli* levels in Hunting Creek and tributaries, and micropollutant levels in sediments and waters of Hunting Creek and Cameron Run. And we completed a second year of benthic macroinvertebrate and water quality sampling on many tributaries of Cameron Run and Hunting Creek.

The Chesapeake Bay, of which the tidal Potomac River is a major subestuary, is the largest and most productive coastal system in the United States. The use of the Bay as a fisheries and recreational resource has been threatened by overenrichment with nutrients which can cause nuisance algal blooms, hypoxia in stratified areas, loss of submersed aquatic vegetation, and declining fisheries. As a major discharger of treated wastewater into Hunting Creek, AlexRenew has been proactive in decreasing nutrient loading since the late 1970's.

The ecological study reported here provides documentation of the current state of water quality and biological resources in Hunting Creek. The year 2017 was characterized by above normal temperatures in April and June with other months being near normal. Precipitation was well above normal in May and July, but well below normal in June. The above normal precipitation in May was reflected in higher than normal freshwater inflows from both the mainstem Potomac and Cameron Run. The large events in July resulted in spikes in freshwater inflow from Cameron Run.

Water temperature tracked air temperature on a seasonal basis with little difference among the stations at the tidal stations. As in 2016, specific conductance and chloride showed a general decline from April to May and then grew steadily through September. Dissolved oxygen (DO) was generally near saturation at tidal stations, but consistent low values found at AR2 are of concern since they were below 4 mg/L on several occasions in late summer. Supersaturation was observed in late June at AR3. Field and lab pH was typically in the 7.3-8.3 range. Correlation analysis confirmed the close correlation between DO and pH, and their relationship to SAV activity. Total alkalinity was fairly

constant after a clear decline from late April to May. The exception was a spike down in the wake of the early May precipitation event.

Water transparency as Secchi depth was generally in the range 0.6-1.0 m. On numerous dates, the disk could be seen on the bottom or at the top of a dense weedbed meaning that valid measurements were not possible. Light attenuation coefficient and turbidity followed similar trends fairly consistent values and correlation analysis revealed that the three measures of water transparency were indeed correlated.

Ammonia and nitrate nitrogen both were highest in spring and declined through summer and fall. Organic nitrogen values were generally in the range of 0.2-0.6 mg/L with little clear seasonal or spatial pattern except at AR1. Total and ortho phosphorus both showed a steady seasonal decline. N:P ratio varied greatly through the year, but always remained in a range that was consistent with P limitation of phytoplankton growth. After being a bit high in April TSS and VSS exhibited a gradual decline at the embayment stations with some ups and downs. TSS and VSS at AR4, the river station, was quite variable. Significant intercorrelation was observed for TSS, VSS, and total P reflecting the association of P with particles. Total P was also negatively correlated with N:P ratio. Ammonia nitrogen was negatively correlated with pH which may be another product of coincident seasonal changes.

Water quality measurements at tidal stations for 2017 generally fell within the range observed in the previous three years. Again, the low DO values at AR2 during the summer in 2017 were noteworthy. Also apparent was the trend to higher TSS and turbidity values at AR4 than in most years. Nitrate values continued to be lower in 2017 than in 2013 and 2014 and the decline of nitrate seasonally was found as in previous years. N:P ratio in 2017 were slightly higher than in 2015 and 2016. Seasonal patterns found in previous years were generally reinforced by 2017 data.

Water quality was measured in 2017 again at a range of tributary stations. Temperature was quite similar at all stations following a pattern that matched air temperature except at AR13 which was cooler in the summer consistent with underground in pipe runoff flow. Specific conductance and chloride exhibited a clear increase in early May (perhaps due to residual road salt flushing) followed by a general seasonal decline at all tributary stations. Dissolved oxygen values were generally near saturation at tributary stations. A marked drop was observed in early July at all stations with a major decline at AR11. Lake Cooks whose outlet was sampled at AR11 was undergoing restoration and exhibited unusual characteristics in late July and August and became unsampleable thereafter. Field and lab pH generally remained in the range of 6.5-8.0 in all tributaries. Turbidity was generally quite low in the tributaries except after the storm in early August and especially at Lake Cook during July and August due to construction. Chlorophyll levels were generally very low except at stations affected by Lake Cook. Phytoplankton growing in and being flushed from Lake Cook are the source of these elevated chlorophyll values.

Total alkalinity at the tributary stations were generally in the normal range. Total phosphorus was generally at a low level except for an early July spike at AR13. Nitrate nitrogen values were consistently elevated at AR13 (Hoffs Run) and AR23 across from the Alex Renew outfall. Values were consistently high at the Hoffs Run station.

Especially high readings were sometimes observed at AR23 across from the Alex Renew outfall. TSS and VSS were generally low except at the Lake Cook outlet station.

Phytoplankton biomass at the tidal stations was quantified using chlorophyll a. Levels were generally quite low (<10 µg/L). Exceptions were significant peaks in early July and late August at AR4. Phytoplankton density (cells/mL) was fairly constant through the year except for a strong peak in late July at both AR2 and AR4. This peak corresponded to large numbers of cyanobacteria of the genera *Oscillatoria* and *Merismopedia*. The lack of correspondence of the chlorophyll peaks and cell density peak is explainable by considering the small size of most cyanobacterial cells. Phytoplankton biovolume (μm^3/mL) is calculated by taking the volumes of individual cells of each species and multiplying by the number of cells per mL for each species giving a size-weighted total. Diatoms, being larger, assumed more importance overall and cyanobacteria, being smaller, assumed a lesser importance. Furthermore, the peak in phytoplankton biovolume in early July corresponded with the peak in chlorophyll a at AR4. On this date, there was a surge in diatoms of the genus *Melosira* which accounts for the peak in chlorophyll in that sample.

Phytoplankton biomass (as measured by chlorophyll a) continued a gradual decline over the five year monitoring period at the shallow tidal stations (AR2 and AR3). At the mainstem station (AR4) values were generally lower in 2016 and 2017 than in the first three years of the study. One difference between shallow and mainstem stations on a seasonal basis is that at AR4 highest values are found in mid to late summer whereas at AR2 and AR4 values decline in these months. This is attributable to the inhibition of phytoplankton by SAV in the shallow areas during these months. Phytoplankton cell density has not shown a clear interannual trend although the last two years were typical. The seasonal pattern of increasing cell density to an August peak continued to be apparent when 2017 data were added to the other years with cyanobacteria being most responsible for the overall seasonal pattern. Diatoms exhibited a similar seasonal pattern at AR4, but did not show an August peak at AR2. Total phytoplankton biovolume was in the midrange of previous years.

As is typical, the small-bodied rotifers were the most numerous zooplankters, generally found in the range of 50-400/L. Among the cladocera, the small-bodied *Bosmina* attained the highest densities with peak values in early summer at AR2 and AR4 and the highest density at AR4 in late September. *Diaphanosoma*, a larger bodied cladoceran, was found in substantial levels in late June at AR2, but otherwise was scarce. Other mostly planktonic cladoceran species were also restricted to late June and found at peak levels from less than 100 to nearly 1000 per m^3. Two taxa characteristic of SAV beds, Chydoridae and Macrothricidae, were observed mainly in late August and only at AR2, but reached high density at this time. Copepod nauplii, the immature stage of copepods, were found at both stations in appreciable numbers mainly in mid-summer. Generally the most abundant larger zooplankter, the calanoid copepod *Eurytemora affinis*, was mainly found in late August at AR4 at somewhat lower than normal levels. On the other hand, another calanoid, *Diaptomus pallidus*, was found at exceptionally high values (nearly 9000/m^3 in late June at AR2.

Total rotifer density in 2017 was similar to that in previous years. An interesting seasonal pattern showing a substantial drop in May and subsequent buildup to peak values in July and August continues to emerge from the pooled data analyzed by month. Most of the crustacean zooplankton exhibited similar densities in 2016 as in previous years. A major difference was the dominance of *Diaptomus* over *Eurytemora* in 2017.

Ichthyoplankton collections were dominated by Gizzard Shad, Blueback Herring, and Alewife, all members of the family Clupeidae. A large number of additional larvae were identifiable to family level as Clupeidae bringing the total of larvae in the family Clupeidae to over 80% of all identifiable fish larvae. The rest of the identifiable larvae were split between Inland Silverside and *Morone* sp. (mostly white perch). There were somewhat more larvae collected at AR4 than AR2. Inland Silverside larvae were collected in greater numbers at AR2 and Gizzard Shad, White Perch, and Striped Bass larvae were more abundant at AR4.

White Perch made up the overwhelming majority of individuals collected by trawling in 2016. Centrarchids including sunfish and bass comprised about 10%. Total catch via trawling was greatly increased in 2017 over the atypically low number found in 2016. Seine sampling was highly dominated by Banded Killifish which comprised over 60% of the total catch. A distant second was Inland Silverside which made up about 10% of the seine catch. The highest seine collections were in early June and early August. Somewhat more fish were seined at AR6 in the Hunting Creek embayment proper than at AR5 off Jones Point, the principal difference being that Inland Silverside were almost exclusively collected at AR6. A new gear was introduced in 2016 to overcome the drawbacks of trawling in dense SAV, the fyke net. The fyke net is a passive gear that can be deployed in shallow water. The net is static; the natural movement of the fish funnel individuals into the gear and they are generally well retained. This gear was deployed semimonthly starting in May at two locations near trawl site AR3. Centrarchids were the most abundant group in the fyke nets in 2017 as opposed to 2016 when bandied killifish were dominant.

Data from the VIMS aerial survey indicated that virtually the entire study area with depths less than 2 m was covered at a 70-100% density class by SAV. SAV species mapping indicated that the native plant Coontail was the most abundant with the normally dominant Hydrilla also being very common Clumps of Water Star-grass were found scattered through the area especially in August. There was some overgrowth of SAV by filamentous algae in the Hunting Creek embayment in August.

Benthic invertebrate data from the tidal stations indicated that 2017 values and trends were similar to other years. A moderate diversity of organisms were observed at all three tidal stations with flatworms, oligochaetes, and chironomids being most abundant at AR2, bivalves and amphipods most abundant at AR3, and isopods most abundant at AR4. Total abundance was somewhat lower than in previous years of the study. In 2016 a benthic macroinvertebrate sampling program was implemented for the flowing tributary streams. Six stations were sampled in November. Flatworms, chironomids, oligochaetes, baetid mayflies, and hydropsychid caddisflies were the dominant taxa, all of which are taxa tolerant of pollution indicating that the tributaries have been degraded by the impacts of urban development, mostly stormwater pulses and nonpoint pollution. Application of

an index of biotic integrity indicated that all streams were categorized as “poor”, but some were approaching “fair”. The values observed were typical of streams draining urban areas.

Anadromous fish sampling was conducted on a weekly basis from March 24 to May 25 in 2017 at a station just above the head of tide on Cameron Run. Hoop nets were deployed for a 24 hour period each week to collect spawning fish moving upstream and ichthyoplankton nets were deployed to collect fish larvae drifting downstream. Fourteen adult Alewife were collected in the hoop nets, less than in 2015 and 2016, but still substantially more than in 2013 and 2014. A total of 24 positively identified Alewife larvae and six other clupeid larvae were collected in the plankton nets. Larvae of several other fish such as Gizzard Shad and White Perch were also collected. Extrapolation from the sample collected to the total period of spawning yielded an estimate 122 adult Alewife spawning and about three-quarters of a million river herring larvae produced in Cameron Run in 2017.

E. coli sampling was expanded to a total of 12 stations in 2016, adding four additional tributary stations as part of the semimonthly sampling program. However, during the 2017 field season, two of the stations, AR22 and AR11, became inaccessible due to construction. The data continue to support a conclusion that the entire area sampled, including the mainstem of the Potomac River (AR4) is impaired for the bacteriological criterion (*E. coli* content) under Section 9VAC25-260-170 of the Virginia Water Quality Standards for contact recreational use of surface waters. In 2017 AR4 exceeded the 235 per 100 mL criterion five times whereas it exceeded that level only twice in 2016. More of the stations exceeded the standard in 2017 than in 2016. While some of the highest values occurred in June and July there was no clear seasonal trend in 2017.

Micropollutants have been detected in water, sediments and fish at nanogram to microgram per gram (or liter) concentrations. Analyses in 2017 focussed on personal care products and antidepressants. Preliminary results from 2017 along with some data from previous years was presented in this report. We are continuing to replace GC-MS methods with LC-MS to allow a greater number of micropollutants to be analyzed in water, sediments and fish. Future methods development includes replacing LC/-MS methods with LC-MS/MS methods to achieve lower detection limits, a greater number of included analytes, and improved accuracy and precision in the chemical analysis.

We recommend that:

1. The basic ecosystem monitoring should continue. A range of climatic conditions is needed to effectively establish baseline conditions in Hunting Creek. Interannual, seasonal and spatial patterns are starting to appear, but need validation with future years’s data.
2. Water quality mapping should be continued. This provides much needed spatial resolution of water quality patterns as well as allowing mapping of SAV distributions.
3. Fyke nets have proven to be a useful new gear to enhance fish collections and should be continued.

4. Anadromous fish sampling is an important part of this monitoring program and has gained interest now that the stock of river herring has collapsed, and a moratorium on these taxa has been established in 2012. The discovery of river herring spawning in Cameron Run increases the importance of continuing studies of anadromous fish in the study area.
5. We recommend that micropollutant sampling and analysis work be continued to better understand the source of residues observed in the Hunting Creek area. We are synthesizing our findings to date and refining our protocols and instrumentation to achieve better results.
6. We recommend continuing the more intensive *E. coli* sampling plan which seems to be giving better insight into the dynamics of *E. coli* in the study area.
7. We recommend continuing macroinvertebrate studies the tributaries of Hunting Creek to further ascertain overall aquatic biota health.

List of Abbreviations

BOD	Biochemical oxygen demand
cfs	cubic feet per second
DO	Dissolved oxygen
ha	hectare
l	liter
LOWESS	locally weighted sum of squares trend line
m	meter
mg	milligram
MGD	Million gallons per day
NS	not statistically significant
NTU	Nephelometric turbidity units
SAV	Submersed aquatic vegetation
SRP	Soluble reactive phosphorus
TP	Total phosphorus
TSS	Total suspended solids
um	micrometer
VSS	Volatile suspended solids
#	number

This page intentionally left blank.

The Aquatic Monitoring Program for the Hunting Creek Area of the Tidal Freshwater Potomac River 2017

FINAL REPORT
March 21, 2018

by

R. Christian Jones
Professor, Department of Environmental Science and Policy
Director, Potomac Environmental Research and Education Center
George Mason University
Project Director

Kim de Mutsert
Assistant Professor, Department of Environmental Science and Policy
George Mason University
Co-Principal Investigator

Amy Fowler
Assistant Professor, Department of Environmental Science and Policy
George Mason University
Co-Principal Investigator

to

Alexandria Renew Enterprises
Alexandria, VA

ACKNOWLEDGEMENTS

The authors wish to thank the numerous individuals and organizations whose cooperation, hard work, and encouragement have made this project successful. We wish to thank the Alexandria Renew Enterprises especially CEO Karen Pallansch for her vision in initiating the study and to Aster Tekle, Charlie Logue, Steve Schemmel, and Sean Stephan for their advice and cooperation during the study.

Without a dedicated group of field and laboratory workers this project would not have been possible. Thanks go to Laura Birsa for managing water quality/plankton/benthos field trips and to field/lab workers Kristen Reck, Chelsea Gray, Michael Cagle, Morgan Collier, Tabitha King, Mary Randolph, Adam Schwoerer, and Steven Chan.

Special thanks go to C.J. Schlick who has put together the figures and tables of the fish section of the report, and to Joris van der Ham, who has operated as the field manager of the fish collections. Others that have helped in the field and in the laboratory to collect and process all fish samples include Casey Pehrson, CJ Schlick, Beverly Bachmann, Sammie Alexander, Maziar Nourizadeh, Alex van Plantinga, Jessie Melton, Michael Rollins, Heather Nortz, Tabitha King, Lisa McAnulty, Michael Cagle, and Rachel Kelmartin.

Claire Buchanan served as a voluntary consultant on plankton identification. Roslyn Cress, Natasha Hendrick, and Lisa Bair were vital in handling personnel and procurement functions.

DEDICATION

This report is dedicated to Larin Michael Isdell who contributed his grittiness and good cheer to field and lab work alike. Larin was our go-to guy for in depth macroinvertebrate taxonomy and a real team player. He was in the final stages of writing his MS thesis on PCB's in sediment, fish, and fish diet in Hunting Creek when he was taken from us on November 11, 2017.

INTRODUCTION

This section reports the results of the fourth year of an aquatic monitoring program conducted for Alexandria Renew Enterprises by the Potomac Environmental Research and Education Center (PEREC) in the College of Science at George Mason University. Three other sections of the report include an anadromous fish study of Cameron Run, a study of the incidence of PCB's and endocrine disrupting chemicals in Hunting Creek, a survey of *Escherichia coli* levels in the Hunting Creek area of the tidal Potomac River, and a benthic macroinvertebrate survey of tributaries to Cameron Run and Hunting Creek.

This work was in response to a request from Karen Pallansch, Chief Executive Officer of Alexandria Renew Enterprises (Alex Renew), operator of the wastewater reclamation and reuse facility (WRRF) which serves about 350,000 people in the City of Alexandria and the County of Fairfax in northern Virginia. The study is patterned on the long-running Gunston Cove Study which PEREC has been conducting in partnership with the Fairfax County Department of Public Works and Environmental Services since 1984. The goal of these projects is to provide baseline data and on-going trend analysis of the ecosystems receiving reclaimed water from wastewater treatment facilities with the objective of adaptive management of these valuable freshwater resources. This will facilitate the formulation of well-grounded management strategies for maintenance and improvement of water quality and biotic resources in the tidal Potomac. A secondary but important educational goal is to provide training for Mason graduate and undergraduate students in water quality and biological monitoring and assessment.

Setting of Hunting Creek

Hunting Creek is an embayment of the tidal Potomac River located just downstream of the City of Alexandria and the Woodrow Wilson Bridge. Waters are shallow with the entire embayment having a depth of 2 m or less at mean tide. According to the "Environmental Atlas of the Potomac Estuary" (Lippson et al. 1981), the mean depth of Hunting Creek is 1.0 m, the surface area is 2.26 km^2, and the volume of 2.1 x 10^6 m^3.

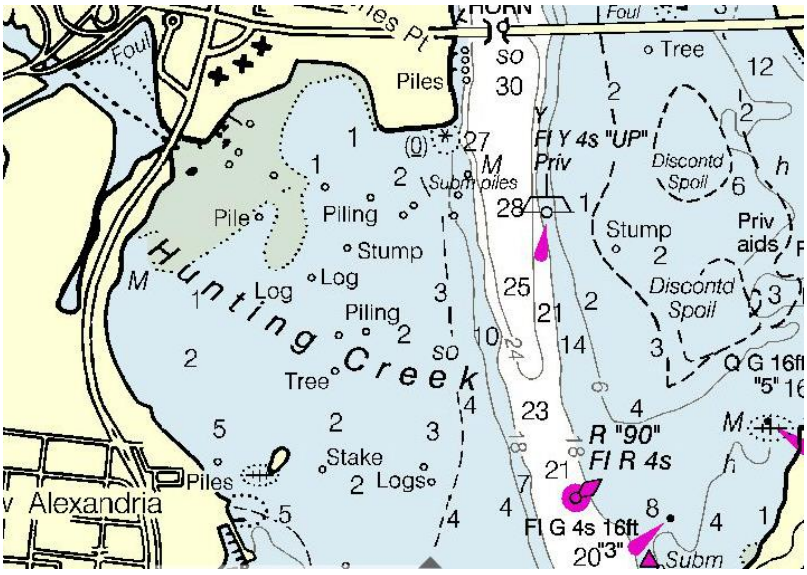

On the left is the Hunting Creek embayment. The Woodrow Wilson Bridge spans the tidal Potomac River at the top of the map. The Potomac River main channel is the whitish area running from north to south through the middle of the map. Soundings (numbers on the map) are in feet at mean low water. For the purposes of this report "Hunting Creek" will extend to the head of tide, roughly to Telegraph Rd.

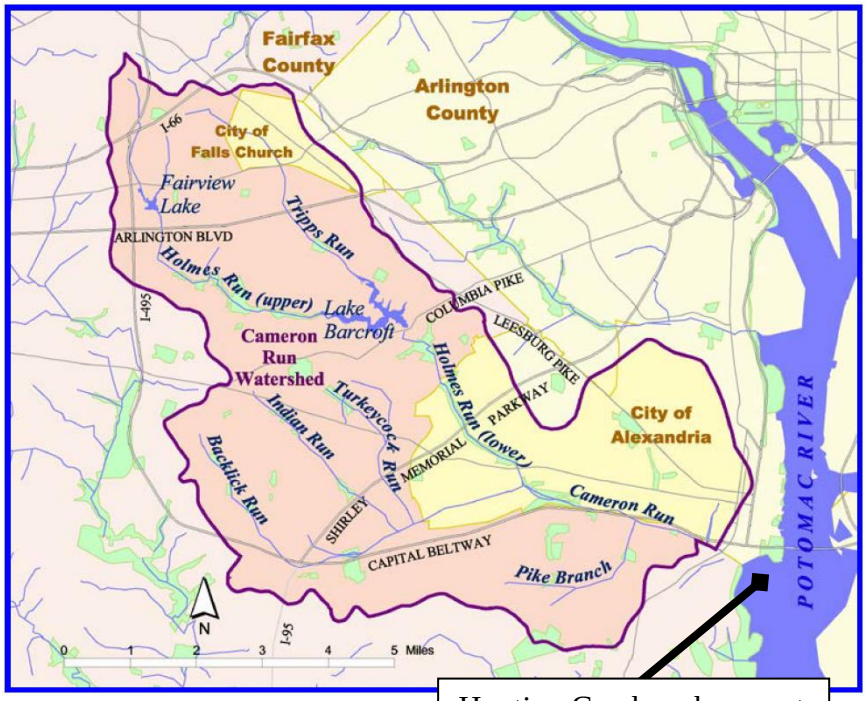

On the left is a map of the Hunting Creek watershed. Cameron Run is the freshwater stream which drains the vast majority of the watershed of Hunting Creek. The watershed is predominantly suburban in nature with areas of higher density commercial and residential development. The watershed has an area of 44 square miles and drains most of the Cities of Alexandria and Falls Church and much of east central Fairfax County. A major aquatic feature of the watershed is Lake Barcroft. The suburban land uses in the watershed are a source of nonpoint pollution to Hunting Creek.

Hunting Creek embayment

The Alex Renew WRRF serves an area similar in extent to the Cameron Run watershed with the addition of some areas along the Potomac shoreline from Four Mile Run to Dyke Marsh. The effluent of the Alexandria Renew Enterprises plant enters the upper tidal reach of Hunting Creek under the Rt 1/I-95 interchange.

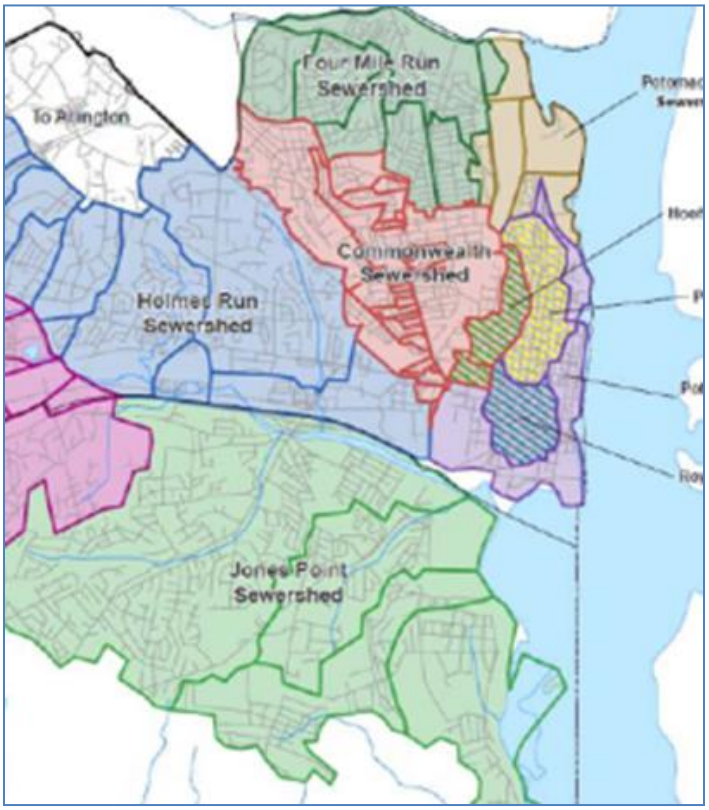

The map at the left shows the sewersheds which contribute to the AlexRenew WRRF. Of particular note are the shaded areas within the City of Alexandria. These sewersheds (Hooff Run, Pendleton, and Royal St.) all contain combined sewers meaning that domestic wastewater is co-mingled with street runoff. Under most conditions, all of this water is directed to the AlexRenew WRRF for treatment. But in extreme runoff conditions (like torrential rains), some may be diverted directly into the tidal Potomac via a Combined Sewer outfall (CSO).

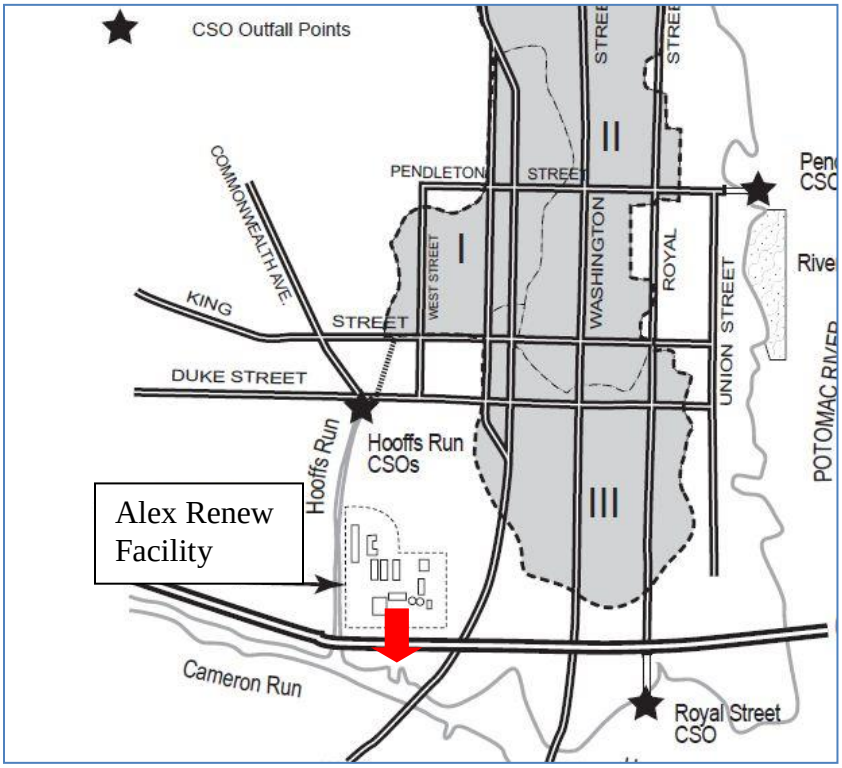

The map at the left is an enlargement of the area where the Alex Renew WRRF is found and where the discharge sites of the CSO's are located. Note the close proximity of two of the CSO's to the Alex Renew WRRF discharge (shown as red arrow).

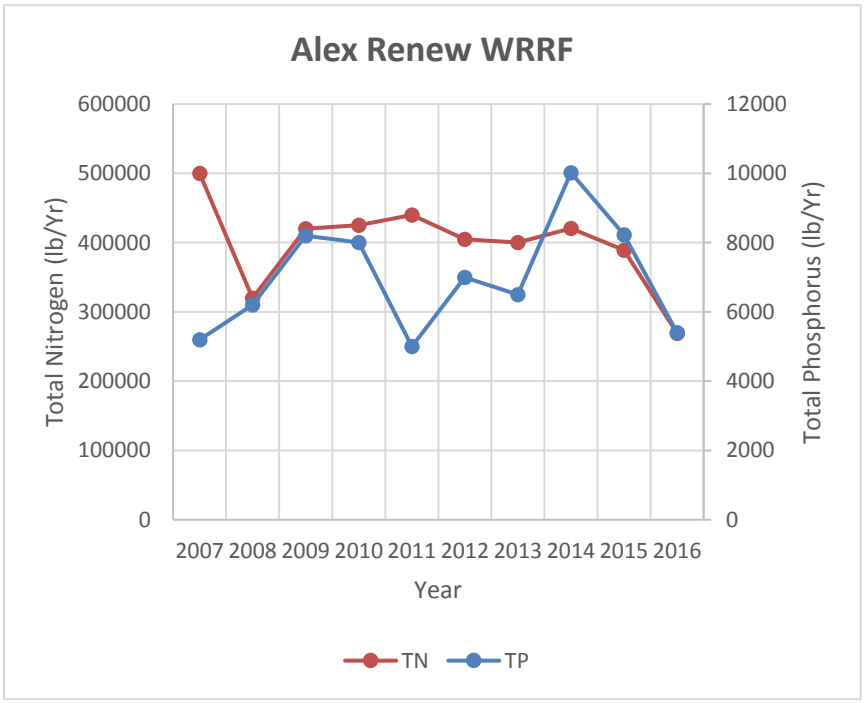

The graph at the left shows the loading of nitrogen and phosphorus from the Alexandria Renew WRRF for the last seven years. Loadings of both nutrient elements were among the lowest in the last decade in 2016: 269,000 lb/yr for nitrogen and 5,400 lb/yr for phosphorus.

Ecology of the Freshwater Tidal Potomac

The tidal Potomac River is an integral part of the Chesapeake Bay tidal system and at its mouth the Potomac is contiguous to the bay proper. The tidal Potomac is often called a subestuary of the Chesapeake Bay and as such it is the largest subestuary of the bay in terms of size and amount of freshwater input. The mixing of freshwater with saltwater is the hallmark of an estuary. While the water elevation in an estuary is "sea level", the water contained in an estuary is not pure sea water such as found in the open ocean. Pure ocean sea water has a salt concentration of about 35 parts per thousand by weight (ppt). Water in Chesapeake Bay ranges from about 30 ppt near its mouth to 0 ppt in the upper reaches where there is substantial freshwater inflow such as in the upper tidal Potomac River. Salinity at a given location is determined by the balance between freshwater input and salt water mixing in from the ocean. It generally varies with season being lower in spring when freshwater inflows are greater and higher in summer when there is less freshwater inflow. In the Hunting Creek study area, the salinity is essentially 0 yearround.

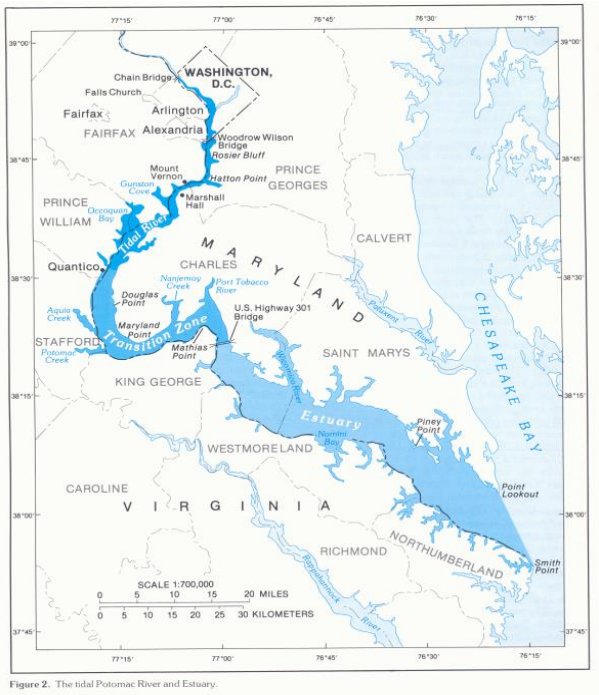

Figure 2. The tidal Potomac River and Estuary.

(map courtesy USGS)

The tidal Potomac is generally divided into three salinity zones as indicated by the map to the left:
-Estuarine or Mesohaline zone (6-14 ppt)
-Transition or Oligohaline zone (0.5-6 ppt)
-Tidal River or Tidal Fresh zone (<0.5 ppt)
Hunting Creek is in the upper part of the Tidal River/Tidal Fresh zone and as such it never experiences detectable salinity

Within the tidal freshwater zone, the flora and fauna are generally characterized by the same species that would occur in a freshwater lake in this area and the food web is similar. Primary producers are freshwater species of submersed aquatic vegetation (SAV) such as native taxa *Vallisneria americana* (water celery), *Potomogeton* spp, (pondweeds), and *Ceratophyllum* (coontail) as well as introduced species such as *Hydrilla verticallata* (hydrilla) and *Myriophyllum spicatum* (water milfoil). Historical accounts indicate that most of the shallow areas of the tidal freshwater Potomac were colonized by SAV when observations were made around 1900 (Carter et al. 1985).

The other group of important primary producers are phytoplankton, a mixed assemblage

of algae and cyanobacteria which may turn over rapidly on a seasonal basis. The dominant groups of phytoplankton in the tidal freshwater Potomac are diatoms (considered a good food source for aquatic consumers) and cyanobacteria (considered a less desirable food source for aquatic consumers). For the latter part of the 20th century, the high nutrient loadings into the river favored cyanobacteria over both diatoms and SAV resulting in large production of undesirable food for consumers. In the last decade or so, as nutrient reductions have become manifest, cyanobacteria have decreased and diatoms and SAV have increased.

The biomass contained in the cells of phytoplankton nourishes the growth of zooplankton and benthic macroinvertebrates which provide an essential food supply for the juvenile and smaller fish. These in turn provide food for the larger fish like striped bass and largemouth bass. The species of zooplankton and benthos found in the tidal fresh zone are similar to those found in lakes in the area, but the fish fauna is augmented by species that migrate in and out from the open interface with the estuary.

Resident fish species include typical lake species such as sunfish (*Lepomis* spp.), bass (*Micropterus* spp.), and crappie (*Pomoxis* spp.) as well as estuarine species such as white perch (*Morone americana*) and killifish (*Fundulus* spp.). Species which spend part of their year in the area include striped bass (*Morone saxitilis*) and river herrings and shad (*Alosa* spp.). Non-native fish species have also become established in the tidal freshwater Potomac such as northern snakehead (*Channa argus*) and blue catfish (*Ictalurus furcatus*).

Larval fishes are transitional stages in the development of juvenile fishes. They range in development from newly hatched, embryonic fish to juvenile fish with morphological features similar to those of an adult. Many fishes such as clupeids (herring family), white perch, striped bass, and yellow perch disperse their eggs and sperm into the open water. The larvae of these species are carried with the current and termed “ichthyoplankton”. Other fish species such as sunfish and bass lay their eggs in “nests” on the bottom and their larvae are rare in the plankton.

After hatching from the egg, the larva draws nutrition from a yolk sack for a few days. When the yolk sack diminishes to nothing, the fish begins a life of feeding on other organisms. This post yolk sack larva feeds on small planktonic organisms (mostly small zooplankton) for a period of several days. It continues to be a fragile, almost transparent larva and suffers high mortality to predatory zooplankton and juvenile and adult fishes of many species, including its own. When it has fed enough, it changes into an opaque juvenile, with greatly enhanced swimming ability. It can no longer be caught with a slow-moving plankton net, but is soon susceptible to capture with the seine or trawl net.

METHODS

A. Profiles and Plankton: Sampling Day

Sampling was conducted on a semimonthly basis at stations representing both Hunting Creek and the Potomac mainstem (Figure 1a). One station (AR 1) was located near the mouth of Cameron Run at the George Washington Parkway bridge. Two stations (AR 2 & 3) were located in the Hunting Creek embayment proper. A fourth station was located in the river channel about 100 m upstream from Buoy 90. Dates for sampling as well as weather conditions on sampling dates and immediately preceding days are shown in Table 1. Note that certain dates such as April 28, June 23, and August 22 had significant rainfall in days preceding sampling which may have impacted conditions in Hunting Creek due to it shallow nature and relatively large watershed contributing runoff.

Figure 1a. Hunting Creek area of the Tidal Potomac River showing water quality, plankton, and benthos sampling stations. AR1, AR2, AR3, AR4, AR22, AR23 represent water quality stations, AR2 and AR4 are the phytoplankton and zooplankton stations and AR2, AR3, and AR4 are benthos stations. Red bar is 0.5 km.

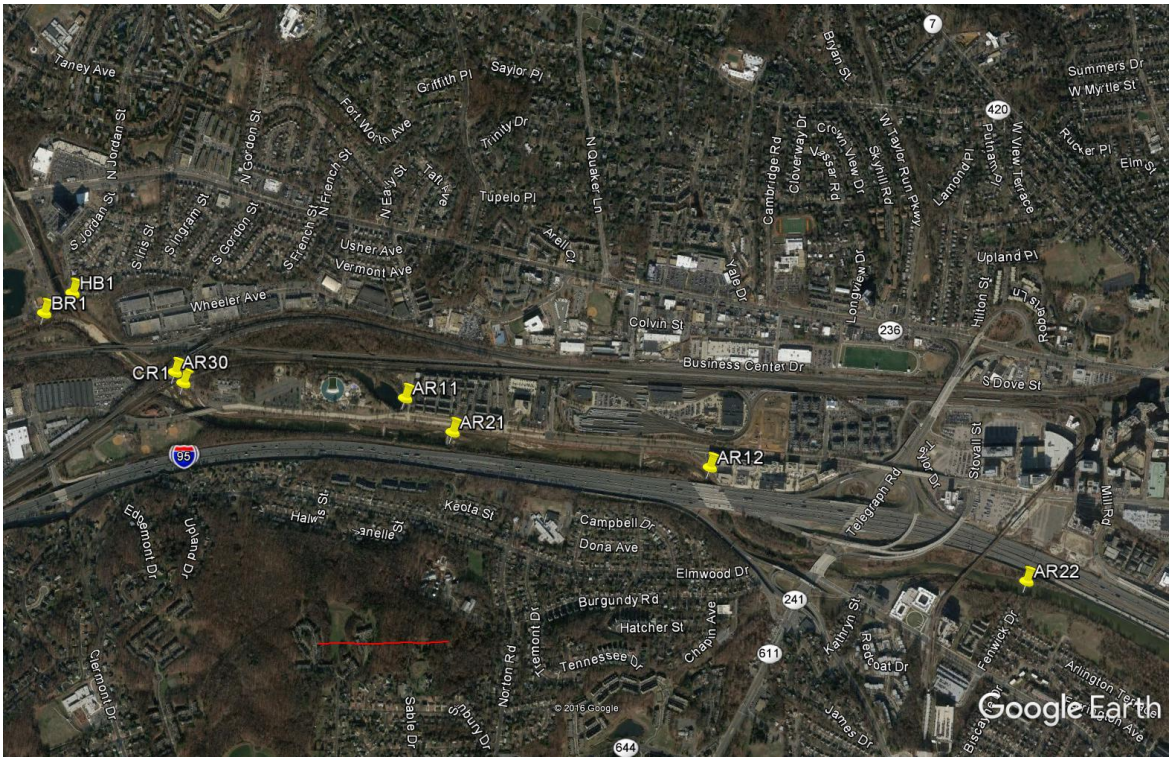

Figure 1b. Cameron Run portion of the study area showing water quality stations.

Figure 1c. Hunting Creek area of the Tidal Potomac River showing fish monitoring stations.

Table 1
Hunting Creek Study: Sampling Dates and Weather Data for 2017

	Type of Sampling						Avg Daily Temp (°C)		Precipitation (cm)	
Date	WP	B	D	T	S	F	1-Day	3-Day	1-Day	3-Day
April 26	X						18.3	15.0	0.03	0.81
April 28				X	X		23.9	21.3	T	0.05
May 10	X	X					17.2	14.8	0	0
May 16				X	X	X	19.4	18,9	0	T
May 24	X						16.7	17.6	0.66	1.68
May 31					X	X	22.8	22.2	0.05	0.50
June 7	X	X					17.8	20.9	0	T
June 13				X	X	X	29.4	28.9	0	0
June 21	X						27.2	26.9	0	1.36
June 26				X	X	X	24.4	26.3	0	0.18
July 5	X	X					26.1	28.0	1.78	1.88
July 11				X	X	X	28.9	27.2	T	T
July 12			X				30.0	28.7	0	T
July 20	X						31.7	30.6	0	T
July 26				X	X	X	25.0	26.1	0	T
August 8				1	X	X	24.4	23.7	0.10	3.85
August 9	X	X					24.4	23.9	0	3.84
August 10			X				23.9	24.3	0	0.10
August 22				1	X	X	28.9	27.8	0	0.03
August 23	X						26.7	28.0	0	0.03
September 6	X	X					19.4	22.4	1.40	1.57
September 12			X	1	1	X	22.2	19.6	0	0
September 20	X						26.1	24.6	0	0

Type of Sampling: WP: Water quality (samples to AlexRenew Lab), profiles and plankton, B: benthos (station numbers indicated), D: dataflow (water quality mapping), T: fish collected by trawling, S: fish collected by seining. F: fish collected by fyke net. T under Precipitation equals "trace". X indicates full station suite on that date. 1 on Trawl indicates only AR4. 1 on Seine indicates only one seine site was sampled.

Sampling was initiated about 10:00 am. Four types of measurements or samples were obtained at each station: (1) depth profiles of temperature, conductivity, dissolved oxygen, pH, and irradiance (photosynthetically active radiation, PAR) measured directly in the field; (2) water samples for GMU lab determination of chlorophyll *a* and phytoplankton species composition and abundance; (3) water samples for determination of N and P forms, BOD, COD, alkalinity, hardness, suspended solids, chloride, and pH by the Alexandria Renew Enterprises lab; (4) net sampling of zooplankton and ichthyoplankton.

Profiles of temperature, conductivity, and dissolved oxygen were conducted at each station using a YSI 6600 datasonde with temperature, conductivity, dissolved oxygen and pH probes. Measurements were taken at 0.3 m increments from surface to bottom at the embayment stations. In the river measurements were made with the sonde at depths of 0.3 m and 2.0 m increments to the bottom. Meters were checked for calibration before and after sampling. Profiles of irradiance (photosynthetically active radiation, PAR) were collected with a LI-COR underwater flat scalar PAR probe. PAR measurements were taken at 10 cm intervals to a depth of 1.0 m. Simultaneous measurements were made with a terrestrial probe in air during each profile to correct for changes in ambient light if needed. Secchi depth was also determined. The readings of at least two crew members were averaged due to variability in eye sensitivity among individuals. If the Secchi disk was still visible at the bottom or if its path was block by SAV while still visible, a proper reading could not be obtained.

A 1-liter depth-composited sample for GMU lab work was constructed from equal volumes of water collected at each of three depths (0.3 m below the surface, middepth, and 0.3 m off of the bottom) using a submersible bilge pump. A 100-mL aliquot of this sample was preserved immediately with acid Lugol's iodine for later identification and enumeration of phytoplankton at stations AR2 and AR4. The remainder of the sample was placed in an insulated cooler with ice. A separate 1-liter surface sample was collected from 0.3 m using the submersible bilge pump and placed in the insulated cooler with ice for lab analysis of surface chlorophyll *a*.

At embayment and river mainstream sampling stations (AR2, AR3, and AR4), 2-liter samples were collected monthly at each station from just below the surface (0.3 m) and near the bottom (0.3 m off bottom) at each station using the submersible pump. At tributary stations (AR1, AR 10, AR11, AR12, AR13, AR21, AR22, AR23, and AR30), 2-liter samples were collected by hand from just below the surface. This water was promptly delivered to the nearby Alexandria Renew Laboratory for determination of nitrogen, phosphorus, BOD, TSS, VSS, pH, total alkalinity, and chloride.

At stations AR2 and AR4, microzooplankton was collected by pumping 32 liters from each of three depths (0.3 m, middepth, and 0.3 m off the bottom) through a 44 μm mesh sieve. The sieve consisted of a 12-inch long cylinder of 6-inch diameter PVC pipe with a piece of 44 μm nitex net glued to one end. The 44 μm cloth was backed by a larger mesh cloth to protect it. The pumped water was passed through this sieve from each depth and then the collected microzooplankton was backflushed into the sample bottle. The resulting sample was treated with about 50 mL of club soda and then preserved with formalin containing a small amount of rose bengal to a concentration of 5-10%.

At stations AR2 and AR4, macrozooplankton was collected by towing a 202 µm net (0.3 m opening, 2 m long) for 1 minute at each of three depths (near surface, middepth, and near bottom). Ichthyoplankton (larval fish) was sampled by towing a 333 µm net (0.5 m opening, 2 m long) for 2 minutes at each of the same depths at Stations AR2 and AR4. In the embayment, the boat traveled from AR2 toward AR3 during the tow while in the river the net was towed in a linear fashion along the channel. Macrozooplankton tows were about 300 m and ichthyoplankton tows about 600 m. Actual distance depended on specific wind conditions and tidal current intensity and direction, but an attempt was made to maintain a constant slow forward speed (approximately 2 miles per hour) through the water during the tow. The net was not towed directly in the wake of the engine. A General Oceanics flowmeter, fitted into the mouth of each net, was used to establish the exact towing distance. During towing the three depths were attained by playing out rope equivalent to about 1.5-2 times the desired depth. Samples which had obviously scraped bottom were discarded and the tow was repeated. Flowmeter readings taken before and after towing allowed precise determination of the distance towed and when multiplied by the area of the opening produced the total volume of water filtered.

Macrozooplankton were preserved immediately with rose bengal formalin with club soda pretreatment. Ichthyoplankton was preserved in 70% ethanol. Macrozooplankton was collected on each sampling trip; ichthyoplankton collections ended after July because larval fish were normally not found after this time.

Benthic macroinvertebrate samples were collected monthly at stations AR2, AR3, and AR4. Three samples were collected at each station using a petite ponar grab. The bottom material was sieved through a 0.5 mm stainless steel sieve and resulting organisms were preserved in rose bengal formalin for lab analysis.

Samples for water quality determination were maintained on ice and delivered to the Alexandria Renew Enterprises (AlexRenew) Laboratory by 2 pm on sampling day and returned to GMU by 3 pm. At GMU 10-15 mL aliquots of both depth-integrated and surface samples were filtered through 0.45 µm membrane filters (Gelman GN-6 and Millipore MF HAWP) at a vacuum of less than 10 lbs/in^2 for chlorophyll a and pheopigment determination. During the final phases of filtration, 0.1 mL of $MgCO_3$ suspension (1 g/100 mL water) was added to the filter to prevent premature acidification. Filters were stored in 20 mL plastic scintillation vials in the lab freezer for later analysis. Seston dry weight and seston organic weight were measured by filtering 200-400 mL of depth-integrated sample through a pretared glass fiber filter (Whatman 984AH).

Sampling day activities were normally completed by 5:30 pm.

B. Profiles and Plankton: Follow-up Analyses

Chlorophyll *a* samples were extracted in a ground glass tissue grinder to which 4 mL of dimethyl sulfoxide (DMSO) was added. The filter disintegrated in the DMSO and was ground for about 1 minute by rotating the grinder under moderate hand pressure.

The ground suspension was transferred back to its scintillation vial by rinsing with 90% acetone. Ground samples were stored in the refrigerator overnight. Samples were removed from the refrigerator and centrifuged for 5 minutes to remove residual particulates.

Chlorophyll *a* concentration in the extracts was determined fluorometrically using a Turner Designs Model 10 field fluorometer configured for chlorophyll analysis as specified by the manufacturer. The instrument was calibrated using standards obtained from Turner Designs. Fluorescence was determined before and after acidification with 2 drops of 10% HCl. Chlorophyll *a* was calculated from the following equation which corrects for pheophytin interference:

$$\text{Chlorophyll } a\ (\mu g/L) = F_s R_s (R_b - R_a)/(R_s - 1)$$

where F_s=concentration per unit fluorescence for pure chlorophyll *a*
R_s=fluorescence before acid/fluorescence after acid for pure chlorophyll *a*
R_b=fluorescence of sample before acid
R_a=fluorescence of sample after acid

All chlorophyll analyses were completed within one month of sample collection.

Phytoplankton species composition and abundance was determined using the inverted microscope-settling chamber technique (Lund et al. 1958). Ten milliters of well-mixed algal sample were added to a settling chamber and allowed to stand for several hours. The chamber was then placed on an inverted microscope and random fields were enumerated. At least two hundred cells were identified to species and enumerated on each slide. Counts were converted to number per mL by dividing number counted by the volume counted. Biovolume of individual cells of each species was determined by measuring dimensions microscopically and applying volume formulae for appropriate solid shapes.

Microzooplankton and macrozooplankton samples were rinsed by sieving a well-mixed subsample of known volume and resuspending it in tap water. This allowed subsample volume to be adjusted to obtain an appropriate number of organisms for counting and for formalin preservative to be purged to avoid fume inhalation during counting. One mL subsamples were placed in a Sedgewick-Rafter counting cell and whole slides were analyzed until at least 200 animals had been identified and enumerated. A minimum of two slides was examined for each sample. References for identification were: Ward and Whipple (1959), Pennak (1978), and Rutner-Kolisko (1974). Zooplankton counts were converted to number per liter (microzooplankton) or per cubic meter (macrozooplankton) with the following formula:

$$\text{Zooplankton } (\#/L \text{ or } \#/m^3) = NV_s/(V_c V_f)$$

where N = number of individuals counted
V_s = volume of reconstituted sample, (mL)
V_c = volume of reconstituted sample counted, (mL)

V_f = volume of water sieved, (L or m^3)

Larval fish were picked from the ethanol-preserved ichthyoplankton samples with the aid of a stereo dissecting microscope. Identification of ichthyoplankton was made to family and further to genus and species where possible. If the number of animals in the sample exceeded several hundred, then the sample was split with a plankton splitter and the resulting counts were multiplied by the subsampling factor. The works Hogue et al. (1976), Jones et al. (1978), Lippson and Moran (1974), and Mansueti and Hardy (1967) were used for identification. The number of ichthyoplankton in each sample was expressed as number per 10 m^3 using the following formula:

Ichthyoplankton (#/10m^3) = 10N/V
where N = number ichthyoplankton in the sample
V = volume of water filtered, (m^3)

C. Adult and Juvenile Fish

Fishes were sampled by trawling at stations AR3 and AR4, and seining at stations AR5 and AR6 (Figure 1). For trawling, a try-net bottom trawl with a 15-foot horizontal opening, a ¾ inch square body mesh and a ¼ inch square cod end mesh was used. The otter boards were 12 inches by 24 inches. Towing speed was 2-3 miles per hour and tow length was 5 minutes. The trawls were towed upriver parallel to the channel at AR4, and following the curve away from the channel at AR3. The direction of tow should not be crucial. Dates of sampling and weather conditions are found in Table 1.

Seining was performed with a bag seine that was 50 feet long, 3 feet high, and made of knotted nylon with a ¼ inch square mesh. The bag is located in the middle of the net and measures 3 ft^3. The seining procedure was standardized as much as possible. The net was stretched out perpendicular to the shore with the shore end right at the water line. The net was then pulled parallel to the shore for a distance of 100 feet by a worker at each end moving at a slow walk. Actual distance was recorded if in any circumstance it was lower than 100 feet. At the end of the prescribed distance, the offshore end of the net was swung in an arc to the shore and the net pulled up on the beach to trap the fish. Dates for seine sampling were the same as those for trawl sampling (Table 1).

Due to extensive submerged aquatic vegetation (SAV) cover in Hunting Creek, we adjusted our sampling regime in 2016. The trawl at AR3 has been impeded more frequently each year due to this vegetation, and two fyke nets were set in the area close to AR3 (Figure 1). The fyke net sampling stations are called ‘fyke near’ and ‘fyke far’ in reference to their distance from shore. These fyke nets were set within the SAV to sample the fish community that uses the SAV cover as habitat. Fyke nets were set for 4 hours to passively collect fish. The fyke nets have 5 hoops, a 1/4 inch mesh size, 16 feet wings and a 32 feet lead. Fish enter the net by actively swimming and/or due to tidal motion of the water. The lead increases catch by capturing the fish swimming parallel to the wings. Fyke nets were set each sampling date, and trawling in this location (AR3) became impossible by mid-July (Table 1). Utilizing the fyke nets when trawling is still possible

allows for gear comparison.

After the catch from each of these three gear types was hauled in, the fishes were measured for standard length and total length to the nearest mm. Standard length is the distance from the front tip of the snout to the end of the vertebral column and base of the caudal fin. This is evident in a crease perpendicular to the axis of the body when the caudal fin is pulled to the side. Total length is the distance from the tip of the snout to the tip of the longer lobe of the caudal fin, measured by straightening the longer lobe toward the midline.

If the identification of the fish was not certain in the field, a specimen was preserved in 70% ethanol and identified later in the lab. Fishes kept for chemical analysis were kept on ice wrapped in aluminum foil until frozen in the lab. All fishes retained for laboratory analysis or identification were first euthanized by submerging them in an ice sludge conforming to the AICUC protocol. Identification was based on characteristics in dichotomous keys found in several books and articles, including Jenkins and Burkhead (1983), Hildebrand and Schroeder (1928), Loos et al (1972), Dahlberg (1975), Scott and Crossman (1973), Bigelow and Schroeder (1953), Eddy and Underhill (1978), Page and Burr (1998), and Douglass (1999).

D. Submersed Aquatic Vegetation

Data on coverage and composition of submersed aquatic vegetation (SAV) are generally obtained from the SAV webpage of the Virginia Institute of Marine Science (http://www.vims.edu/bio/sav). Information on this web site is obtained from aerial photographs near the time of peak SAV abundance as well as ground surveys which are used to determine species composition. We also recorded SAV relative abundance on a 0-3 scale at 4 minute intervals using visual observations and rake tow during data mapping cruises.

E. Benthic Macroinvertebrates

Benthic macroinvertebrates were sampled monthly using a petite ponar sampler at embayment stations AR2, AR3, and AR4. Triplicate samples were collected at each station monthly. Bottom samples were sieved on-site through a 0.5 mm stainless steel sieve and preserved with rose bengal formalin. In the laboratory benthic samples were rinsed with tap water through a 0.5 mm sieve to remove formalin preservative and resuspended in tap water. All organisms were picked, sorted, identified and enumerated.

In 2017 for the second year, benthic invertebrates were also sampled at selected flowing tributary stations which possessed natural riffle-run areas. At each site one-minute kick samples were collected at one riffle and one run and composited in a single bottle. The sample was preserved with formalin to a concentration of 5%. In the lab the sample was sieved through a 0.5 mm mesh (same as the kick net) and thoroughly washed with tap water before picking and sorting. Following sorting animals were enumerated by taxon and held in ethanol-glycerin. Sampling sites for tributary macroinvertebrate

sampling are shown in Figure 1d.

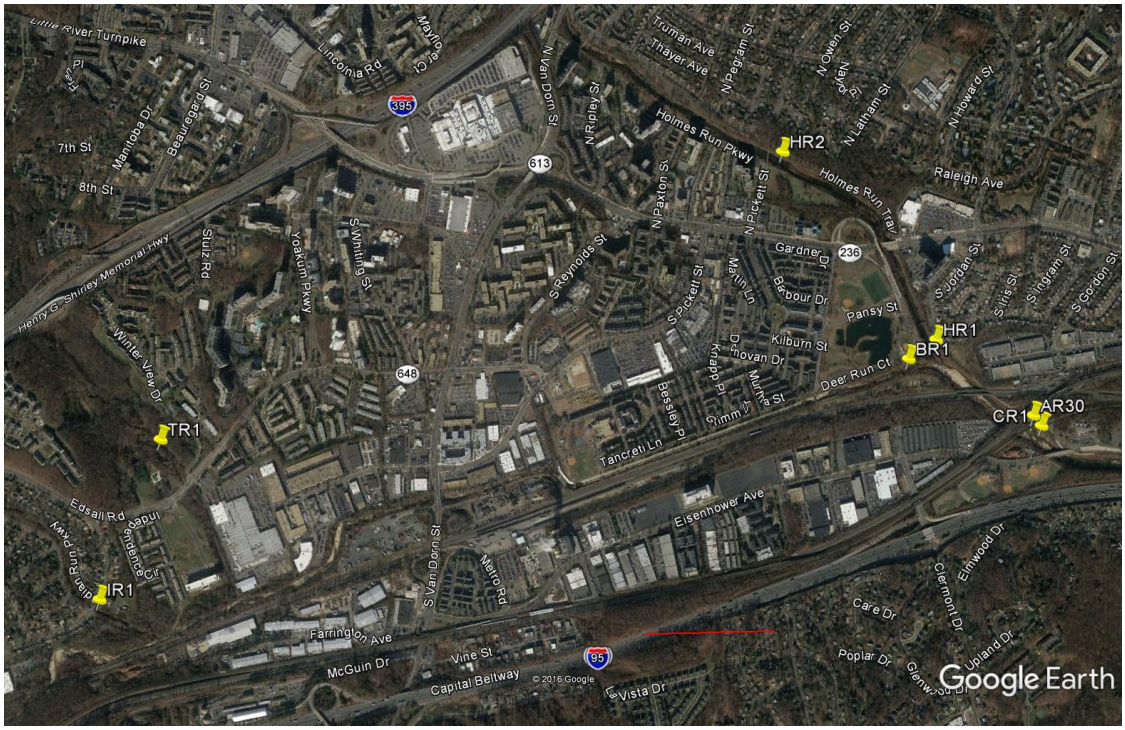

Figure 1d. Western portion of the study area showing benthic sampling stations on flowing tributaries of Cameron Run. CR1: Cameron Run: HR1, HR2: Holmes Run; BR: Backlick Run; IR: Indian Run; TR: Turkeycock Run. Red bar is 0.5 km.

F. Water Quality Mapping (Dataflow)

On two additional dates in 2017 (July 12 and August 10) *in situ* water quality mapping was conducted by slowly transiting through much of the Hunting Creek study area as water was pumped through a chamber containing a YSI 6600 sonde equipped with temperature, specific conductance, dissolved oxygen, pH, turbidity, and chlorophyll probes. Readings were recorded at 15 second intervals along with simultaneous GPS position readings. Every 2 minutes SAV relative abundance by species was recorded and every 4 minutes water samples were collected for extracted chlorophyll and TSS determination. Some areas of the Hunting Creek embayment could not be surveyed due to shallow water or heavy SAV growth. These surveys allowed a much better understanding of spatial patterns in water quality within the Hunting Creek area which facilitated interpretation of data from the fixed stations. This approach is in wide use in the Chesapeake Bay region by both Virginia and Maryland under the name “dataflow”.

G. Data Analysis

Data for each parameter were entered into spreadsheets (Excel or SigmaPlot) for graphing of temporal and spatial patterns. SYSTAT was used for statistical calculations and to create illustrations of the water quality mapping cruises. JMP v8.0.1was used for fish graphs. Other data analysis approaches are explained in the text.

RESULTS

A. Climatic and Hydrologic Factors - 2017

In 2017 air temperature was substantially above average in April and June, but near normal the remainder of the year (Table 2). July was the warmest month, with June being untypically warmer than August. There were 33 days with maximum temperature above 32.2°C (90°F) during 2017 which is near the median number over the last decade. Precipitation was well above normal during May and July, near normal in March, April and August, and below normal in the other months. The largest daily rainfall totals during the period of sampling was 8.41 cm on July 28. Over two days on July 22-23, 6.02 cm were observed. Both May and July exhibited mean discharges that were over twice the long-term average in Cameron Run (Table 3). May mean discharge was elevated in the river mainstem.

Table 2. Meteorological Data for 2017. National Airport. Monthly Summary.

	Air Temp (°C)		Precipitation (cm)	
MONTH				
March	8.4	(8.1)	8.1	(9.1)
April	18.2	(13.4)	6.7	(7.0)
May	18.8	(18.7)	14.1	(9.7)
June	25.5	(23.6)	2.9	(8.0)
July	27.7	(26.2)	23.3	(9.3)
August	25.1	(25.2)	11.6	(8.7)
September	22.8	(21.4)	3.7	(9.6)
October	----	(14.9)	----	(8.2)
November	----	(9.3)	----	(7.7)
December	----	(4.2)	----	(7.8)

Note: 2017 monthly averages or totals are shown accompanied by long-term monthly averages (1971-2000). Source: Local Climatological Data. National Climatic Data Center, National Oceanic and Atmospheric Administration.

Table 3. Monthly mean discharge at USGS Stations representing freshwater flow into the study area. (+) 2017 month > 2x Long Term Avg. (-) 2017 month < ½ Long Term Avg.

	Potomac River at Little Falls (cfs)		**Cameron Run at Wheeler Ave (cfs)**	
	2017	**Long Term Average**	**2017**	**Long Term Average**
January	14863	13700	37.4	41
February	8645	16600	11.8 (-)	45
March	9517 (-)	23600	37.5	55
April	15646	20400	39.4	42
May	26578	15000	86.6 (+)	41
June	8528	9030	15.8 (-)	38
July	6408	4820	119.0 (+)	31
August	6860	4550	56.1 (+)	28
September		5040	16.0 (-)	38
October		5930		33

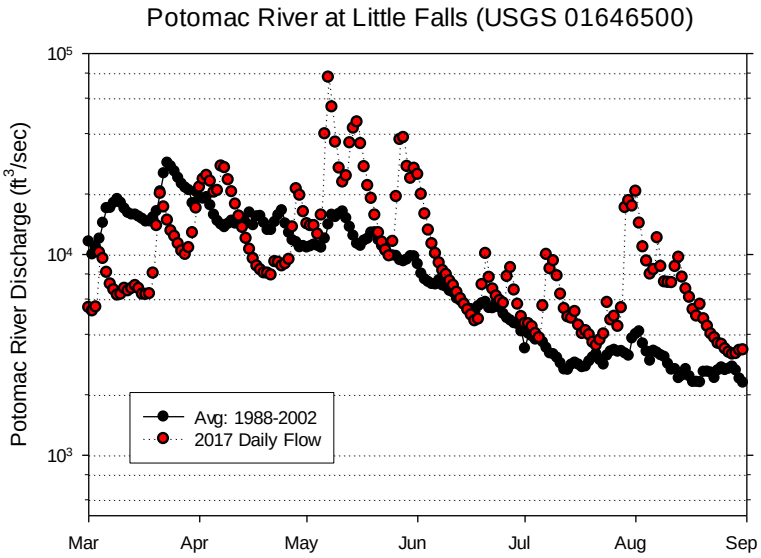

In a tidal freshwater system like the Potomac River, river flow entering from upstream is important in maintaining freshwater conditions and also serves to bring in dissolved and particulate substances from the watershed. High freshwater flows may also flush planktonic organisms downstream and bring in suspended sediments that decrease water clarity. The volume of river flow per unit time is referred to as "river discharge" by hydrologists. Note the general long term seasonal pattern of higher discharges in winter and spring and lower discharges in summer and fall.

Figure 2. Mean Daily Discharge: Potomac River at Little Falls (USGS Data). Month tick is at the beginning of the month.

Potomac River discharge during 2017 was below normal during most of March and April (Table 3, Figure 2). From May through early June Potomac flows were consistently above the long-term mean. In July and August Potomac flows were consistently above average. In Hunting Creek flows were generally below the long term average except for a few one-day spikes associated with storms. On a monthly basis, May and July were above average and June was below average. Water quality/plankton sampling dates that may have been particularly affected by immediately prior storm events included May 24, July 5 and August 8/9 (Table 1).

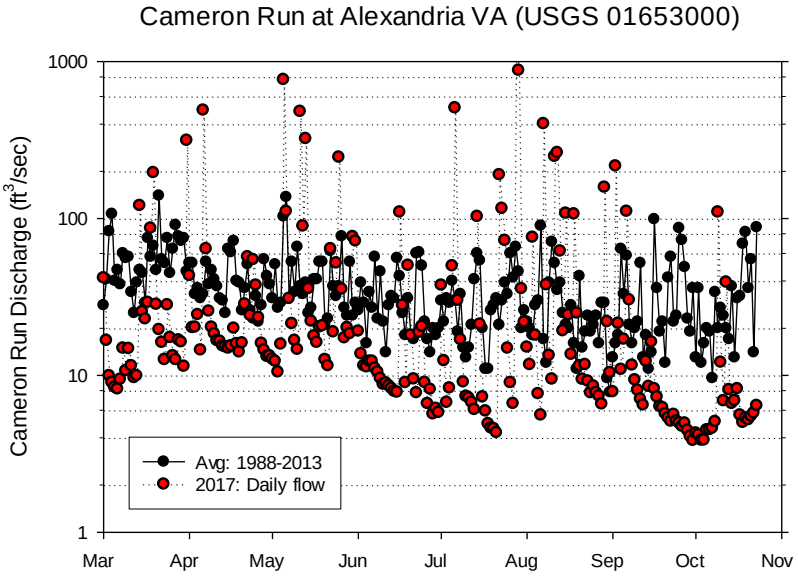

In the Hunting Creek region of the tidal Potomac, freshwater discharge is occurring from both the major Potomac River watershed upstream (measured at Little Falls) and from immediate tributaries, principally Cameron Run which empties directly into Hunting Creek. The gauge on Cameron Run at Wheeler Avenue is located just above the head of tide and covers most area which contributes runoff directly to the Hunting Creek embayment from the watershed. The contributing area to the Wheeler Ave gauge is 33.9 sq mi. (USGS)

.

Figure 3. Mean Daily Discharge: Cameron Run at Alexandria (Wheeler Ave) (USGS Data).

B. Physico-chemical Parameters: Embayment and River Stations – 2017

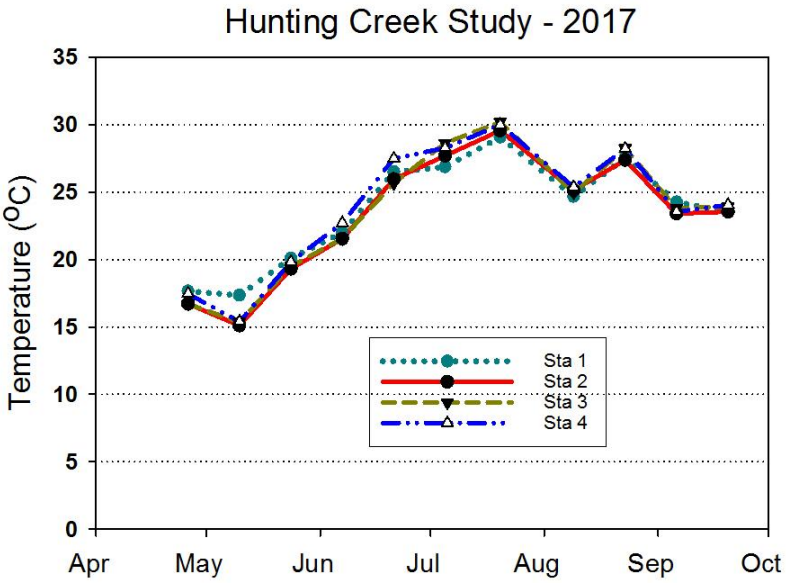

Water temperature is an important factor affecting both water quality and aquatic life. In a well-mixed system like the tidal Potomac, water temperatures are generally fairly uniform with depth. In a shallow mixed system such as the tidal Potomac, water temperature often closely tracks daily changes in air temperature.

Figure 4. Water Temperature (ºC). GMU Field Data. Month tick is at first day of month.

In 2017, water temperature followed the typical seasonal pattern at all stations (Figure 4). Values were unusually high in late April, but consistently increased from May through late July. Maximum temperature was just below 30°C at all sites on July 25, declined in early August, went up again in late August, and then declined through September. Mean daily air temperature showed similar patterns (Figure 5)

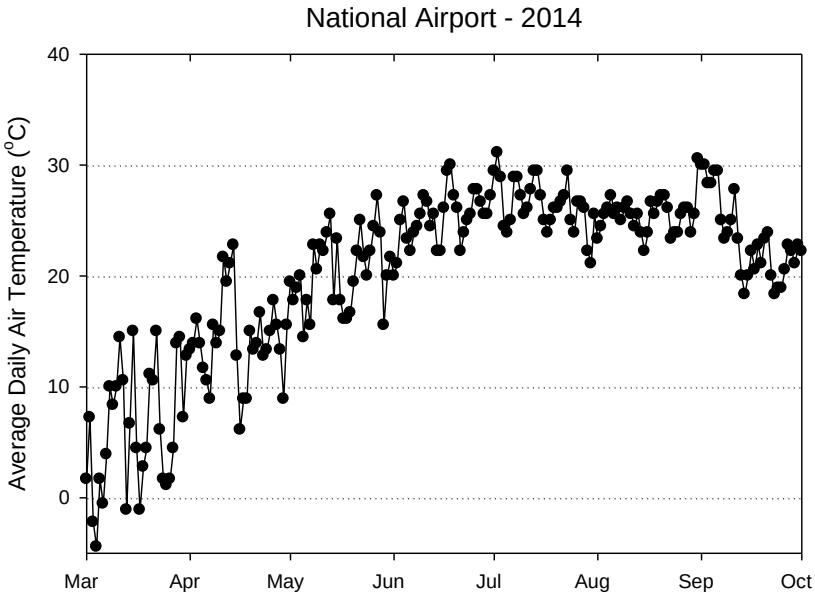

Mean daily air temperature (Figure 5) was a good predictor of water temperature (Figure 4).

Figure 5. Average Daily Air Temperature (ºC) at Reagan National Airport.

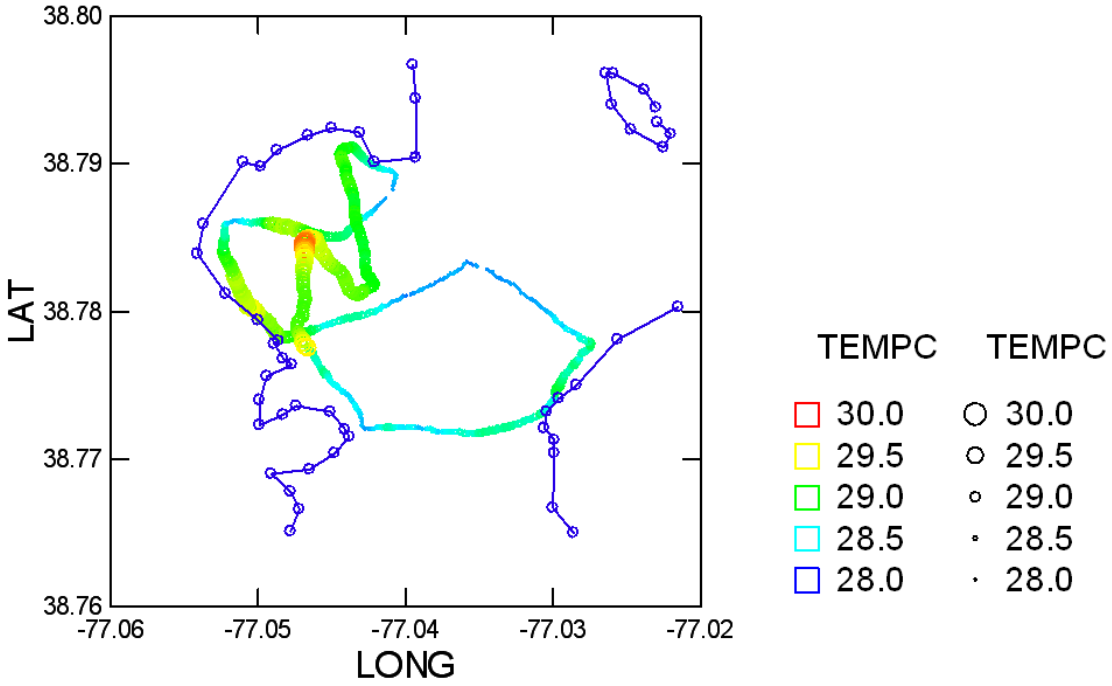

Figure 6a. Water Quality Mapping. July 12, 2017. Temperature (°C).

Mapping of water temperature was conducted on two dates in 2017: July 12 and August 10. In July temperatures were noticably warmer in Hunting Creek than in areas nearer the river mainstem (Figure 6a). This can be explained by the fact that July 12 was near the end of a weeklong period of increasing temperatures. The shallow water areas naturally responded more quickly to these changing weather conditions. In August temperatures were generally lower reflecting a period of cooling (Figure 6b).

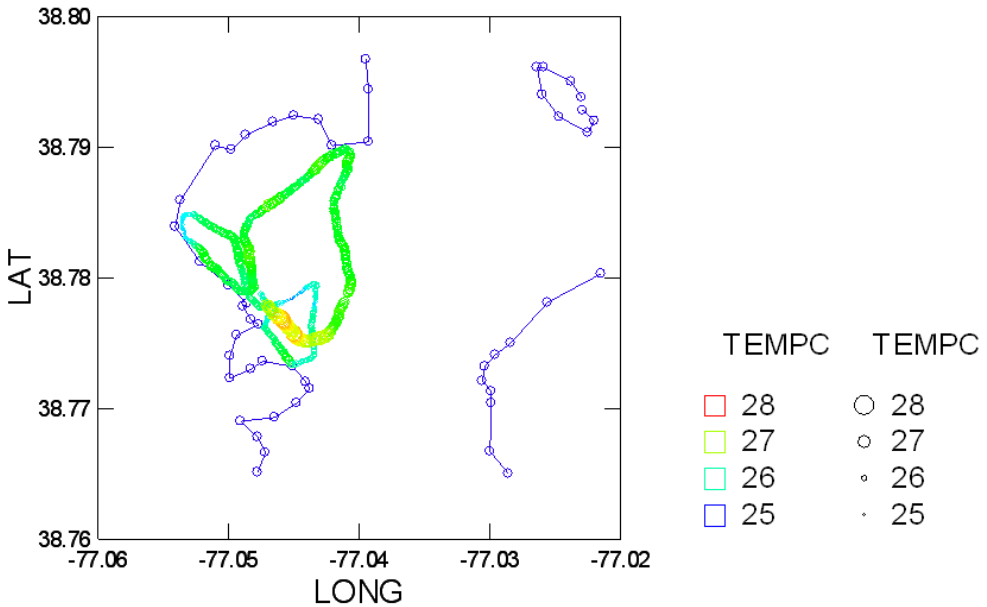

Figure 6b. Water Quality Mapping. August 10, 2017. Temperature (°C).

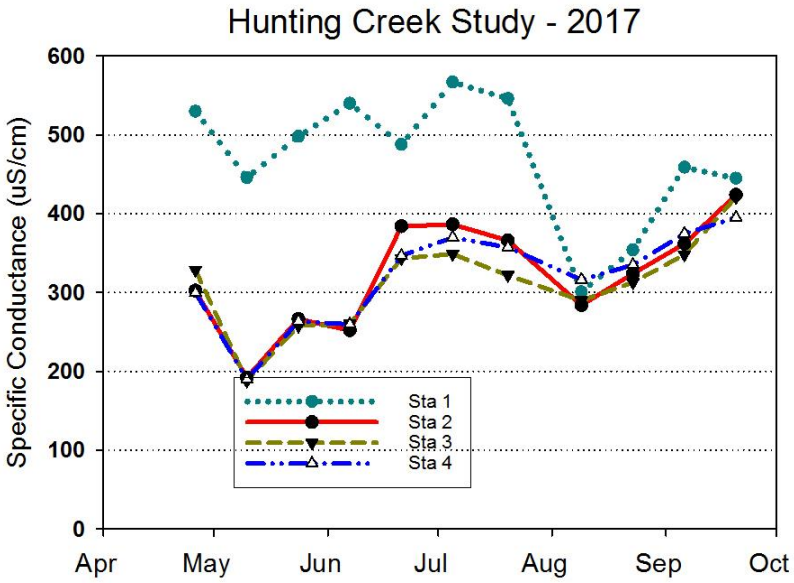

Specific conductance measures the capacity of the water to conduct electricity standardized to 25°C. This is a measure of the concentration of dissolved ions in the water. In freshwater, conductivity is relatively low. Ion concentration generally increases slowly during periods of low freshwater inflow and decreases during periods of high freshwater inflow. Sewage treatment facilities can be a source of elevated conductivity. In winter road salts can be a major source of conductivity in urban streams.

Figure 7. Specific Conductance (µS/cm). GMU Field Data. Month tick is at first day of month.

Specific conductance was generally substantially higher at AR1 than the other stations. This reflects its location just downstream of the Alex Renew treatment plant and Cameron Run, potential sources of ions contributing to conductivity (Figure 7). Following a marked decline in early May, a general pattern of increase was observed at AR2, AR3, and AR4 for the remainder of the year. AR1 showed a major decline in early August following a strong runoff event and with its levels increasing gradually along with the other stations for the remainder of the year. Chloride seasonal patterns (Figure 8) were very similar to specific conductance at all stations.

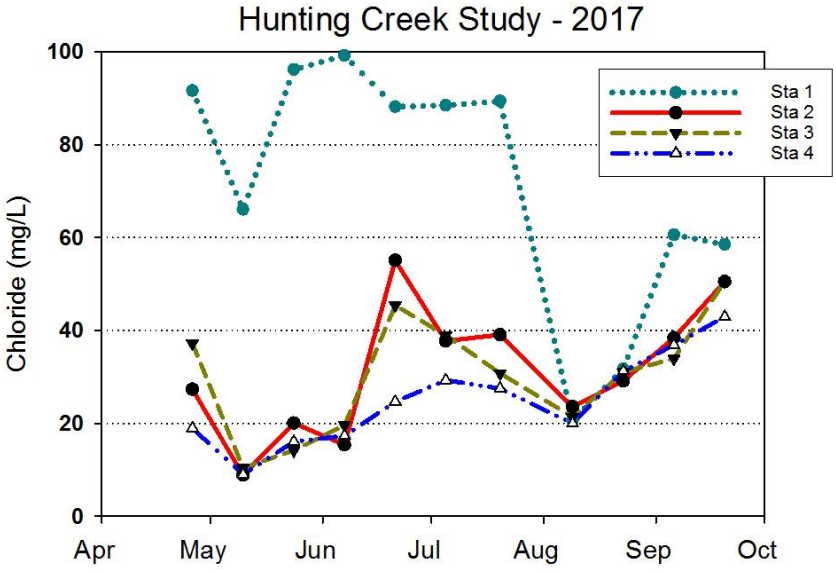

Chloride ion (Cl-) is a principal contributor to conductance. Major sources of chloride in the study area are sewage treatment plant discharges, road salt, and brackish water from the downriver portion of the tidal Potomac. Chloride concentrations observed in the Hunting Creek area are very low relative to those observed in brackish, estuarine, and coastal areas of the Mid-Atlantic region. Chloride may increased slightly in late summer or fall when brackish water from down estuary may reach the area as freshwater discharge declines.

Figure 8. Chloride (mg/L). Alexandria Renew Lab Data. Month tick is at first day of month.

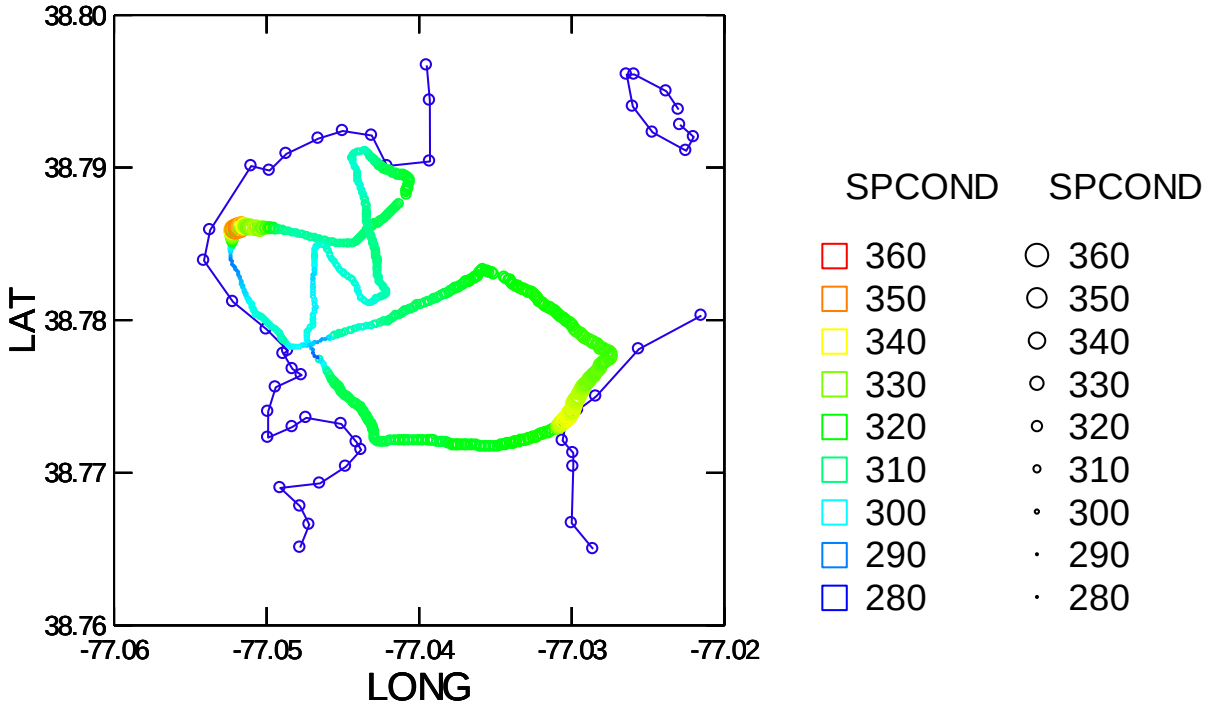

Figure 9a. Water Quality Mapping. July 12, 2017. Specific conductance (µS).

Mapping of specific conductance July 12 showed minor variations over most of the study area with lowest values along the Hunting Creek shoreline (Figure 9a). On August 10, again only minor variations were observed through the study area (Figure 9b).

.

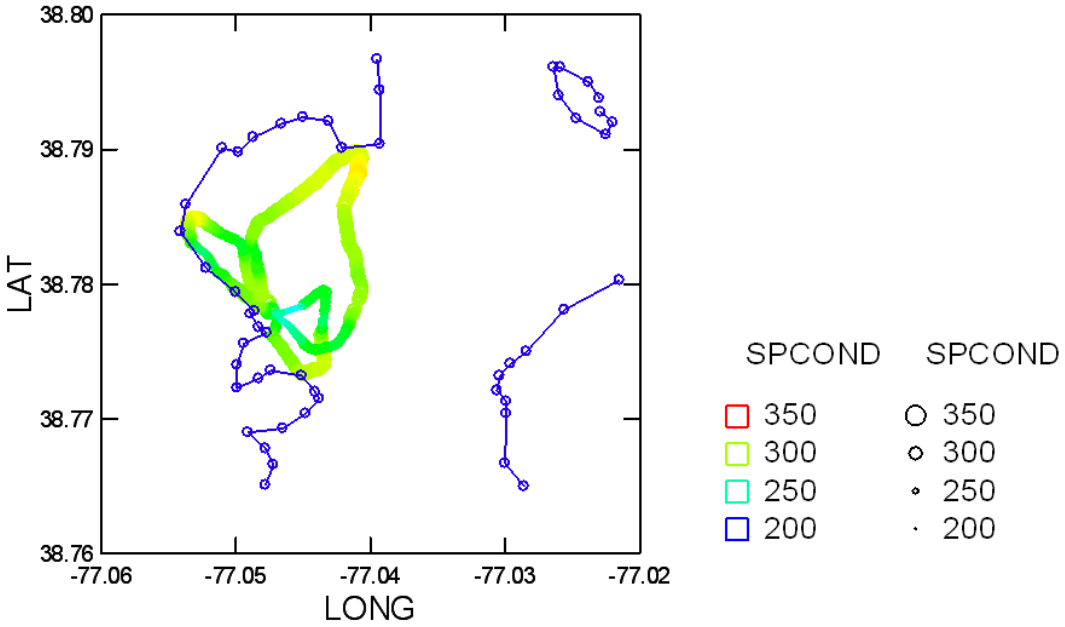

Figure 9b. Water Quality Mapping. August 10, 2017. Specific conductance (µS).

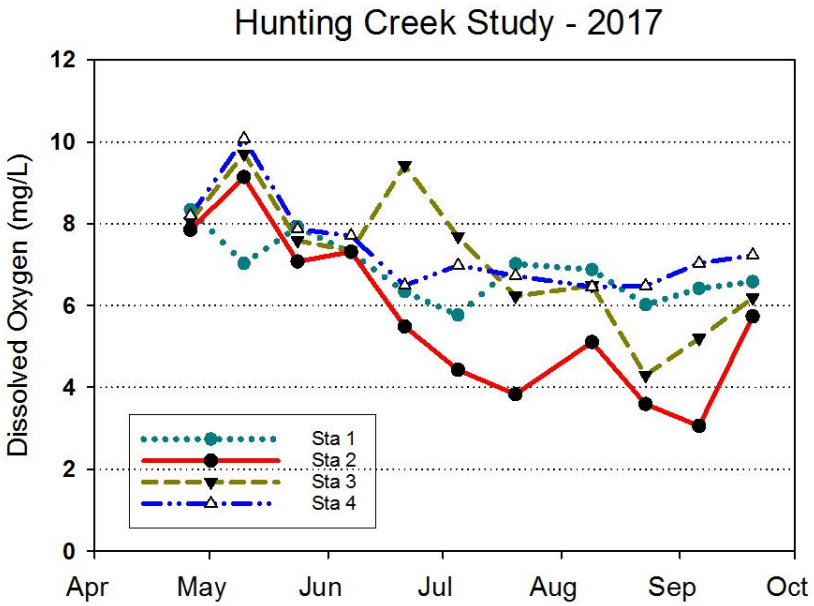

Oxygen dissolved in the water is required by freshwater animals for survival. The standard for dissolved oxygen (DO) in most surface waters is 5 mg/L. Oxygen concentrations in freshwater are in balance with oxygen in the atmosphere, but oxygen is only weakly soluble in water so water contains much less oxygen than air. This solubility is determined by temperature with oxygen more soluble at low temperatures.

Figure 10. Dissolved Oxygen (mg/L). GMU Field Data. Month tick is at first day of month.

The general pattern for dissolved oxygen (mg/L) was a seasonal decline from May through September (Figure 10). Values at AR1 exhibited a clear decline in early May corresponding to the major tributary flow event. At AR3 there was a distinct peak in late June. Looking at DO as percent saturation (Figure 11), the basic seasonal pattern was less pronounced indicating that most of the seasonal pattern in Figure 10 was explained by temperature changes in saturation capacity of water. The high value of about 120% observed at AR3 in late June indicates high rates of photosynthesis due to the thick beds of SAV at this site.

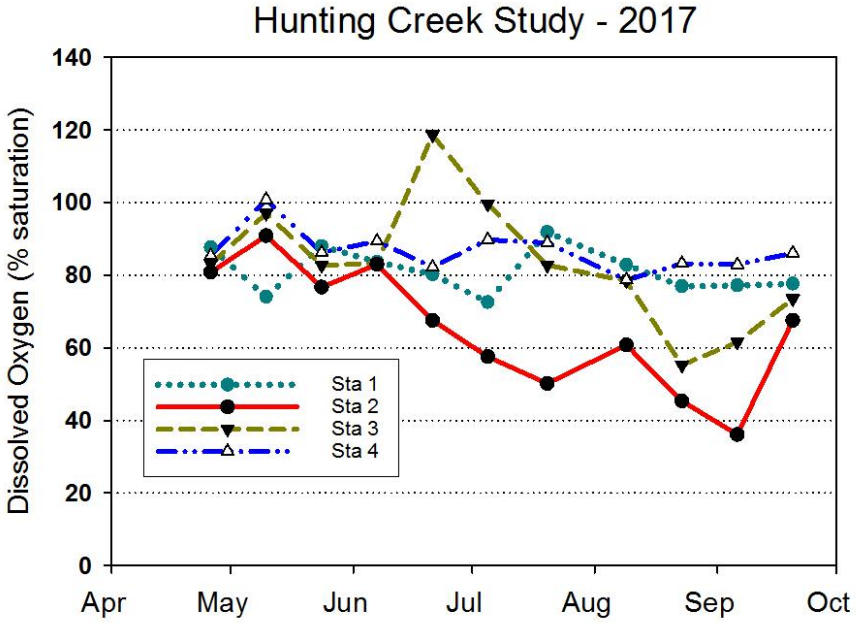

The temperature effect on oxygen concentration can be removed by calculating DO as percent saturation. This allows examination of the balance between photosynthesis and respiration both of which also impact DO. Photosynthesis adds oxygen to the water while respiration removes it. Values above 120% saturation are indicative of intense photosynthesis while values below 80% reflect a preponderance of respiration or decomposition.

Figure 11. Dissolved Oxygen (% saturation). GMU Field Data. Month tick is at first day.

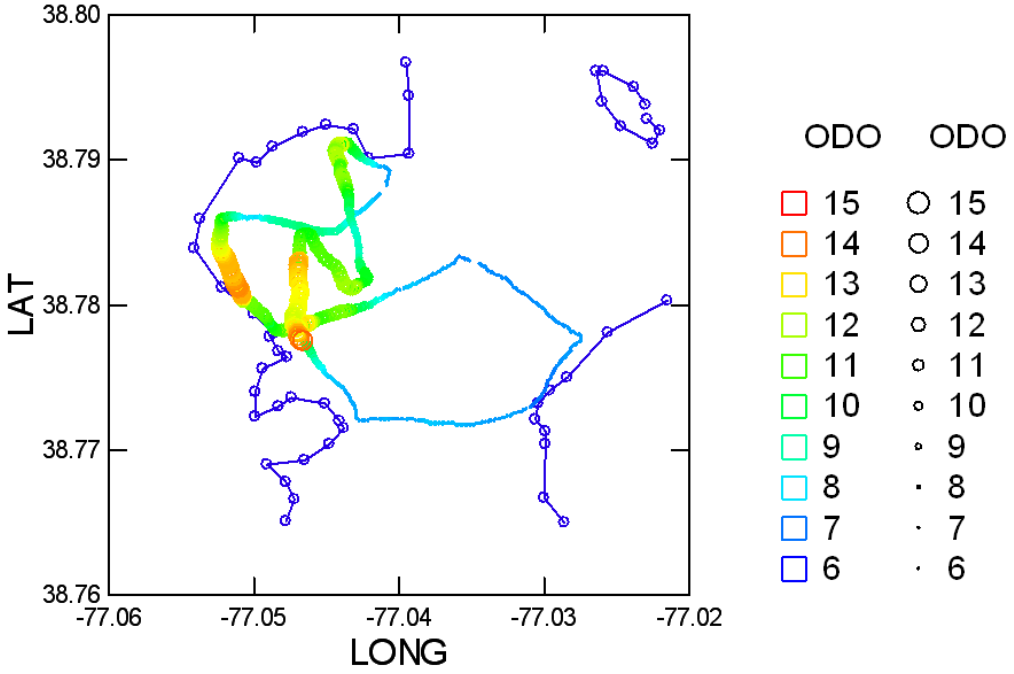

Figure 12a. Water Quality Mapping. July 12, 2017. Dissolved oxygen (mg/L).

On July 12 dissolved oxygen (both mg/L and percent saturation) exhibited clear spatial variation (Figures 12a&b). DO levels in Hunting Creek proper were clearly elevated to levels reaching 200% saturation compared with about 100% saturation over the rest of the cruise track. This was clearly a result of strong photosynthetic production of oxygen, mostly by submersed aquatic vegetation.

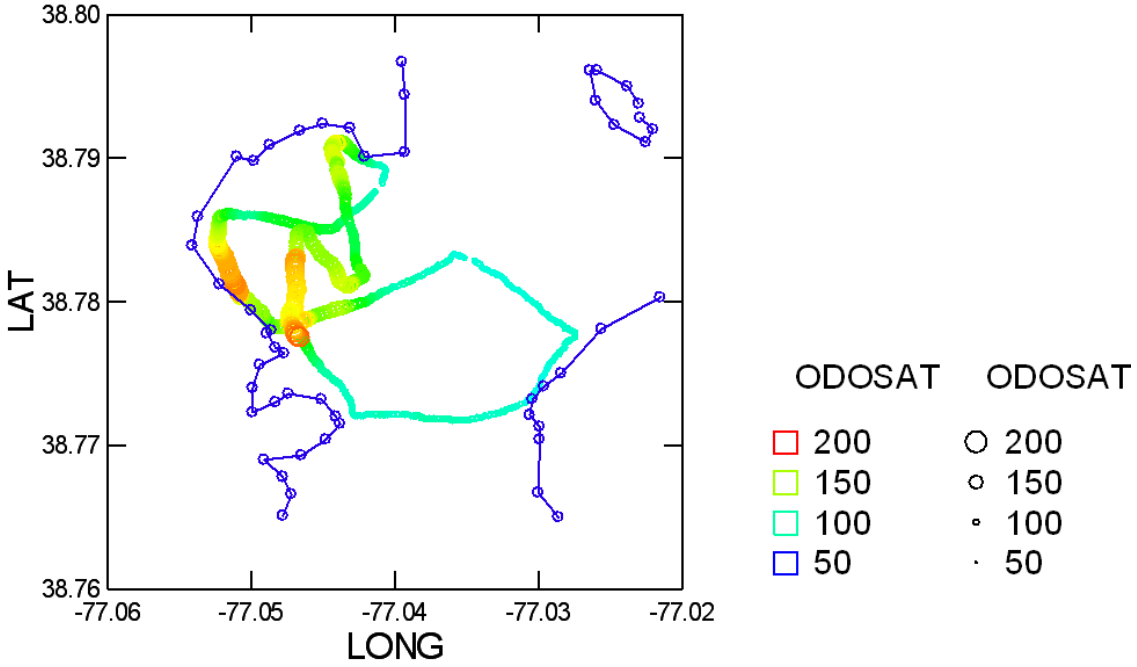

Figure 12b. Water Quality Mapping. July 12, 2017. Dissolved oxygen (percent saturation).

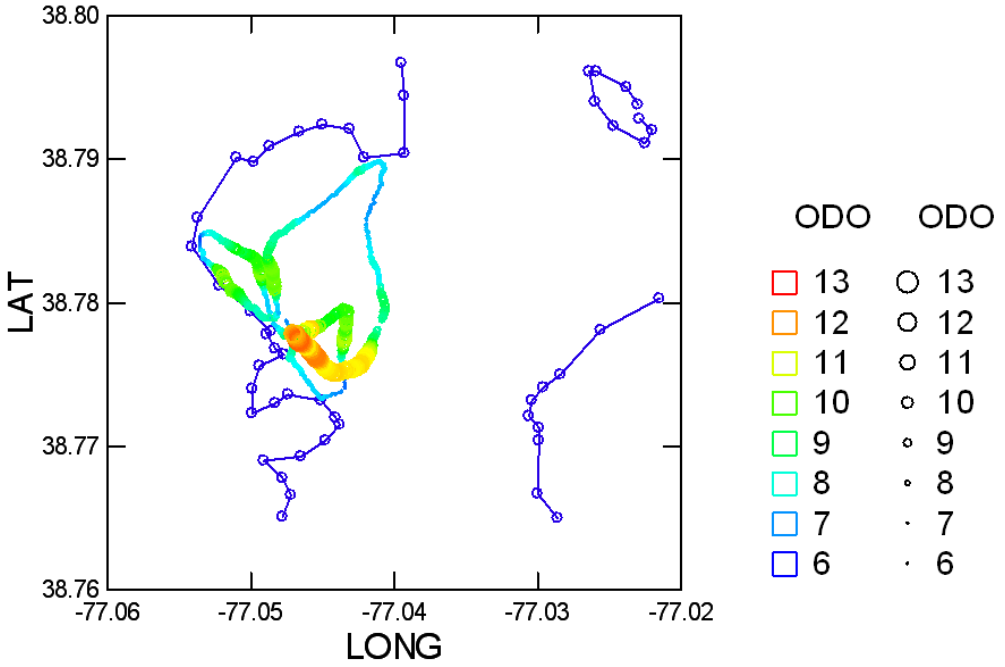

Figure 13a. Water Quality Mapping. August 10, 2017. Dissolved oxygen (mg/L).

The August 10 cruise showed a similar, but more intense and localized pattern (Figures 13a&b). The elevated values were confined to a rather small area around AR3.The subdued concentrations in the northern part of Hunting Creek may have been a lingering effect of a large runoff event in early August.

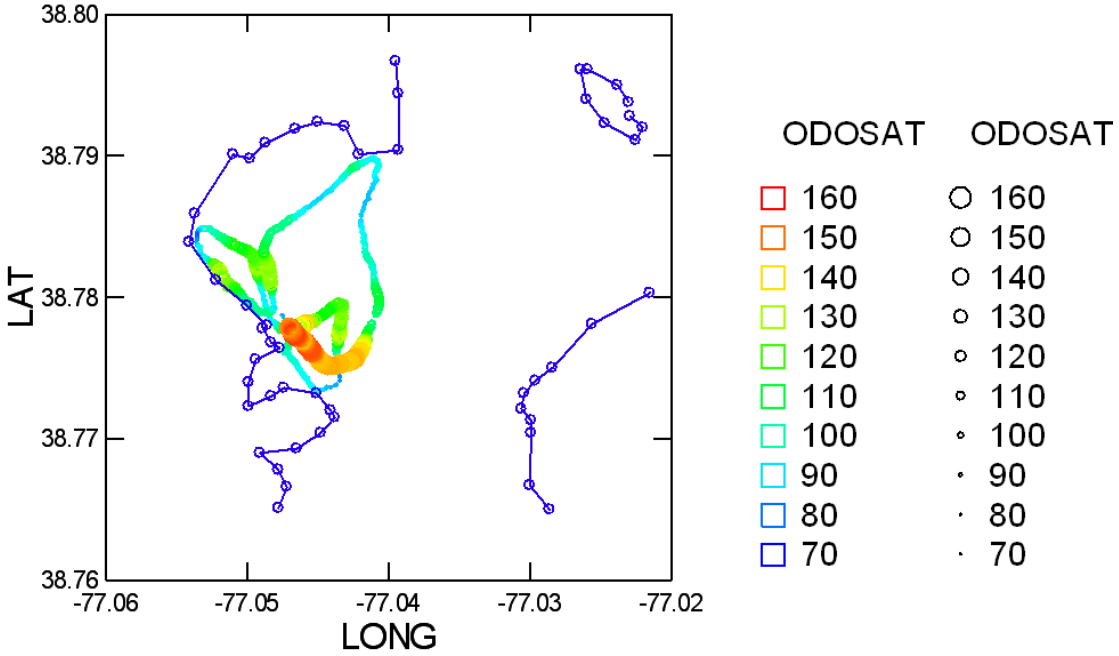

Figure 13b. Water Quality Mapping. August 10, 2017. Dissolved oxygen (percent saturation).

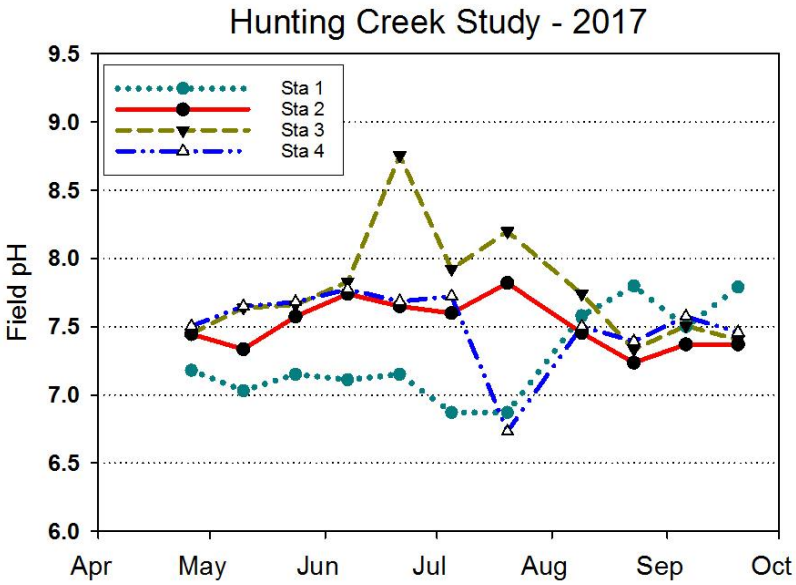

pH is a measure of the concentration of hydrogen ions (H+) in the water. Neutral pH in water is 7. Values between 6 and 8 are often called circumneutral, values below 6 are acidic and values above 8 are termed alkaline. Like DO, pH is affected by photosynthesis and respiration. In the tidal Potomac, pH above 8 indicates active photosynthesis and values above 9 indicate intense photosynthesis. A decrease in pH following a rainfall event may be due to acids in the rain or in the watershed.

Figure 14. pH. GMU Field Data. Month tick is at first day of month.

Field pH and lab pH showed a range of seasonal and spatial patterns in 2017 (Figure 14, 15). The river mainstem site (AR 4) was fairly constant through time, generally in the 7.5-8.0 range, except for a clear decrease in late July. AR3 was elevated in late June and July, but AR2 remained rather constant. At AR1, pH was rather low from April through July, but increased in August and September.

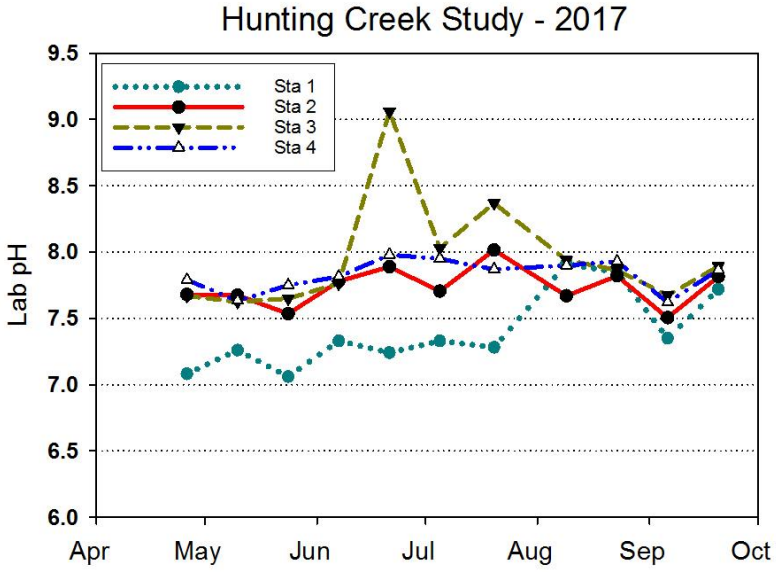

pH may be measured in the field or in the lab. Field pH is more reflective of in situ conditions while lab pH is done under more stable and controlled laboratory conditions and is less subject to error. Newer technologies such as the Hydrolab and YSI sondes used in GMU field data collection are more reliable than previous field pH meters and should give results that are most representative of values actually observed in the river.

Figure 15. pH. AlexRenew Lab Data. Month tick is at first day of month.

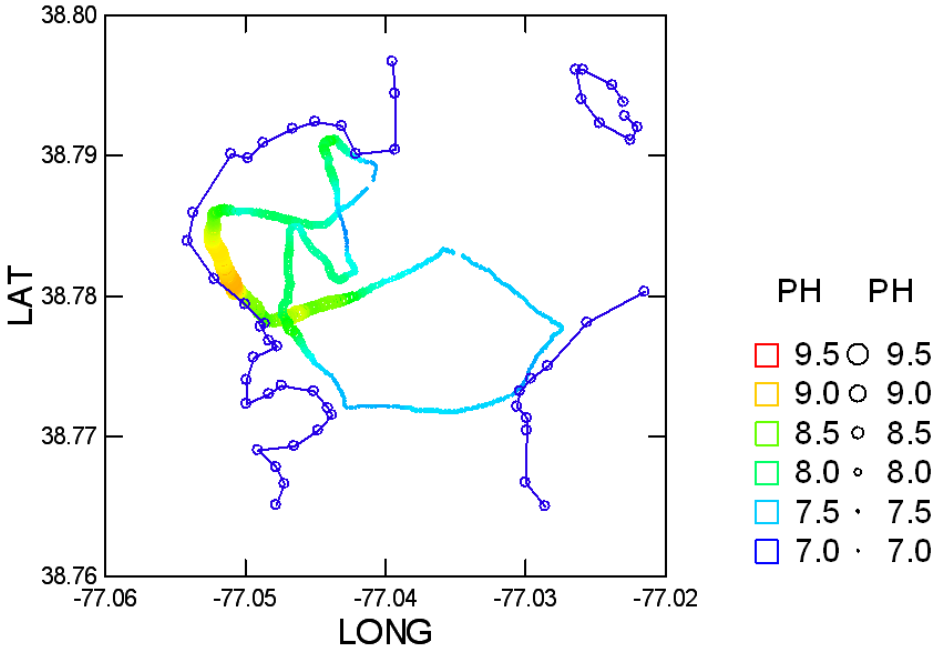

Figure 16a. Water Quality Mapping. July 12, 2017. pH.

Water quality mapping on both dates showed elevated pH in the Hunting Creek embayment due to heavy SAV growth (Figure 16a&b). Values in both months reached a value of 9.5; this was consistent with the elevated DO values also observed in the embayment indicating strong photosynthesis as a likely cause.

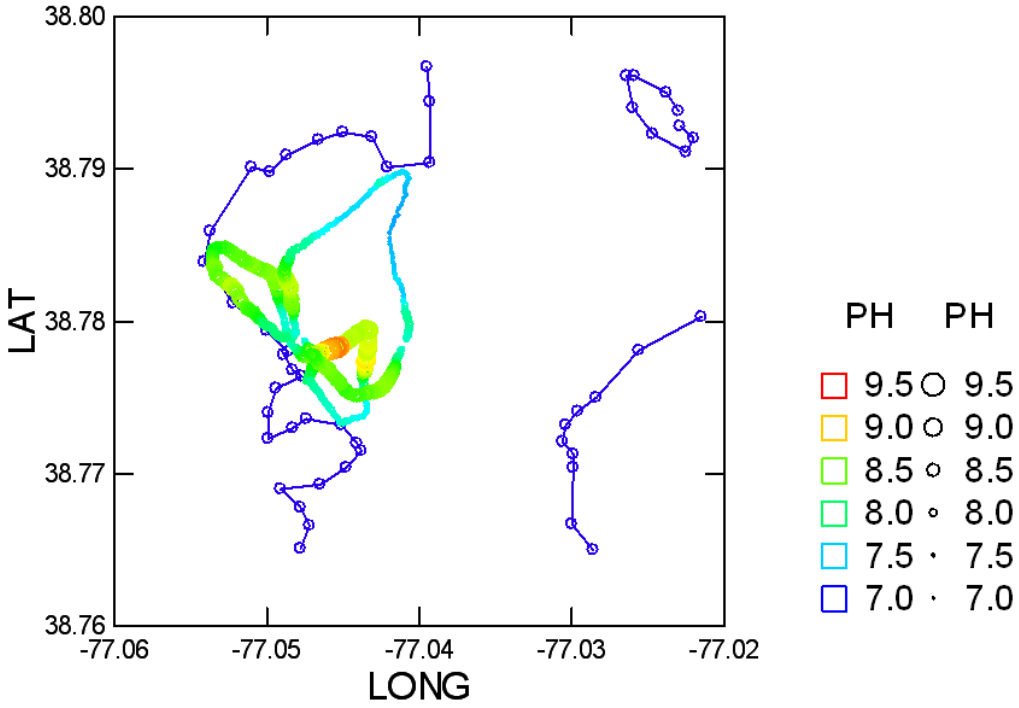

Figure 16b. Water Quality Mapping. August 10, 2017. pH.

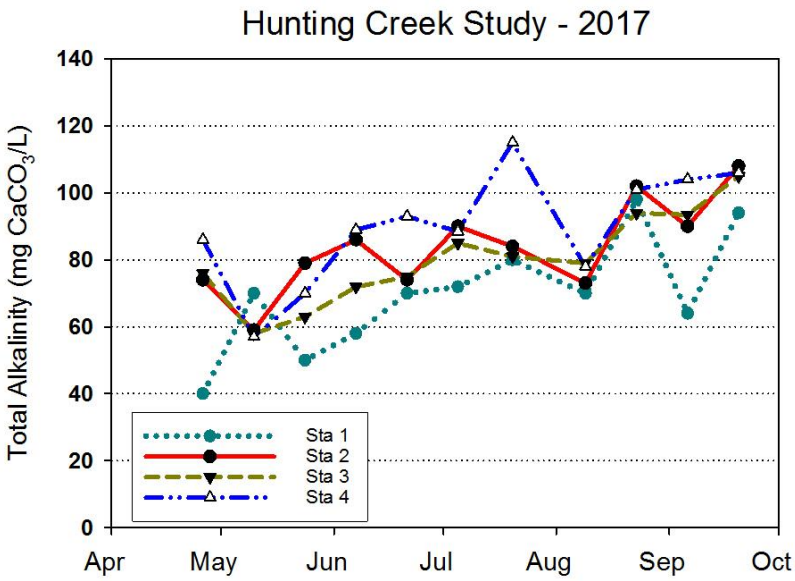

Total alkalinity measures the amount of bicarbonate and carbonate dissolved in the water. In freshwater this corresponds to the ability of the water to absorb hydrogen ions (acid) and still maintain a near neutral pH. Alkalinity in the tidal freshwater Potomac generally falls into the moderate range allowing adequate buffering without carbonate precipitation.

Figure 17. Total Alkalinity (mg/L as $CaCO_3$). AlexRenew Lab data. Month tick is at first day.

Total alkalinity was generally in the range 60-100 mg/L as $CaCO_3$ (Figure 17). There was a gradual trend of increasing values as the year went along. Water clarity as reflected by Secchi disk transparency was generally in the range 0.6 to 1.0 m during 2017 (Figure 18). Values were low at all sites in early May. Accurate values were missing from AR2 and AR3 during most of the year as the Secchi disk was visible to the bottom of the bay or to the top of the SAV which was about 1 m. A markedly high value of 1.5 m was found in late August at AR3. At AR4 in the channel, transparency reached a low value of about 0.6 m in early May and early September.

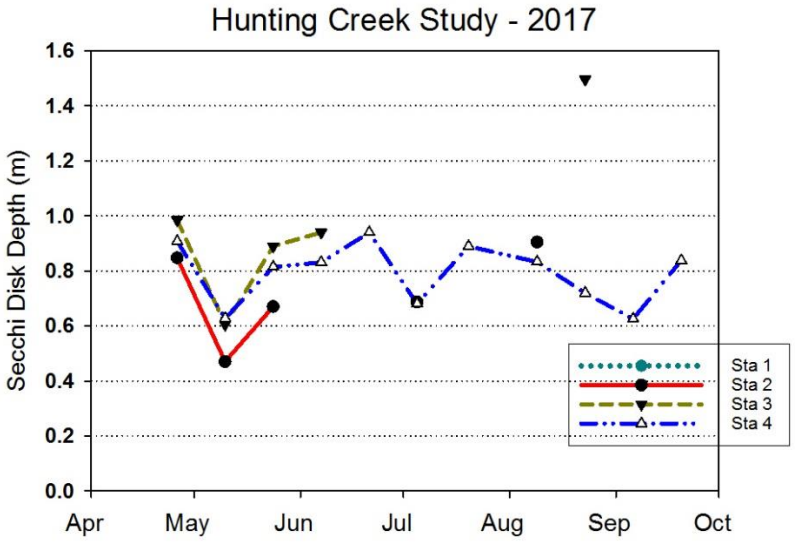

Secchi Depth is a measure of the transparency of the water. The Secchi disk is a flat circle of thick sheet metal or plywood about 6 inches in diameter which is painted into alternate black and white quadrants. It is lowered on a calibrated rope or rod to a depth at which the disk disappears. This depth is termed the Secchi Depth. This is a quick method for determining how far light is penetrating into the water column. Light is necessary for photosynthesis and thereby for growth of aquatic plants and algae.

Figure 18. Secchi Disk Depth (m). GMU Field Data. Month tick is at first day of month.

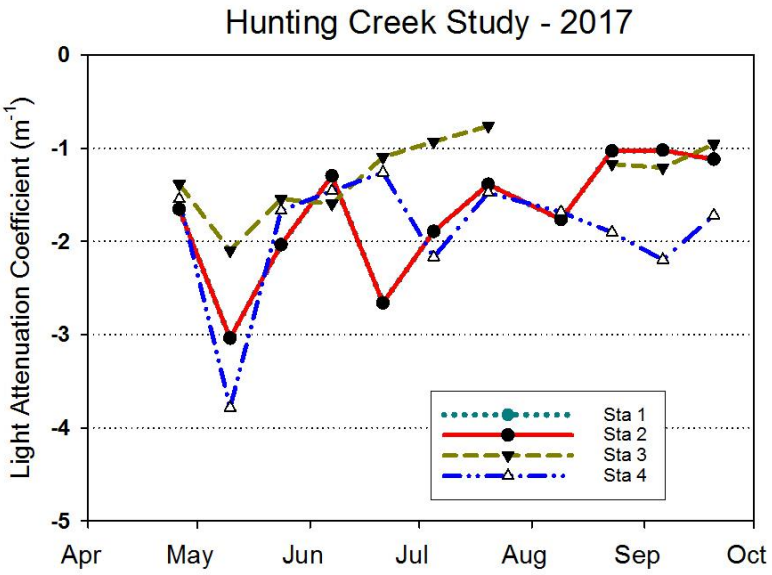

Light Attenuation is another approach to measuring light penetration. This is determined by measuring light levels at a series of depths starting near the surface. The resulting relationship between depth and light is fit to a semi-logarithmic curve and the resulting slope is called the light attenuation coefficient. This relationship is called Beer's Law. It is analogous to absorbance on a spectrophotometer. The greater the light attenuation, the faster light is absorbed with depth. More negative values indicate greater attenuation. Greater attenuation is due to particulate and dissolved material which absorbs and deflects light.

Figure 19. Light Attenuation Coefficient (m^{-1}). GMU Field Data. Month tick is at first day of month.

Light attenuation coefficient data generally fell in the range -1.0 to -3.0 m^{-1} (Fiigure 19). More negative values indicate lower light penetration. Values dropped strongly in early May due to heavy rains 5 days earlier. Turbidity also showed this effect with values increasing markedly. Turbidity values showed a general decrease through the study period.

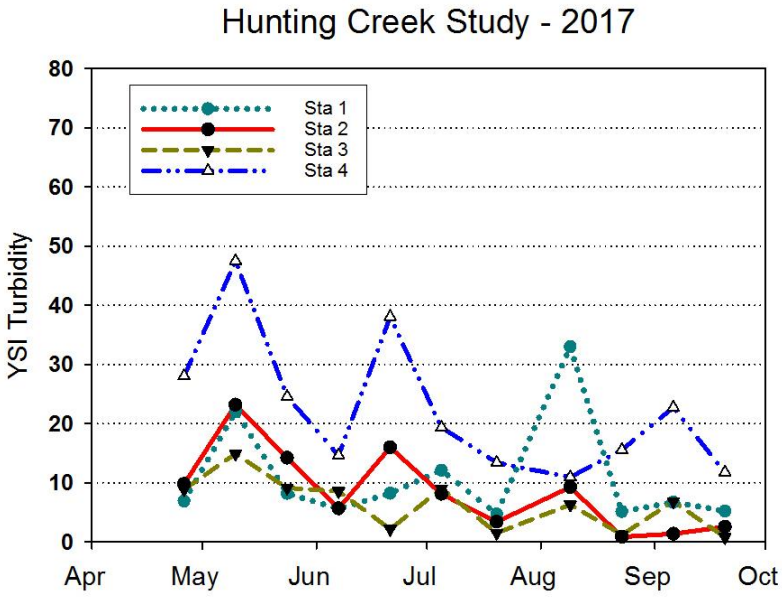

Turbidity is yet a third way of measuring light penetration. Turbidity is a measure of the amount of light scattering by the water column. Light scattering is a function of the concentration and size of particles in the water. Small particles scatter more light than large ones (per unit mass) and more particles result in more light scattering than fewer particles.

Figure 20. Turbidity (NTU). GMU Lab Data. Month tick is at first day of month.

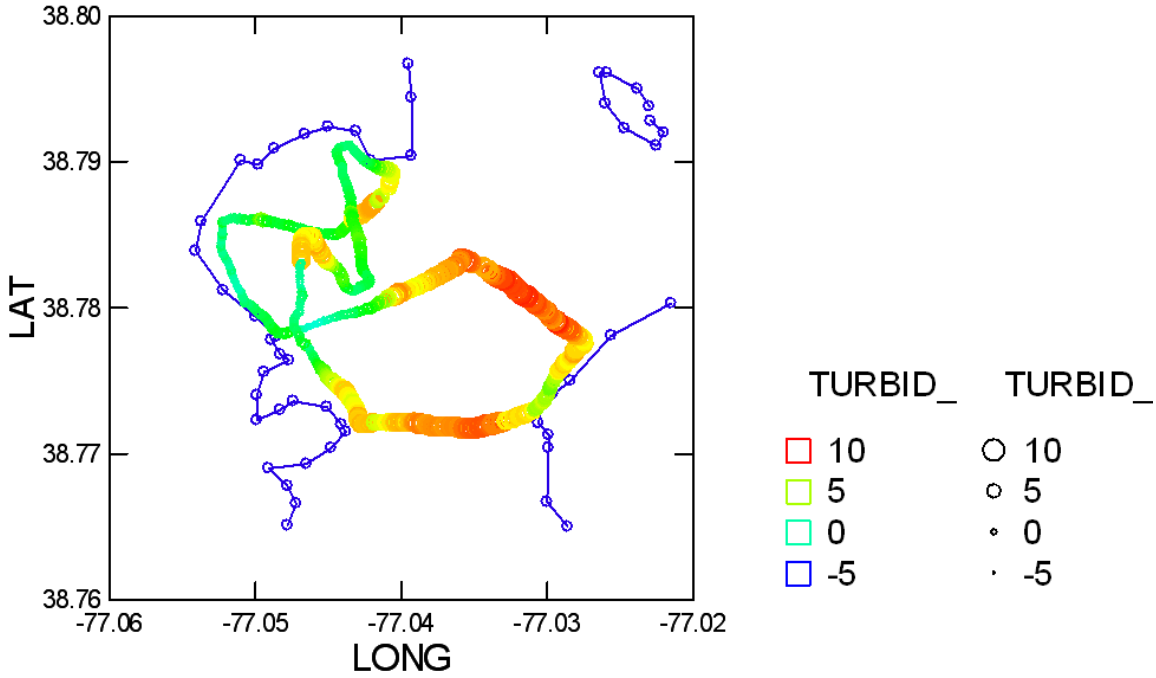

Figure 21a. Water Quality Mapping. July 12, 2017. Turbidity YSI.

On the July 12 mapping turbidity showed a strong spatial gradient, being highest in the river channel and consistently lower in the SAV beds (Figure 21a). Within Hunting Creek values were generally in the 0-10 NTU range. In August turbidity was generally low in the area surveyed which was mostly in the embayment (Figure 21b).

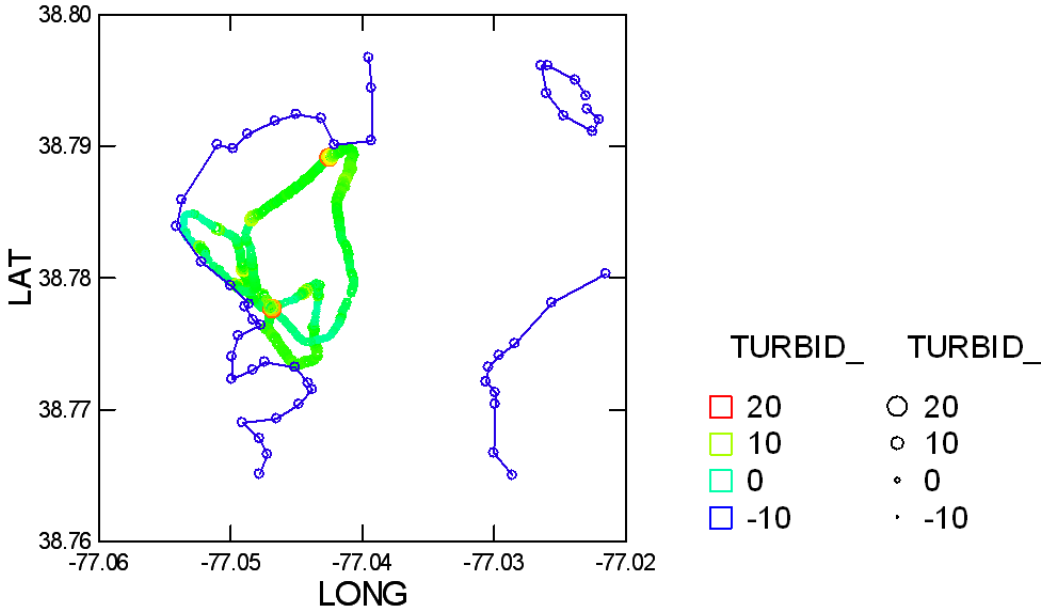

Figure 21b. Water Quality Mapping. August 10, 2017. Turbidity YSI.

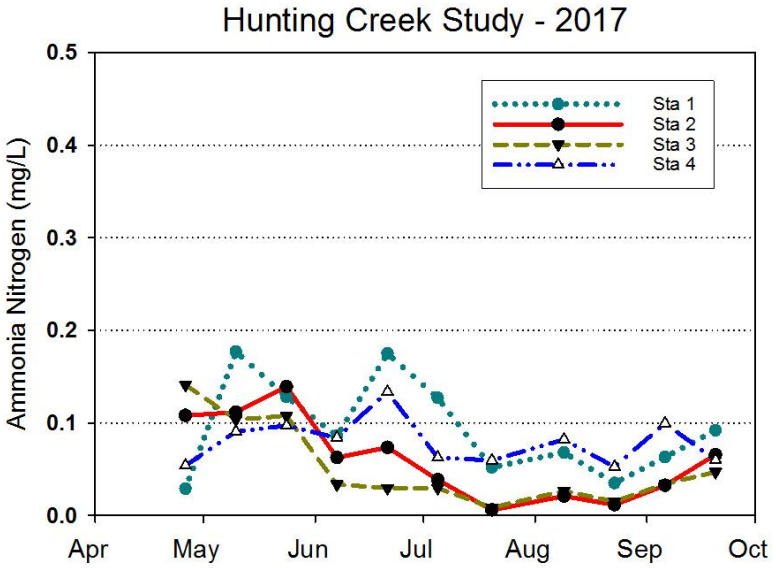

Ammonia nitrogen measures the amount of ammonium ion (NH_4^+) and ammonia gas (NH_3) dissolved in the water. Ammonia nitrogen is readily available to algae and aquatic plants and acts to stimulate their growth. While phosphorus is normally the most limiting nutrient in freshwater, nitrogen is a close second. Ammonia nitrogen is rapidly oxidized to nitrate nitrogen when oxygen is present in the water so high ammonia levels suggest proximity to a source.

Figure 22. Ammonia Nitrogen (mg/L). AlexRenew Lab Data. Month tick is at first day of month.

Ammonia nitrogen was consistently low (<0.2 mg/L) for the entire study period (Figure 22). A clear seasonal pattern was seen at AR1, AR2, and AR3 with a general decline. At AR4 ammonia values were consistently below 0.1 mg/L and did not show much seasonality. Nitrate nitrogen levels did not show much of a seasonal trend at AR4 remaining between 0.5 and 1.0 mg/L (Figure 23). At AR2 and AR3 values were near 1.0 mg/L in the spring and declined to below 0.5 mg/L during the active growth of SAV in midsummer. Nitrate nitrogen at AR1 was generally in the same range as the other sites, but bumped up on late May-early June and September.

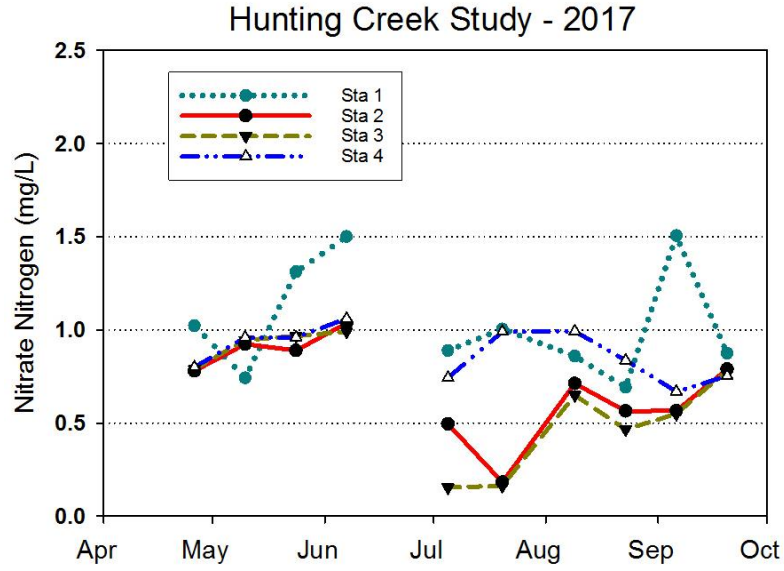

Nitrate Nitrogen refers to the amount of N that is in the form of nitrate ion (NO_3^-). Nitrate ion is the most common form of nitrogen in most well oxidized freshwater systems. Nitrate concentrations are increased by input of wastewater, nonpoint sources, and oxidation of ammonia in the water. Nitrate concentrations decrease when algae and plants are actively growing and removing nitrogen as part of their growth.

Figure 23. Nitrate Nitrogen (mg/L). AlexRenew Lab Data. Month tick is at first day of month.

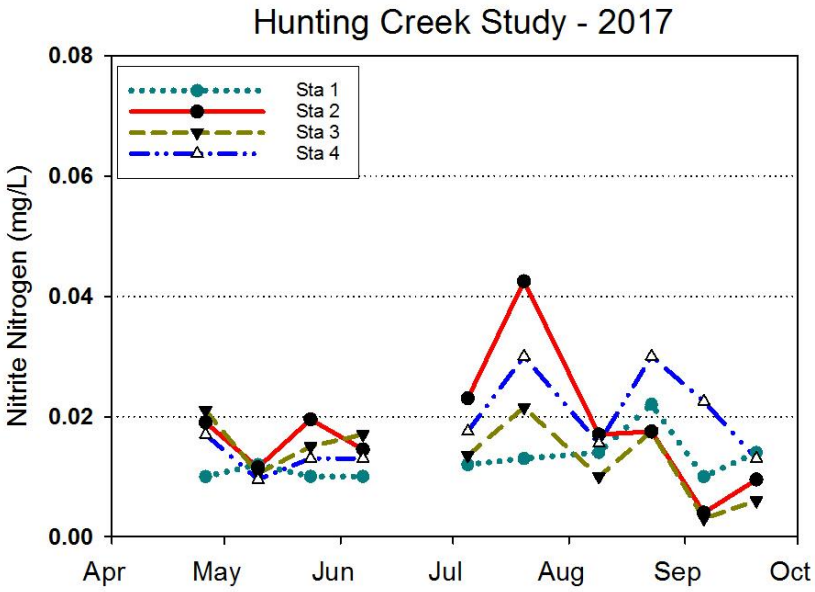

Nitrite nitrogen consists of nitrogen in the form of nitrite ion (NO_2^-). Nitrite is an intermediate in the oxidation of ammonia to nitrate, a process called nitrification. Nitrite is usually in very low concentrations unless there is active nitrification.

Figure 24. Nitrite Nitrogen (mg/L). AlexRenew Lab Data. Month tick is at first day of month.

Nitrite nitrogen was generally low (<0.03 mg/L) throughout the year (Figure 24). Some slightly elevated levels were observed in late July and late Autust. Organic nitrogen values were generally in the range of 0.2-0.6 mg/L with little clear seasonal or spatial pattern at most stations (Figure 25). The exception was AR1 which had elevated values from April through July.

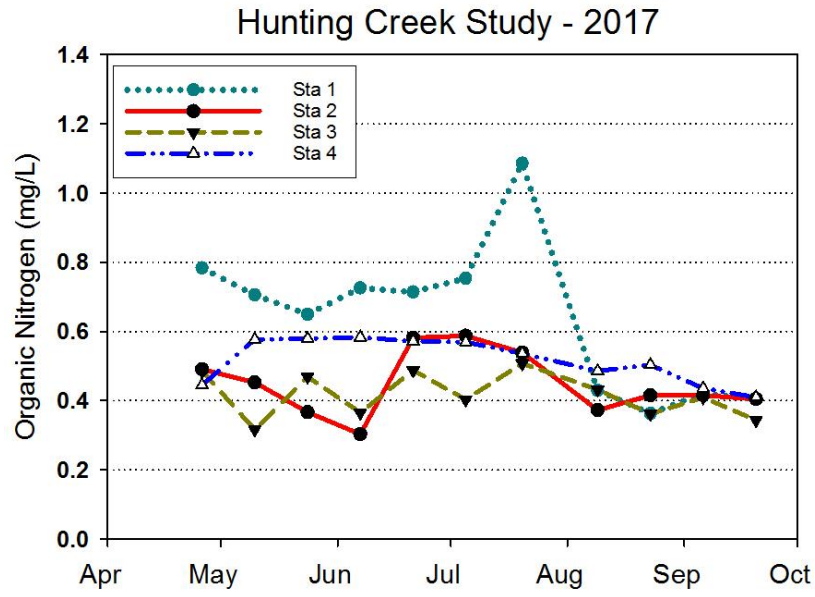

Organic nitrogen measures the nitrogen in dissolved and particulate organic compounds in the water. Organic nitrogen comprises algal and bacterial cells, detritus (particles of decaying plant, microbial, and animal matter), amino acids, urea, and small proteins. When broken down in the environment, organic nitrogen results in ammonia nitrogen. Organic nitrogen is determined as the difference between total Kjeldahl nitrogen and ammonia nitrogen.

Figure 25. Organic Nitrogen (mg/L). AlexRenew Lab Data. Month tick is at first day of month.

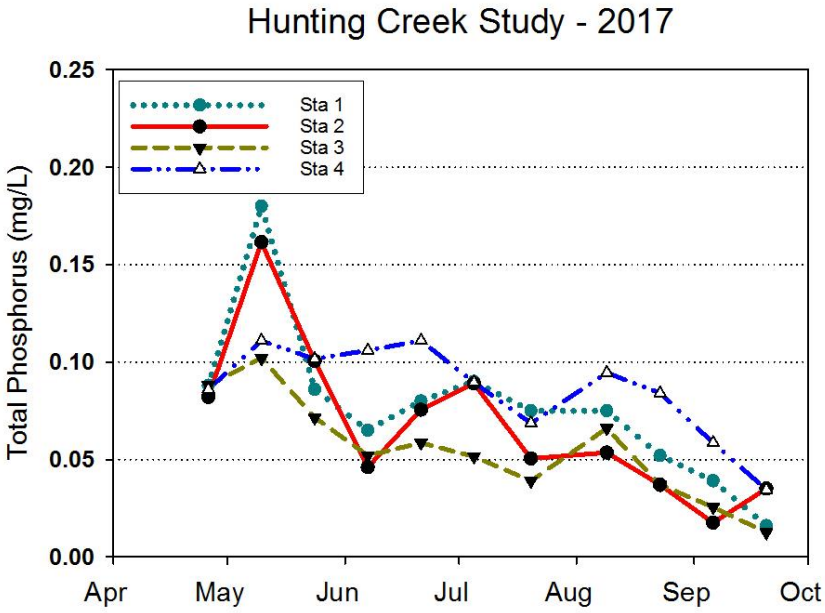

Phosphorus (P) is often the limiting nutrient in freshwater ecosystems. As such the concentration of P can set the upper limit for algal growth. Total phosphorus is the best measure of P availability in freshwater since much of the P is tied up in biological tissue such as algal cells. Total P includes phosphate ion (PO_4^{-3}) as well as phosphate inside cells and phosphate bound to inorganic particles such as clays.

Figure 26. Total Phosphorus (mg/L). AlexRenew Lab Data. Month tick is at first day of month.

Total phosphorus showed general pattern of decreasing values over the study period at all stations with values dropping from about 0.10 mg/L to less than 0.05 mg/L (Figure 26). An upward spike was observed at AR1 and AR2 in early May following major storm inflow. Otherwise, AR2 was generally highest. Ortho-phosphorus was generally quite low (<0.04 mg/L) and showed a downward trend, especially in June and July (Figure 27).

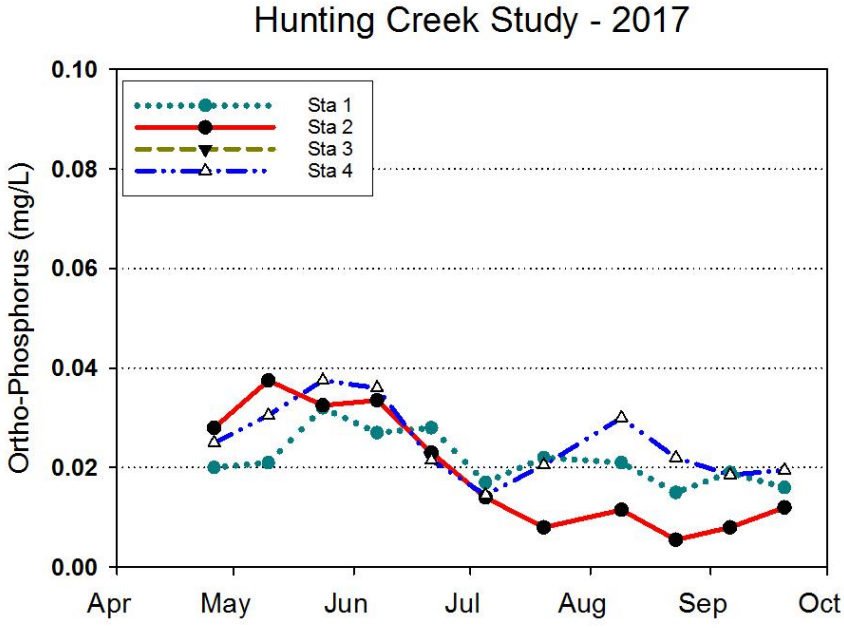

Soluble reactive phosphorus (SRP) is a measure of phosphate ion (PO_4^{-3}). Phosphate ion is the form in which P is most available to primary producers such as algae and aquatic plants in freshwater. However, SRP is often inversely related to the activity of primary producers because they tend to take it up so rapidly. So, higher levels of SRP indicate either a local source of SRP to the waterbody or limitation by a factor other than P.

Figure 27. Soluble Reactive Phosphorus (mg/L). AlexRenew Lab Data. Month tick is at first day of month.

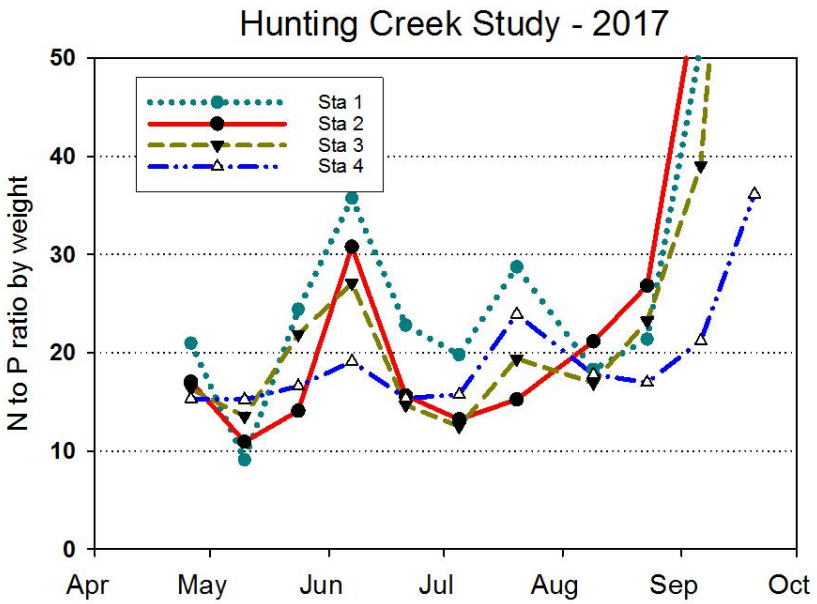

N:P ratio is determined by summing all of the components of N (ammonia, nitrate, nitrite, and organic nitrogen) and dividing by total P. This ratio gives an indication of whether N or P is more likely to be limiting primary production in a given freshwater system. Generally, values above 7.2 are considered indicative of P limitation while values below 7.2 suggest N limitation. N limitation could lead to dominance by cyanobacteria who can fix their own N from the atmosphere.

Figure 28. N/P Ratio (by mass). AlexRenew Lab Data. Month tick is at first day of month.

N/P ratio consistently pointed to P limitation, being greater than 7.2 in all samples (Figure 28). A Values were generally in the 10 to 20 range, but increased strongly in September, mainly due to falling total P concentrations. Biochemical oxygen demand (BOD) was generally below detection limit at all stations at all times (Figure 29). The detection limit is 2 mg/L which was plotted at 1 mg/L in the graph.

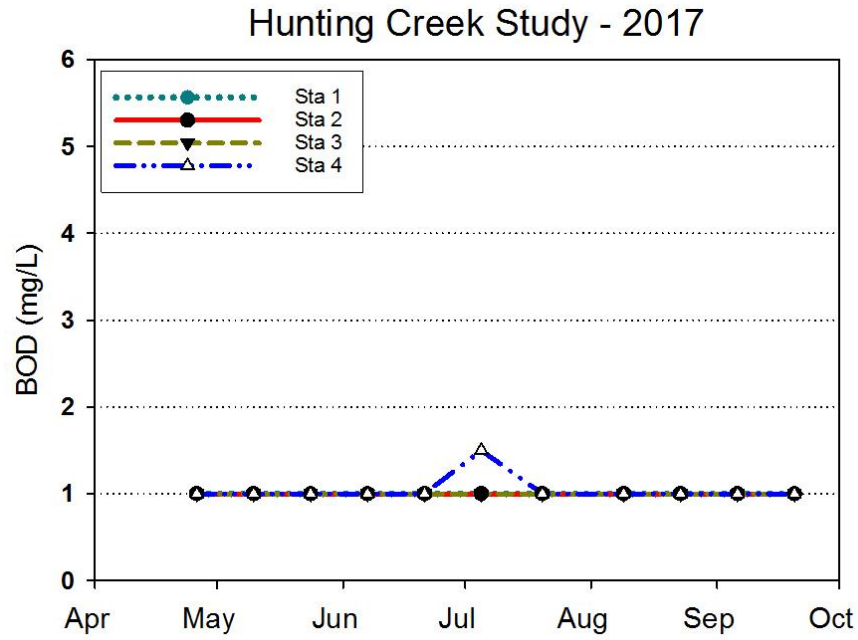

Biochemical oxygen demand (BOD) measures the amount of decomposable organic matter in the water as a function of how much oxygen it consumes as it breaks down over a given number of days. Most commonly the number of days used is 5. BOD is a good indicator of the potential for oxygen depletion in water. BOD is composed both dissolved organic compounds in the water as well as microbes such as bacteria and algae which will respire and consume oxygen during the period of measurement.

Figure 29. Biochemical Oxygen Demand (mg/L). AlexRenew Lab Data. Month tick is at first day of month.

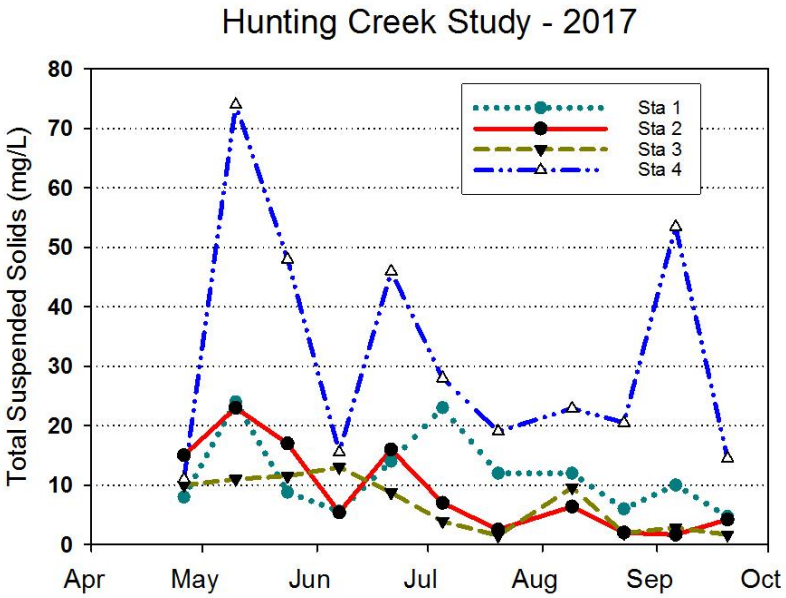

Total suspended solids (TSS) is measured by filtering a known amount of water through a fine filter which retains all or virtually all particles in the water. This filter is then dried and the weight of particles on the filter determined by difference. TSS consists of both organic and inorganic particles. During periods of low river and tributary inflow, organic particles such as algae may dominate. During storm flow periods or heavy winds causing resuspension, inorganic particles may dominate.

Figure 30. Total Suspended Solids (mg/L). AlexRenew Lab Data. Month tick is at first day of month.

Total suspended solids was generally in the range 0-20 mg/L at AR1, AR2, and AR3 (Figure 30). There was a general seasonal decline at AR2 and AR3 through the year. AR1 readings were more variable. Surface and bottom samples were averaged at AR2, AR3, and AR4.The substantially higher values observed at AR4 were mainly due to elevated readings in the bottom samples due to scouring by tidal flow; depth variations were not found at AR2 and AR3. VSS values were generally much lower, but followed similar patterns (Figure 31). Both TSS and VSS were highly elevated in late June corresponding to the major runoff event.

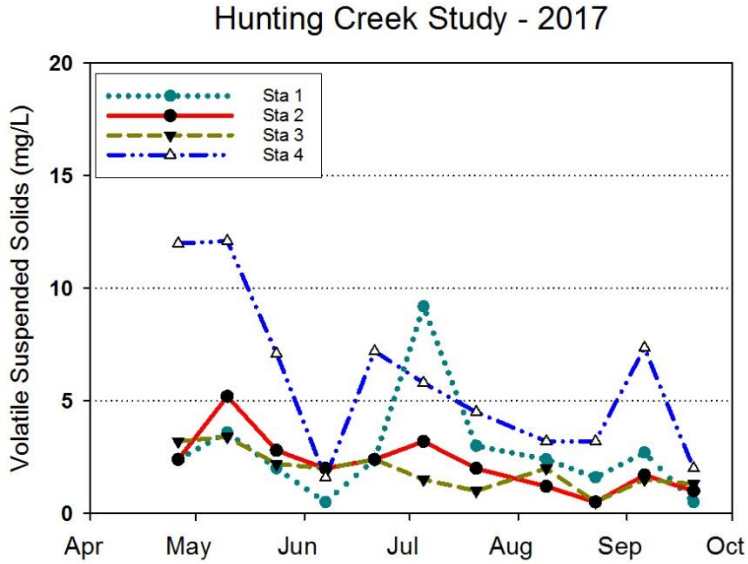

Volatile suspended solids (VSS) is determined by taking the filters used for TSS and then ashing them to combust (volatilize) the organic matter. The organic component is then determined by difference. VSS is a measure of organic solids in a water sample. These organic solids could be bacteria, algae, or detritus. Origins include sewage effluent, algae growth in the water column, or detritus produced within the waterbody or from tributaries. In summer in Gunston Cove a chief source is algal (phytoplankton) growth.

Figure 31. Volatile Suspended Solids (mg/L). AlexRenew Lab Data. Month tick is at first day of month.

C. Physico-chemical Parameters: Tributary Stations – 2017

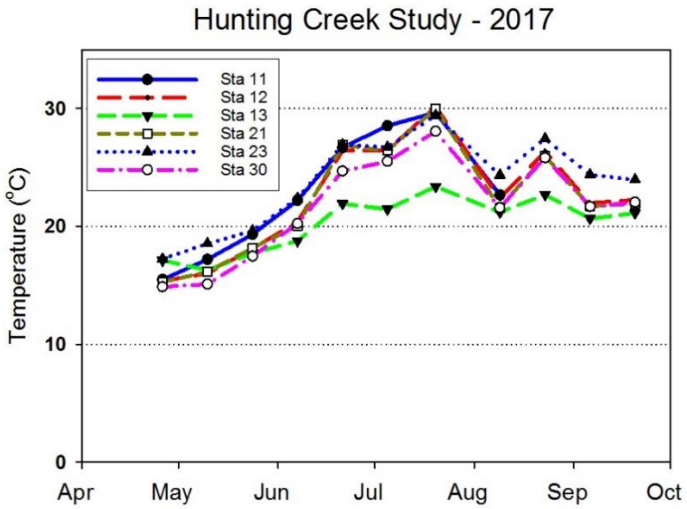

Figure 32. Water Temperature (°C). GMU Field Data. Month tick is at first day of month.

Water quality data for the tributary stations was combined into a series of graphs by parameter. Temperatures at almost all stations closely followed air temperatures (Figure 32). The most obvious exception was AR13 which exhibited lower temperatures during most of the year. The water at AR13 is just emerging from underground storm sewers and is buffered from the higher air temperatures. Specific conductance was generally in the 400-600 uS/cm range (Figure 33). Higher values were observed at AR12, AR21, and AR30 in early May following a major flow event. All of these stations are on the mainstem of Cameron Run above Telegraph Rd. and they tracked each other closely the whole time. AR11, the outlet of Cook Lake, was generally lowest in specific conductance. The lake was drained late in 2017.

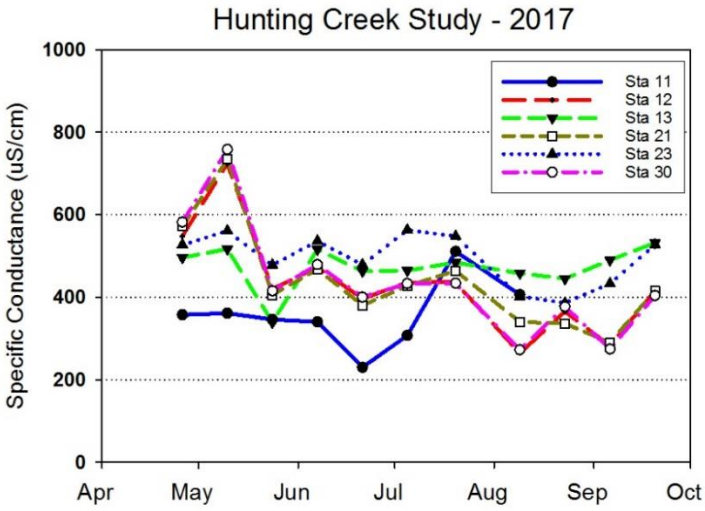

Figure 33. Specific Conductance (uS/cm). GMU Field Data. Month tick is at first day of month.

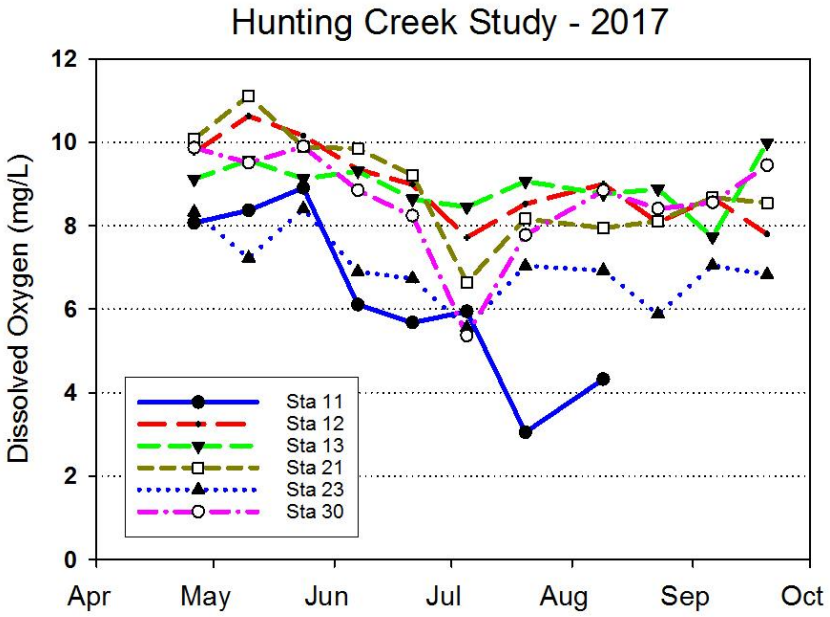

Figure 34. Dissolved Oxygen (mg/L) GMU Field Data. Month tick is at first day of month.

Dissolved oxygen (mg/L) in the tributaries exhibited a clear seasonal pattern that was probably reflective of changes in DO saturation with temperature (Figure 34). The most obvious departure were the very low values observed at AR11, the outlet of Cook Lake, in late July and early August. When expressed in percent saturation, most of the seasonal pattern disappeared (Figure 35). The very low values at AR11 remain and the other obvious effect at all stations was a clear depression in values in early July. This was probably due to a significant runoff event preceding sampling that day.

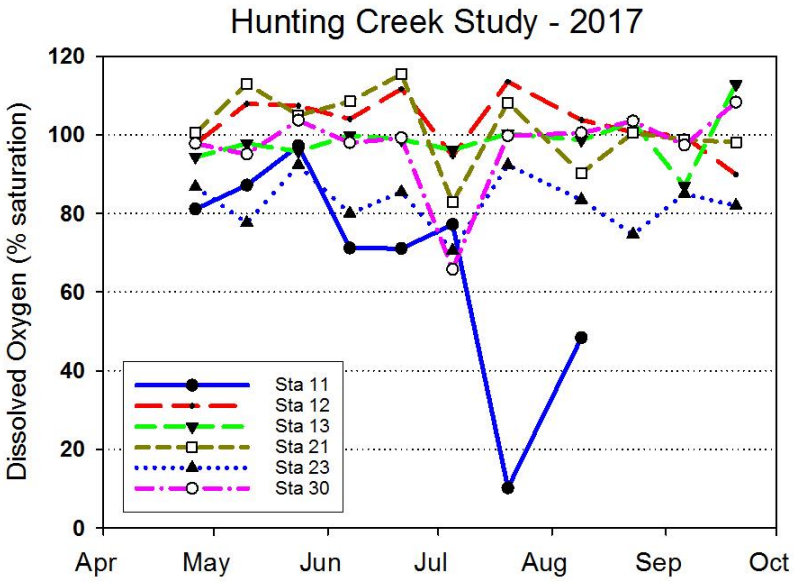

Figure 35. Dissolved Oxygen (% saturation) GMU Field Data. Month tick is at first day of month.

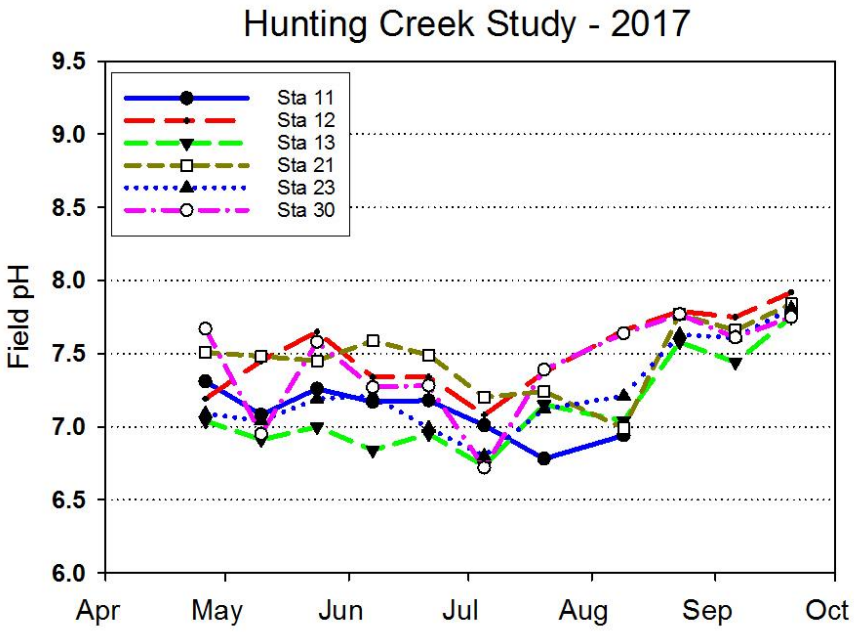

Figure 36. Field pH. GMU Field Data. Month tick is at first day of month.

Field pH was consistently in the 6.8 to 7.8 range at tributary stations (Figures 36 and 37). AR12 exhibited one value above 8.0 in early July. These values are clearly in the range supportive of aquatic life. Field pH showed a trend of slowly rising values in August and September.

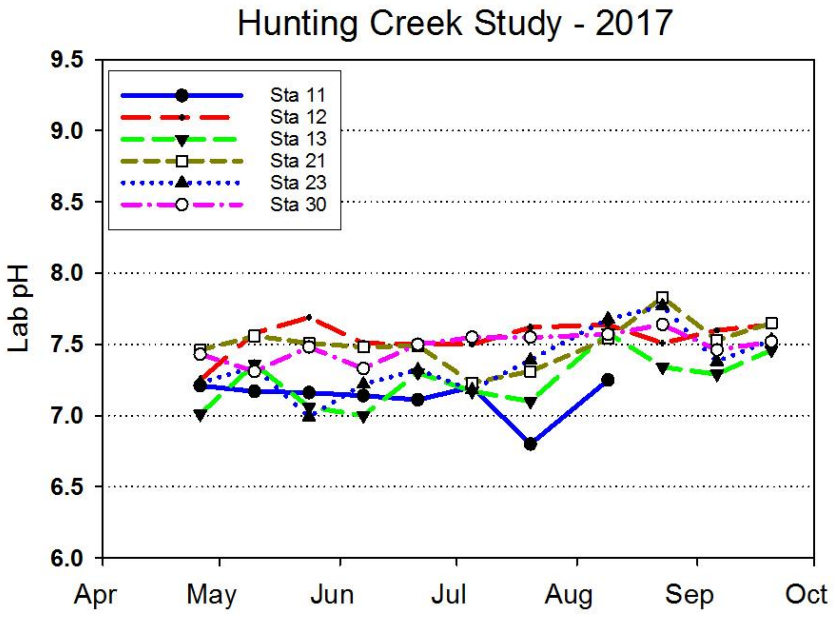

Figure 37. Lab pH. Alex Renew Lab Data. Month tick is at first day of month.

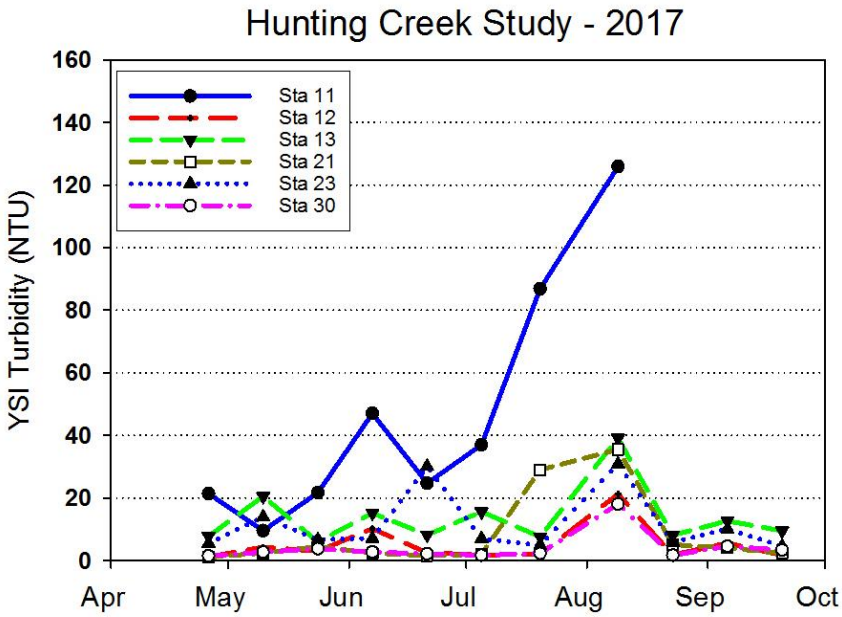

Figure 38. YSI Turbidity. GMU Field Data. Month tick is at first day of month.

Turbidity values were generally fairly low (<20 units) at all tributary stations (Figure 38). The major exception was AR11 at the outlet of Cook Lake. Construction work was occurring at Cook Lake during the summer of 2017 and apparently was responsible for the elevated values. At the other stations there was a distinct increase in early August following a major flow event. Chlorophyll was generally very low at all stations except Cook Lake where algae grew fairly abundantly (Figure 39). AR21 also showed some elevated readings being in Cameron Run just downstream of the Cook Lake outlet.

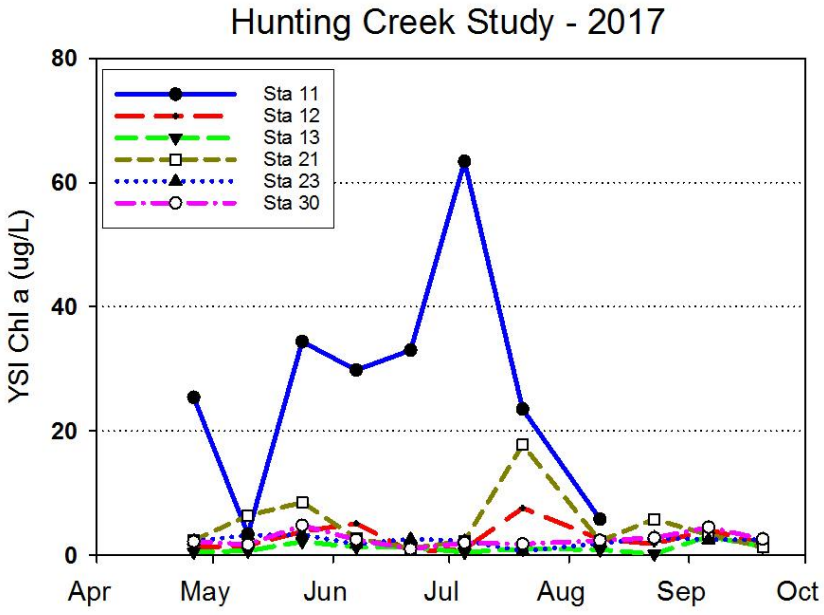

Figure 39. YSI Chlorophyll a. GMU Field Data. Month tick is at first day of month.

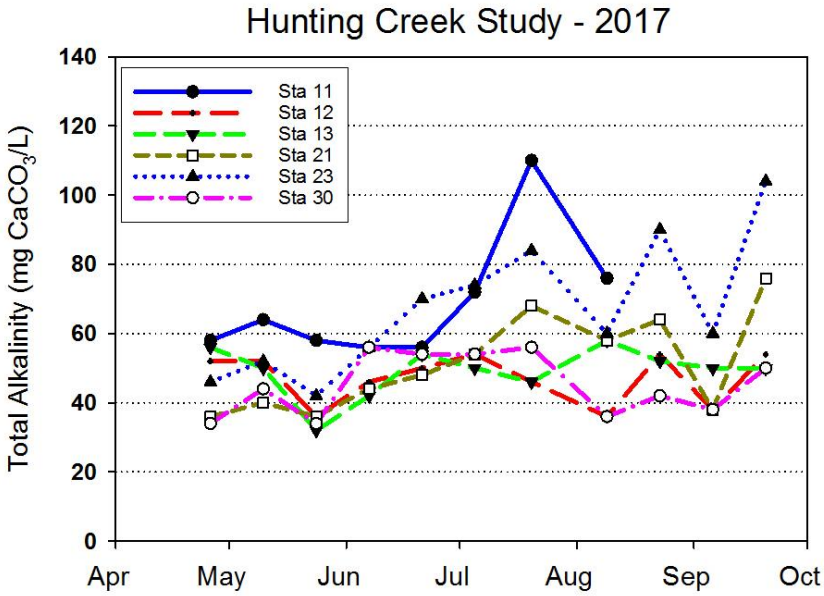

Figure 40. Total Alkalinity (mg/L as $CaCO_3$) AlexRenew Lab Data. Month tick is at first day of month.

Total alkalinity was generally in the 40-60 mg/L range (Figure 40). There was a general trend of increasing values at AR23 over the study period interrupted in early August and early September by flow events which diluted the ions. Chloride levels declined seasonally at most stations following a spike in early May at the Cameron Run mainstem stations (Figure 41). AR13 (Hoofs Run) did not exhibit a seasonal pattern.

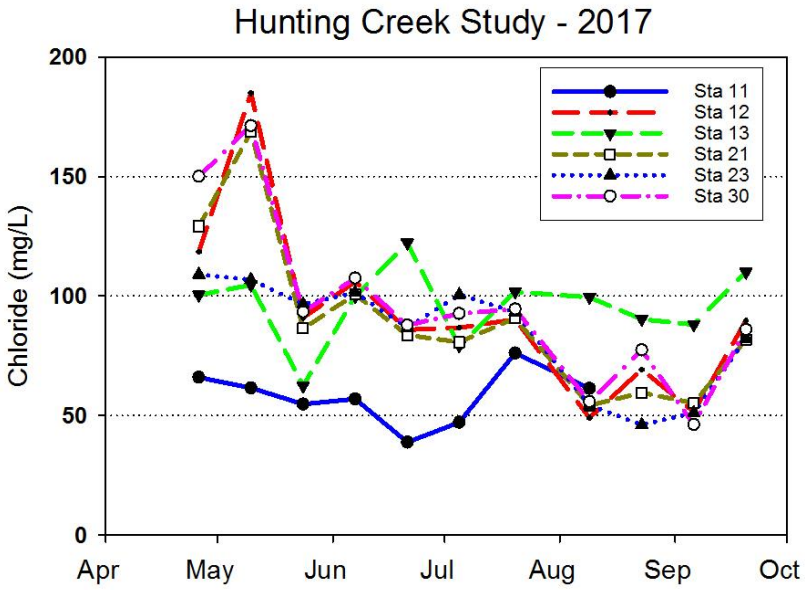

Figure 41. Chloride (mg/L) AlexRenew Lab Data. Month tick is at first day of month.

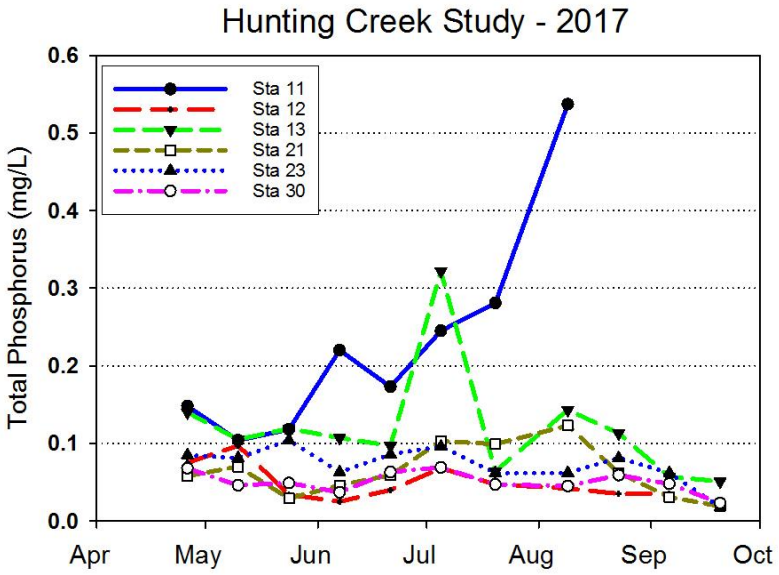

Figure 42. Total Phosphorus (mg/L) AlexRenew Lab Data. Month tick is at first day of month.

Total phosphorus levels were generally relatively low at most tributary stations and did not vary much seasonally (Figure 42). Highest and most variable values were observed at Lake Cook outlet and Hooff Run outlet. Ortho phosphorus levels hovered around 0.02 mg/L (Figure 43).

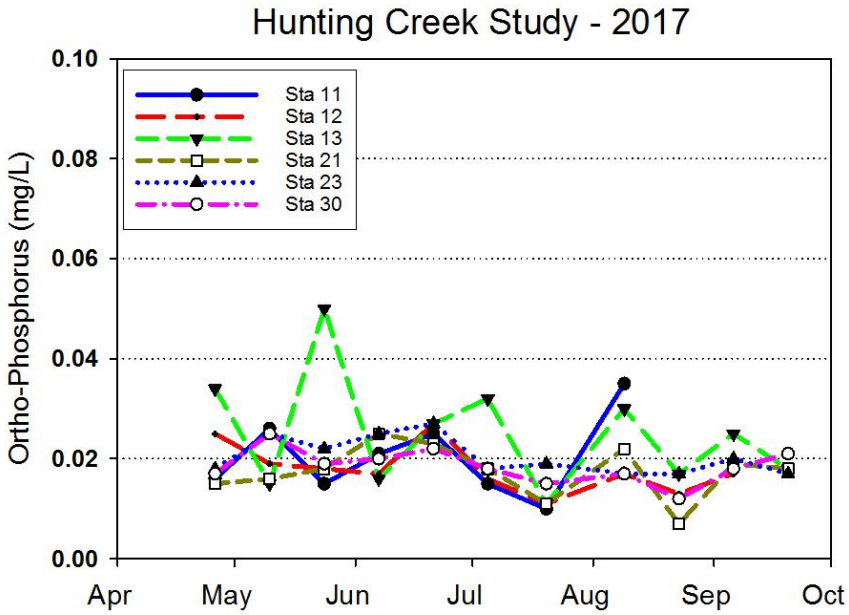

Figure 43. Ortho-Phosphorus (mg/L) AlexRenew Lab Data. Month tick is at first day of month.

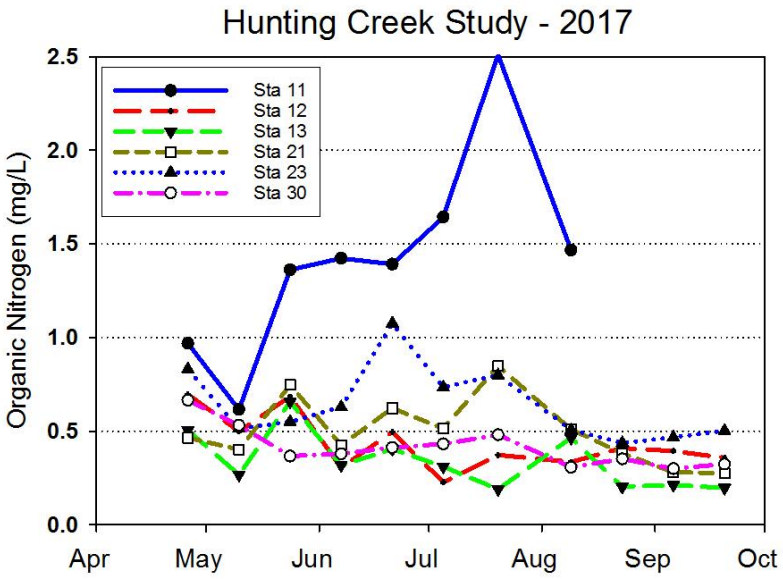

Figure 44. Organic Nitrogen (mg/L) AlexRenew Lab Data. Month tick is at first day of month.

Tributary levels of organic nitrogen are depicted in Figure 44. At AR21 and AR23 values hovered between 0.5 mg/L through July whereas at most of the other stations values were 0.2-0.5 mg/L. Organic nitrogen in the Lake Cook outlet was highly elevated. Ammonia nitrogen values were quite low (<0.2 mg/L) over most of the period at all stations (Figure 45). However, in late July and August values were very high coming out of Lake Cook (AR11) and downstream of its outlet in Cameron Run (AR21).

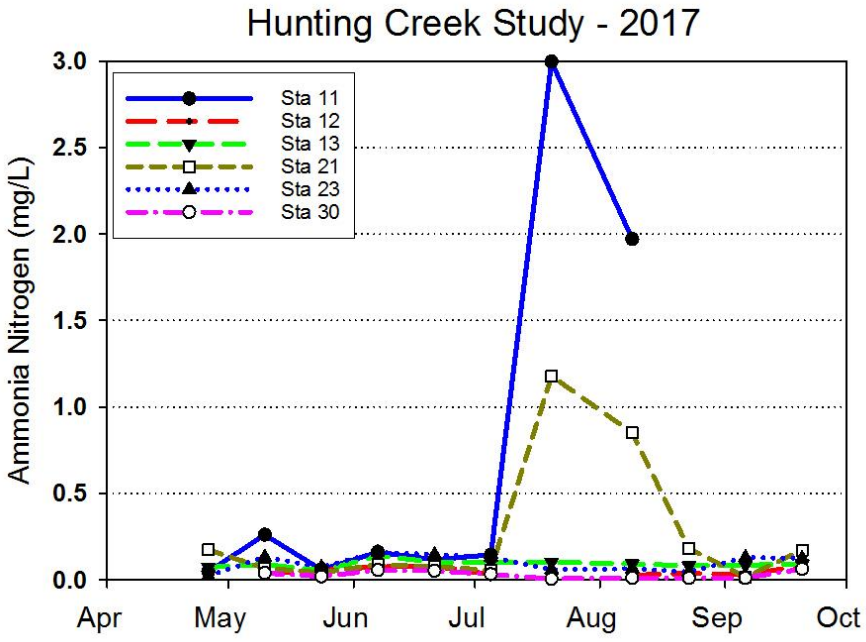

Figure 45. Ammonia Nitrogen (mg/L) AlexRenew Lab Data. Month tick is at first day of month.

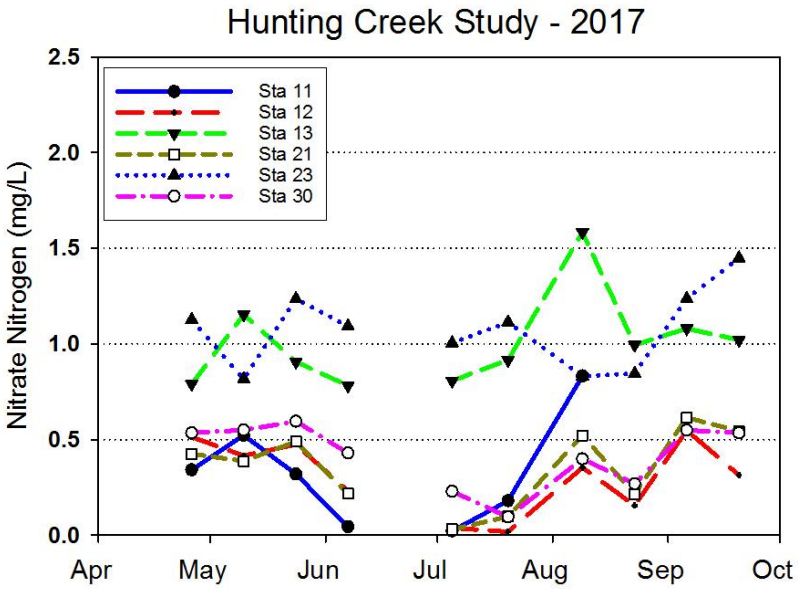

Figure 46. Nitrate Nitrogen (mg/L) AlexRenew Lab Data. Month tick is at first day of month.

Nitrate nitrogen values exhibited clear spatial variation (Figure 46). Values were elevated at AR23 and AR13 but probably for different reasons. AR13, with values hovering around 1 mg/L, is primarily runoff from urbanized areas of Alexandria and so the nitrogen at AR13 probably originates from nonpoint sources. AR23 is downstream from the Alex Renew outfall which probably accounts for the elevated levels there. Nitrite nitrogen was generally quite low at all stations (Figure 47).

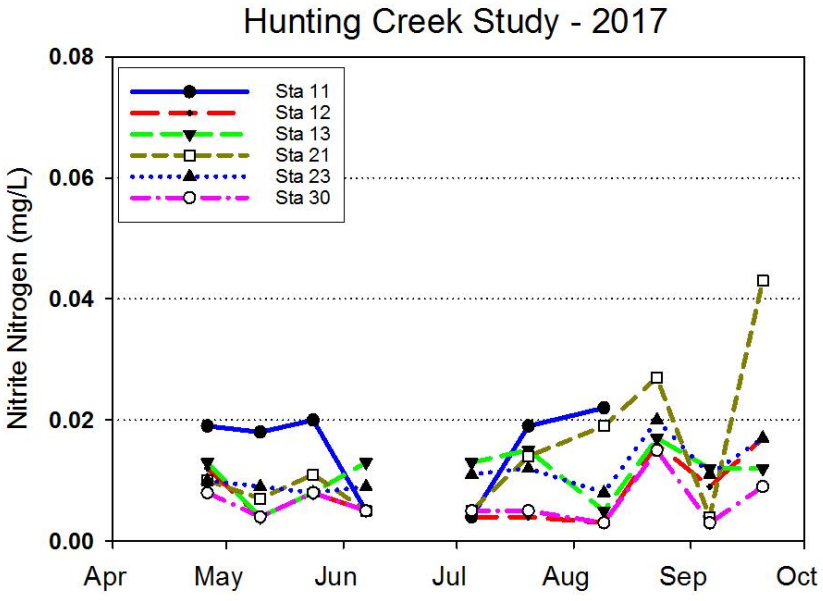

Figure 47. Nitrite Nitrogen (mg/L) AlexRenew Lab Data. Month tick is at first day of month.

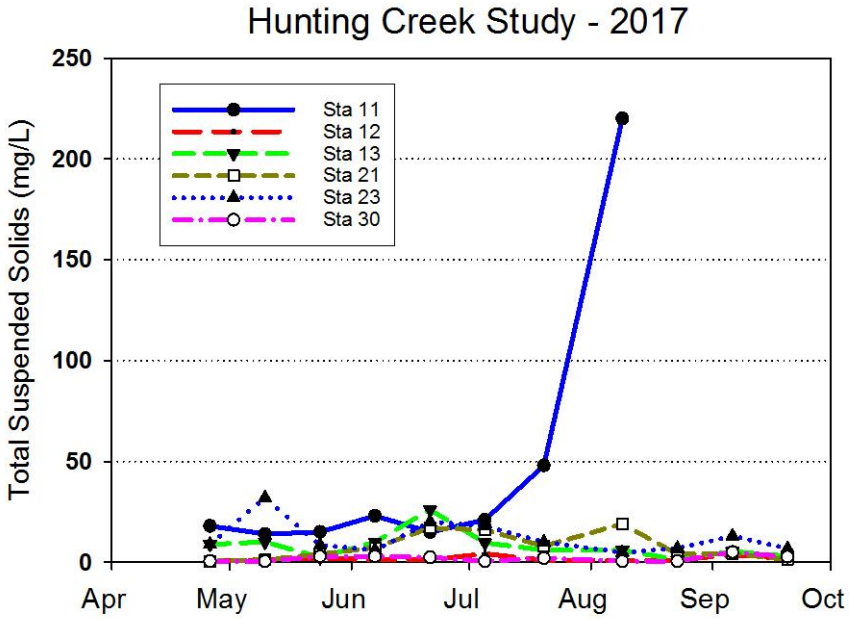

Figure 48. Total Suspended Solids (mg/L) AlexRenew Lab Data. Month tick is at first day of month.

Total suspended solids concentrations at tributary stations are shown in Figure 48. TSS was quite low (<20 mg/L) at most stations for most of the year. The exception, again was Lake Cook which had extremely high values in early September. Similar trends were observed volatile suspended solids (Figure 49) with some higher values also observed at AR23.

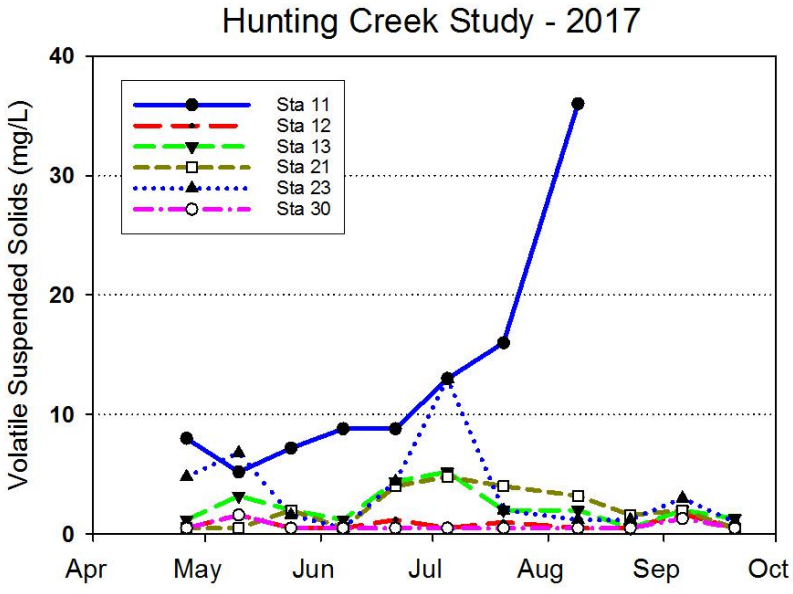

Figure 49. Volatile Suspended Solids (mg/L) AlexRenew Lab Data. Month tick is at first day of month.

D. Phytoplankton -2017

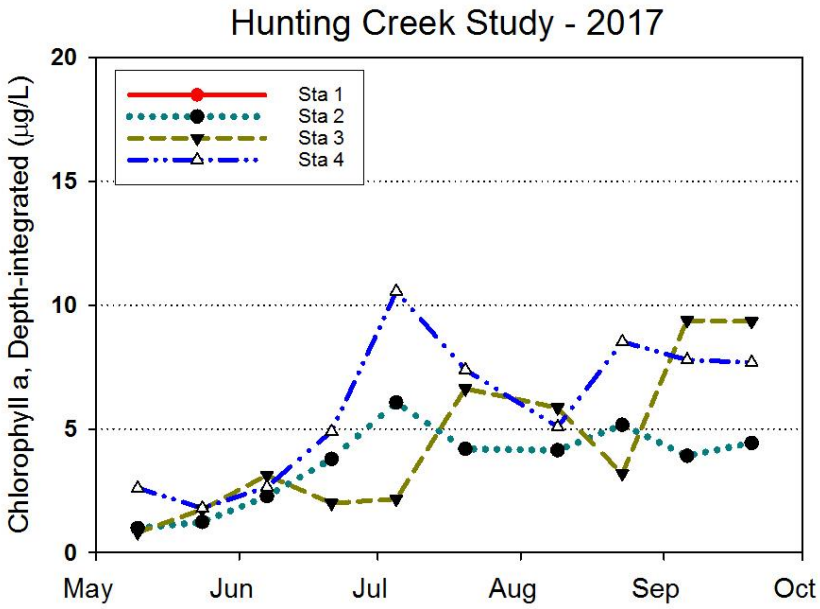

Chlorophyll *a* is a measure of the amount of algae growing in the water column. These suspended algae are called phytoplankton, meaning "plant wanderers". In addition to the true algae (greens, diatoms, cryptophytes, etc.) the term phytoplankton includes cyanobacteria (sometimes known as "blue-green" algae). Both depth-integrated and surface chlorophyll values are measured due to the capacity of phytoplankton to aggregate near the surface under certain conditions.

Figure 50. Chlorophyll *a* (µg/L). Depth-integrated. GMU Lab Data. Month tick is at the first day of month.

Chlorophyll *a* began the year at low concentrations (<3 ug/L) at all stations (Figures 50&51). At AR4 there was an increase in late June and early July which carried values to 10 ug/L. Another peak was found in late August. At AR1, AR2 and AR3 chlorophyll mainly was less than 5 mg/L, but increased above that level on at least one date. Depth-integrated samples were not available for the April sampling.

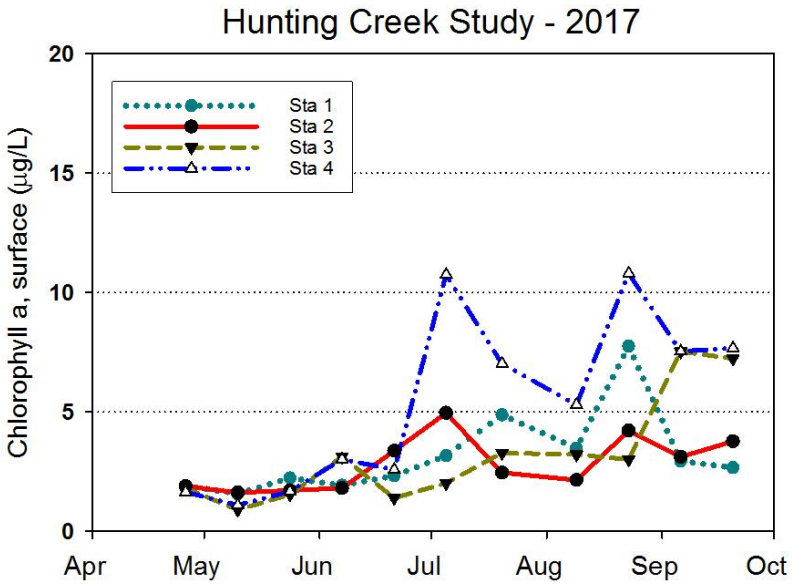

In the tidal freshwater Potomac generally, there is very little difference in surface and depth-integrated chlorophyll levels because tidal action keeps the water well-mixed which overcomes any potential surface aggregation by the phytoplankton. Summer chlorophyll concentrations above 30 ug/L are generally considered characteristic or eutrophic conditions.

Figure 51. Chlorophyll *a* (µg/L). Surface. GMU Lab Data. Month tick is at first day of month.

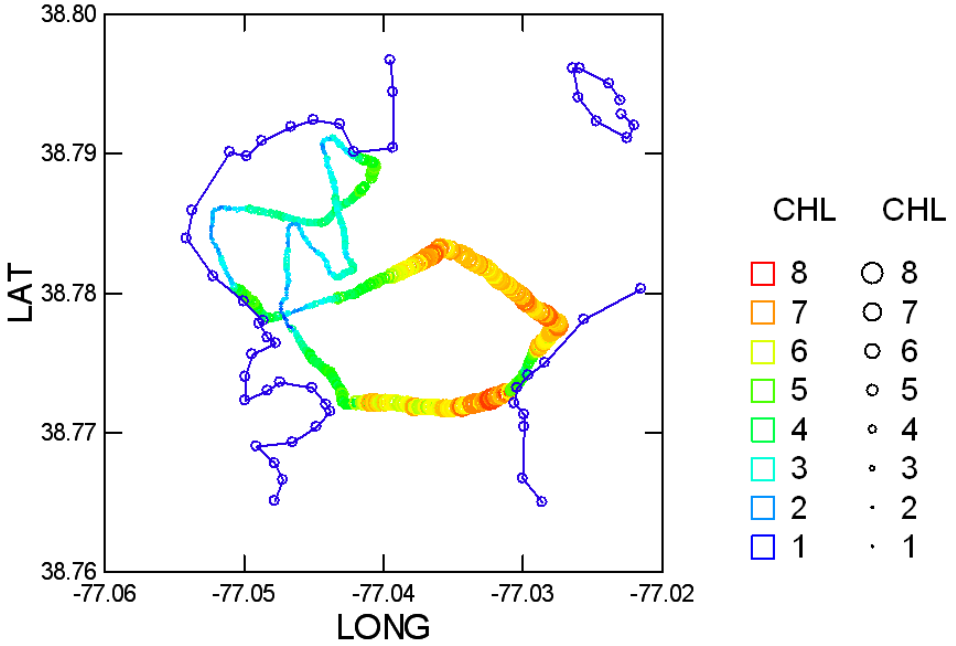

Figure 52a. Water Quality Mapping. July 12, 2017. Chlorophyll YSI (mg/L).

On the July sampling date a distinct spatial pattern was observed in chlorophyll with higher values in the river mainstem and lower levels in the Hunting Creek embayment (Figure 52a). The values observed were consistent with the extracted chlorophyll readings at AR2, AR3, and AR4. On August 10, some very high values were observed at one site in the embayment which may have been due to algae knocked off of the SAV (Figure 52b).

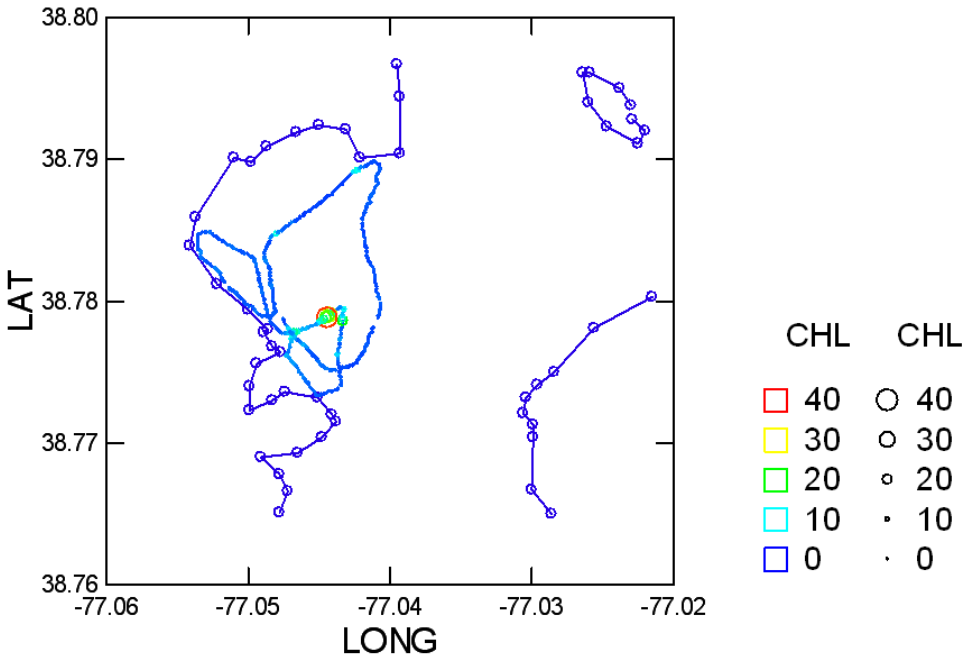

Figure 52b. Water Quality Mapping. August 10, 2017. Chlorophyll YSI (mg/L).

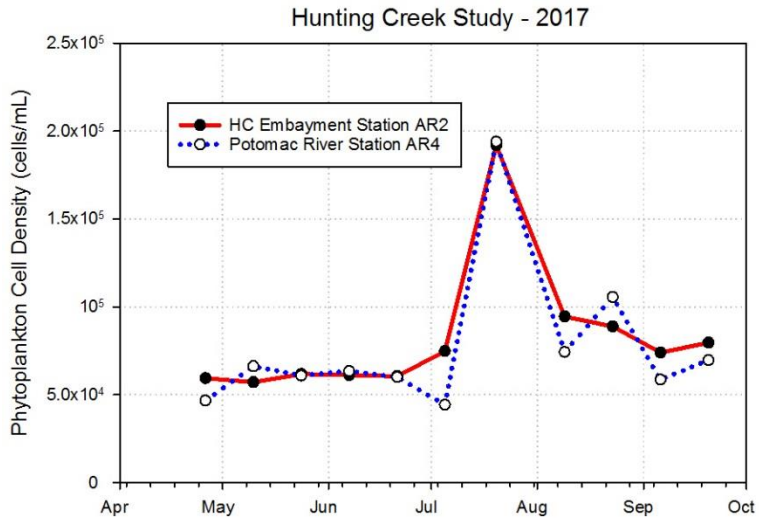

Phytoplankton cell density provides a measure of the number of algal cells per unit volume. This is a rough measure of the abundance of phytoplankton, but does not discriminate between large and small cells. Therefore, a large number of small cells may actually represent less biomass (weight of living tissue) than a smaller number of large cells. However, small cells are typically more active than larger ones so cell density is probably a better indicator of activity than of biomass. The smaller cells are mostly cyanobacteria.

Figure 53. Phytoplankton Density (cells/mL).

Phytoplankton density was quite similar between the two stations and over all dates except that in late July, the values were much higher than on other dates (Figure 53). Total biovolume exhibited somewhat more variability between dates and stations (Figure 54). In this case there was a very high biovolume calculated in early July at AR4.

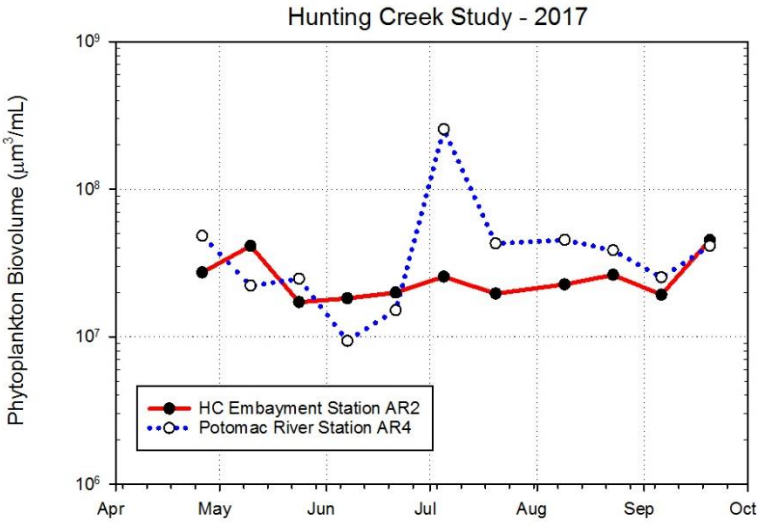

The volume of individual cells of each species is determined by approximating the cells of each species to an appropriate geometric shape (e.g. sphere, cylinder, cone, cube, etc.) and then making the measurements of the appropriate dimensions under the microscope. Total phytoplankton biovolume (shown here) is determined by multiplying the cell density of each species by the biovolume of each cell of that species. Biovolume accounts for the differing size of various phytoplankton cells and is probably a better measure of biomass. However, it does not account for the varying amount of water and other nonliving constituents in cells.

Figure 54. Phytoplankton Biovolume (um^3/mL).

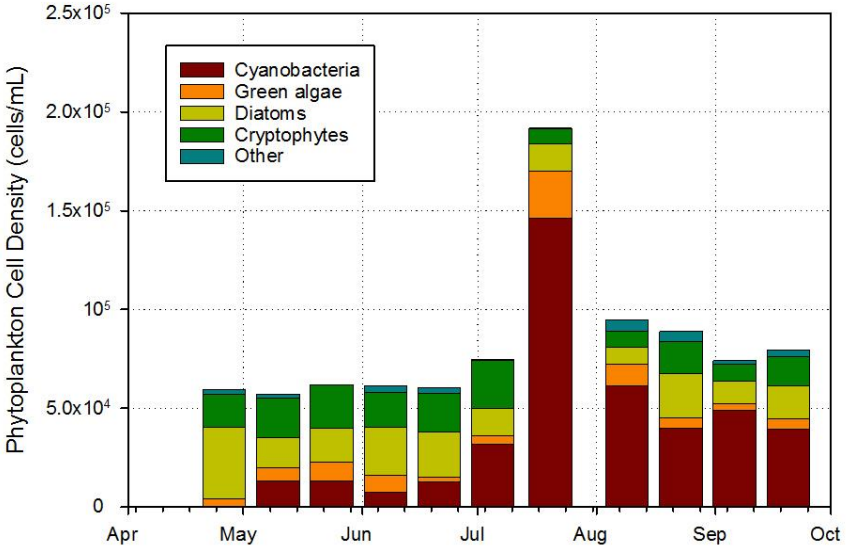

Total phytoplankton cell density can be broken down by major group. **Cyanobacteria** are sometimes called "blue-green algae". **Other** includes euglenoids and dinoflagellates. Due to their small size cyanobacteria typically dominate cell density numbers. Their numbers are typically highest in the late summer reflecting an accumulation of cells during favorable summer growing conditions.

Figure 55. Phytoplankton Density by Major Group (cells/mL). Hunting Creek.

Phytoplankton cell density was distributed fairly evenly among three major groups (cyanobacteria, diatoms, and cryptophytes) at both stations (Figures 55&56). The major exception to this was late July when cyanobacteria were strongly dominant at both stations and responsible for the above-normal values on this date.

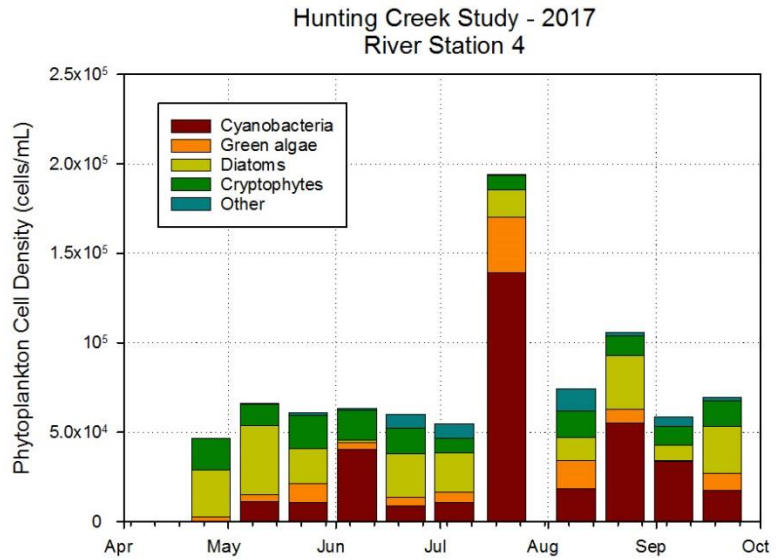

In the river cyanobacteria normally follow similar patterns as in the embayments, but may attain lower abundances. This is probably due to the deeper water column which leads to lower effective light levels and greater mixing. Other groups such as diatoms and green algae tend to be more important on a relative basis than in the embayments.

Figure 56. Phytoplankton Density by Major Group (cells/mL). River.

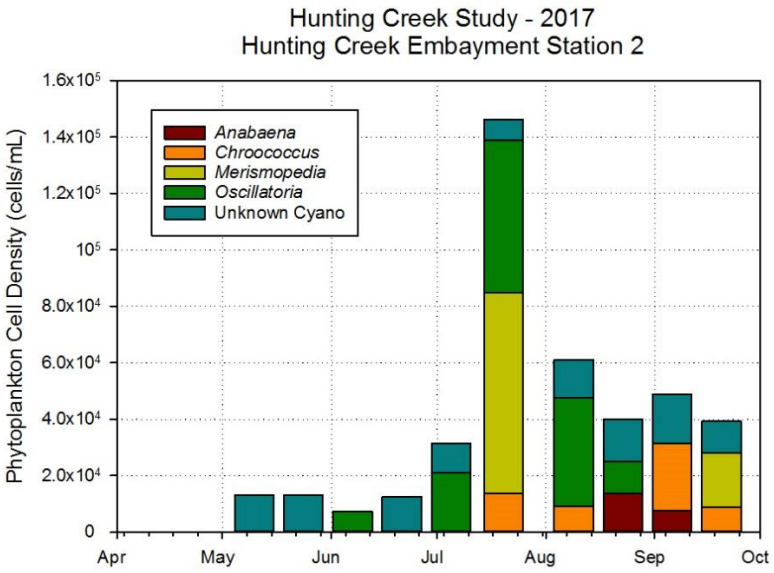

The dominant cyanobacteria on a numerical basis were:
- *Oscillatoria* – a filament with disc-like cells
- *Merismopedia* -- a flat plate of cells in a rectangular arrangement
- *Anabaena* – a filament with bead-like cells & heterocysts
- *Chroococcus* – individual spherical cells
- Unknown cyanobacterium About 2 µm

Figure 57. Phytoplankton Density by Dominant Cyanobacteria (cells/mL). Hunting Creek.

The large peak in cyanobacteria density was attributable to *Oscillatoria* and *Merismopedia* at both stations (Figure 57&58). *Anabaena*, a nitrogen-fixing genus was important in late August and September at both stations.

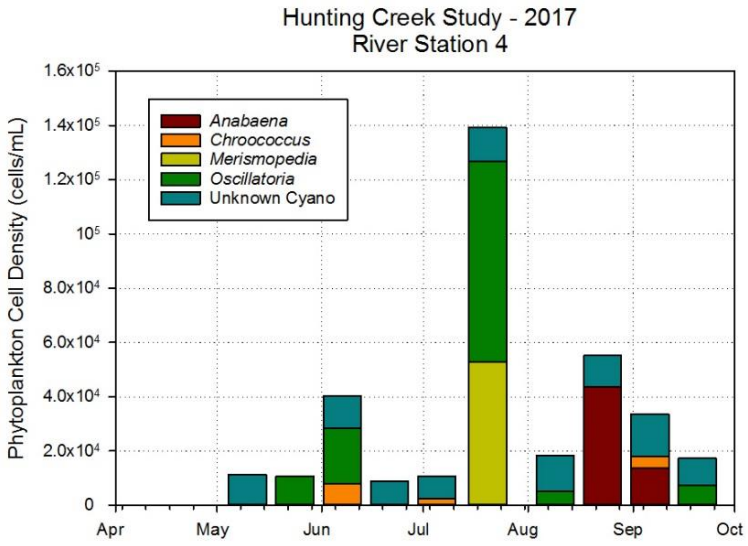

Oscillatoria

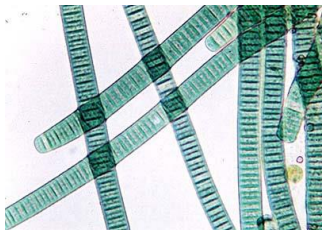

Microcystis

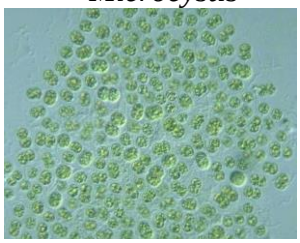

Figure 58. Phytoplankton Density by Dominant Cyanobacteria (cells/mL). River.

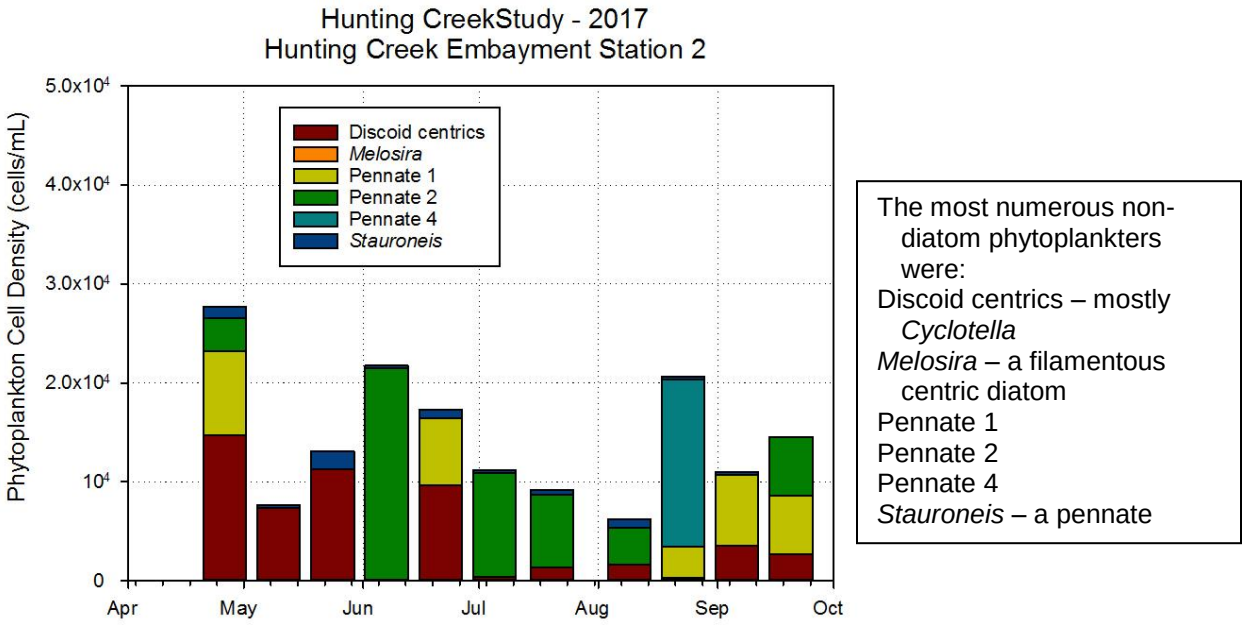

Figure 59. Phytoplankton Density (#/mL) by Dominant Diatom Taxa. Hunting Creek.

Discoid centrics were the most important diatoms in spring and also in late June (Figure 59). Pennat 2 was dominant in early June and July and early August. Pennate 5 was dominant in late August. At the river station AR4 discoid centrics were again dominant in spring, then in July and finally again in late September (Figure 60). Melosira, a filamentous diatom, was notable dominant in early July.

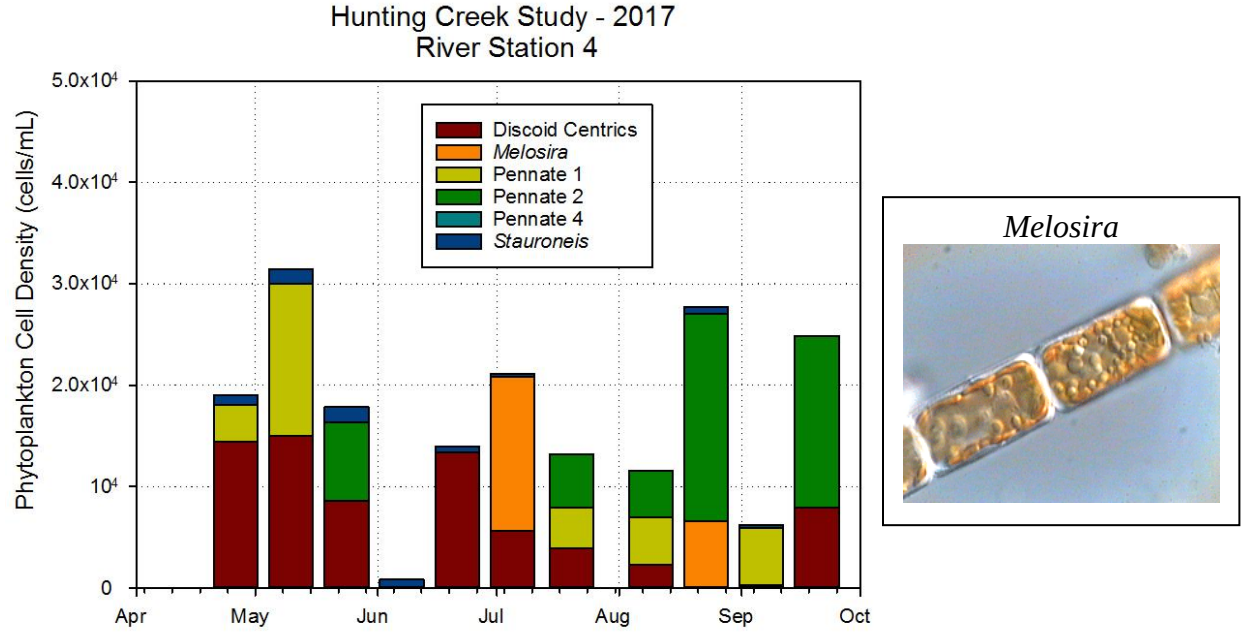

Figure 60. Phytoplankton Density (#/mL) by Dominant Diatom Taxa. River.

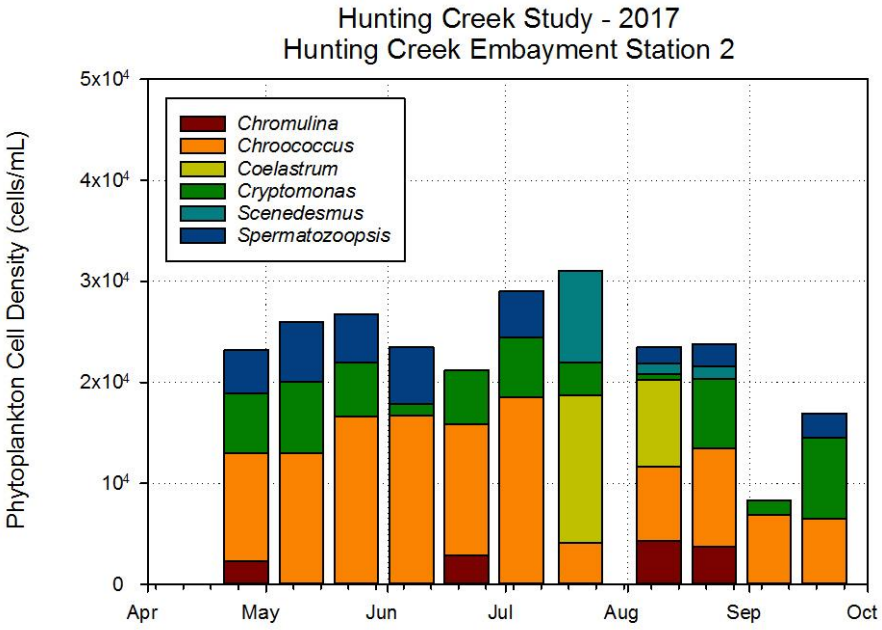

The most numerous other phytoplankton were:

- *Cryptomonas* – an ellipsoidal, flagellated unicell
- *Chroomonas* – a flagellated cryptomonad unicell
- *Spermatozoopsis* – flagellated green unicell
- *Chromulina* – a flagellated chrysophyte
- *Scenedesmus* – a green alga
- *Coelastrum* – a green alga

Figure 61. Phytoplankton Density (#/mL) by Dominant Other Taxa. Hunting Creek.

Phytoplankton species that were neither cyanobacteria nor diatoms were grouped together as "other" for these graphs; these included most numerous taxa of green algae, cryptophytes, euglenoids, and dinoflagellates. At both stations the cryptophytes *Cryptomonas* and *Chroomonas* were consistently the most numerous (Figure 61&62). The green alga *Coelastrum* was important in late July and early August at both stations. Another green alga *Scendesmus* was numerous in late July at both stations.

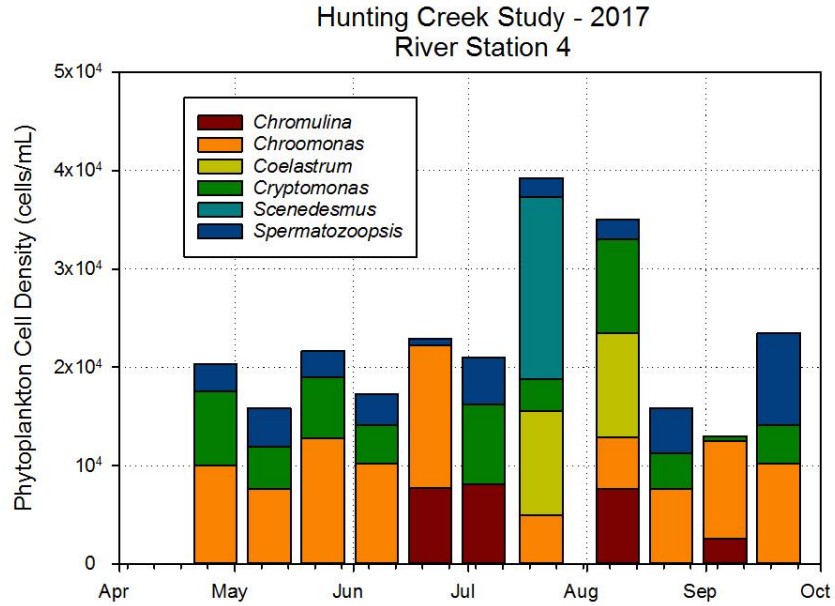

Figure 62. Phytoplankton Density (#/mL) by Dominant Other Taxa. River.

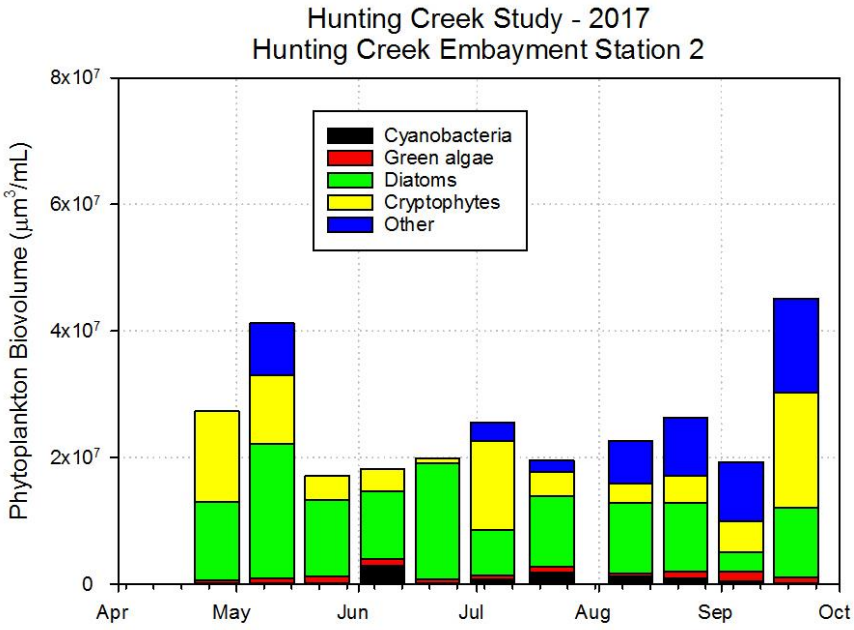

Total phytoplankton biovolume can be broken down into groups:

- **Cyano** – cyanobacteria ("blue-green" algae)
- **Greens** – green algae
- **Diatoms** – includes both centric and pinnate
- **Cryptos** – cryptophytes
- **Other** – includes euglenoids, chrysophytes, and dinoflagellates

Figure 63. Phytoplankton Biovolume (um^3/mL) by Major Groups. Hunting Creek.

At AR 2 in Hunting Creek diatoms were dominant in biovolume in most samples (Figure 63). The highest biovolumes were in early May and late September. Cryptophytes and Other algae were important on some dates. In the river, diatoms were overwhelming in their dominance on many dates (Figure 64). However, in August and September Other algae were generally dominant.

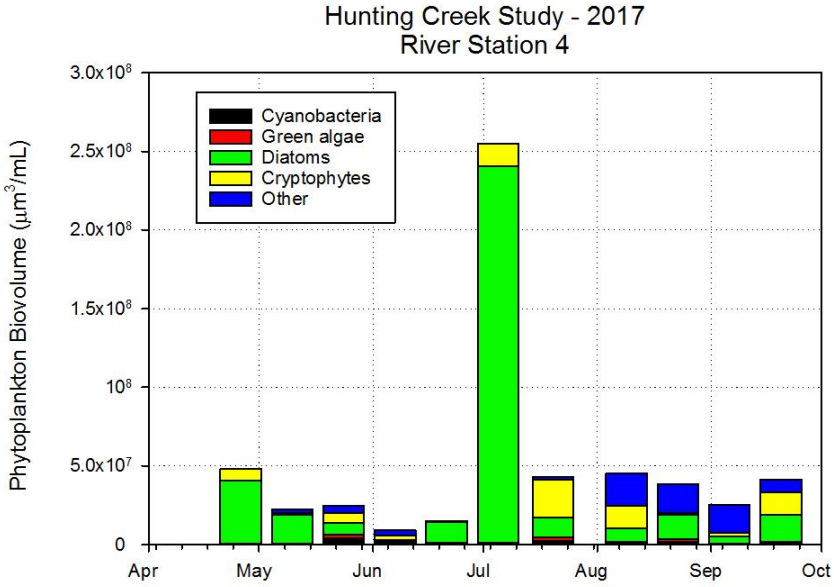

While dominating cell density, cyanobacteria typically make up a much smaller portion of phytoplankton biovolume. Diatoms generally are dominant.

Figure 64. Phytoplankton Biovolume (um^3/mL) by Major Groups. River.

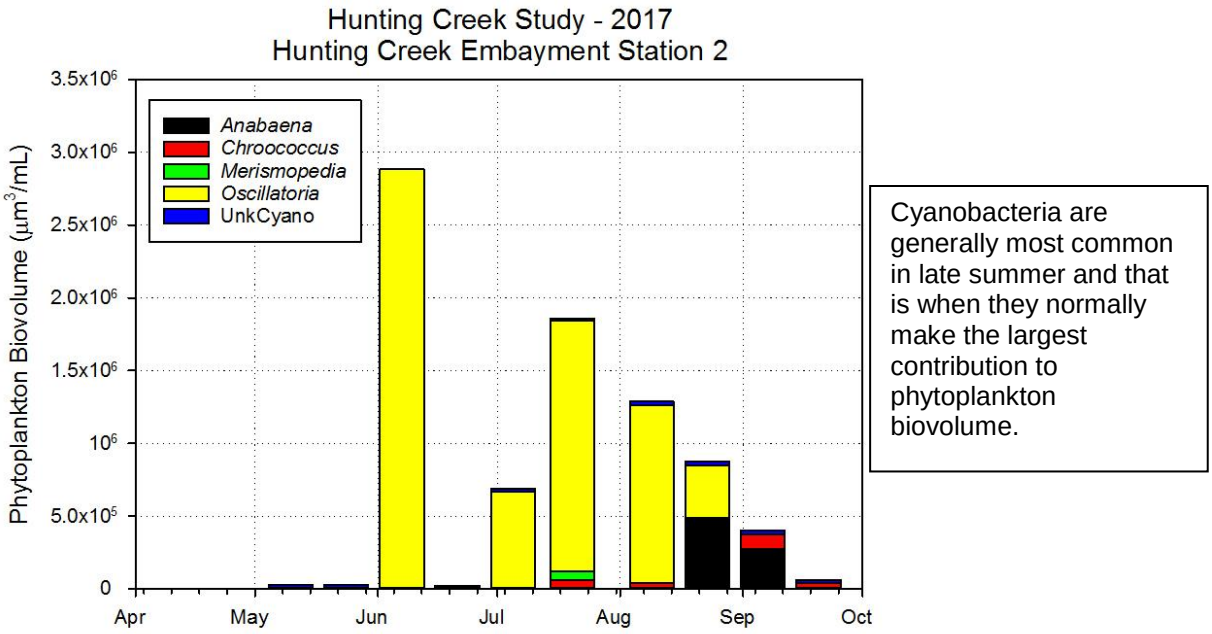

Figure 65. Phytoplankton Biovolume (um³/mL) by Cyanobacteria Taxa. Hunting Creek.

In Hunting Creek *Oscillatoria* was most consistently observed cyanobacterium being very abundant in early June (Figure 65). *Oscillatoria* was generally the most abundant cyanobacterium at the River mainstem station during summer, but a large peak of *Anabaena* was observed in late August and early September (Figure 66).

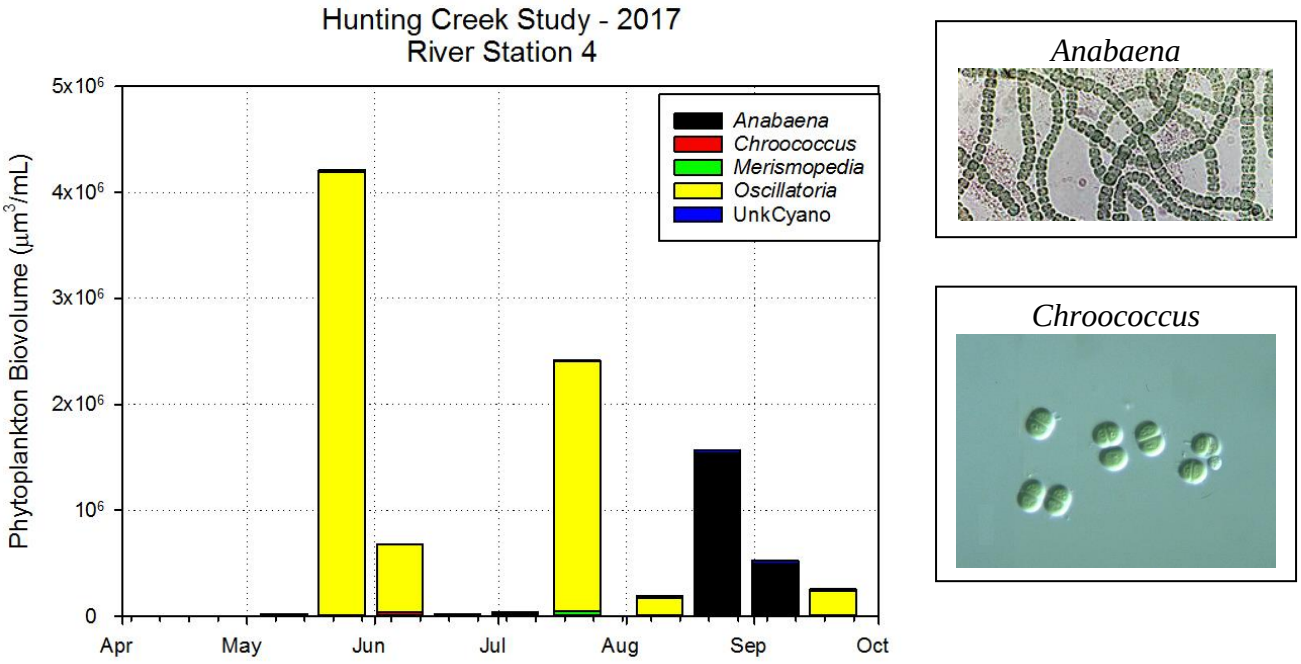

Figure 66. Phytoplankton Biovolume (um³/mL) by Cyanobacterial Taxa. River.

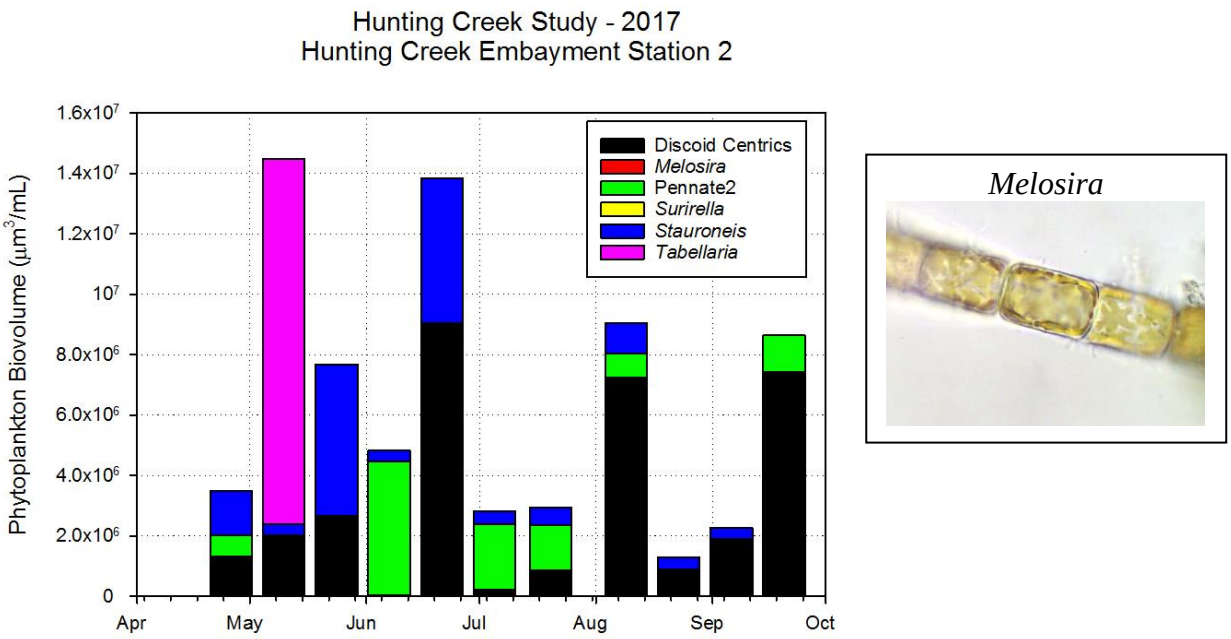

Figure 67. Phytoplankton Biovolume (um^3/mL) by Dominant Diatom Taxa. Hunting Creek.

Tabellaria was the overwhelming dominant in biovolume in early May (Figure 67).On several other dates, discoid centrics, Pennate 2, and *Stauroneis* were important. In the river, *Melosira* was dominant in early July with discoid centrics being substantial on most dates (Figure 68).

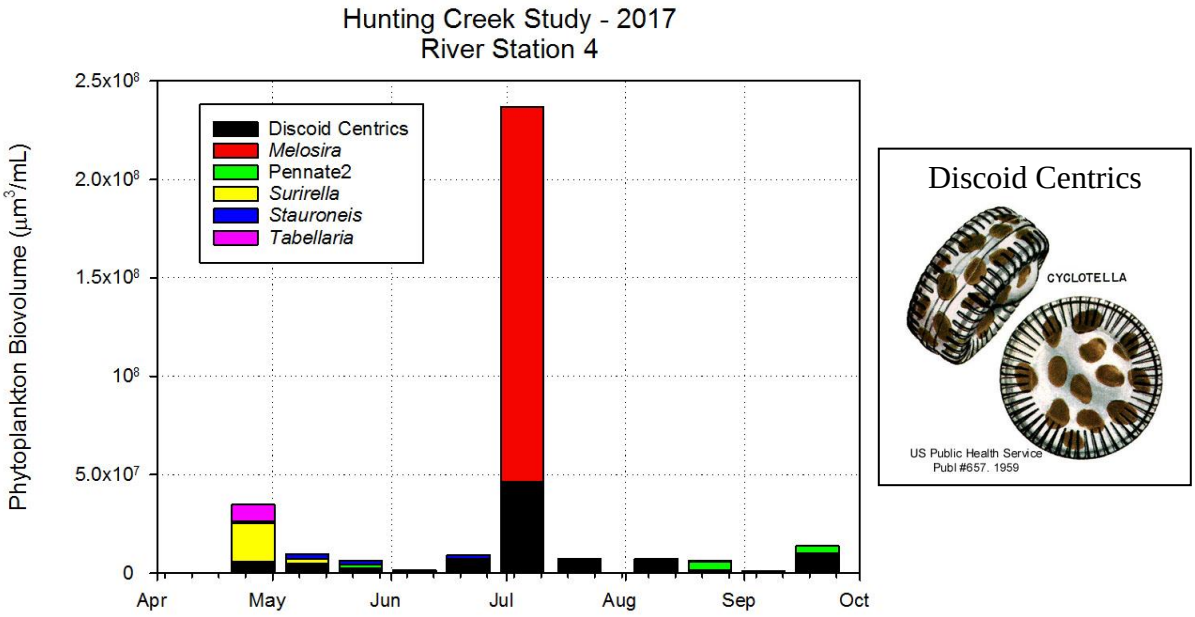

Figure 68. Phytoplankton Biovolume (um^3/mL) by Dominant Diatom Taxon. River.

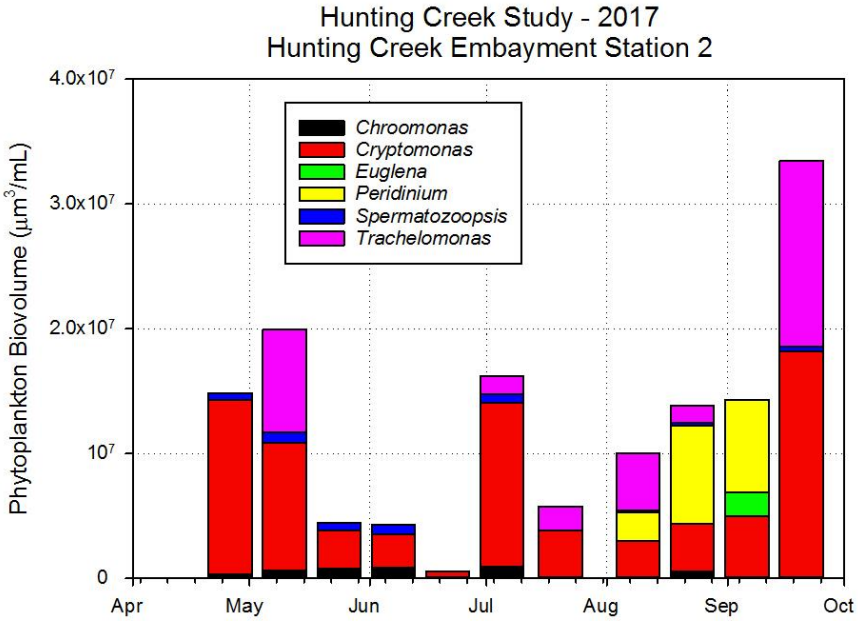

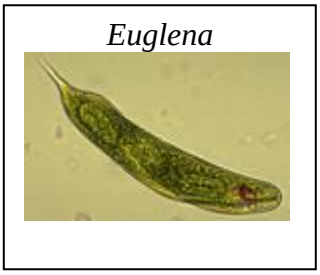

Figure 69. Phytoplankton Biovolume (um³/mL) by Dominant Other Taxa. Hunting Creek.

The cryptophyte *Cryptomonas* was a strong contributor to biovolume in Hunting Creek on all dates (Figure 69). The euglenoid *Trachelomonas* was dominant in early May and late September. The dinoflagellate *Peridinium* was important in late August and early September. In the river *Cryptomonas* was again dominant on most dates with *Trachelomonas* again being important as well as *Euglena* (Figure 70).

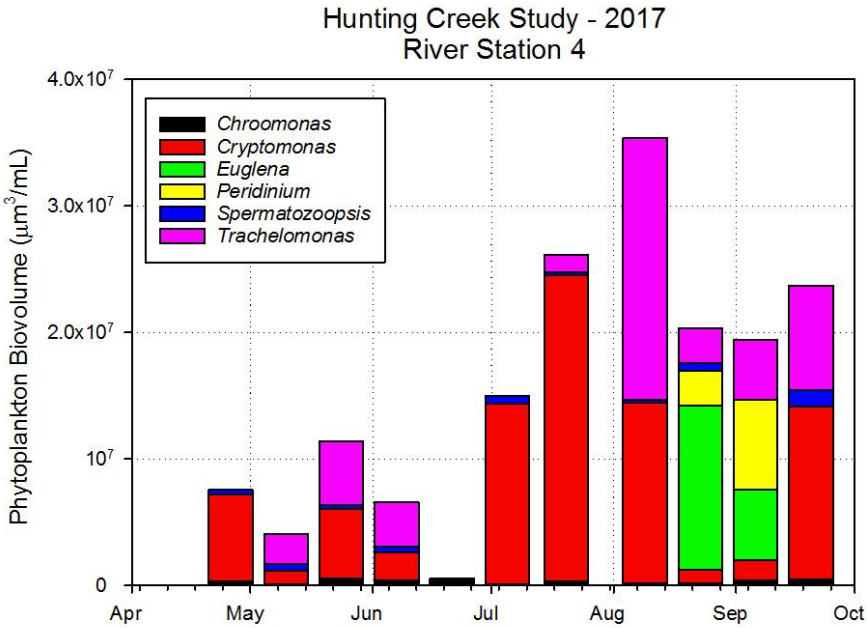

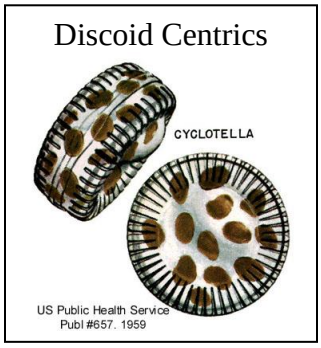

Figure 70. Phytoplankton Biovolume (um³/mL) by Dominant Other Taxon. River.

E. Zooplankton – 2017

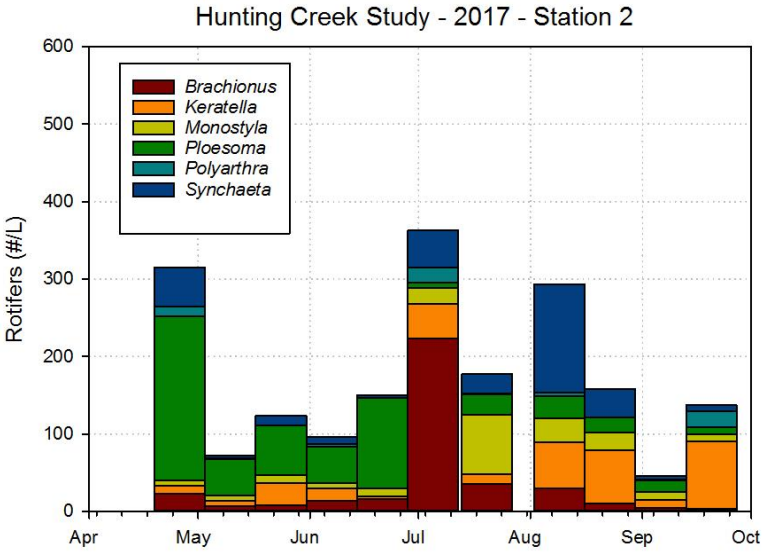

Brachionus (Sta 7, RCJ)

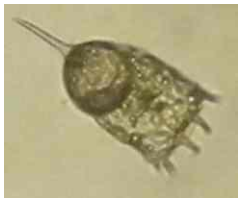

Keratella (Sta 7, RCJ)

Figure 71. Rotifer Density by Dominant Taxa (#/L). Hunting Creek.

In Hunting Creek, rotifers exhibited a peak in late April and again early July (Figure 71). *Ploesoma* dominated from April through June. In early July *Brachionus* increased to dominance. *Polyarthra* and *Keratella* shared dominance for the rest of the year. In the river *Brachionus* and *Keratella* were most important with *Ploesoma* making significant contributions in July (Figure 72).

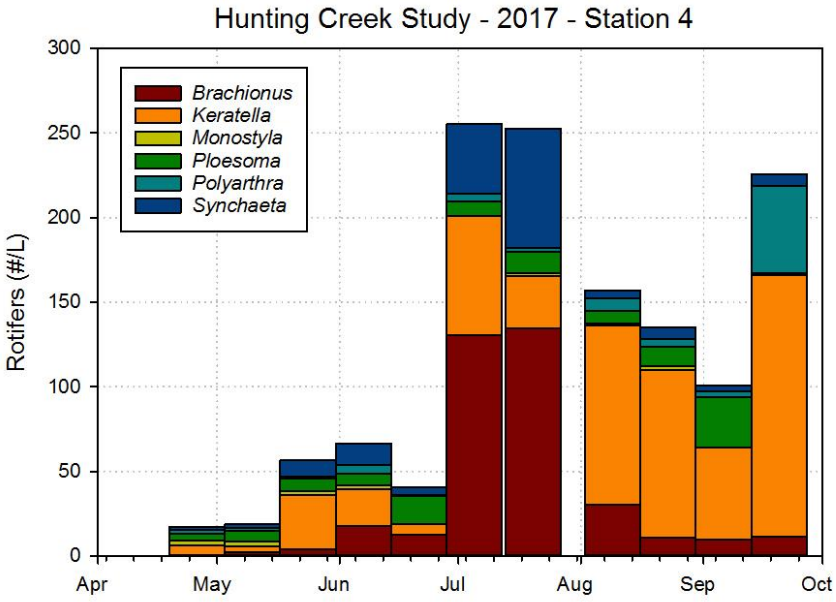

Brachionus (c. 50 um)

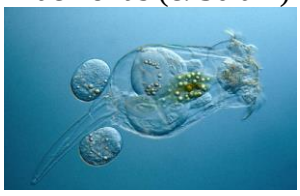

Conochilidae

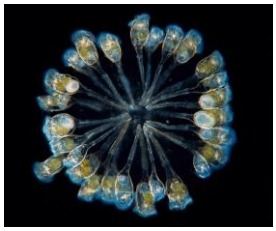

Figure 72. Rotifer Density by Dominant Taxa (#/L). River.

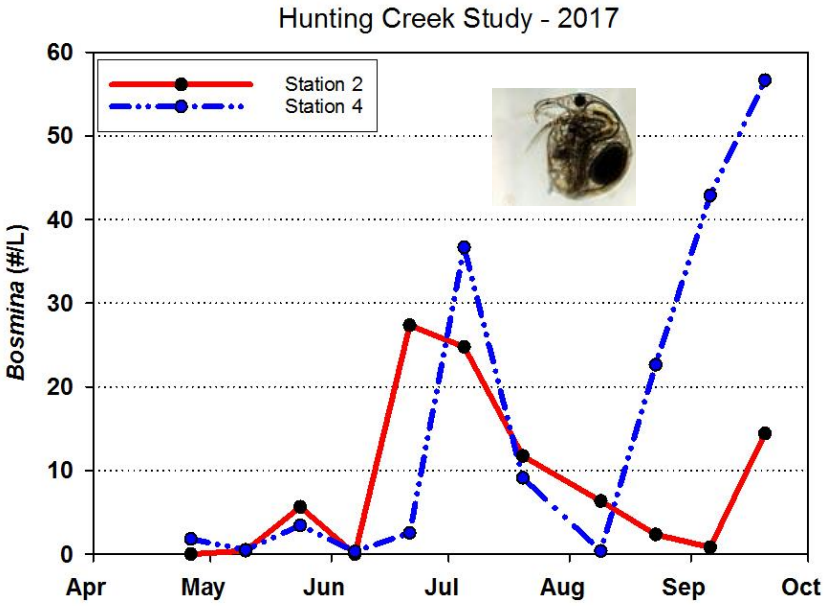

Bosmina is a small-bodied cladoceran, or "waterflea", which is common in lakes and freshwater tidal areas. It is typically the most abundant cladoceran with maximum numbers generally about 100-1000 animals per liter. Due to its small size and relatively high abundances, it is enumerated in the micro-zooplankton samples. *Bosmina* can graze on smaller phytoplankton cells, but can also utilize some cells from colonies by knocking them loose.

Figure 73. *Bosmina* Density by Station (#/L).

In 2017 the small cladoceran *Bosmina* was generally present at low densities at both stations (Figure 73). The highest densities were in late June and early July at both stations and in September at AR4. Even the highest values here are low for the Potomac. *Diaphanosoma*, typically the most abundant larger cladoceran in Gunston Cove, was not very common at AR4, but reached a major peak at AR2 of about 1300/m^3 in late June (Figure 74).

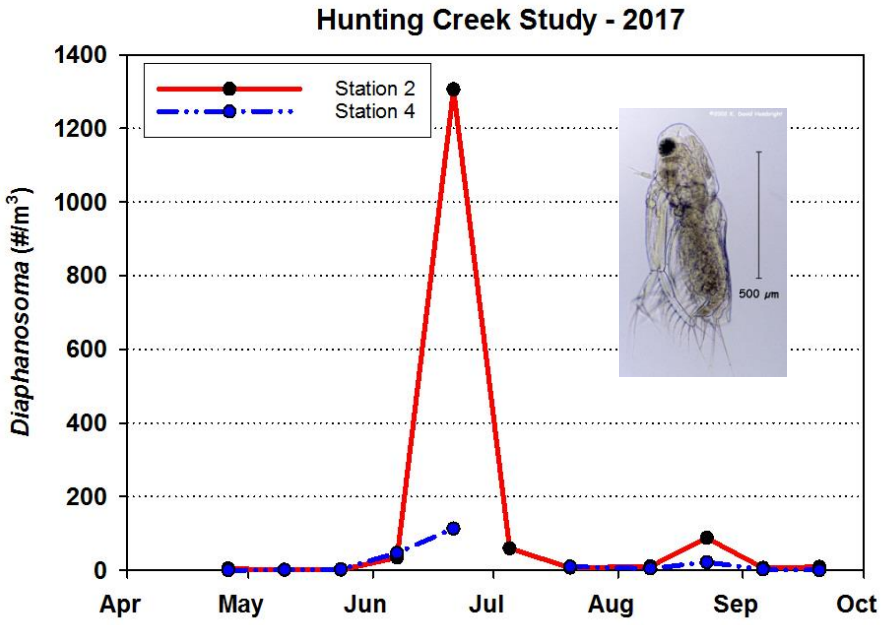

Diaphanosoma is the most abundant larger cladoceran found in the tidal Potomac River. It generally reaches numbers of 1,000-10,000 per m^3 (which would be 1-10 per liter). Due to their larger size and lower abundances, *Diaphanosoma* and the other cladocera are enumerated in the macrozooplankton samples. *Diaphanosoma* prefers warmer temperatures than some cladocera and is often common in the summer.

Figure 74. *Diaphanosoma* Density by Station (#/m^3).

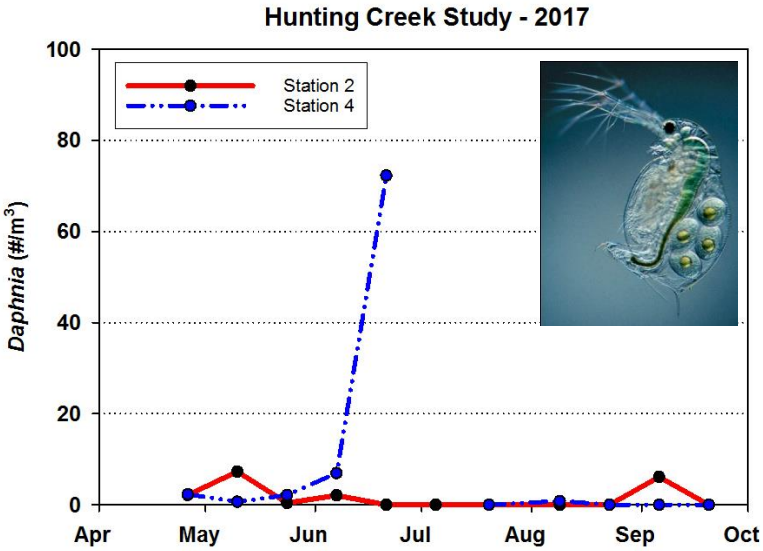

Daphnia, the common waterflea, is one of the most efficient grazers of phytoplankton in freshwater ecosystems. In the tidal Potomac River it is present, but has not generally been as abundant as *Diaphanosoma*. It is typically most common in spring.

Figure 75. *Daphnia* Density by Station (#/m^3).

Daphnia was generally uncommon in the study are in 2017 with a slight outbreak at the river station in late June (Figure 75). *Ceriodaphnia* was very rare at the river station and exhibited moderate peaks in late June and late August in at the embayment station (Figure 76).

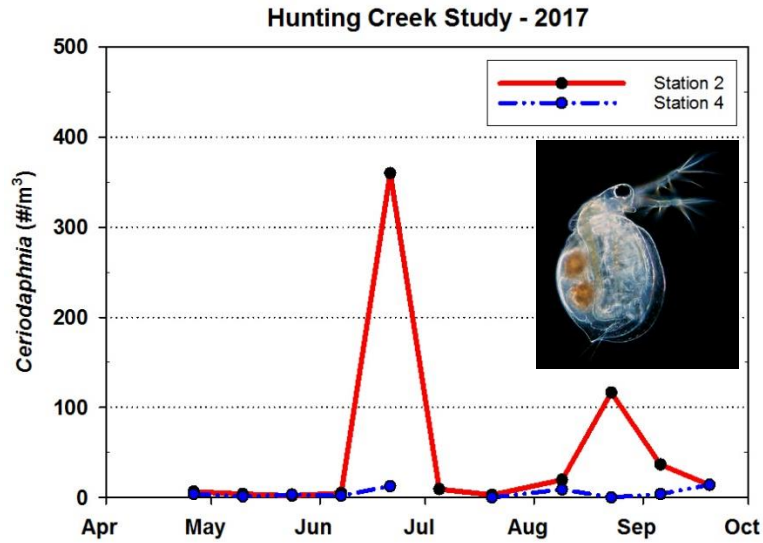

Ceriodaphnia, another common large-bodied cladoceran, is usually present in numbers similar to *Daphnia*. Like all waterfleas, the juveniles look like miniature adults and grow through a series of molts to a larger size and finally reach reproductive maturity. Most reproduction is asexual except during stressful environmental conditions.

Figure 76. *Ceriodaphnia* Density by Station (#/m^3).

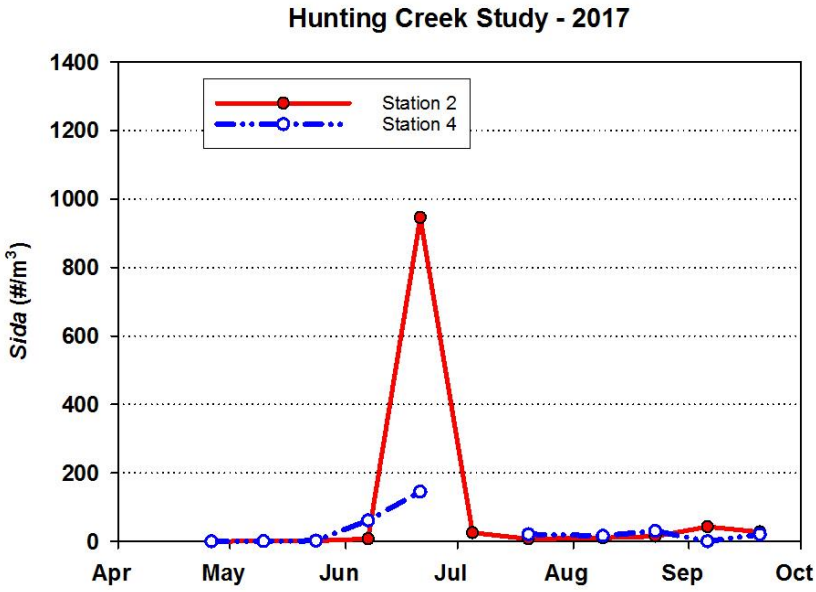

Sida is another waterflea that is often observed in the tidal Potomac River. Like the other cladocera mentioned so far, *Sida* grazes on phytoplankton to obtain its food supply.

Figure 77. *Sida* Density by Station (#/m^3).

Sida was yet another cladoceran whose values peaked in late June at the embayment station (Figure 77). It was also present in lower numbers at the river station. *Leptodora*, the large cladoceran predator, peaked in late June in Hunting Creek at about 50/m^3 and in late July at a lowere level at the river mainstem site AR4 (Figure 78).

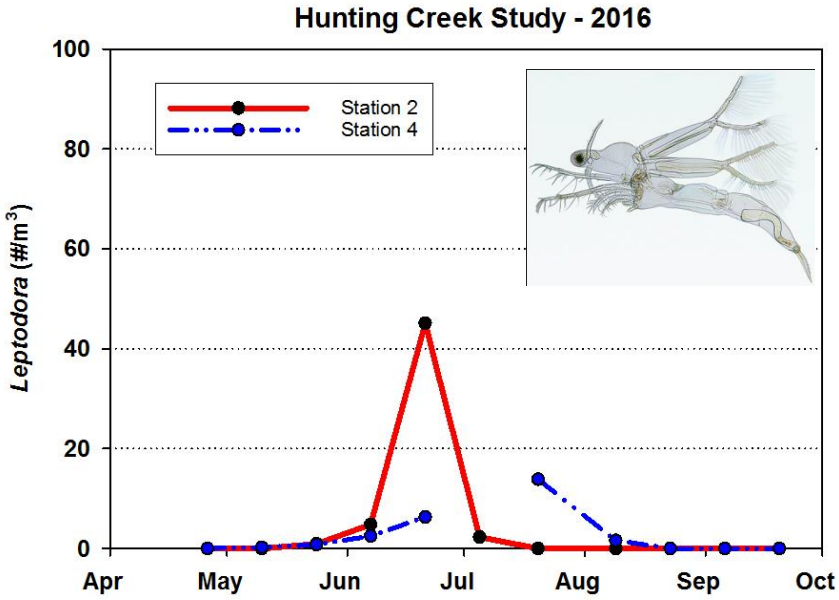

Leptodora is substantially larger than the other cladocera mentioned. Also different is its mode of feeding – it is a predator on other zooplankton. It normally occurs for brief periods in the late spring or early summer.

Figure 78. *Leptodora* Density by Station (#/m^3).

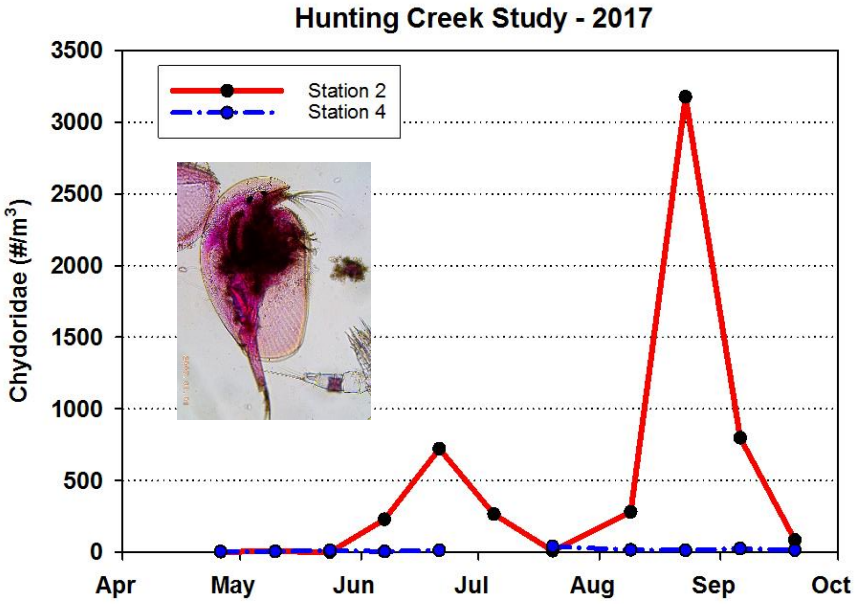

Figure 79. Chydoridae Density by Station (#/m^3). (photo: L. Birsa from HC samples)

Chydoridae is a cladoceran family whose members are associated with SAV (Figure 79). Chydorids were found almost exclusively at the Hunting Creek embayment (AR2), peaking in late June and late August. The late August peak was very large, exceeding 3000/m^3. Macrothricids, another group associated with SAV, were also present exclusively at AR2 and were recorded at over 1200/m^3 in late August (Figure 80).

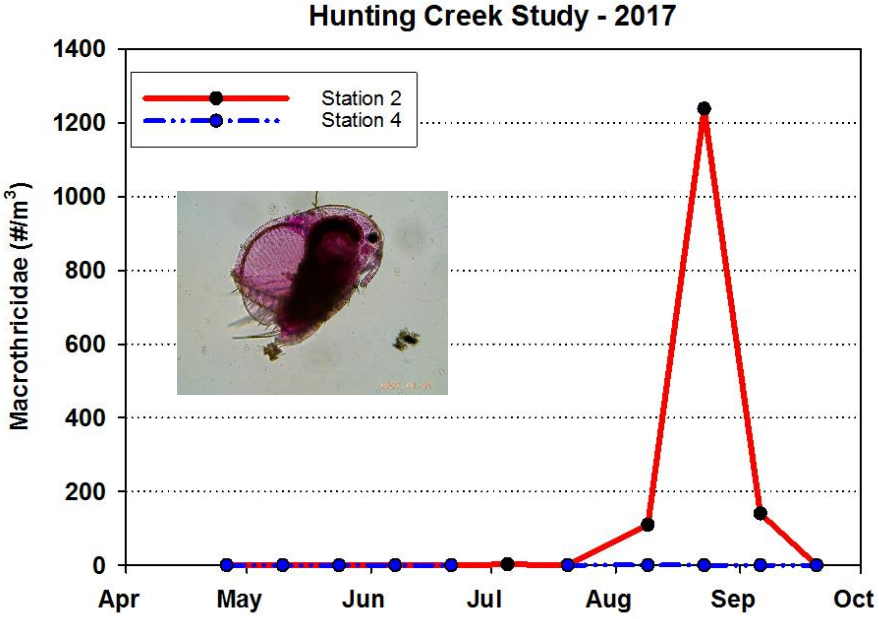

Figure 80. Macrothricid Density by Station (#/m^3). (photo: L. Birsa from HC samples)

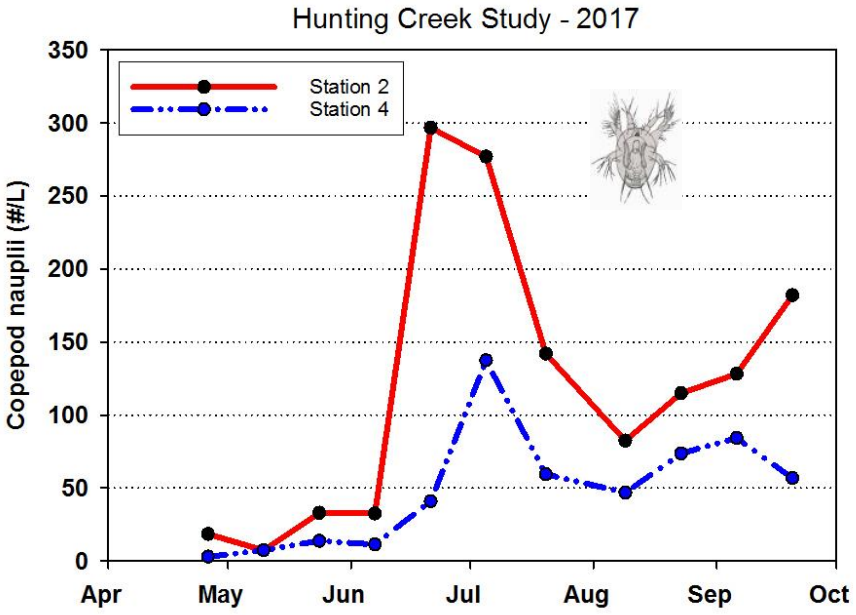

Copepod eggs hatch to form an immature stage called a nauplius. The nauplius is a larval stage that does not closely resemble the adult and the nauplii of different species of copepods are not easily distinguished so they are lumped in this study. Copepods go through 5 naupliar molts before reaching the copepodid stage which is morphologically very similar to the adult. Because of their small size and high abundance, copepod nauplii are enumerated in the micro-zooplankton samples.

Figure 81. Copepod Nauplii Density by Station (#/L).

Copepod nauplii were the most numerous group of crustacean zooplankton. They were present at elevated levels at AR2 in late June and early July reaching 300/L (Figure 81). Levels in the river also peaked in early June at a lower level of about 150/L. *Eurytemora* was abundant in Hunting Creek in April, was scarce for the rest of the year. In the river, densities attained a maximum of about 1,600/m^3 in late June (Figure 82).

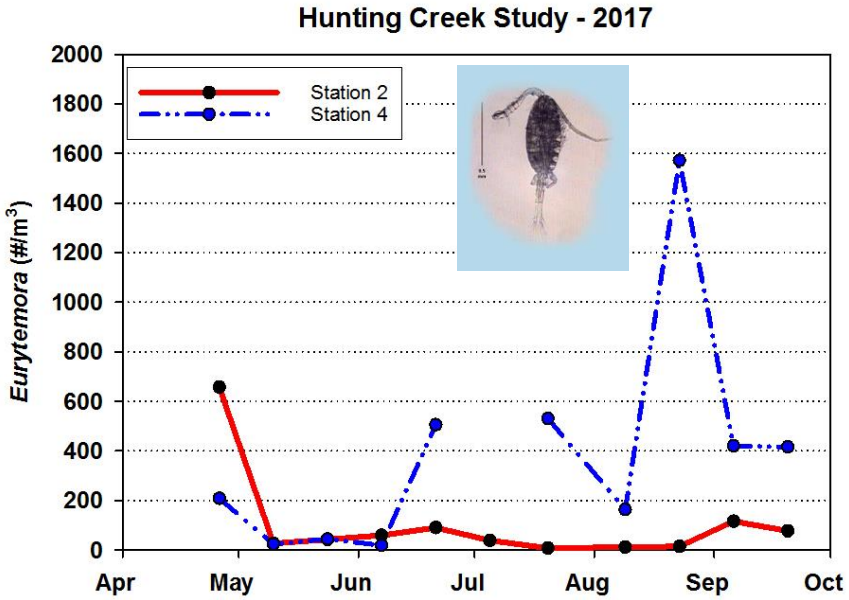

Eurytemora affinis is a large calanoid copepod characteristic of the freshwater and brackish areas of the Chesapeake Bay. *Eurytemora* is a cool water copepod which often reaches maximum abundance in the late winter or early spring. Included in this graph are adults and those copepodids that are recognizable as *Eurytemora*.

Figure 82. *Eurytemora* Density by Station (#/m^3).

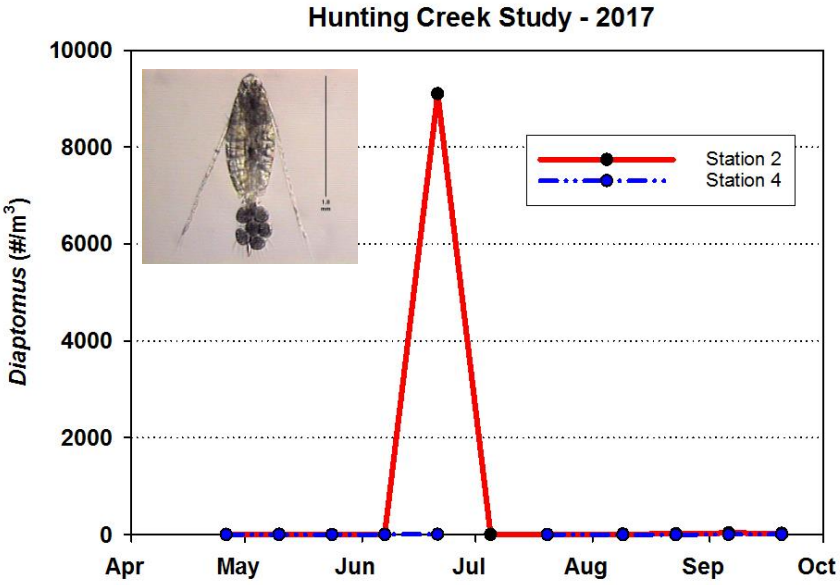

Diaptomus pallidus is a calanoid copepod often found in moderate densities in the Gunston Cove area. *Diaptomus* is an efficient grazer of algae, bacteria, and detrital particles in freshwater ecosystems Included in this graph are adults and those copepodids that are recognizable as *Diaptomus*.

Figure 83. *Diaptomus* Density by Station (#/m^3).

Diaptomus was almost exclusively found in Hunting Creek where it reached a substantial peak of nearly 9000/m^3 in late June (Figure 83). Cyclopoid copepods were present at moderately high numbers in late June and early September at the Hunting Creek embayment station (Figure 84). Cyclopoids were rare in the river mainstem.

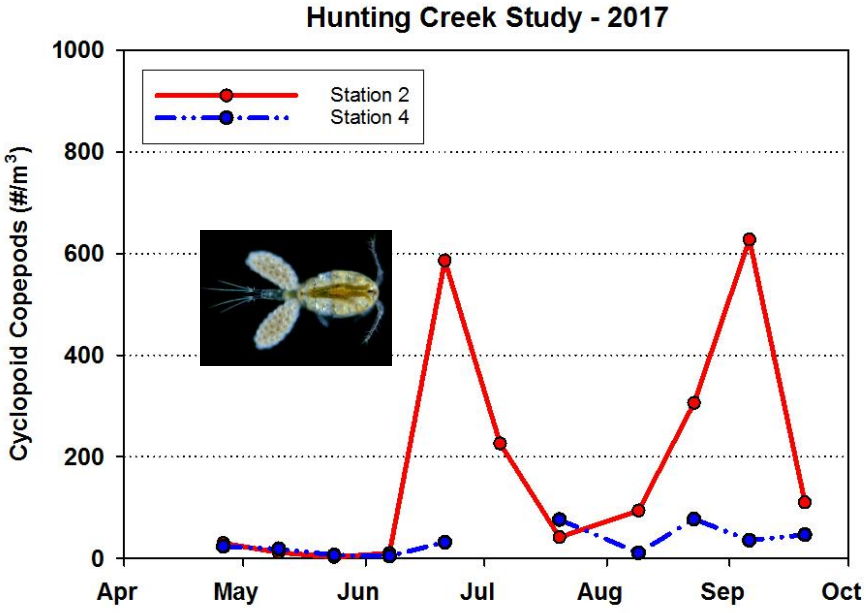

Cyclopoids are the other major group of planktonic copepods. Cyclopoids feed on individual particles suspended in the water including small zooplankton as well as phytoplankton. In this study we have lumped all copepodid and adult cyclopoids together.

Figure 84. Cyclopoid Copepods by Station (#/m^3).

F. Ichthyoplankton – 2017

We collected 14 samples (7 at Station 2 and 7 at Station 4) during the months April through July and found an average total larval density of 503 larvae per 10 m^3 (Table 4), which is more than last year (but less than 2015). The dominant species was Gizzard Shad (*Dorosoma cepedianum*) with an average larval density of 147 larvae per $10m^3$. *Alosa aestivalis* (Blueback Herring) had the second highest density with 103 larvae per $10m^3$. *Alosa pseudoharengus* (Alewife) was present in relative high densities as well: 41 larvae per $10m^3$ on average. Other clupeids present that could positively be identified to the species level are Hickory Shad (*Alosa mediocris*) at an average of 2 larvae per $10m^3$, and American Shad at 1 per $10m^3$. The taxon Clupeidae, which is comprised of clupeids (*Alosa* or *Dorosoma* sp.) that could not be identified to a lower taxonomic level had a density of 97 larvae per $10m^3$.

A different taxon with relatively high representation is Inland Silverside (*Menidia beryllina*) with an average of 30 larvae per $10m^3$. Fishes of the genus *Morone*, which includes White Perch (*M. americana*) and Striped Bass (*M. saxatilis*) were relatively abundant as well, with an average of 2 larvae per $10m^3$ identified to the genus level, plus 9 positively identified as White Perch, and 4 as Striped Bass larvae per $10m^3$.

Table 4. The average larval density (#/$10m^3$) in Hunting Creek (Sta. 2) and the Potomac River (Sta. 4) in 2017.

Scientific Name	Common Name	AR2	AR4	Average
Alosa aestivalis	Blueback Herring	51.05	154.24	102.64
Alosa mediocris	Hickory Shad	0.75	3.53	2.14
Alosa pseudoharengus	Alewife	18.55	63.20	40.87
Alosa sapidissima	American Shad	1.44	1.36	1.40
Carassius auratus	Goldfish	7.02	0.00	3.51
Clupeid species	Unidentified Clupeid	131.15	62.16	96.66
Cyprinus carpio	Carp	2.98	0.00	1.49
Dorosoma cepedianum	Gizzard Shad	75.45	218.05	146.75
Eggs	Eggs	10.50	15.16	12.83
Fundulus diaphanus	Banded Killifish	0.16	0.33	0.25
Hybognathus regius	Eastern Silvery Minnow	0.50	0.00	0.25
Lepisosteus osseus	Longnose Gar	0.25	0.00	0.12
Lepomis cyanellus	Green Sunfish	0.50	0.00	0.25
Lepomis gibbosus	Pumpkinseed	0.99	0.00	0.50
Lepomis macrochirus	Bluegill	0.50	0.00	0.25
Lepomis species	Unidentified Sunfish	7.52	0.72	4.12

Scientific Name	Common Name	AR2	AR4	Average
Menidia beryllina	Inland Silverside	60.11	0.68	30.39
Micropterus dolomieu	Small-mouth Bass	0.25	0.00	0.12
Morone americana	White Perch	6.19	11.35	8.77
Morone saxatilis	Striped Bass	0.30	7.41	3.85
Morone species	Unidentified perch/bass	2.10	1.61	1.85
Notropis hudsonius	Spottail Shiner	2.48	0.00	1.24
Perca flavescens	Yellow Perch	0.50	0.00	0.25
Strongylura marina	Atlantic Needlefish	0.13	0.00	0.07
Unidentified	Unidentified	83.03	1.20	42.11

Clupeid larvae in Figure 56 include Blueback Herring, Hickory Shad, Alewife, American Shad and Gizzard Shad. These have similar spawning patterns so they are lumped into one group for this analysis. Clupeids were present in the sample at the end of April, increased to 160 larvae per 10 m^3 in early June, and decreased again at the end of June (Figure 56). Of these clupeids, Alewife and Blueback Herring are the two species that make up river herring, of which we describe the spawning population at the end of this report.

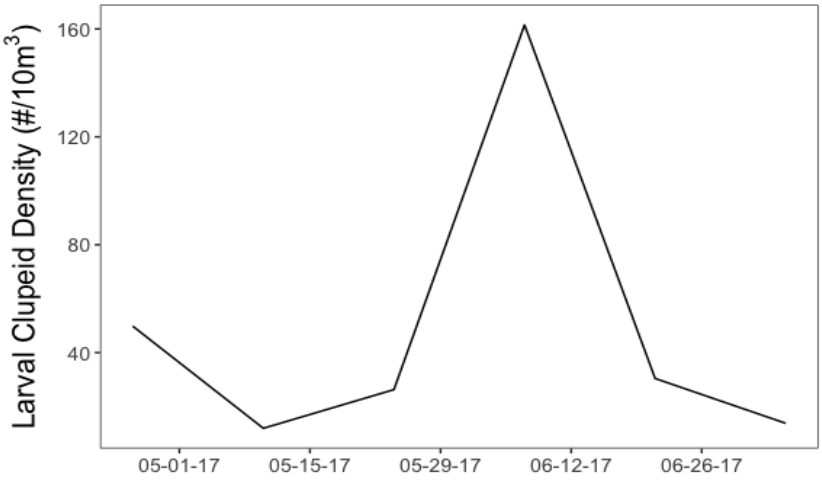

Figure 85. Average Density of clupeid larvae per 10m^3.

White Perch and Striped Bass larvae attained highest density on average at about 7 larvae per 10m^3 at the start of sampling in April (Figure 57), and disappeared from the samples in July. The group of larvae that are not positively identified clupeids or Morone species are dominated by unidentified larvae. Highest densities of unidentified larvae were found mid-June. The unidentified larvae were not intact unknown species, but larvae to mangled for proper identification. Because of the high density of clupeid larvae, most unidentified larvae are likely to be clupeids as well.

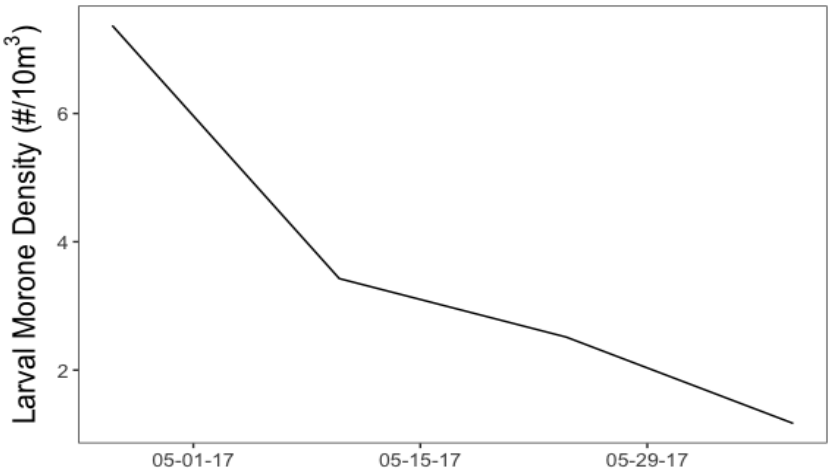

Figure 86. Density of *Morone* sp. (white perch and striped bass) per $10m^3$.

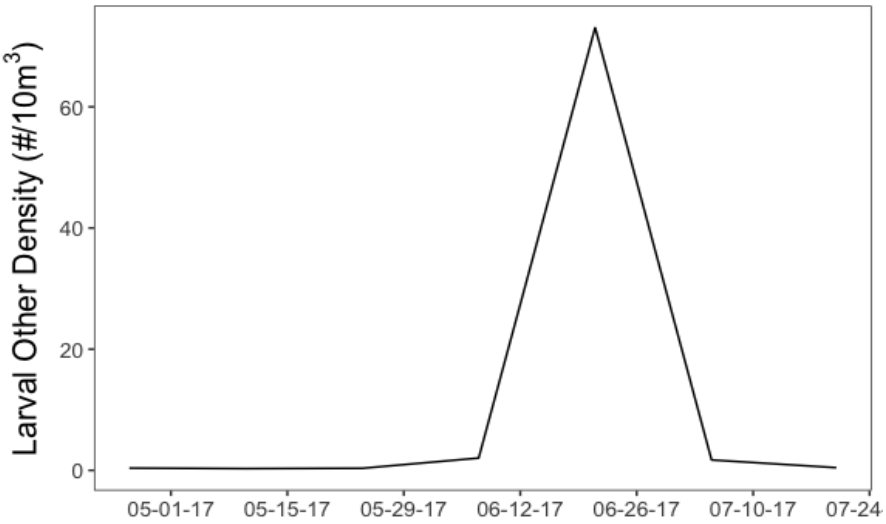

Figure 87. Density of other larvae per $10m^3$.

G. Adult and juvenile fishes – 2017

Trawls

Trawl sampling was conducted between April 28 and September 12 at station 3 and 4. A total of 484 fishes comprising 13 species were collected with trawls (Table 5). This

abundance is about 5 times higher than last year while the diversity is similar. Collections were dominated by White Perch (81%). The second most abundant taxon caught were species in the sunfish family (9%). Another relatively abundant species was Tessellated Darter (3.3%). Other species were observed at low abundances (Tables 5 and 6). An interesting find was the collection of a native catfish (Brown Bullhead), which has seen declining abundances since the invasion of Blue Catfish.

Table 5. Adult and juvenile fish collected by trawling. Hunting Creek - 2017

Scientific Name	Common Name	Abundance	Percent
Morone americana	White Perch	391	80.77
Lepomis species	Unidentified Sunfish	40	8.27
Etheostoma olmstedi	Tessellated Darter	16	3.31
Notropis hudsonius	Spottail Shiner	7	1.45
Ictalurus furcatus	Blue Catfish	6	1.31
Carassius auratus	Goldfish	6	1.24
Lepomis gibbosus	Pumpkinseed	6	1.24
Morone saxatilis	Striped Bass	3	0.62
Cyprinus carpio	Carp	3	0.55
Ameiurus nebulosus	Brown Bullhead	2	0.41
Lepomis macrochirus	Bluegill	2	0.41
Alosa species	Unidentified Herring or shad	1	0.21
Perca flavescens	Yellow Perch	1	0.21
Total		**484**	**100.00**

Trawling collects fish that are located in the open water near the bottom. Due to the shallowness of Hunting Creek, the volume collected is a substantial part of the water column. However, in the river channel, the near bottom habitat through which the trawl moves is only a small portion of the water column. Fishes tend to concentrate near the bottom or along shorelines rather than in the upper portion of the open water.

Table 6. Adult and juvenile fish collected by trawling. Hunting Creek study – 2017

Scientific Name	Common Name	04-28	05-16	05-31	06-13	06-27	07-11	07-26	08-08	08-22	09-12	Total
Alosa species	Unidentified Herring or shad	0	0	0	0	0	0	1	0	0	0	**1**
Ameiurus nebulosus	Brown Bullhead	0	0	2	0	0	0	0	0	0	0	**2**
Carassius auratus	Goldfish	0	0	1	0	1	1	3	0	0	0	**6**
Cyprinus carpio	Carp	0	0	0	0	0	1	0	2	0	0	**3**
Etheostoma olmstedi	Tessellated Darter	0	1	1	4	8	1	1	0	0	0	**16**
Ictalurus furcatus	Blue Catfish	1	0	0	0	0	0	0	3	2	0	**6**
Lepomis gibbosus	Pumpkinseed	1	1	3	1	0	0	0	0	0	0	**6**
Lepomis macrochirus	Bluegill	0	1	0	0	0	0	1	0	0	0	**2**
Lepomis species	Unidentified Sunfish	0	0	0	0	0	0	40	0	0	0	**40**
Morone americana	White Perch	6	16	27	10	99	92	30	87	23	1	**391**
Morone saxatilis	Striped Bass	0	0	0	0	2	1	0	0	0	0	**3**
Notropis hudsonius	Spottail Shiner	0	4	0	0	0	3	0	0	0	0	**7**
Perca flavescens	Yellow Perch	1	0	0	0	0	0	0	0	0	0	**1**
Total		**9**	**23**	**34**	**15**	**110**	**99**	**76**	**92**	**25**	**1**	**483**

The highest catch occurred on June 27, which was due to the high abundance of White Perch in that trawl sample (Table 6). In 2017, most catches occurred in station 4, which is similar to last year but unlike previous years (Table 7). This was due to the high abundance of White Perch collected at station 4. The catch at station 4 was higher than previous years with 325 individuals of 8 species. At Station 3, 159 individuals were collected of 9 species.

Table 7. Adult and juvenile fish collected by trawling. Hunting Creek study - 2017

Scientific Name	**Common Name**	**3**	**4**
Alosa species	Unidentified Herring or shad	0	1
Ameiurus nebulosus	Brown Bullhead	2	0
Carassius auratus	Goldfish	5	1
Cyprinus carpio	Carp	0	3
Etheostoma olmstedi	Tessellated Darter	7	9
Ictalurus furcatus	Blue Catfish	0	6
Lepomis gibbosus	Pumpkinseed	6	0
Lepomis macrochirus	Bluegill	2	0
Lepomis species	Unidentified Sunfish	40	0
Morone americana	White Perch	95	296
Morone saxatilis	Striped Bass	1	2
Notropis hudsonius	Spottail Shiner	0	7
Perca flavescens	Yellow Perch	1	0
Total		**159**	**325**

White Perch was the dominant species as in previous years (only in 2016 we only collected 3 White Perch). High dominance of White Perch at station 4 was also responsible for the large catch at station 4. Looking at species by dominance (Figure 59A and B), White Perch was the dominant species both at station 3 and 4 in 2017. The species distribution is slightly more even in station 3 than station 4.

White perch (*Morone americana*) is the dominant species in Hunting Creek, and continues to be an important commercial and popular game fish. Adults grow to over 30 cm long. Sexual maturity begins the second year at lengths greater than 9 cm. As juveniles they feed on zooplankton and macrobenthos, but as they get larger consume fish as well.

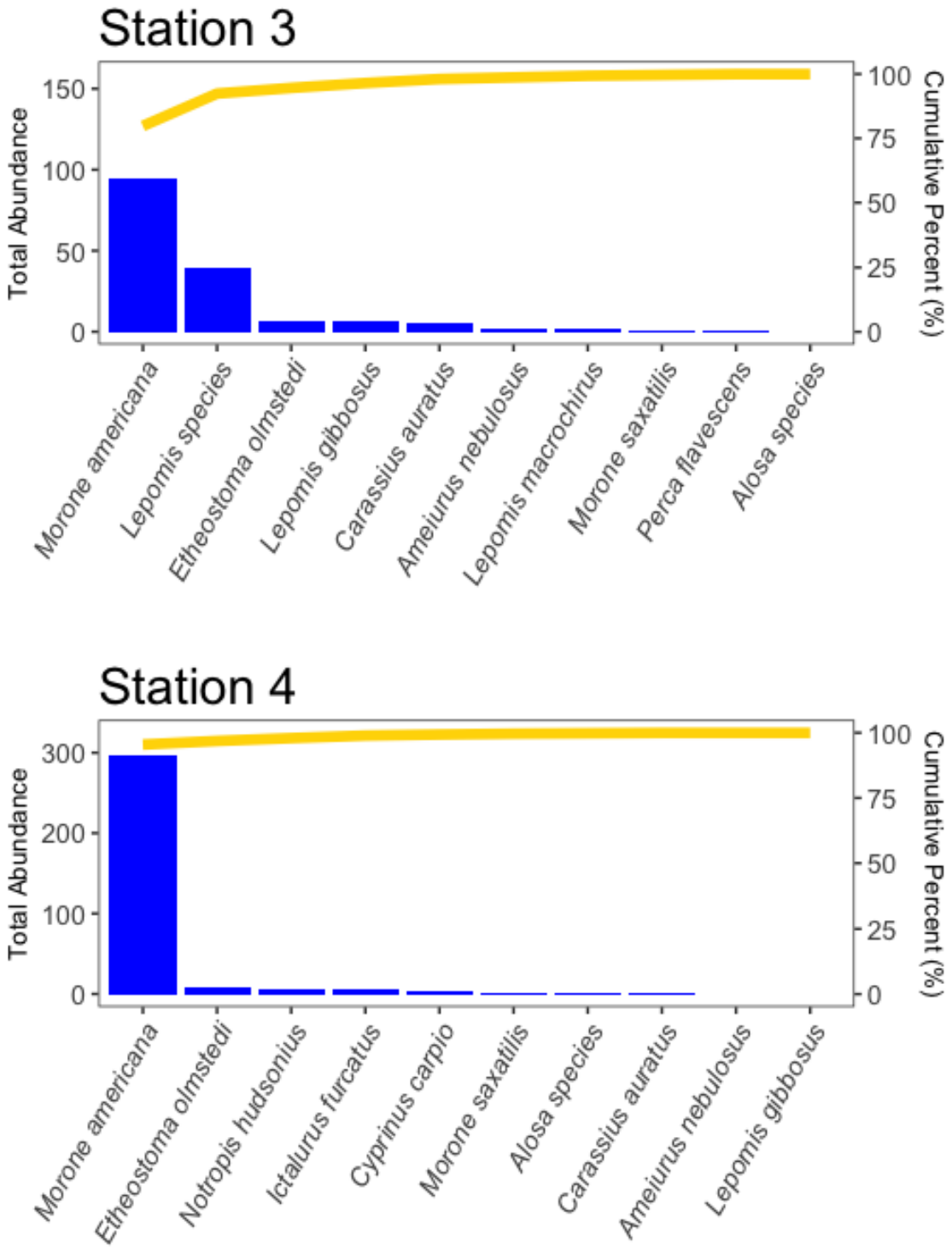

Figure 88A and B. Pareto chart of adult and juvenile fishes collected by trawling. Dominant species by station in total abundance and cumulative percentage of total for Station 3 (top) and Station 4 (bottom)

Spottail shiner (*Notropis hudsonius* is a common fish in the open waters of Hunting Creek. Spawning occurs throughout the warmer months. It reaches sexual maturity at about 5.5 cm and may attain a length of 10 cm. They feed primarily on benthic invertebrates and occasionally on algae and plants.

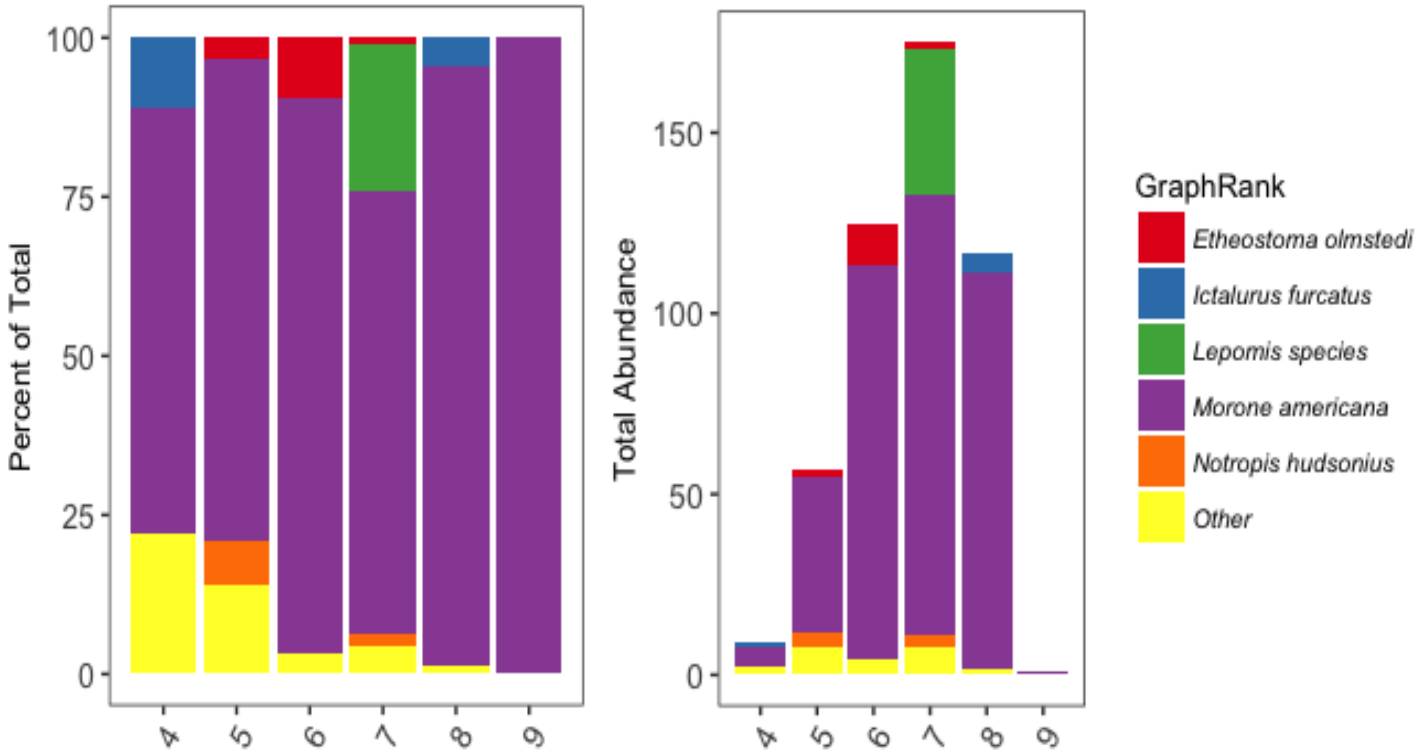

Figure 89 A&B. Adult and juvenile fishes collected by trawling. Dominant species by month in percentage of total (A) and total abundance (B).

From Figure 60 it is clear that White Perch is the dominant species in all months sampled. Sunfish, which is the second most abundant taxon, were all collected during one sampling event in July. Figure 60B also shows how our sampling season captures the representative fish community well, with very low abundances at the start and end of the season. One White Perch was the entire catch of September.

Seines

Seine sampling was conducted between April 28 and September 12 at station 5 and 6. As planned, one sampling trip per month was performed in April and September, and two sampling trips per month from May to August. These two seines stations were selected as sites with shallow sloping shorelines that would enable us to tow a beach seine. The net was towed up onto the beach unless high water completely submerged the beach. In those cases, the net was towed into the boat.

A total of 19 seine samples were conducted, yielding 1125 fishes of 23 species (Table 8). The most dominant species in seine catches was banded Killifish (61.33%). This is similar to last year, although the total number of individuals is about a third of what it was in previous years. Other species that were relatively abundant were Inland Silverside (10.13%), Smallmouth Bass (5.51%), Mummichog (5.51%), and Eastern Silvery Minnow (3.56%). Other species occurred at low abundances (Table 8).
Banded Killifish was present from May to October, and dominant on most collections (Table 9; Figure 62A&B). The most productive month was August; not only due to the high numbers of Banded Killifish present that month, but also those of other species such as Smallmouth Bass and Mummichog. Banded Killifish collections were evenly collected over station 5 and 6 (Table 10). The total number of individuals in station 6 was slightly higher than station 5, mostly due to higher numbers of inland silverside and Smallmouth Bass at station 6. Evenness (of abundance distribution over multiple species was higher than previous years, mostly due to the lower abundance of banded killifish in the collections. The Pareto charts of station 5 and 6 (Figure 61A&B) indicate with higher slopes of the cumulative percent of the catch than last year that Banded Killifish is dominant, but that contributions of other species are slightly higher than last year.

Table 8. Adult and juvenile fish collected by seining. Hunting Creek- 2017

Scientific Name	Common Name	Abundance	Percent
Alosa sapidissima	American Shad	2	0.18
Alosa species	Unidentified Herring or shad	2	0.18
Carassius auratus	Goldfish	12	1.07
Enneacanthus gloriosus	Bluespotted Sunfish	27	2.40
Etheostoma olmstedi	Tessellated Darter	17	1.51
Fundulus diaphanus	Banded Killifish	690	61.33
Fundulus heteroclitus	Mummichog	62	5.51
Gambusia holbrooki	Mosquitofish	1	0.09
Hybognathus regius	Eastern Silvery Minnow	40	3.56
Lepisosteus osseus	Longnose Gar	1	0.09
Lepomis cyanellus	Green Sunfish	4	0.36
Lepomis gibbosus	Pumpkinseed	33	2.93
Lepomis macrochirus	Bluegill	26	2.31
Lepomis megalotis	Longear Sunfish	1	0.09
Lepomis species	Unidentified Sunfish	10	0.89
Menidia beryllina	Inland Silverside	114	10.13
Micropterus dolomieu	Smallmouth Bass	62	5.51
Micropterus salmoides	Largemouth Bass	2	0.18
Morone americana	White Perch	2	0.18
Morone saxatilis	Striped Bass	2	0.18
Notemigonus crysoleucas	Golden Shiner	2	0.18
Notropis hudsonius	Spottail Shiner	4	0.36
Strongylura marina	Atlantic Needlefish	9	0.80
Total		**1125**	**100**

Table 9. Adult and juvenile fish collected by seining. Hunting Creek study – 2017

Scientific Name	Common Name	04-28	05-16	05-31	06-13	06-27	07-11	07-26	08-08	08-22	09-12	Total
Alosa sapidissima	American Shad	0	0	0	0	0	0	0	0	2	0	**2**
Alosa species	Unidentified Herring or shad	1	0	0	0	0	0	1	0	0	0	**2**
Carassius auratus	Goldfish	0	0	0	0	0	0	2	10	0	0	**12**
Enneacanthus gloriosus	Bluespotted Sunfish	0	0	0	0	0	0	0	15	12	0	**27**
Etheostoma olmstedi	Tessellated Darter	0	0	0	7	0	6	2	1	1	0	**17**
Fundulus diaphanus	Banded Killifish	0	56	185	210	1	36	0	143	52	7	**690**
Fundulus heteroclitus	Mummichog	0	0	2	0	0	20	0	17	23	0	**62**
Gambusia holbrooki	Mosquitofish	0	0	0	0	0	0	0	1	0	0	**1**
Hybognathus regius	Eastern Silvery Minnow	0	0	0	23	0	0	0	0	1	16	**40**
Lepisosteus osseus	Longnose Gar	0	0	0	0	1	0	0	0	0	0	**1**
Lepomis cyanellus	Green Sunfish	0	0	0	0	0	0	0	0	2	2	**4**
Lepomis gibbosus	Pumpkinseed	1	1	0	0	1	0	0	5	17	8	**33**
Lepomis macrochirus	Bluegill	0	1	0	0	0	1	2	15	7	0	**26**
Lepomis megalotis	Longear Sunfish	1	0	0	0	0	0	0	0	0	0	**1**
Lepomis species	Unidentified Sunfish	0	0	0	0	0	0	1	2	7	0	**10**
Menidia beryllina	Inland Silverside	52	39	0	1	18	0	4	0	0	0	**114**
Micropterus dolomieu	Smallmouth Bass	0	0	0	0	0	4	4	46	6	2	**62**
Micropterus salmoides	Largemouth Bass	0	1	0	1	0	0	0	0	0	0	**2**
Morone americana	White Perch	0	0	0	0	0	0	0	2	0	0	**2**
Morone saxatilis	Striped Bass	0	0	0	0	0	2	0	0	0	0	**2**
Notemigonus crysoleucas	Golden Shiner	1	1	0	0	0	0	0	0	0	0	**2**
Notropis hudsonius	Spottail Shiner	0	0	1	3	0	0	0	0	0	0	**4**
Strongylura marina	Atlantic Needlefish	0	0	0	7	1	0	1	0	0	0	**9**
Total		**56**	**99**	**188**	**252**	**22**	**69**	**17**	**257**	**130**	**35**	**1125**

Table 10. Adult and juvenile fish collected by seining. Hunting Creek study – 2017

Scientific Name	**Common Name**	**5**	**6**
Alosa sapidissima	American Shad	0	2
Alosa species	Unidentified Herring or shad	1	1
Carassius auratus	Goldfish	0	12
Enneacanthus gloriosus	Bluespotted Sunfish	16	11
Etheostoma olmstedi	Tessellated Darter	17	0
Fundulus diaphanus	Banded Killifish	324	366
Fundulus heteroclitus	Mummichog	60	2
Gambusia holbrooki	Mosquitofish	1	0
Hybognathus regius	Eastern Silvery Minnow	17	23
Lepisosteus osseus	Longnose Gar	1	0
Lepomis cyanellus	Green Sunfish	3	1
Lepomis gibbosus	Pumpkinseed	11	22
Lepomis macrochirus	Bluegill	5	21
Lepomis megalotis	Longear Sunfish	1	0
Lepomis species	Unidentified Sunfish	5	5
Menidia beryllina	Inland Silverside	5	109
Micropterus dolomieu	Smallmouth Bass	7	55
Micropterus salmoides	Largemouth Bass	1	1
Morone americana	White Perch	1	1
Morone saxatilis	Striped Bass	2	0
Notemigonus crysoleucas	Golden Shiner	0	2
Notropis hudsonius	Spottail Shiner	3	1
Strongylura marina	Atlantic Needlefish	6	3
Total		**487**	**638**

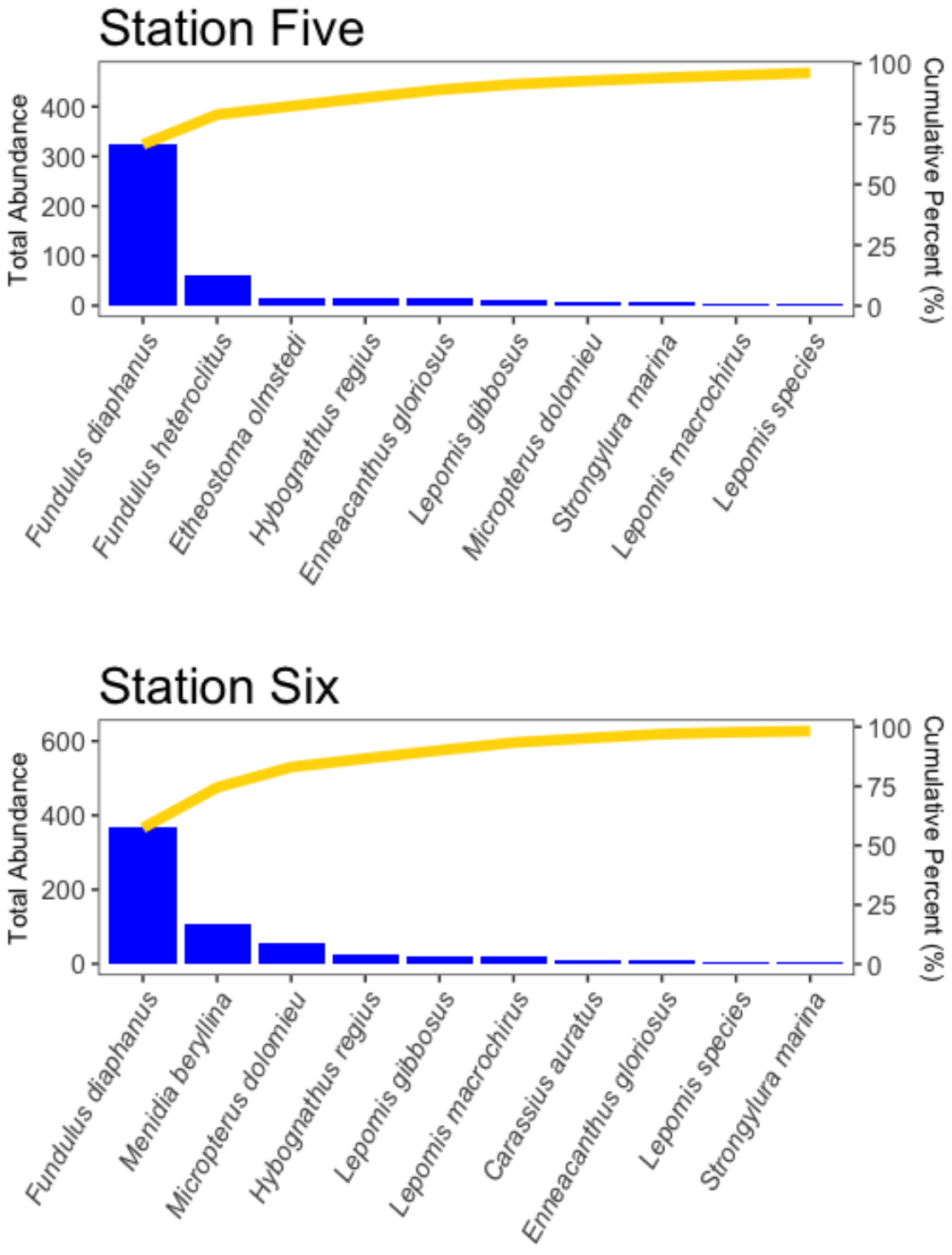

Figure 90A and B. Pareto chart of adult and juvenile fishes collected by seining. Dominant species by station in total abundance and cumulative percentage of total for Station 5 (top) and Station 6 (bottom).

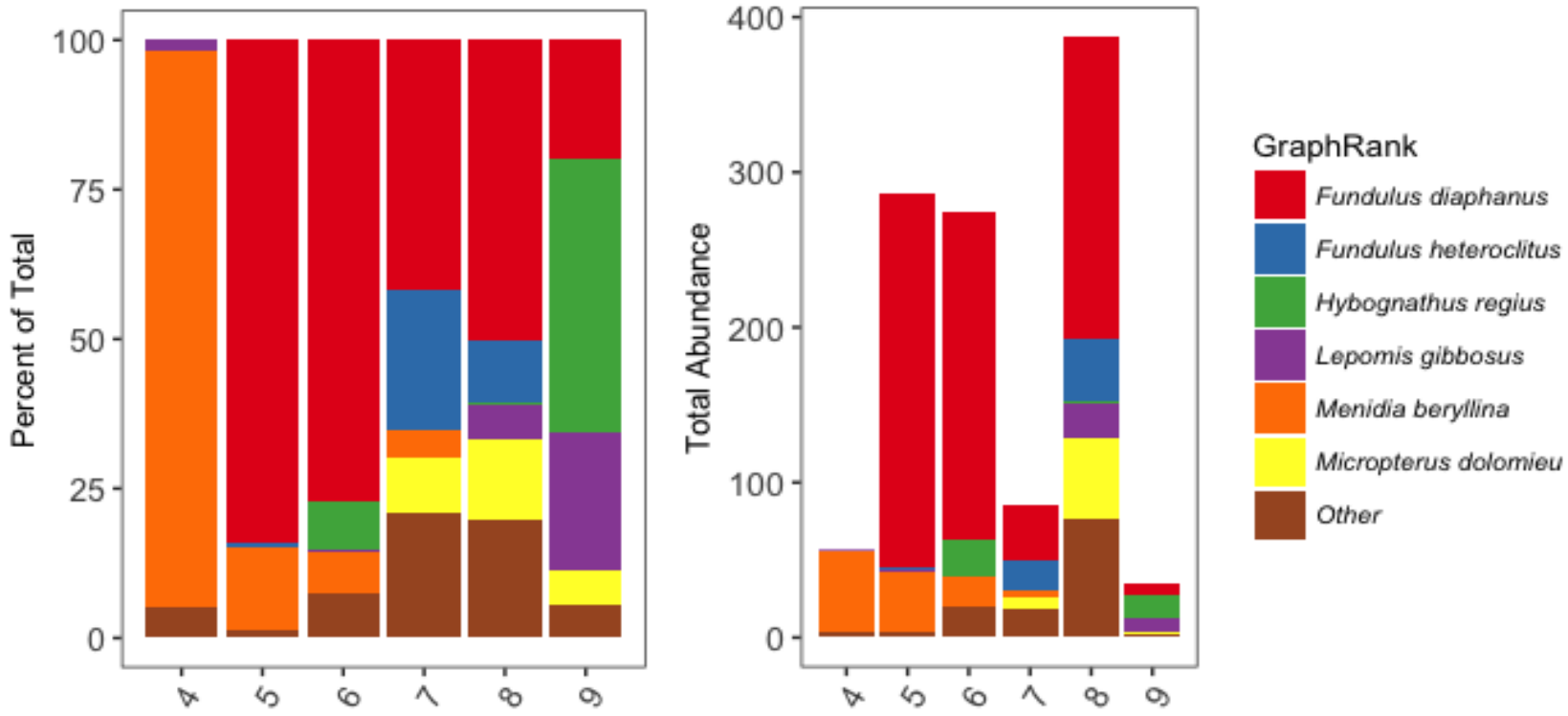

Figure 91A and B. Adult and juvenile fish collected by seining. Dominant species by month in: (a) percentage of total and (b) total abundance.

Fyke Nets

Both fyke nets were set near trawl station 3 (Figure 1), and the total fyke net catch was higher than the total trawl catch at station 3 (855 specimens versus 159). Fyke nets were very effective in 2017, with high abundance reflective of a diversity of species utilizing the SAV habitat. We were able to continue our fyke net sampling when SAV growth had rendered trawling impossible. Fyke nets were set from May 16 to September 12. Except for the first sampling date in April, fyke nets were set during every sampling trip throughout the season (Table 1).

In a total of 18 samples (9 per fyke net), we collected 855 individual fishes from 15 species. Unlike previous years, Banded Killifish was not the dominant species, and it represented 11.23% of the total abundance (Table 11). In 2017 the most dominant species was Bluegill with 23.34% of the total abundance. The percent dominance was distributed fairly evenly over the species collected in fyke nets (Figures 63A&B), and 9 species had a dominance of at least more than 1 % (Table 11). The other species with abundance higher than 1% were Pumpkinseed (20.64%), *Lepomis* sp. (17.36%), Goldfish (12.97%), White Perch (6.75%), Bluespotted Sunfish (3%), Inland Silverside (1.46%), and Smallmouth Bass (1.17%).

Table 11. Adult and juvenile fish collected by fyke nets. Hunting Creek study – 2017

Scientific Name	Common Name	Abundance	Percent
Ameiurus nebulosus	Brown Bullhead	4	0.44
Carassius auratus	Goldfish	111	12.97
Enneacanthus gloriosus	Bluespotted Sunfish	26	3.00
Etheostoma olmstedi	Tessellated Darter	3	0.30
Fundulus diaphanus	Banded Killifish	96	11.23
Lepomis cyanellus	Green Sunfish	4	0.44
Lepomis gibbosus	Pumpkinseed	176	20.64
Lepomis macrochirus	Bluegill	199	23.34
Lepomis species	Unidentified Sunfish	148	17.36
Menidia beryllina	Inland Silverside	12	1.46
Micropterus dolomieu	Smallmouth Bass	10	1.17
Morone americana	White Perch	58	6.75
Morone saxatilis	Striped Bass	4	0.47
Notropis hudsonius	Spottail Shiner	2	0.29
Perca flavescens	Yellow Perch	1	0.15
Total		**855**	**100**

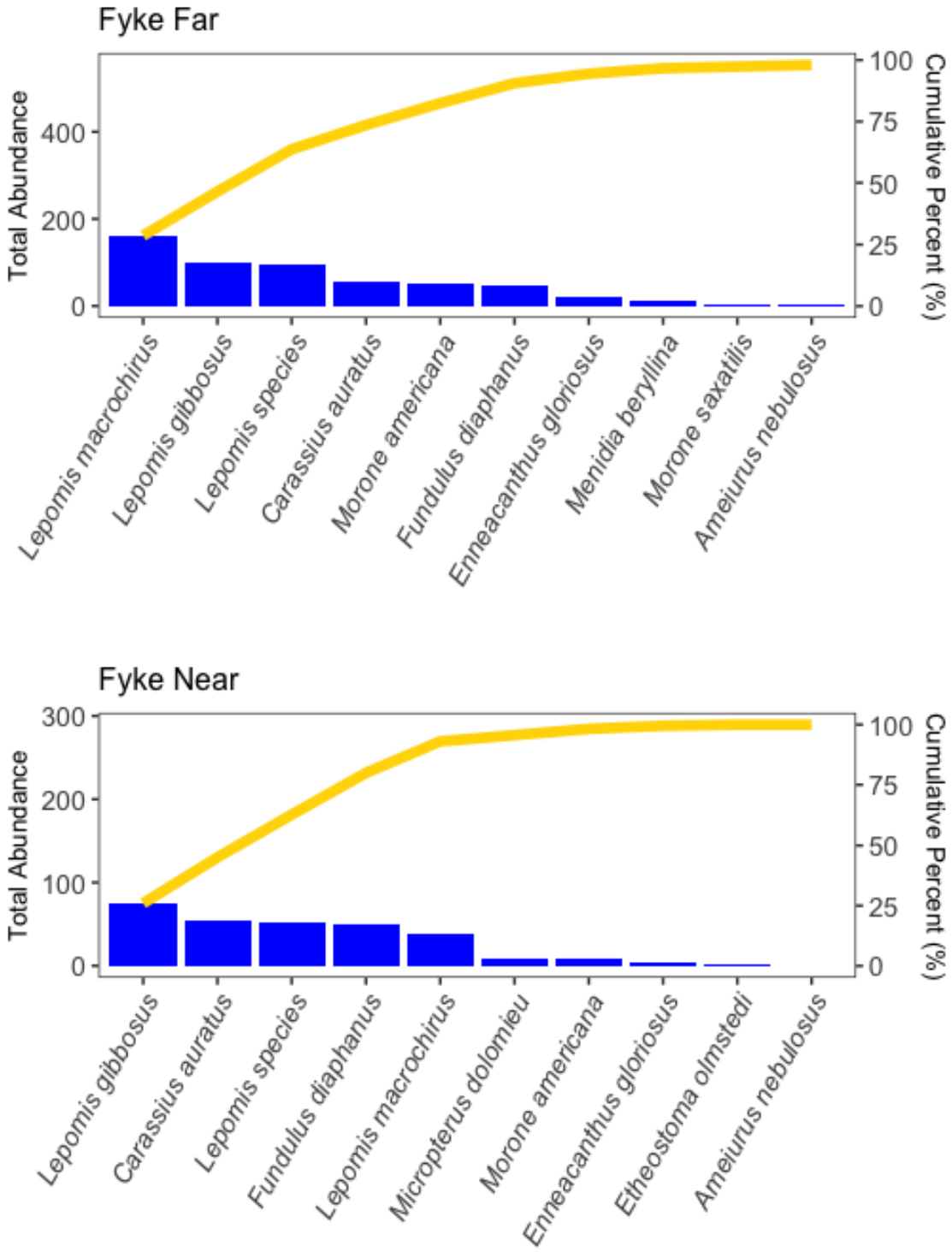

Figure 92a and b. Pareto chart of adult and juvenile fishes collected by fyke nets. Dominant species by station in total abundance and cumulative percentage of total for the Far Fyke (top) and Near Fyke (bottom).

Table 12. Adult and juvenile fish collected by fyke nets. Hunting Creek study - 2017

Scientific Name	Common Name	05-16	05-31	06-13	06-27	07-11	07-26	08-08	08-22	09-12	Total
Ameiurus nebulosus	Brown Bullhead	0	0	2	0	0	0	0	1	0	**4**
Carassius auratus	Goldfish	0	0	0	6	12	52	20	20	0	**111**
Enneacanthus gloriosus	Bluespotted Sunfish	0	0	0	0	0	0	11	15	0	**26**
Etheostoma olmstedi	Tessellated Darter	0	0	0	0	0	1	1	0	0	**3**
Fundulus diaphanus	Banded Killifish	2	1	0	0	25	34	18	15	0	**96**
Lepomis cyanellus	Green Sunfish	0	0	0	0	0	0	0	4	0	**4**
Lepomis gibbosus	Pumpkinseed	0	22	42	12	25	26	5	16	26	**176**
Lepomis macrochirus	Bluegill	2	0	18	0	2	0	84	74	19	**199**
Lepomis species	Unidentified Sunfish	0	0	0	0	9	25	17	90	8	**149**
Menidia beryllina	Inland Silverside	4	0	0	2	0	0	0	6	0	**12**
Micropterus dolomieu	Small-mouth Bass	0	0	0	0	1	9	0	0	0	**10**
Morone americana	White Perch	1	0	0	0	2	26	25	2	0	**58**
Morone saxatilis	Striped Bass	0	0	0	0	0	0	4	0	0	**4**
Notropis hudsonius	Spottail Shiner	0	0	0	1	0	0	0	1	0	**2**
Perca flavescens	Yellow Perch	0	0	0	0	0	1	0	0	0	**1**
Total		**10**	**24**	**62**	**22**	**78**	**175**	**186**	**245**	**52**	**855**

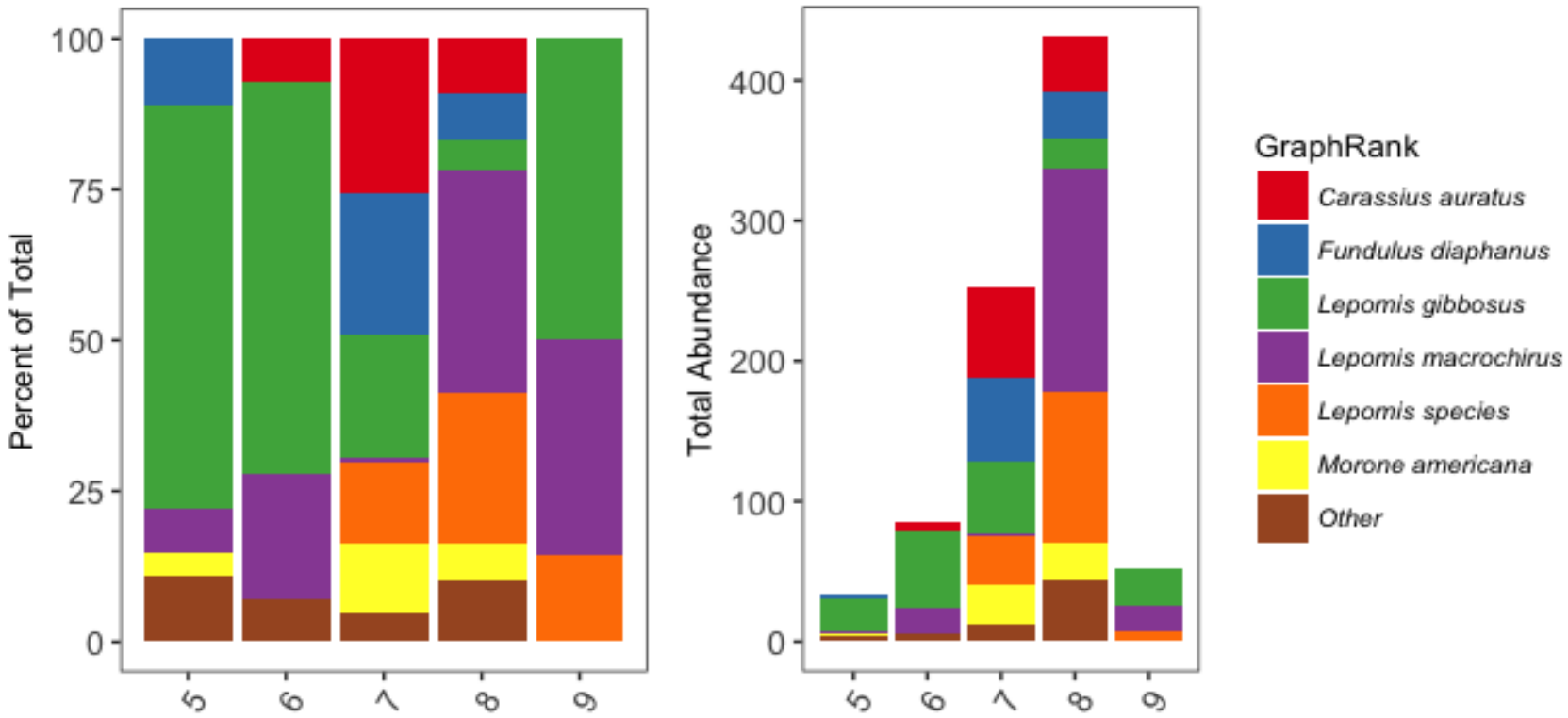

Figure 93a and b. Adult and juvenile fish collected by fyke nets. Dominant species by month in: (a) percentage of total and (b) total abundance.

The highest abundance occurred in the second half of the sampling season, with the highest catch occurring in the month of August and second highest catch in July (Table 12, Figures 64A&B). All species collected had higher abundances in second half of the sampling season, which makes the fyke nets a great addition to the sampling gear, since the trawl could not be towed anymore in August, and in some years already not anymore in July.

Of the two fyke nets, Fyke Far collected twice as much specimens as Fyke Near (Table 13). Fyke Far also collected the highest number of species, with 15 species collected in Fyke far and 9 in Fyke Near. While both fyke nets are close to each other and sample the littoral zone, the fyke net further from shore collects more open water species such as White Perch and Striped Bass (Table 13). The total catch was higher in 2017 than 2016 (855 versus 316), mostly due to higher abundance collected in Fyke Far in 2017. Overall the evenness in the Fyke collections was high in the fyke nets (Figures 63A and B), with representation of several species as a significant portion of the total catch (Figure 64A and B).

Table 13. Adult and juvenile fish collected by fyke nets. Hunting Creek study – 2017

Scientific Name	**Common Name**	**Fyke Far**	**Fyke Near**
Ameiurus nebulosus	Brown Bullhead	4	0
Carassius auratus	Goldfish	56	55
Enneacanthus gloriosus	Bluespotted Sunfish	22	4
Etheostoma olmstedi	Tessellated Darter	1	1
Fundulus diaphanus	Banded Killifish	46	50
Lepomis cyanellus	Green Sunfish	4	0
Lepomis gibbosus	Pumpkinseed	101	75
Lepomis macrochirus	Bluegill	162	38
Lepomis species	Unidentified Sunfish	97	51
Menidia beryllina	Inland Silverside	12	0
Micropterus dolomieu	Smallmouth Bass	2	8
Morone americana	White Perch	50	8
Morone saxatilis	Striped Bass	4	0
Notropis hudsonius	Spottail Shiner	2	0
Perca flavescens	Yellow Perch	1	0
Total		**565**	**289**

H. Submersed Aquatic Vegetation – 2017

SAV data overflights by VIMS were conducted in 2017 as in most previous years (Figure 94). As can be seen the coverage of the shallow portions of the Hunting Creek embayment is almost complete by the end of the growing season as in recent years.

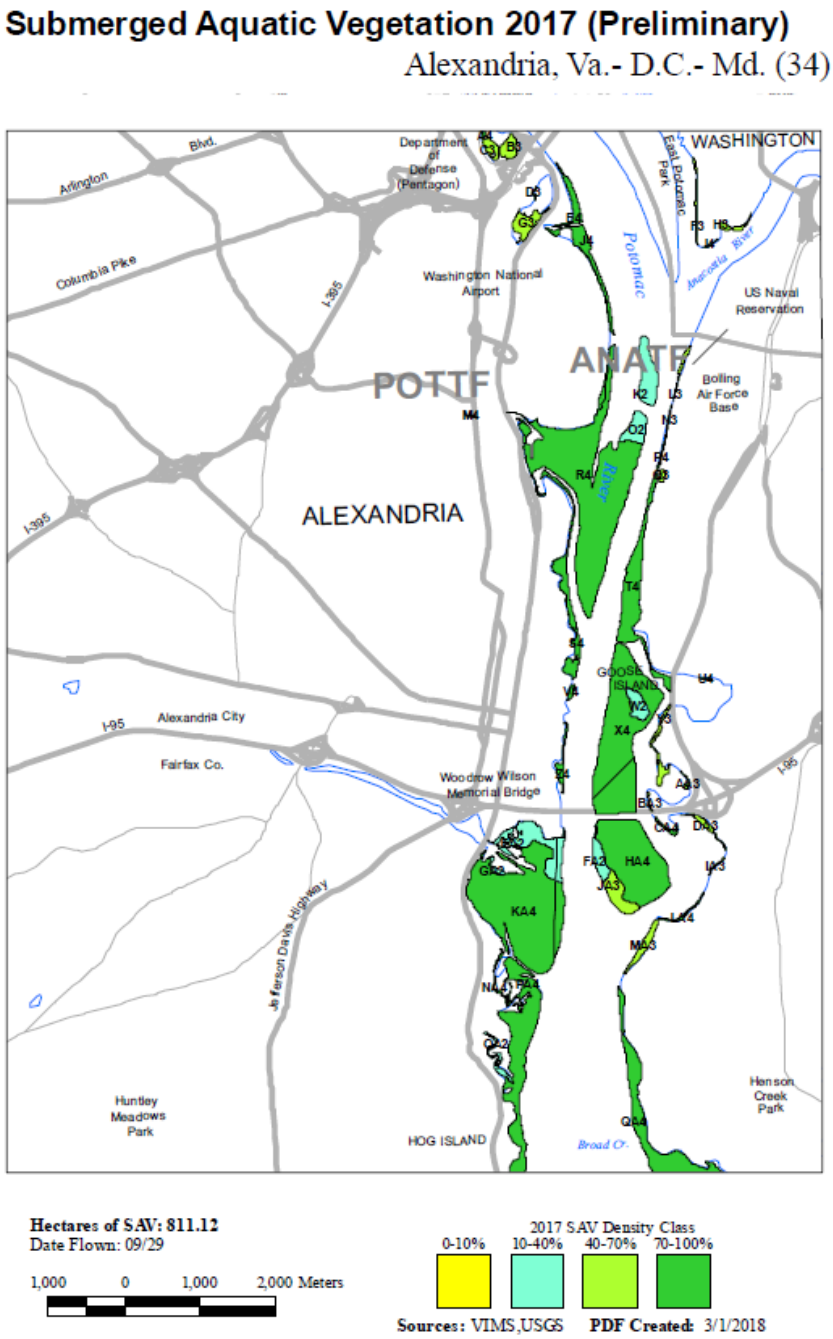

Figure 94. Distribution and density of Submersed Aquatic Vegetation (SAV) in the Hunting Creek area in 2016. VIMS (http://www.vims.edu/bio/sav/index.html). Area enclosed by red square is the area depicted in each of the Figure 112 maps.

We also assessed the relative abundance of various SAV species as part of the data mapping cruises on July 12 and August 10 (Table 14). Coontail, a native species, was the dominant species on both dates and its density did not change appreciably from July to August. Hydrilla, an introduced species which is considered invasive, was second most abundant in July. It decreased slightly in August and was displaced as subdominant by another native species Water Stargrass. Two Naiad species were moderately abundant. Filamentous algae was rare in July, but in August was often found overtopping the angiosperm SAV species.

Table 14. Average Density of Submersed Aquatic Vegetation Species in Transects. Average included all sites with water depth less than or equal to 2 m.

		Average Density per sample by SAV Species	
Taxon Scientific Name	Taxon Common Name	July 12	August 10
Ceratophyllum demersum	Coontail	1.76	1.74
Heteranthera dubia	Water Stargrass	0.19	1.19
Hydrilla verticillata	Hydrilla	0.78	0.32
Najas guadalupensis	Southern Naiad	0.20	0
Najas minor	Spiny Naiad	0.45	0.21
Various	Filamentous algae	0.03	0.43

Some photographs of SAV are also shown below (Figure 95).

Figure 95 (a) Hunting Creek embayment showing almost complete coverage by SAV on July 20, 2017. (b) Clumps of the native SAV species *Heteranthera dubia* (water stargrass) on August 10, 2017.

I. Benthic Macroinvertebrates - 2017

River and Embayment Samples

Triplicate petite ponar samples were collected AR2, AR3, and AR4 monthly from May through September. Averages over samples collected at each station are shown in Figure 96.

Taxonomic Groups: Annelid worms (including Oligochaetes, Polychaetes, and Leeches) were found in high numbers (total N = 1,740) at each site over all dates. Overall, they accounted for 57% of all benthic organisms found. Oligochaetes were the dominant taxonomic group, accounting for 95% of individuals.

Crustaceans (including Gammarid amphipods and isopods) were the second highest in abundance across sites and dates, accounting for 23% of all individuals (N = 696). Gammarid amphiods (scuds) dominated this group, accounting for 94% of all crustaceans observed.

The remainder of the taxonomic groups accounted for minor components of the overall diversity. These included Bivalvia (N = 107; 3.5% of total abundance), Turbellarians (i.e., flatworms) (N = 196; 6.4%), Gastropods (N = 183; 6%), and Insecta (N = 151; 4.9%). All of these taxonomic groups were found at each site and sampling month. The bivalve group was dominated by the invasive Asian clam, *Corbicula fluminea*, which accounted for 85% of all bivalves documented. Other individuals were from the family Sphaeriidae. The gastropod (i.e., snails) group was composed of taxa from Planorbidae, Viviparidae, Lymaneidae, Bithyniidae, Hydrobiidae. The most dominant family was Viviparidae, accounting for 72% of all gastropods found. Insects from multiple orders were found, but they were dominated by Chironomids (midges) which accounted for 87% of all insects. The remainder was composed of small numbers of phantom midges, riffle beetles, dragonfly nymphs, crane fly larvae, and caddisfly larvae.

Spatial trends: The total and average abundance of organisms was highest at the AR2 site over time, which is the closest location to Hunting Creek, and decreased spatially as sites were sampled further into the Potomac River. In general, all three sites were dominated by Annelida, driven by high abundances of Oligochaete, and Crustaceans (mostly Gammarid amphipods). Sites AR2 and AR3 had a higher diversity of taxa than the Potomac River site, likely due to differences in sediment and flow characteristics. Other dominant taxa at the AR2 and AR3 sites included Insecta (mostly Chironomids and Caddisflies), Turbellairans (i.e., flatworms), and Gastropoda (i.e., snails). The only taxa to increase in abundance from the bay to the river site were Bivalva (mostly the invasive Asian clam *Corbicula fluminea*).

Temporal trends: Across the months, Annelids (mostly Oligochaetes) were the dominant taxa except for July when Crustaceans (mostly Gammarid amphipods) dominated. Insecta (mostly Chironomids and Caddisflies) also contributed as dominant taxa during the early part of the sampling period, while Turbellairans (i.e., flatworms) were dominant later. There was a seasonal increase in Crustaceans driven by Gammarid amphipods, which peaked during July most likely due to recruitment. Across the months, Bivalve abundances, consisting mostly of the invasive Asian clam *Corbicula fluminea*, stayed constant. Turbellairan abundances increased later in the

sampling period during August and September. The lowest abundances of insect larvae across all sites occurred during July, but abundances were relatively constant outside of July. Annelids, composed of Oligochaete, Polychaetes, and Leeches, were dominant taxa recorded during all months but had highest abundances during September. Gastropod abundances were also highest during the later part of the sampling period and were driven by abundances of snails from the Viviparidae and Hydrobiidae families. Overall, larger increases in abundances over the sampling period for many of the taxa described above are in direct relation to seasonal changes and recruitment.

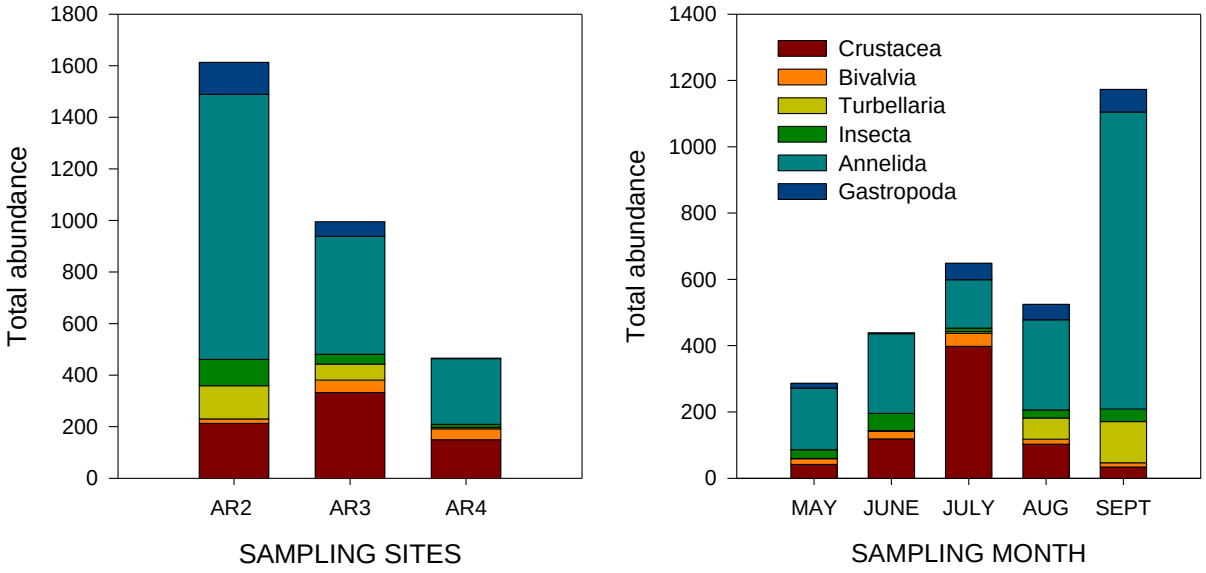

Figure 96a and b. Total abundance of benthic macroinvertebrate taxa in petite ponar samples collected in 2017 separated by: (a) site and (b) month.

Tributary Samples

Duplicate kick net samples were taken in six tributaries of Hunting Creek during October 2017. The exact locations of the sampling sites is given in Table 15. The first 200 randomly selected individuals from each sample were identified to lowest taxonomic unit, usually genus, except for Oligochaetes (aquatic worms) and Chironomidae (midges).

Table 15. Location of Tributary Benthos Sampling Stations

Station ID	Stream	Sampling Date	Location on Stream
CR1	Cameron Run	Oct 17 2017	Just below Metrorail bridge
BR1	Backlick Run	Oct 17 2017	At trail bridge just upstream of the confluence with Holmes Run
TR1	Turkeycock Run	Oct 2 2017	In Bren Mar Park just above Edsall Road
IR1	Indian Run	Oct 2 2017	Just below Bren Mar Drive crossing
HR1	Holmes Run	Oct 17 2017	First riffle upstream of confluence with Backlick Run
HR2	Holmes Run	Oct 2 2017	Holmes Run Park just below pedestrian bridge at Pickett Street

Taxonomic Groups: The five most abundant taxa observed included three groups of insect larvae – Chironomids (midges), Trichoptera (caddisflies of the family Hydropsychidae), and Ephemeroptera (mayflies of the family Baetidae). In addition, Turbellarians (i.e., flatworms) and Oligochaete worms were dominant groups (Figure 97a). All other taxa were significantly less abundant and included Trichoptera (caddisflies of the family Philopotamidae), Crustaceans (Gammarid amphipods), and Dipteran larvae (family Tipulidae). Of the less abundant taxa, none of these were present at all sites, and only the Philopotamidae reached a total abundance across sites of >100 (Figure 97b).

Spatial trends: Cameron Run and Holmes Run-2 had the highest abundances of the five dominant taxa (N = 385 and 386, respectively). Interestingly, dominant taxa differed by site. Hydropsychidae larvae (caddisflies) were the dominant group (N>100) at 2 of the sites (i.e., Backlick Run and Holmes Run-1), and Baetidae larvae were dominant at both Holmes Run-2 and Turkeycock Run. Cameron Run was dominated by Oligochaetes, which were the highest values observed across all sites. Indian Run had highest numbers of Philopotamidae larvae (characterized by very low abundances of <50 at other sites).

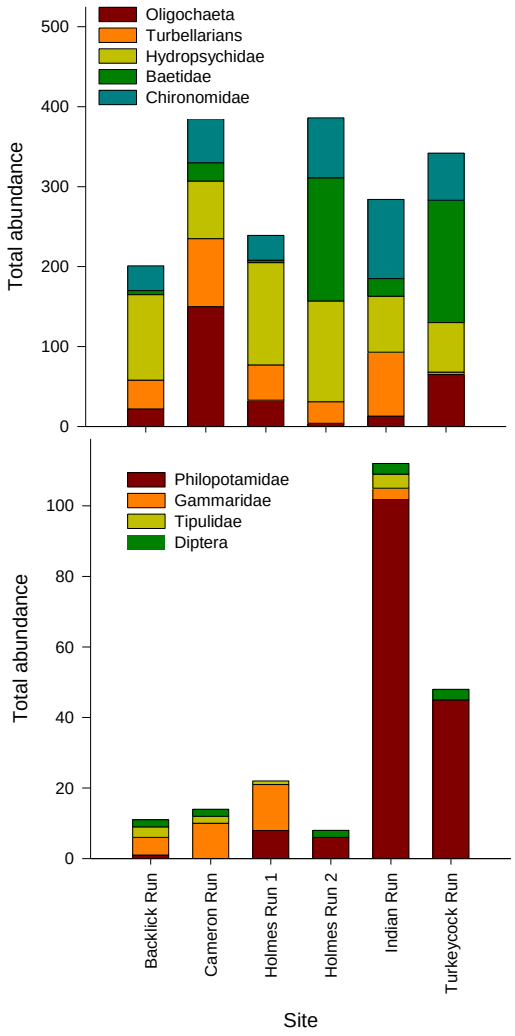

Figure 97a and b. TOP (a): Total abundance of the five dominant benthic invertebrate taxa in tributary kick samples. BOTTOM (b): Total abundance of four less dominant benthic invertebrate taxa in tributary kick samples.

Benthic Invertebrate Community Metrics: In general, increasing taxa richness reflects increasing water quality, habitat diversity, or habitat suitability. Taxa richness across all five sites ranges from 9 to 13 taxa, with lowest richness at Cameron Run and Holmes Run 1 and highest richness at Backlick Run and Turkeycock Run (Table 16).

A subset of abundance, EPT abundance is the cumulative abundance of individuals from the generally more environmentally sensitive Insecta groups Ephemeroptera, Plecoptera, and Trichoptera. In general, if the EPT abundance is ≤ 1, then conditions are poor. If between 2 and 5, then conditions are moderate. If ≥ 5, then conditions are good. EPT abundance in each of the five sampled locations was between 2 and 4, indicating that the environmental conditions at these sites is moderate.

The Insecta group Ephemeroptera is considered a particularly environmentally sensitive group. Calculating the percentage of total organisms that are Ephemeroptera provides another metric for stream condition. In this case, if the value is >40%, then conditions are good. If the value is between 20 and 40%, then conditions are moderate. If the value is < 20%, then conditions are poor. In all cases, percentage values are <20% (poor conditions) except for Holmes Run 2 and Turkeycock Run, both of which have ~38% Ephemeroptera, indicating moderate conditions.

The Hilsenhoff Biotic Index (HBI) estimates the overall tolerance of the community in a sampled area toward organic (nutrient) enrichment, weighted by the relative abundance of each taxonomic group (family, genus, etc.). Organisms are assigned a tolerance number from 0 to 10 pertaining to that group's known sensitivity to organic pollutants; 0 is most sensitive, 10 is most tolerant. Low HBI values reflect a higher abundance of sensitive groups, thus a lower level of pollution. Family-level tolerance values from USEPA (Barbour et al. 1999) were used for organisms that could not be identified to the genus level because of size or condition. Taxa with tolerance values ≤3 were considered *intolerant*, whereas those with values ≥7 were considered *tolerant.* Low HBI (≤3.75) values reflect a higher abundance of sensitive groups, indicative of a lower level of pollution. Only one site, Holmes Run 1, is considered "good" with some organic pollution probable (values between 4.26 and 5). Three others (Backlick Run, Cameron Run, and Indian Run) are considered "fair" with fairly substantial organic pollution likely (values 5.01-5.75), and two (Holmes Run 2, Turkeycock Run) would be considered "fairly poor" with substantial organic pollution likely (values 5.76 – 6.50).

The percent of organisms that are clingers, which are those that have fixed retreats or adaptations for attachment to surfaces in flowing water is another indicator of environmental quality. Increasing metric values indicate increasing substrate stability. In this case, if the value is >40%, then conditions are good. If the value is between 20 and 40%, then conditions are moderate. If the value is < 20%, then conditions are poor. Two locations (Backlick Run and Holmes Run 1) had values >40%, indicating good substrate stability, while one location (Cameron Run) had poor conditions. The three other sites were considered to be moderate.

Using these five measures of biological health, we can calculate a summary statistic of relative overall health of these streams. In this case, we assign values of high (5), moderate (3), or low (1) health for each metric at each site, sum these values for each site and divide by 25 (i.e., the maximum score achievable). Streams characterized as "good" would achieve summary statistics of 90% or better of the maximum summary statistic. "Moderate" streams would be between 75 and 89%, and "poor" streams would come in at 75% of the summary statistic. Using the criteria for each metric laid out above, all of the streams scored between 44% and 68% of the maximum summary statistic. This indicates that all sampled streams are in poor condition based on these five metrics.

Table 16. Benthic invertebrate community metrics. EPT include the Insecta from Ephemeroptera, Plecoptera, and Tricoptera. % E refers to just those from the Ephemeroptera.

	Taxa Richness	EPT Abundance	% E	Hilsenhoff Biotic Index	% Clingers	Summary Statistic
Backlick Run	13	4	2.75	5.19	50.00	60%
Cameron Run	9	2	5.75	5.38	18.00	44%
Holmes Run 1	9	3	1.12	4.83	50.75	68%
Holmes Run 2	11	4	38.75	5.90	33.75	52%
Indian Run	12	3	5.50	5.67	43.25	60%
Turkeycock Run	13	3	38.25	5.82	27.75	52%

Water quality variables were measured on the date of benthic sampling (Table 17) and were generally supportive of aquatic life. It is important to note that all streams were at base flow conditions during the sampling period; water quality is expected to be more degraded during high flow.

Table 17. Water Quality Results from Tributary Benthos Sampling

Station ID	Temp (°C)	SpCond (uS/cm)	DO (mg/L)	DO (%)	pH	Turbidity YSI units	Chlorophyll a (µg/L)
CR1	17.78	408	11.87	125	7.09	2.5	2.1
BR1	14.84	447	9.40	93.1	7.30	33.7	1.4
TR1	15.49	492	8.81	88.2	7.41	-1.4	1.2
IR1	15.29	499	8.58	85.8	7.31	-0.5	0.8
HR1	16.37	301	9.87	101.1	7.55	2.2	2.1
HR2	18.94	395	9.82	105.9	7.73	0.3	1.5

DISCUSSION

A. 2017 Synopsis

In 2017 air temperature was substantially above average in April and June, but near normal the remainder of the year. July was the warmest month, with June being untypically warmer than August. Precipitation was well above normal during May and July, near normal in March, April and August, and below normal in the other months. To better understand relationships between flow events and Hunting Creek ecology, time course graphs were constructed overlaying the sequence of precipitation, stream/river flow, and water quality/plankton sampling dates (Fig. 98a,b). During May and July Cameron Run flows were often substantially elevated due to frequent precipitation events. These would be expected to affect water quality in the study area especially AR2 and AR3. In the mainstem Potomac flows were below normal in April, but well above normal in May. These would have most relevant for events at AR4.

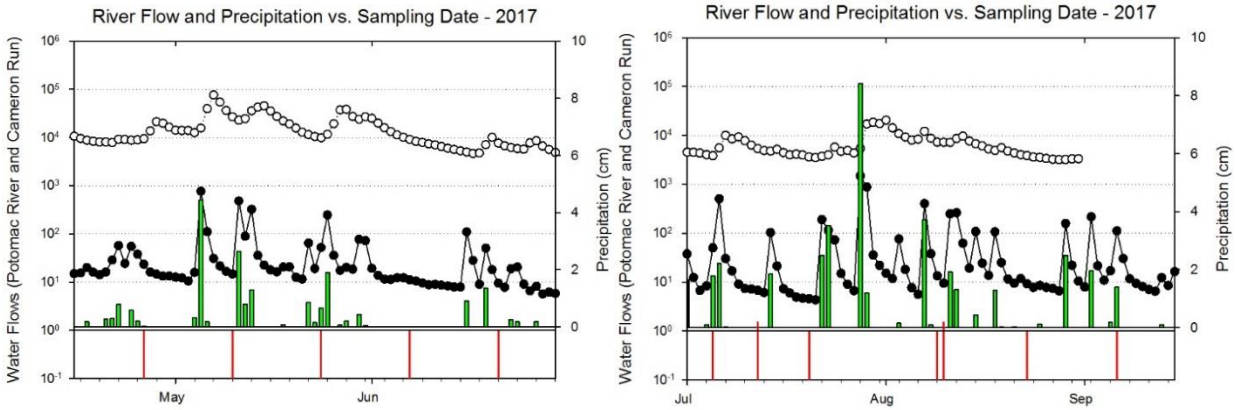

Figures 98a, b. Precipitation (green bars), Cameron Run flows (solid circles), Potomac River flows (open circles) and water quality/plankton sampling events (red lines at bottom).

Based on these graphs and the antecedent precipitation data from Table 1, it appears that May 10, May 24, July 5, and August 9 were the profile-plankton sampling dates predicted to be most strongly affected by water runoff from rainfall events. The largest one day rainfall total was in late July, but the next sampling date after this was August 9.

Water temperature followed a typical seasonal pattern at all stations. The temporary cooling events observed in early May and early August both followed cold front passage through the area. The data mapping cruises generally showed higher temperatures in the shallow embayment than in the river mainstem. Following a decline in early May, specific conductance and chloride showed a general gradual increase seasonally with another decline in early August in the wake of increased inflow. AR1, at the GW Parkway bridge, had elevated specific conductance and chloride throughout the year except in August. Dissolved oxygen was generally in the 80-120 percent saturation range indicating that neither photosynthesis nor respiration was excessive. Exceptions to this pattern were most of the year at AR2 and during late summer at AR3. The consistent low values at AR2 are of special concern as they dropped below 4 mg/L on several occasions. On the two data mapping dates, low DO's were not observed. Field pH was generally in the 7-8.5 range at all stations. Exceptions to this were higher values observed at AR3 in late

June and late July due to SAV photosynthesis and lower values at AR1 and AR 4 in late July of unknown origin. Data mapping showing small areas of elevated pH in the embayment on each date. Total alkalinity was generally 60-100 mg/L as $CaCO_3$. Values tended to increase over the study period.

Secchi disk depth was generally 0.6-1.0 m. For most of the year values were missing at AR2 and AR3 because the Secchi disk reached bottom or plant growth before disappearing. Light attenuation coefficient was quite low (clear water) in April, but increased by early May to values between -2.0 and -4.0 m^{-1} presumably due to the water runoff input from the recent storms in the days leading up to sampling. The July 5 and August 9 values did not seem to be affected by those runoff events. AR3 in the middle of the SAV beds had consistently clearer water. Turbidity was generally in the range 0-25 NTU at AR1, AR2, and AR3. All stations exhibited an increase in turbidity (less clear water) in early May and there was also an increase on August 9, but no clear signal on July 5. The data mapping confirmed the observation from biweekly data that the river mainstem was generally more turbid (less clear) than the Hunting Creek embayment.

Ammonia nitrogen showed a general decrease from May through September with lower values generally at AR2 and AR3 and higher values at AR1 and AR4. But all values were quite low (<0.2 mg/L). Nitrate nitrogen showed a clear seasonal decline at AR2 and AR3 from values of about 1.0 mg/L in spring to levels below 0.5 mg/L in late summer, probably due to phytoplankton and macrophyte uptake. Little seasonal change was observed at the other two stations. Nitrite was very low at all stations and did not show consistent seasonal patterns. Organic nitrogen was mostly in the range 0.3-0.7 mg/L with little seasonal change. Total phosphorus was less than 0.1 mg/L except for the early May storm aftermath at AR1 and AR2. Ortho-P showed a general gradual decline seasonally starting in May. N/P ratio exhibited some seasonal patterns, but remained above 7.2, consistently pointed to P limitation of primary producers. Biochemical oxygen demand was usually below detection limit so this data is not very useful anymore. Total suspended solids was generally in the range 0-20 mg/L except at AR2 where values were consistently higher. There was some increase at the other stations in early May and at AR1 in early July. VSS values were generally much lower. Again, highest values were normally at AR4.

In the tributaries, water temperature also generally followed air temperature with a gradual rise in the spring and summer through late July. An early August cooling period was apparent followed by warmer temperatures in late August. Specific conductance was generally 400-600 uS/cm except in early May at Cameron Run mainstem sites when values were clearly elevated. High chlorides were observed at the same time suggesting elevated salt concentrations. Dissolved oxygen was generally 80-120 percent saturation with a marked decline in early July. pH values were consistently 7-8, fairly constant in lab readings, but with a slight increase late in the year in field readings. AR11, the Lake Cook station, showed by far the highest turbidity and chlorophyll a readings probably due to the impounded nature of the water and the work that was going on in the lake. Total alkalinity was fairly uniform in all of the tributaries early in the year, but became more variable later. Total phosphorus and ortho-phosphorus were low on most dates and at most tributary stations. Lake Cook (AR11) showed greatly elevated levels in summer. Organic nitrogen and ammonia nitrogen were also elevated at AR11 later in the year with higher levels in ammonia also observed at AR21, Cameron Run just below the Lake Cook inflow.

Nitrate nitrogen showed a different pattern with elevated values at AR13 and AR23, Hoof Run and Cameron Run below Hoof Run. TSS and VSS were low to moderate at all stations except at AR11 in late summer.

Phytoplankton biomass as indicated by chlorophyll a remained low in the spring (< 3 µg/L) through June. By early July chlorophyll a had increased substantially in the river at AR4 to levels of about 10 µg/L. Levels at the other stations increased less dramatically. At AR4 chlorophyll declined in late July and early August and reached another peak near 10 µg/L in late August. At AR3 relatively high levels were found in September. The data mapping cruise in July confirmed that the higher levels at AR4 were indicative of the river channel. It is important to note that even the highest levels observed are quite low relative to historical levels.

Phytoplankton cell density was generally fairly constant and very similar at AR2 and AR4. The major exception was in late July when cell density increased strongly at both stations. These peaks in cell density did not correspond with peaks in chlorophyll a. At both sites, cyanobacteria were dominant at the time of the cell density peak with *Oscillatoria* and *Merismopedia* being the most numerous genera.

Phytoplankton biovolume exhibited a dramatic peak in early July at AR4 and this did correspond with a peak in chlorophyll a. On this date at AR4 biovolume was strongly dominated by the filamentous diatom *Melosira*. In general, biovolume was strongly dominated by diatoms on most dates at both AR2 and AR4 with discoid centrics being the most common dominants.

Ploesoma dominated rotifer populations in the cove from April through June with *Brachionus* most important in early July and mixed dominance for the rest of the year. In the river *Keratella* was dominant in the spring, *Brachionus* in July and *Keratella* again in August and September. Maximum rotifer densities were lower than in most previous years and similar in both areas. The small bodied cladoceran *Bosmina* was generally present at lower than normal densities except for a strong surge in September at AR4. The larger-bodied cladoceran *Diaphanosoma* attained fairly high levels of about 1200/m^3 in late June at AR2, but was virtually absent at AR4. *Daphnia* was virtually absent at both stations in 2017. *Ceriodaphnia* showed a single sharp peak at AR2, but was scarce at AR4. *Sida* was similarly abundant in late June at AR2. *Leptodora* reached a peak of 40/m^3 in late June at AR2 at a lower peak of 15/m^3 at AR4 in late July. Chydoridae and Macrothricidae were found at high levels in late August almost exclusively at AR2 consistent with their affinity for the SAV habitat. Copepod nauplii were generally more abundant at AR2, but followed a similar seasonal pattern at both sites with a strong peak in late June. *Eurytemora* was fairly abundant at both stations in late April, but bloomed strongly in late August at AR4 attaining a density of almost 1600/m^3. *Diaptomus* exhibited a stronger than normal peak in late June at AR2. Cyclopoid copepods exhibited two respectable peaks at AR2, late June and early September.

B. Correlation Analysis of Hunting Creek Data: 2013-2017

To better understand the ecological relationships in Hunting Creek and the nearby Potomac River, relationships among parameters were assessed using correlation analysis. Due to the uncertain statistical distribution of some parameters, the correlations were conducted using the

Spearman rank correlation coefficient rather than the Pearson coefficient. Since all samples were collected by PEREC personnel at the same time, it was possible to pool the data on all field and lab water quality parameters at the level of depth-averages and/or surface samples. Three tables were constructed: PEREC field and lab parameters with each other, ARE lab parameters with each other, and PEREC field parameters against ARE lab parameters.

Table 16 shows the correlations among PEREC-collected water quality parameters from the regular sampling. These reflect relationships over all five years. Indicators of photosynthesis (DOPPM, DOSAT, Field pH) were highly intercorrelated. Also, measures of particles in the water column and resultant water clarity (turbidity, Secchi disk depth, and extinction coefficient) were also highly intercorrelated. Interestingly, phytoplankton chlorophyll was not significantly correlated with indicators of photosynthesis, suggesting that another photosynthetic group, SAV, was the major driver of photosynthesis. There was a very good correlation between the different measures of extracted chlorophyll and pheopigment. Overall there was a fairly good correlation between depth-integrated and surface chlorophyll (measured by extraction in the lab) and YSI chlorophyll (measured *in situ* with a less refined sensor). Interestingly, there was a significant correlation between specific conductance and depth-integrated chlorophyll which may related to the fact that both tend to increase seasonally.

Table 16. Correlations among PEREC collected water quality parameters from regular sampling. Depth-integrated samples unless otherwise indicated. All Stations. 2013-2017. Strongest correlations (r>0.400) are have **bolded** text. Yellow: indicators of photosynthesis. Blue: indicators of water clarity. Green: indicators of phytoplankton abundance.

Spearman Correlation Matrix	TEMP	SPC	DOPPM	DOSAT	SD	CHLDI	PHEODI	CHLSF	PHEOSF	FLDPH	EXTCOE	YSITUR	YSICHL
TEMPC	1.000												
SPC	0.199	1.000											
DOPPM	-0.380	-0.277	1.000										
DOSAT	-0.022	-0.230	**0.899**	1.000									
SECCHI	0.081	0.097	0.054	0.055	1.000								
CHLDI	0.328	**0.457**	-0.087	0.039	-0.092	1.000							
PHEODI	0.388	**0.476**	-0.237	-0.115	-0.153	**0.833**	1.000						
CHLSF	0.337	0.288	-0.110	0.043	-0.144	**0.941**	**0.792**	1.000					
PHEOSF	0.295	0.315	-0.197	-0.088	-0.278	**0.808**	**0.875**	**0.844**	1.000				
FIELDPH	0.117	-0.350	**0.468**	**0.518**	0.217	0.055	-0.015	0.050	0.021	1.000			
EXTCOEF	0.164	0.122	-0.055	-0.014	**0.802**	-0.075	-0.153	-0.122	-0.228	0.201	1.000		
YSITURB	-0.128	-0.279	0.084	0.049	**-0.602**	0.187	0.267	0.193	0.209	-0.129	**-0.627**	1.000	
YSICHL	0.259	0.089	-0.084	0.018	-0.324	**0.618**	**0.589**	**0.638**	**0.630**	0.169	-0.250	0.338	1.000

TEMP – water temperature (°C), SPC – specific conductance (µS), DOPPM – dissolved oxygen (mg/L), DOSAT – dissolved oxygen (% saturation), SD - secchi disk depth (m), CHLDI – depth-integrated chlorophyll a (µg/L), PHEODI – depth-integrated pheopigiment (µg/L), CHLSF – surface chlorophyll a (µg/L), PHEOSF – surface pheopigment (µg/L), FLDPH – field pH, EXTCO (light attenuation coefficient (m^{-1}), YSITUR – Turbidity as measured by YSI sonde *in situ*, YSICHL – chlorophyll a (µg/L) as measured by YSI sonde *in situ*. n = 146-211.

The correlation coefficients among AR lab parameters are shown in Table 17. Among the most highly correlated variables in this dataset were TSS and VSS (0.855). Total P was positively

correlated with TSS and VSS. Most phosphorus is bound to particles so these correlations make sense. TP was negatively correlated with N to P ratio and this makes sense since it is in the denominator of this ratio. Lab pH was negatively correlated with ammonia nitrogen, but this may just reflect that lab pH is highest in summer when ammonia nitrogen is lowest. Other correlations were not strong.

Table 17. Correlation coefficients between AR lab parameters. All Stations. 2013-2017. Strongest correlations highlighted in yellow.

	PHLAB	ALK	TP	OP	ON	NO3	NH4	NO2	CLD	TSS	VSS	BOD	NTOP
PHLAB	1.000												
ALK	0.371	1.000											
TP	-0.256	-0.312	1.000										
OP	-0.376	-0.300	0.190	1.000									
ON	-0.242	-0.142	0.387	-0.101	1.000								
NO3	-0.286	-0.270	0.369	0.147	-0.082	1.000							
NH4	**-0.527**	-0.274	**0.496**	**0.411**	0.205	0.365	1.000						
NO2	-0.035	0.135	0.073	-0.034	0.273	-0.048	0.220	1.000					
CLD	-0.228	0.014	-0.052	-0.094	0.209	0.099	0.069	0.085	1.000				
TSS	-0.183	-0.030	**0.637**	0.141	0.272	0.360	**0.488**	0.132	-0.164	1.000			
VSS	-0.185	-0.016	**0.588**	0.196	0.342	0.238	**0.417**	0.193	-0.130	**0.855**	1.000		
BOD	0.040	-0.143	0.357	-0.013	0.297	0.194	0.132	0.298	0.025	0.256	0.355	1.000	
NTOP	-0.097	0.102	**-0.664**	-0.088	-0.148	0.261	-0.121	0.035	0.222	-0.339	-0.362	-0.076	1.000

PHLAB – lab pH, ALK – total alkalinity (mg/L as $CaCO_3$), TP – total phosphorus (mg/L), OP – orthophosphorus (mg/L), NO3N – nitrate nitrogen (mg/L), NH4N – ammonia nitrogen (mg/L), NO2N – nitrite nitrogen (mg/L), CLD – chloride (mg/L), TSS – total suspended solids (mg/L), VSS – volatile suspended solids (mg/L), BOD – biochemical oxygen demand (mg/L), NTOP – nitrogen to phosphorus ratio by mass. n= 164-211.

Table 18. Correlation coefficients between PEREC and AR parameters. 2013-2017.

	TEMPC	SPC	DOPPM	DOSAT	SECCHI	CHLDI	CHLSF	FIELDPH	EXTCOEF	YSITURB	YSICHL
PHLAB	0.349	-0.134	0.230	0.353	0.398	0.209	0.201	0.636	0.351	-0.142	0.261
ALK	0.388	0.217	-0.247	-0.138	0.309	**0.412**	0.344	0.184	0.329	-0.134	0.175
TP	-0.174	-0.191	0.044	-0.017	**-0.432**	0.072	0.051	-0.249	**-0.485**	**0.584**	0.035
OP	-0.262	-0.207	0.148	0.051	-0.071	-0.312	-0.271	-0.098	-0.202	0.155	-0.250
ON	0.163	0.395	-0.189	-0.108	-0.307	**0.406**	0.294	-0.305	-0.217	0.151	0.199
NO3	-0.374	-0.100	0.165	0.054	-0.235	-0.054	-0.029	-0.278	-0.234	0.274	-0.121
NH4	-0.382	0.046	-0.126	-0.285	-0.320	0.017	0.017	**-0.434**	**-0.475**	0.388	-0.055
NO2	0.288	0.233	-0.374	-0.296	-0.158	0.263	0.269	-0.219	-0.099	0.125	0.254
CLD	0.117	**0.554**	-0.193	-0.193	-0.052	0.089	-0.007	-0.336	0.004	-0.208	-0.137
TSS	-0.170	-0.189	-0.008	-0.032	**-0.420**	0.283	0.287	-0.180	**-0.495**	**0.764**	0.235
VSS	-0.072	-0.134	0.017	0.020	**-0.414**	0.311	0.283	-0.155	**-0.521**	**0.685**	0.252
BOD	0.147	-0.029	-0.046	0.037	-0.256	0.327	0.343	-0.078	-0.121	0.243	0.306
COD	0.076	0.015	0.172	0.204	-0.377	0.149	-0.011	-0.269	-0.184	0.315	-0.193
NTOP	-0.020	0.303	-0.095	-0.084	0.137	0.054	0.033	-0.133	0.272	-0.350	-0.087

See Table 16 and 17 for most abbreviations. n = 121-211.

Table 18 contains the correlation coefficients between PEREC and AR parameters. As expected YSI Turbidity was highly correlated with TSS and VSS and also with TP. EXTCOEF and SD

showed similar, but slightly weaker correlations with TSS, VSS and TP. The correlation between SPC and CLD would also be expected as chloride is the dominant anion contributing to SPC.

C. Water Quality: Comparison among Years

Since five years of data are now available for the Hunting Creek area, comparisons were made for each parameter among years. And many of the parameters vary seasonally as well as among stations. In order to assess overall patterns in the data among years, stations, and seasonally, box plots were constructed. In a box plot, the spread of the middle 50% of the data is shown by a box with a line in the middle which is the median. Two plots were constructed for each parameter: one comparing years by station, the other comparing months by station. In the month graph months were indicated by a number starting with 4 for April.

Temperature did not show much difference between the years with the medians in the 22-26ºC range at all sites and years (Figure 99a). A more distinct pattern was observed seasonally with all stations showing a clear and steady rise in spring from values near 17ºC in April to 25-30ºC in July and August followed by seasonal decline in September (Figure 99b). This trend was apparent across all stations and seasons.

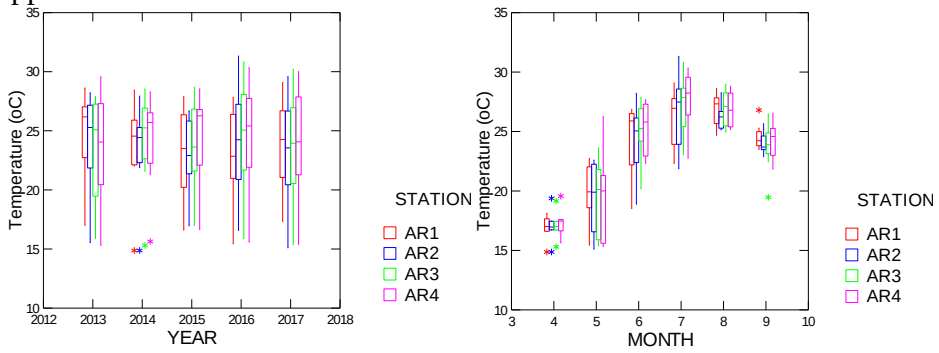

Figure 99. Box plots comparing values of Temperature between years (left) and by season (right).

Specific conductance showed clear differences among stations with AR 1 consistently higher, probably due to input from AR effluent although in 2016, the values at AR1 overlapped extensively with the other stations (Figure 100a). There was little consistent difference among years among the other three stations. At these three other sites, there was a clear seasonal pattern with a general increase from April through September (Figure 100b). At AR 1 values showed less consistent seasonal patterns.

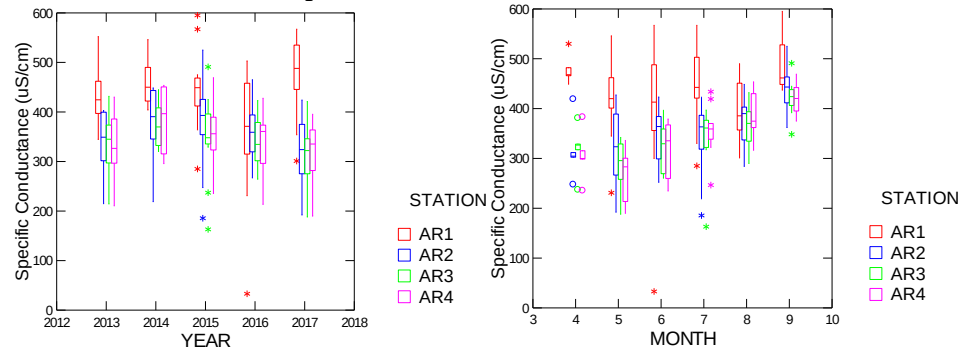

Figure 100. Box plots comparing values of Specific Conductance between years (left) and by season (right)

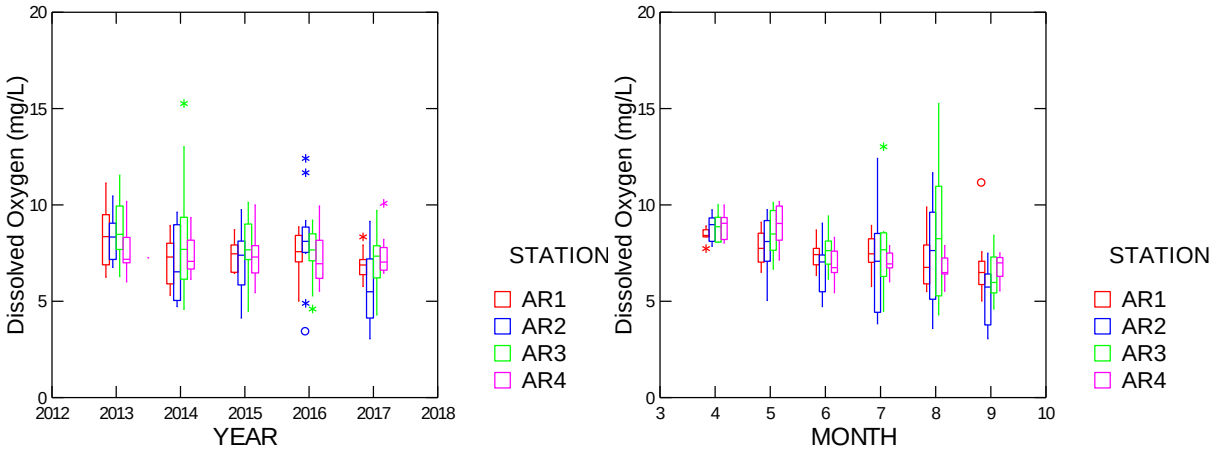

Figure 101. Box plots comparing values of dissolved oxygen as mg/L between years (left) and by season (right).

The most obvious aspect of 2017 data was that the median and interquartile range at AR2 indicated lower values in 2017 than in other years (Figure 101a). The interquartile range at AR3 was higher than normal indicating a greater range of values. There were several readings at AR2 that was below the DO standard of 5 mg/L. Values were generally highest in April, except at AR2 and AR3 where July and August exhibited some higher values due to photosynthesis (Figure 101b). Dissolved oxygen (as % saturation) exhibited similar patterns (Figure 102a,b).

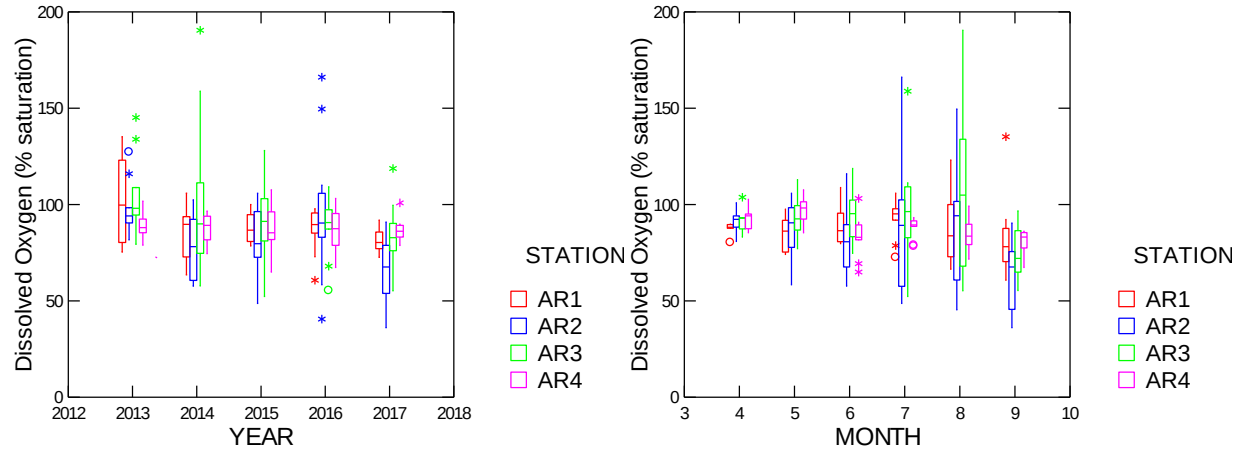

Figure 102. Box plots comparing values of dissolved oxygen as percent saturation between years (left) and by season (right).

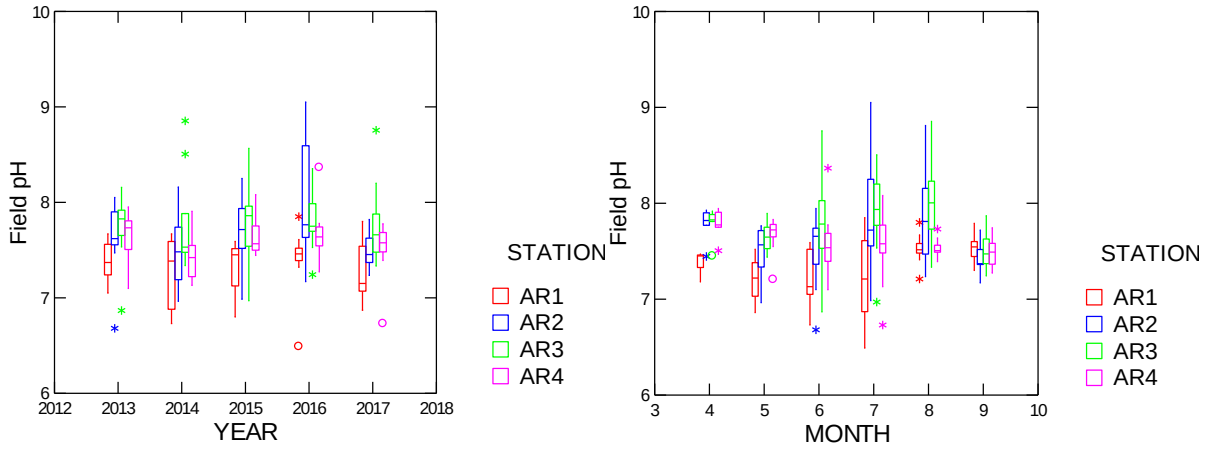

Figure 103. Box plots comparing values of field pH between years (left) and by season (right).

Field pH was consistently lowest at AR1 though still in a healthy range (Figure 103a). Generally AR3 was the highest and AR2 was second highest and the elevated values at these sites was most obvious in July and August (Figure 103b), periods of high SAV abundance. Secchi disk depth (Figure 104a) did not show any obvious interannual or seasonal patterns, but was generally highest at AR3. There are many missing values at AR2 and AR3 in the summer and fall due to the encroachment of SAV into the watercolumn and the shallow dept of these areas (Figure 104b). Secchi disk measurements were discontinued at AR1 when a new sampling protocol was instituted there.

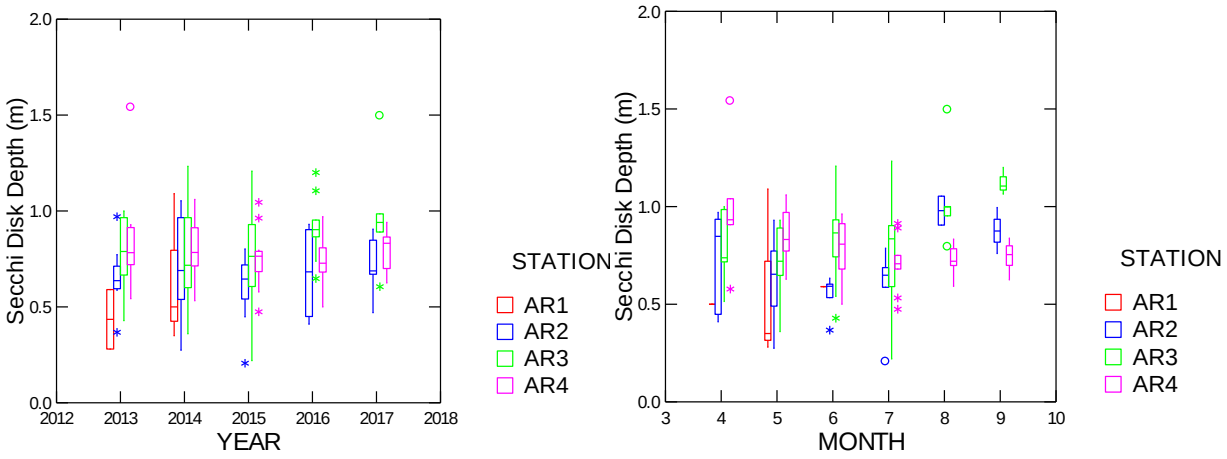

Figure 104. Box plots comparing values of Secchi disk depth between years (left) and by season (right).

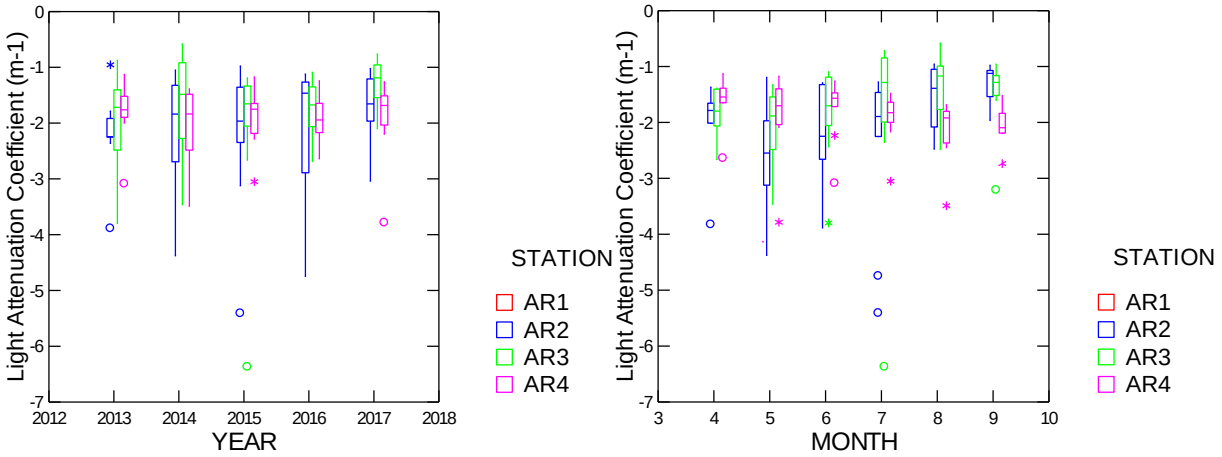

Figure 105. Box plots comparing values of Light Attenuation Coefficient between years (left) and by season (right).

Light attenuation coefficient and turbidity are two other ways of measuring water clarity: less negative values of light attenution coefficient indicate clearer water. Median values in light attenuation coefficient were similar from year to year (Figure 105a). The range of values was greatest at AR2. There was little consistent seasonal pattern at most stations, but at AR3 less negative values were observed in July and August (Figure 105b).

Turbidity, another measure of water clarity, increased at AR4 from 2013 to 2014 and has remained generally higher that at the other stations (Figure 106a). At the other stations, interannual trends in median values was not apparent, but their was great variability within a year in 2015. When viewed seasonally, AR4 tended to show increasing values from April through September (Figure 106b). Values at AR2 and AR3 generally declined through the months similar to trends in light attenuation coefficient.

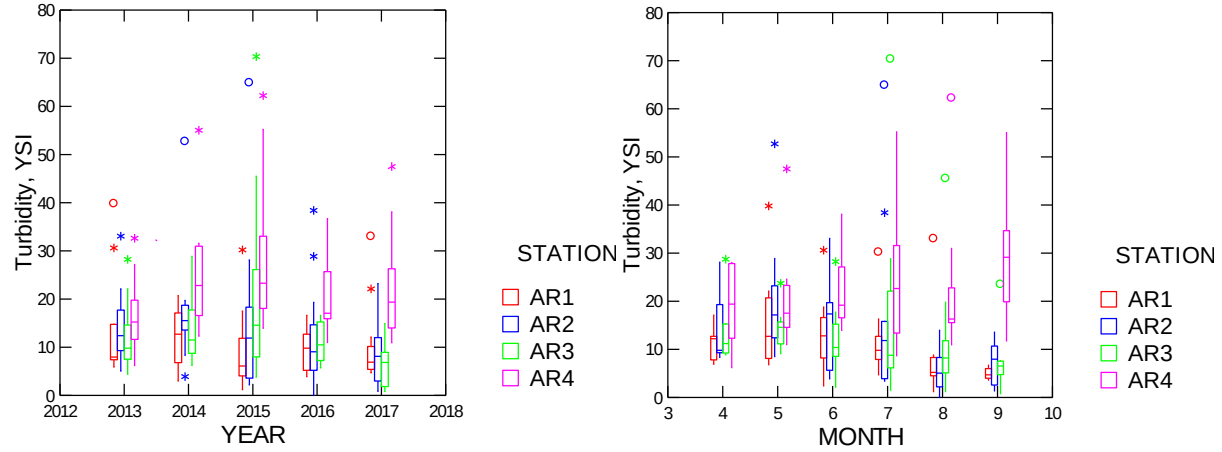

Figure 106. Box plots comparing values of Turbidity between years (left) and by season (right).

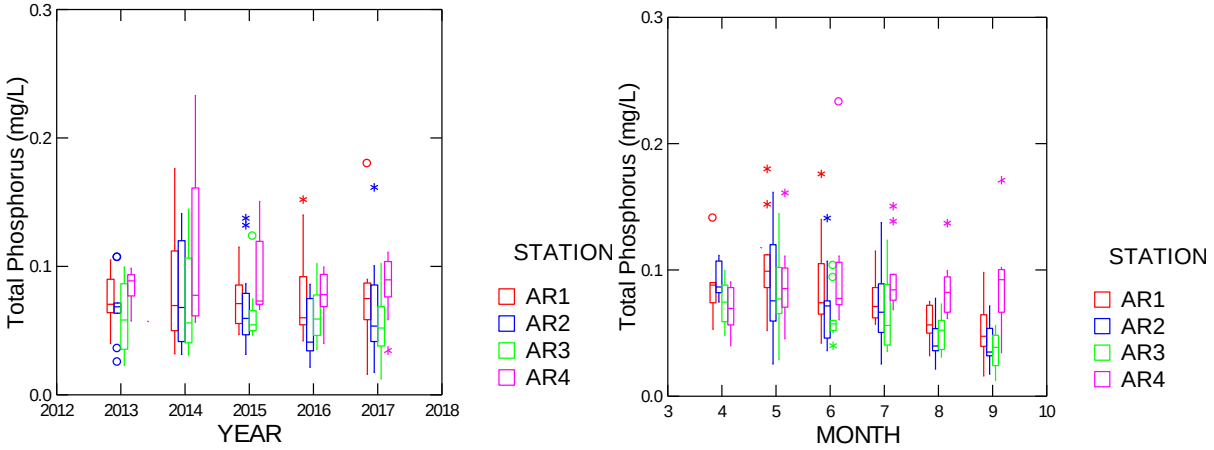

Figure 107. Box plots comparing values of Total Phosphorus between years (left) and by season (right).

Total phosphorus did not exhibit any clear patterns between years (Figure 107a). Seasonally, there was a steady decline in Total P from spring through fall in the embayment stations (AR1, AR2, and AR3) while the river station (AR4) did not show much seasonal trend (Figure 107b). Organic nitrogen was generally higher at AR1 than at the other stations (Figure 108a). This effect was most pronounced in spring when there was a pattern of decreasing values from AR1 to AR2 to AR3 to AR4 (Figure 108b). This pattern started breaking down in July and disappeared in August and September.

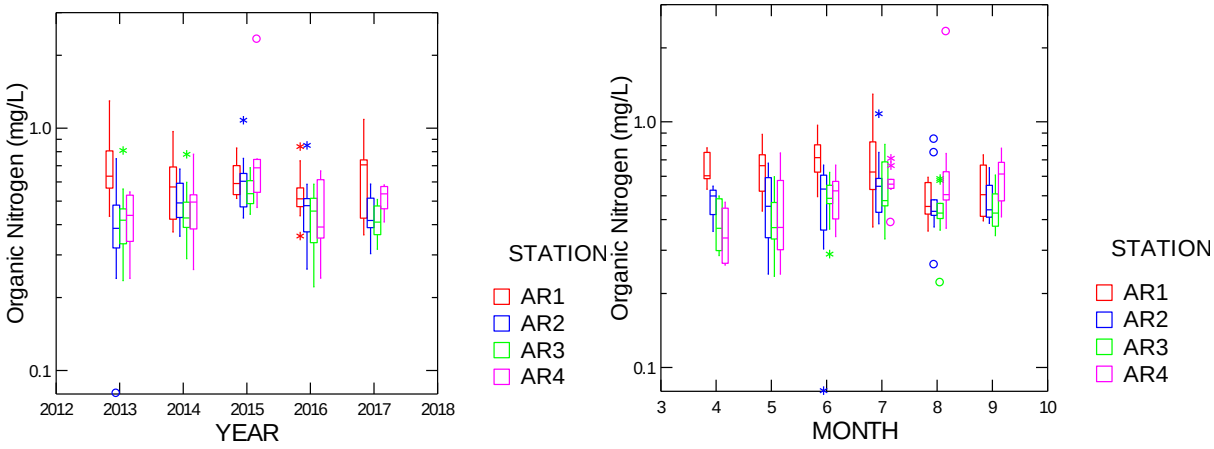

Figure 108. Box plots comparing values of Organic Nitrogen between years (left) and by season (right).

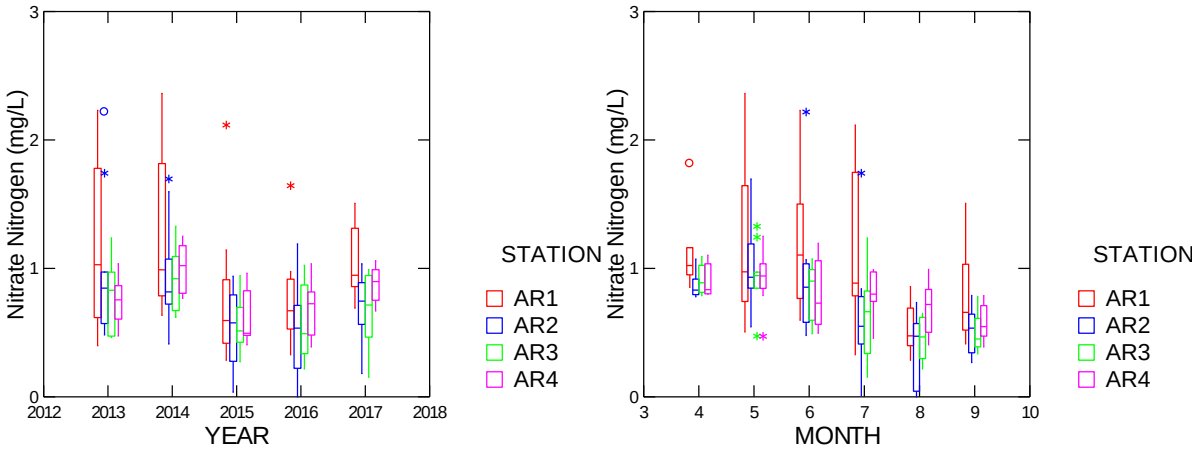

Figure 109. Box plots comparing values of Nitrate Nitrogen between years (left) and by season (right).

Nitrate nitrogen values continued to be substantially lower than in the first two years of the study (Figure 109a). A seasonal pattern in nitrate values was observed with a decline at all stations in summer attributable to uptake by phytoplankton and SAV (Figure 109b). Ammonia nitrogen values did not show any systematic variation among the years (Figure 110a). A seasonal pattern, however was apparent with values in the period July to September being substantially lower than observed in the previous months (Figure 110b).

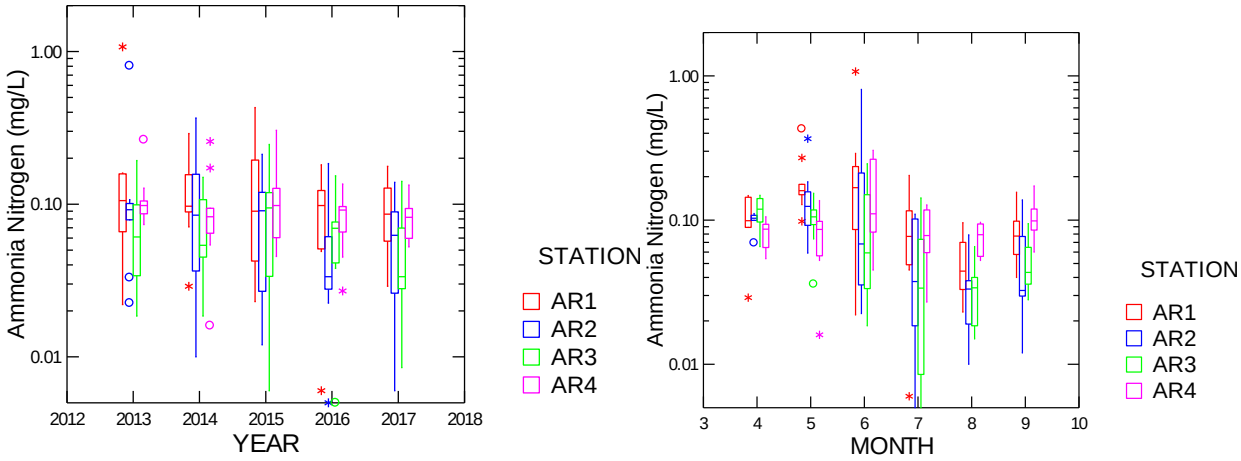

Figure 110. Box plots comparing values of Ammonia Nitrogen between years (left) and by season (right).

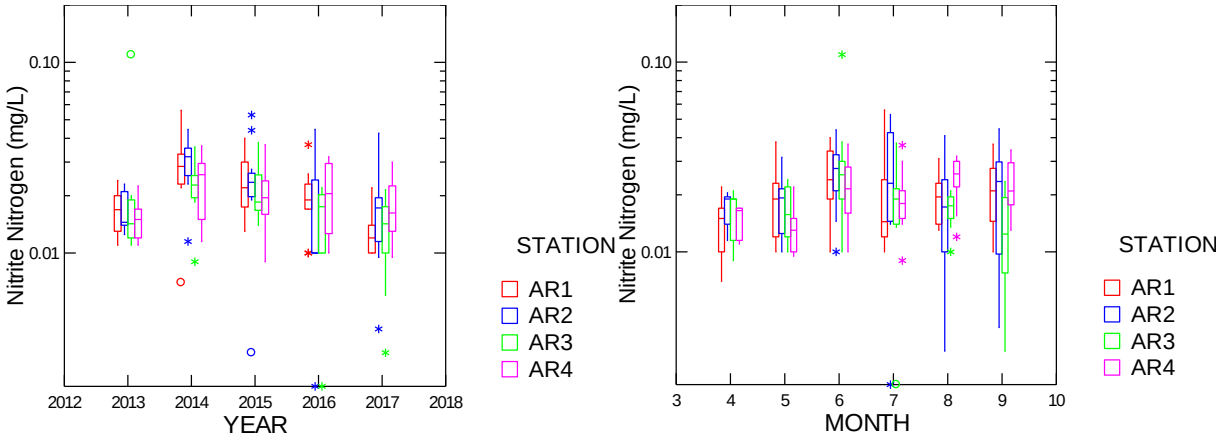

Figure 111. Box plots comparing values of Nitrite Nitrogen between years (left) and by season (right).

Nitrite nitrogen values were highest in 2014 with lowest in 2013; levels in 2017 were closer to 2013 (Figure 111a). Seasonally, there was a general increase in nitrite through mid summer followed by a decline at all stations (Figure 130b). N to P ratio seemed to show a decline over the study period (Figure 112a). Seasonal patterns were not apparent (Figure 112b).

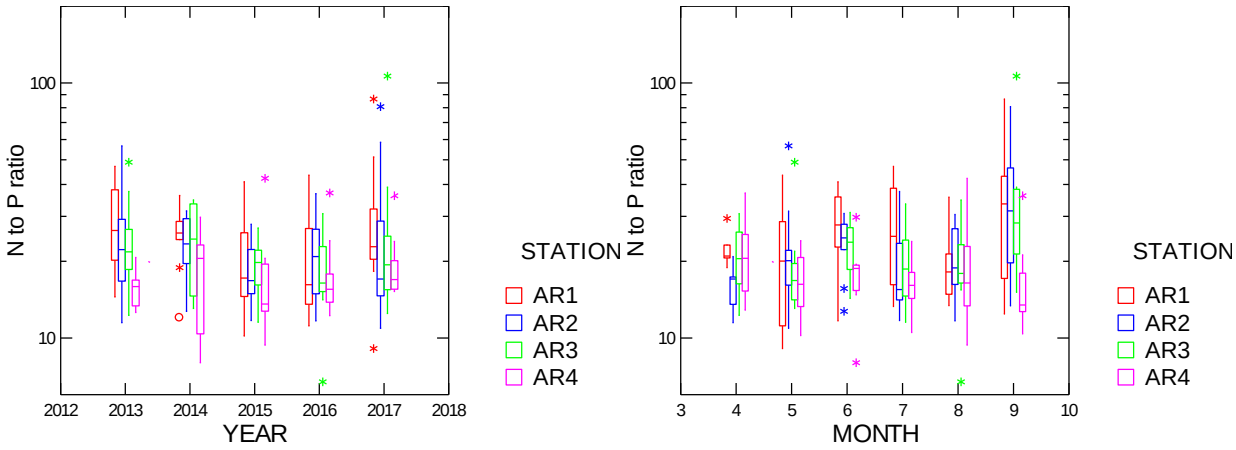

Figure 112. Box plots comparing values of N to P ratio between years (left) and by season (right).

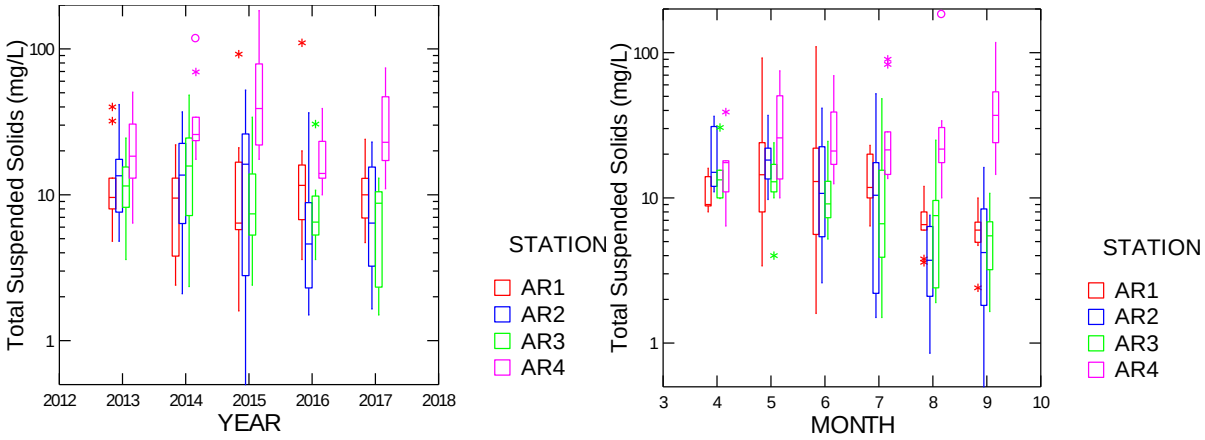

Figure 113. Box plots comparing values of Total Suspended Solids between years (left) and by season (right).

Total suspended solids (TSS) values have shown a slight decline over the five years of the study at AR2 and AR3 (Figure 113a). Values have been consistently highest at AR4. Seasonal patterns were different between the river mainstem site (AR4) and the Hunting Creek embayment stations (AR1, AR2, AR3). At AR4 TSS tended to rise through the study period whereas at the other sites it showed a marked decline particulary when the SAV beds were highly developed in August and September (Figure 113b).

VSS exhibited markedly less systematic variation among years, but AR4 was consistently greater than the other stations and a seasonal decline was observed at AR2 and AR3, but not at AR1 (Figure 114a,b).

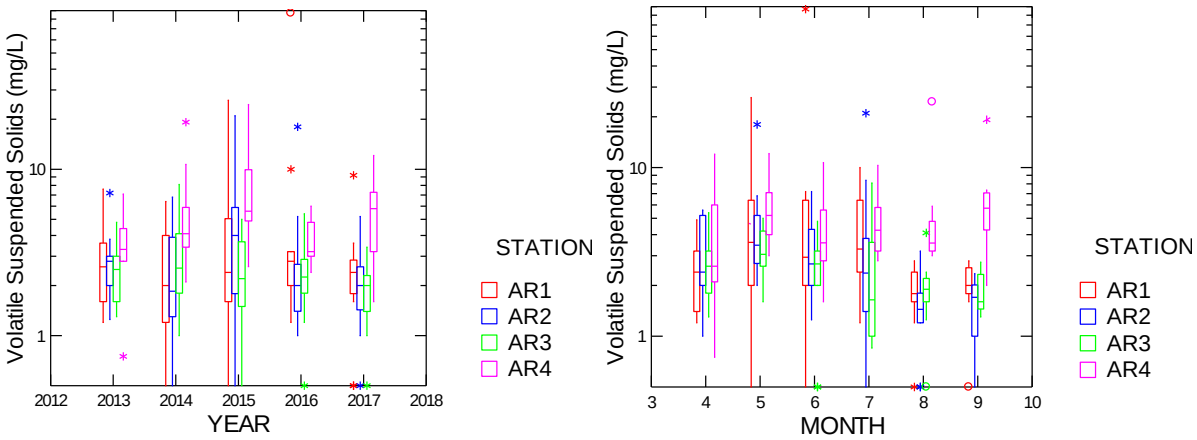

Figure 114. Box plots comparing values of Volitile Suspended Solids between years (left) and by season (right).

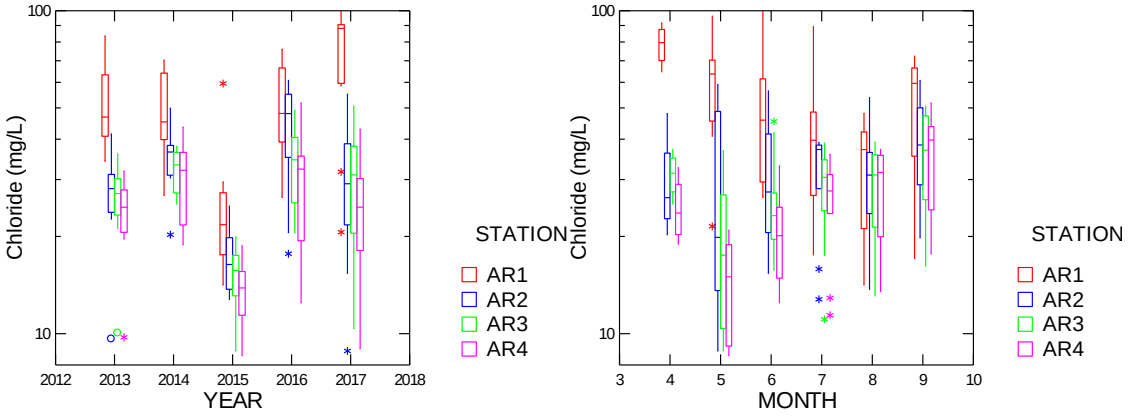

Figure 115. Box plots comparing values of Chloride between years (left) and by season (right).

Chloride levels showed a clear spatial pattern with highest values at AR1 (Figure 115a). Chloride was lower at all sites during 2015 than other years. At AR1 there was a consistent seasonal decline from April through July with possible increase in September (Figure 115b). At AR4 a consistent decrease was observe in May with steady increase through the remainder of the year. A seasonal pattern in chloride was not observed at AR2 or AR3. Total alkalinity has shown a slight, but steady increase over the years (Figure 116a). Seasonally values were lower in spring and early summer and increased in late summer (Figure 116b). Values were also lowest at AR1 and consistently highest at AR4.

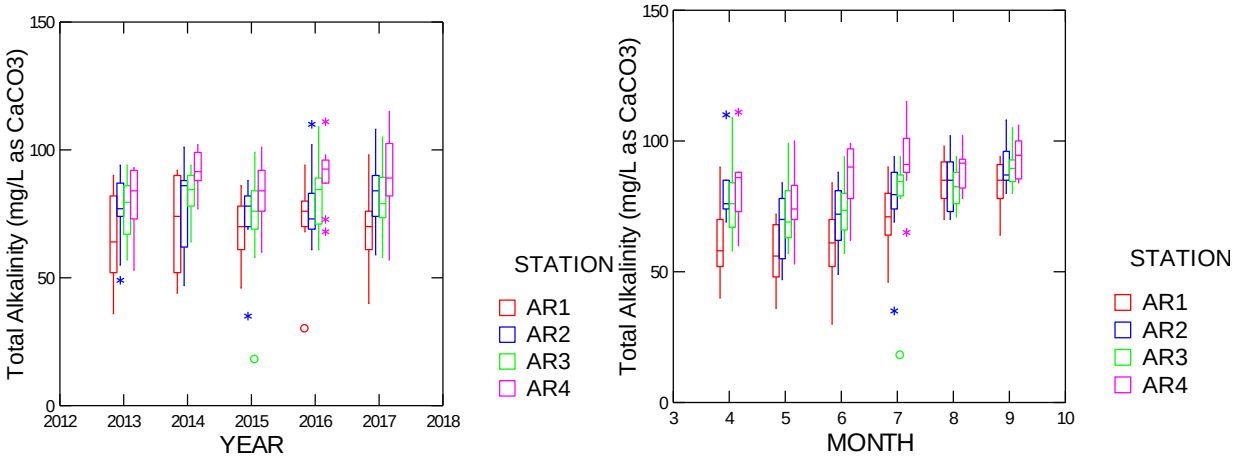

Figure 116. Box plots comparing values of Total Alkalinity between years (left) and by season (right).

D. Phytoplankton: Comparison among Years

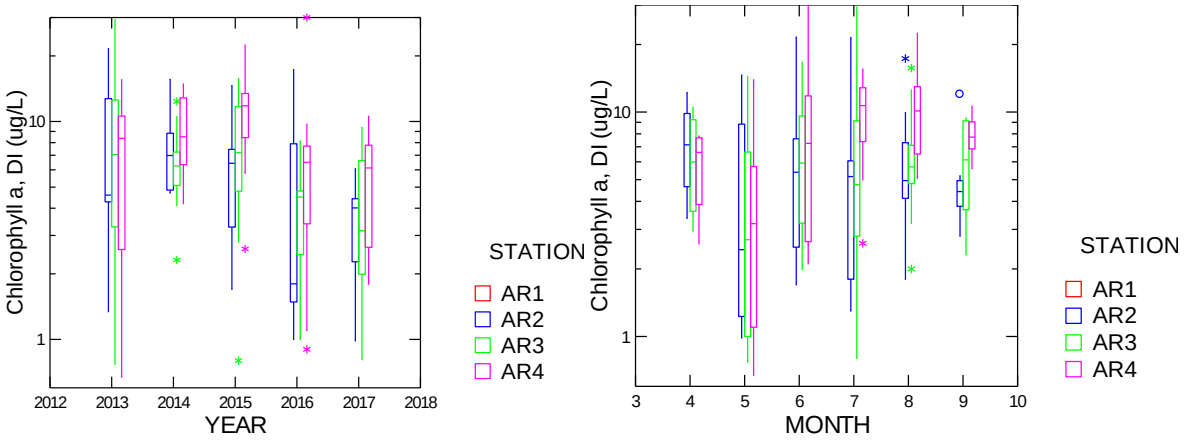

Figure 117. Box plots comparing values of depth-integrated Chlorophyll a among years (left) and by month (right).

A general decline in depth-integrated chlorophyll was observed at AR2 and AR3 over the study period (Figure 117a). Values at AR4 were lower in 2016 and 2017 than in previous years. A seasonal increase with maximum in July and August was clearly indicated at AR4, whereas AR2 and AR3 did not show a consistent seasonal effect (Figure 117b). Similar results were observed with surface chlorophyll (Figure 118a,b). Chlorophyll values in the water are a measure of phytoplankton populations which compete with phytoplankton for light and nutrients.

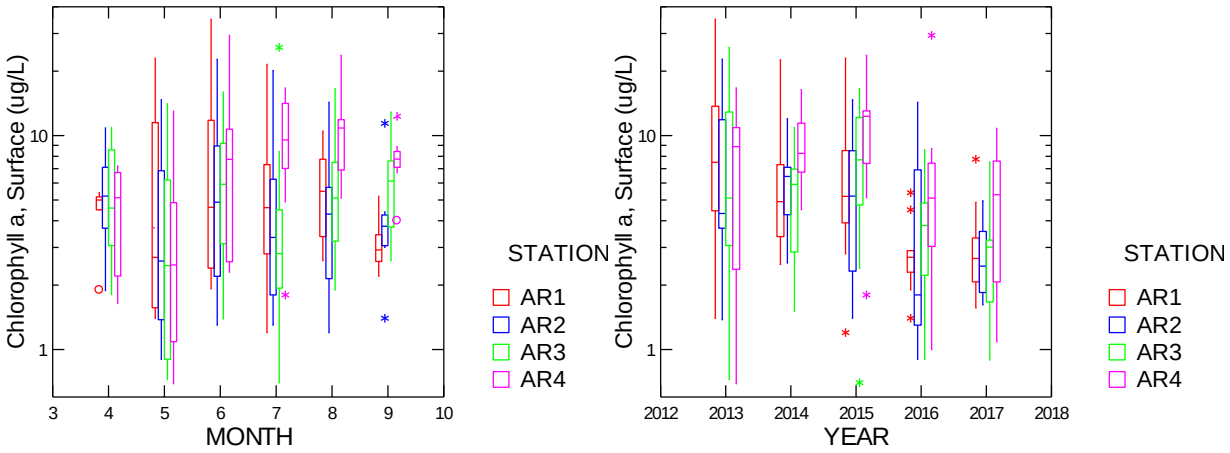

Figure 98. Box plots comparing values of surface Chlorophyll a among years (left) and by month (right).

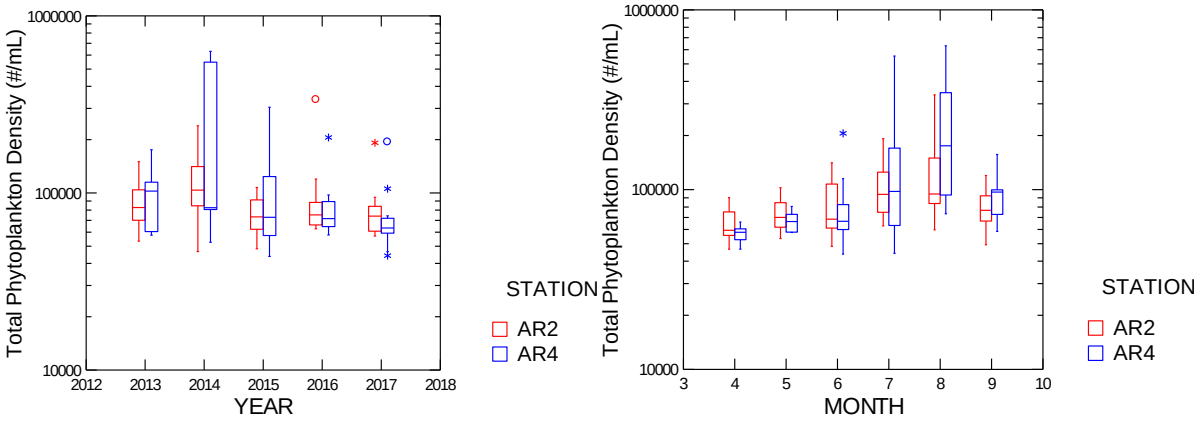

Figure 119. Box plots comparing values of Total Phytoplankton Density among years (left) and by month (right).

The median values for total phytoplankton cell density were similar among the five years, although there were more high values in 2014 especially at AR4 (Figure 119a). Both stations showed a seasonal increase in phytoplankton (Figure 119b). The increase followed a similar pattern at both stations through July, but in August AR4 (river mainstem) continued to increase whereas at AR2 (Hunting Creek) values leveled off. Total cyanobacterial cell density was clearly higher in 2014 at both stations than in the other four years (Figure 120a). The main difference between the two stations was the greater variability observed at AR4. The seasonal pattern in cyanobacterial density was very similar to the patterns noted above in total phytoplankton cell density as cyanobacteria often make up the majority of phytoplankton cells (Figure 120b).

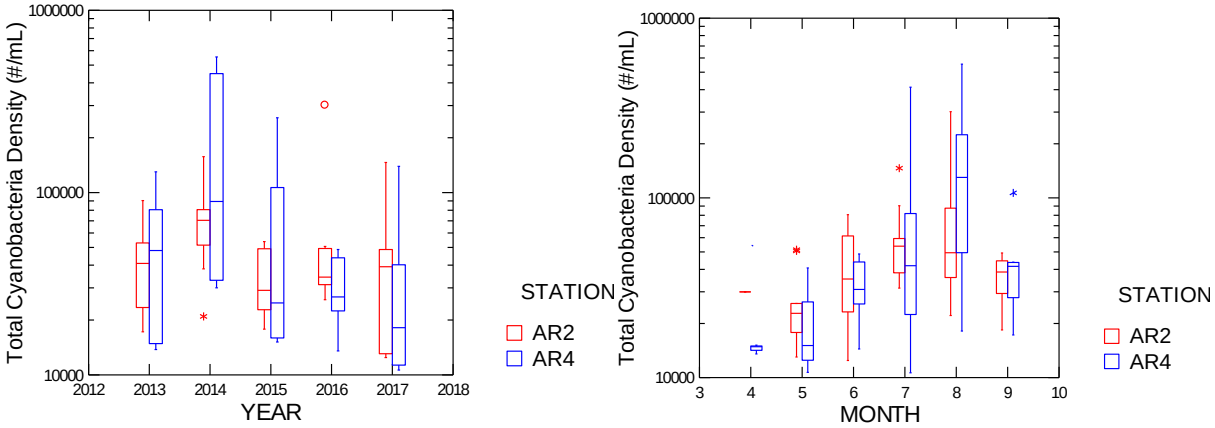

Figure 120. Box plots comparing values of Cyanobacterial Density among years (left) and by month (right).

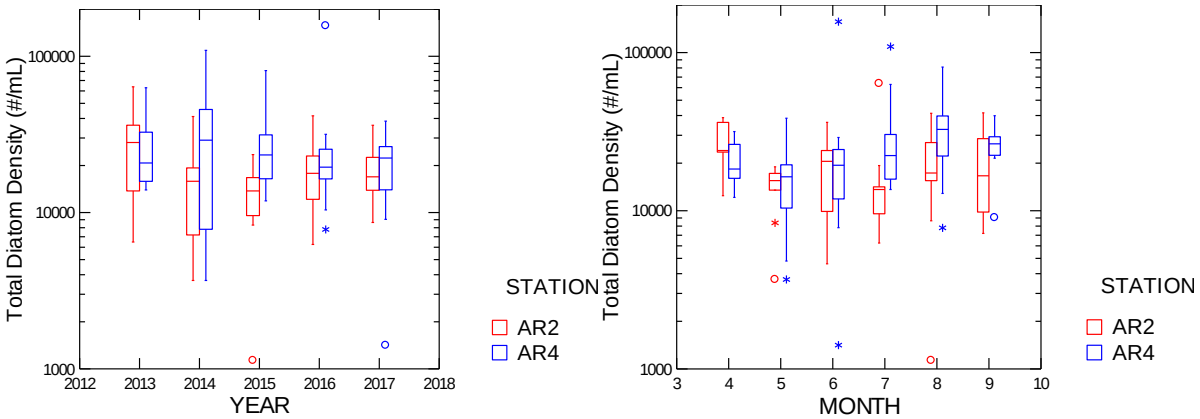

Figure 121. Box plots comparing values of Diatom Density among years (left) and by month (right).

Median diatom densities overall were fairly constant among all years at AR4 (Figure 121a). At AR2, lower medians were found in 2014 and 2015 relative to the other years. Median diatom densities were highest in April at AR2, lowest in May, June and July (Figure 121b). At AR4 a decline was observed in May and then values increased through August.

Green algal cell densities were very similar across the five years (Figure 122a). There was essentially no consistent seasonal pattern in green algal cell densities at either station (Figure 122b).

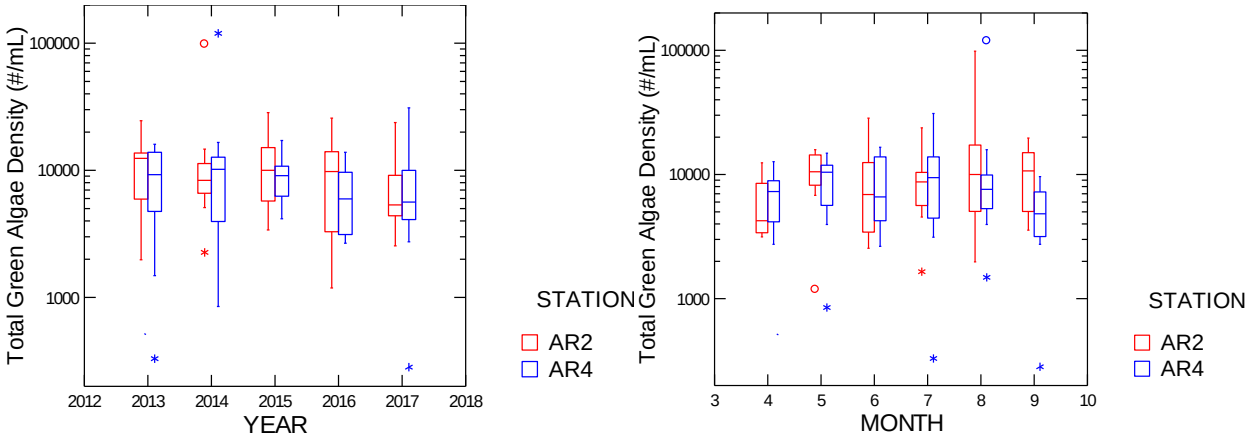

Figure 122. Box plots comparing values of Green Algal Density among years (left) and by month (right).

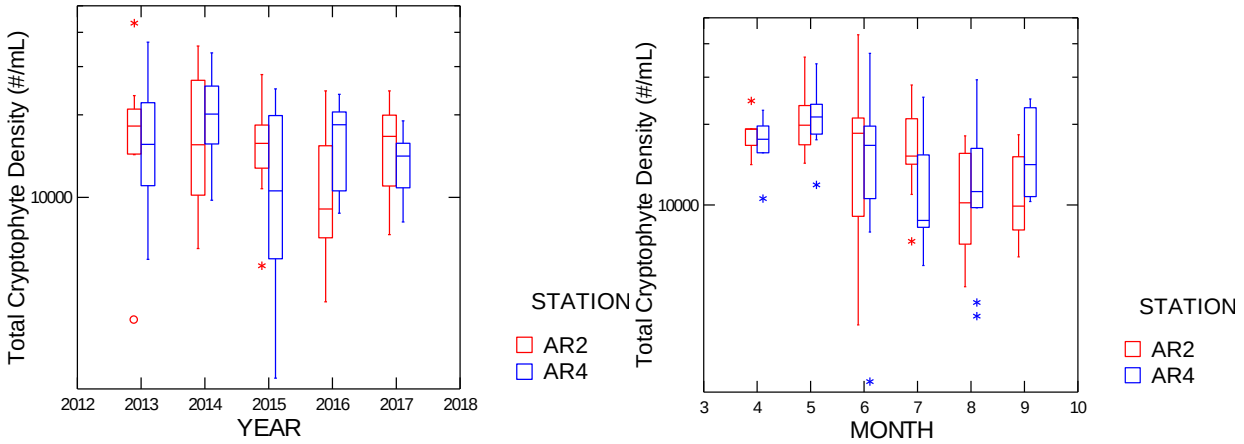

Figure 123. Box plots comparing values of Cryptophyte Density among years (left) and by month (right).

Median cryptophyte cell densities have not shown a consistent interannual pattern of the years at either station (Figure 123a). A general seasonal pattern of higher values in spring and a tapering for the rest of the year was found at both stations (Figure 123b).

Miscellaneous taxa includes those species of phytoplankton in groups not tallied above. These are mainly dinoflagellates, crysophytes and euglenoids whose abundances are somewhat sporadic in the study area. This is reflected in interannual and seasonal patterns which did not reveal any clear patterns (Figure 124a,b).

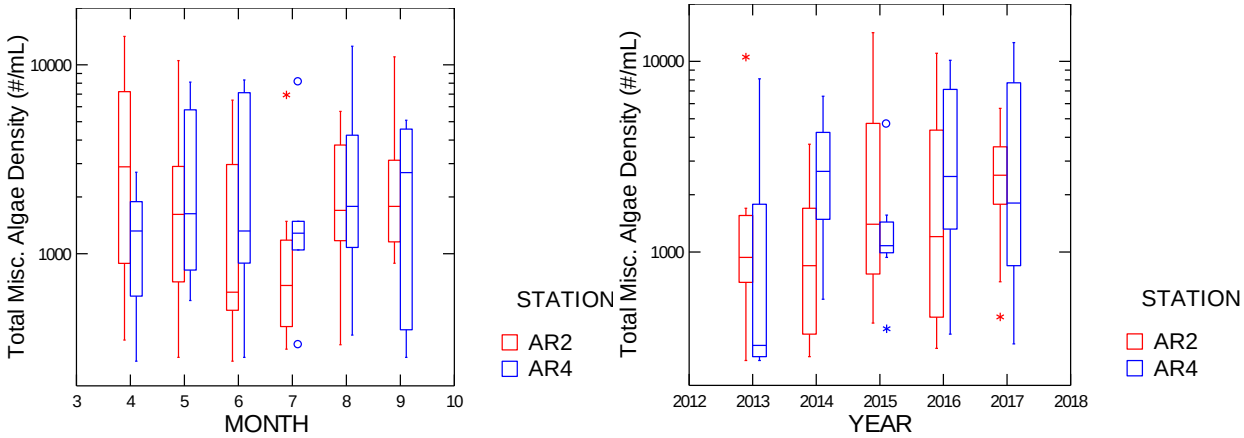

Figure 124. Box plots comparing values of Miscellaneous Taxa Density among years (left) and by month (right).

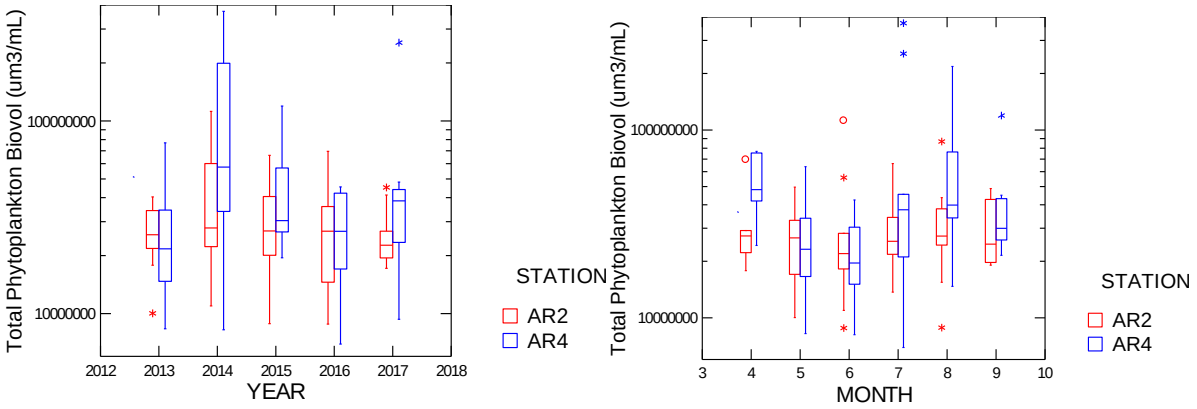

Figure 125. Box plots comparing values of Total Phytoplankton Biovolume among years (left) and by month (right).

Biovolume takes into account both the number of cells and their relative size. Mean values of total phytoplankton biovolume were similar over all five years at AR2 (Figure 125a). At AR4 total phytoplankton biovolume was markedly higher in 2014 than in the other two years. At AR2 there was little seasonal pattern, but at AR4 a general decline was observed in May and June followed by an increase in July and August (Figure 125b).

Total cyanobacterial biovolume exhibited a steady decline in median values through 2015, but values rebounded at both sites in 2016 and 2017 (Figure 126a). Seasonally both values at both stations increased through August. AR2 increased steadily in spring and early summer and declined in September; AR4 was higher in August and September (126b).

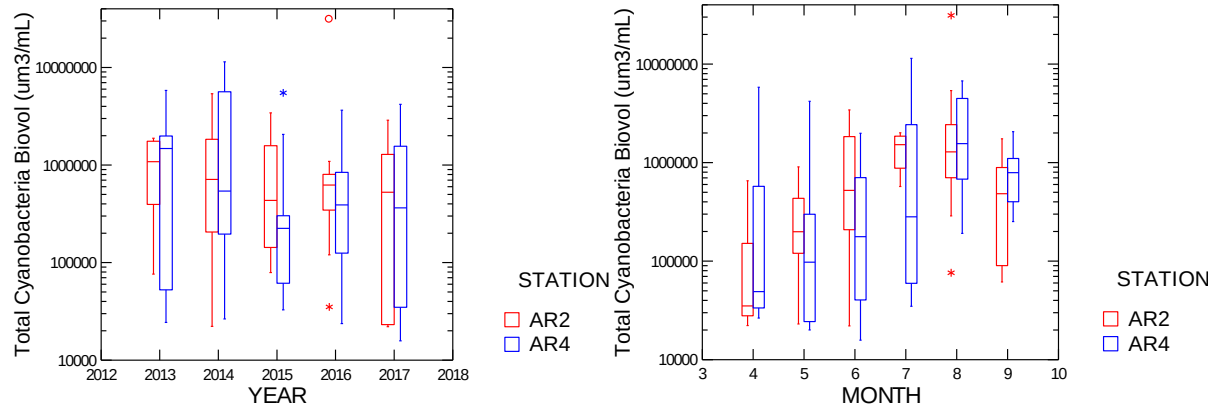

Figure 126. Box plots comparing values of Cyanobacterial Biovolume among years (left) and by month (right).

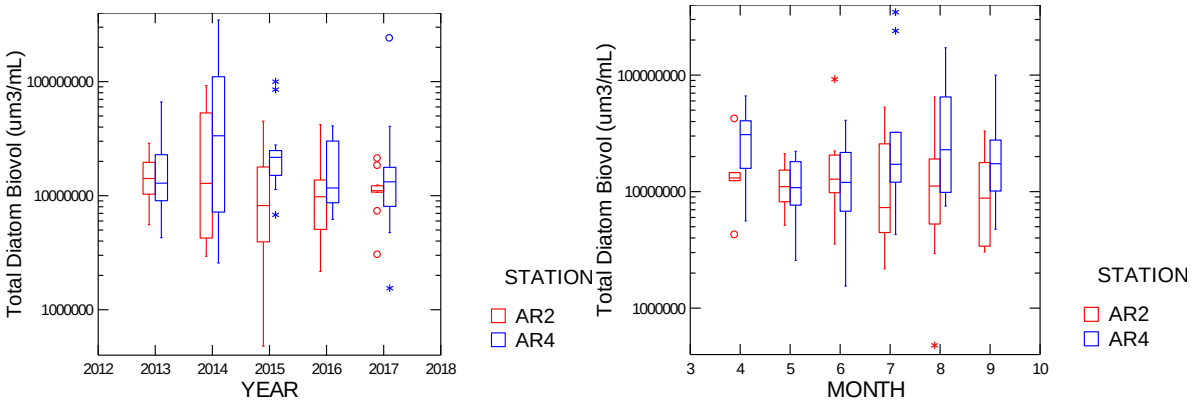

Figure 127. Box plots comparing values of Diatom Biovolume among years (left) and by month (right).

Median diatom biovolume did not show a consistent trend over the five years of the study (Figure 127a). Seasonal patterns revealed that a general increase was observed at AR4 from May through August (Figure 127b). AR2 did not show a clear seasonal pattern.

Median values in green algal biovolume increased in 2015 and 2016, but dropped back in 2017 (Figure 128a). The seasonal pattern was complex, but similar at both stations (Figure 128b).

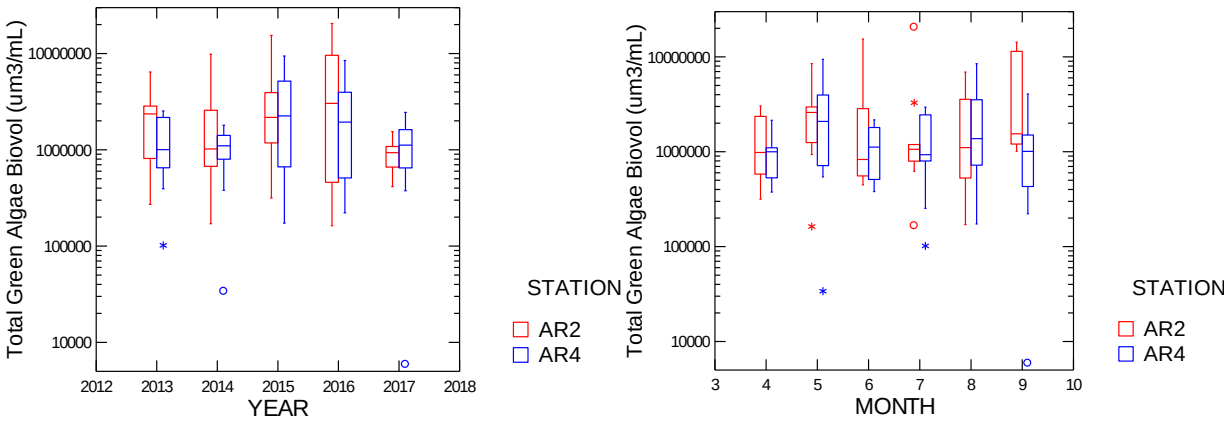

Figure 128. Box plots comparing values of Green Algal Biovolume among years (left) and by month (right).

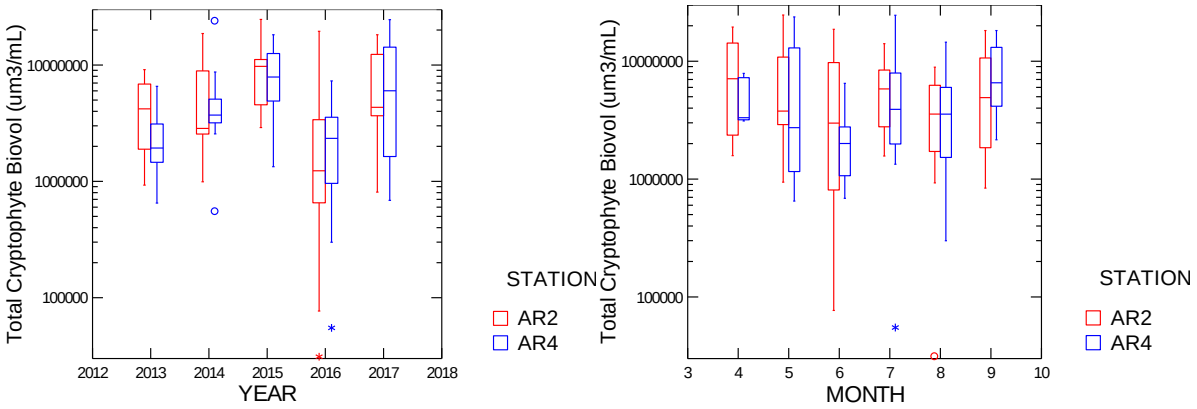

Figure 129. Box plots comparing values of Cryptophyte Biovolume among years (left) and by month (right).

Cryptophyte biovolume exhibited a clear gradual increase from 2013 through 2015 at both sites, but dropped back markedly in 2016 (Figure 129a). They rebounded again in 2017. The seasonal pattern showed a decline through June, but rose again at both stations later in the year (Figure 129b).

The patterns in Miscellaneous Taxa Biovolume were a bit sporadic. The main interannual pattern was that in 2014 values at AR4 were higher than in the other year-station groups (Figure 130a). Seasonal patterns were a little clearer. At AR2 there was a steady decline in the miscellaneous group from April through July followed by a clear increase through August and a decline in September (Figure 130b). A similar pattern was observed in median values at AR4, but there was a very large amount of variability.

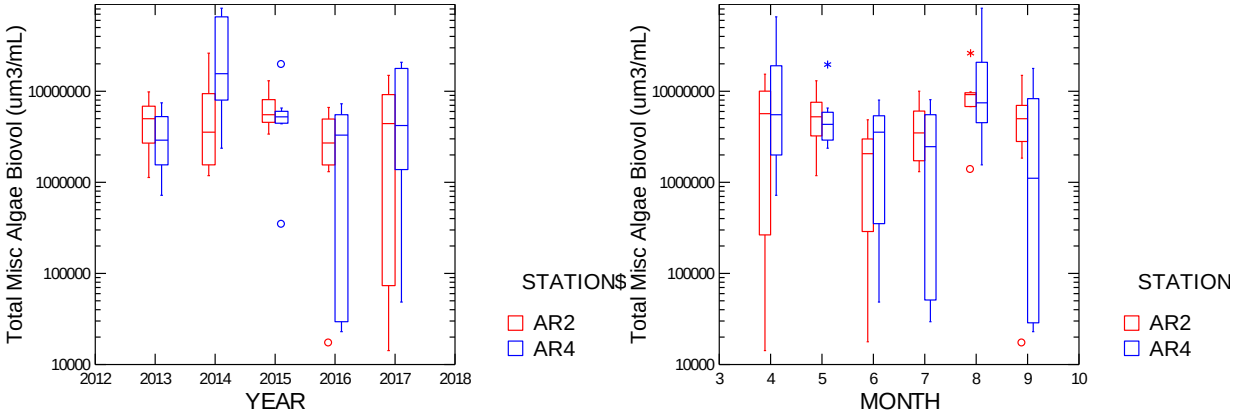

Figure 130. Box plots comparing values of Miscellaneous Biovolume among years (left) and by month (right).

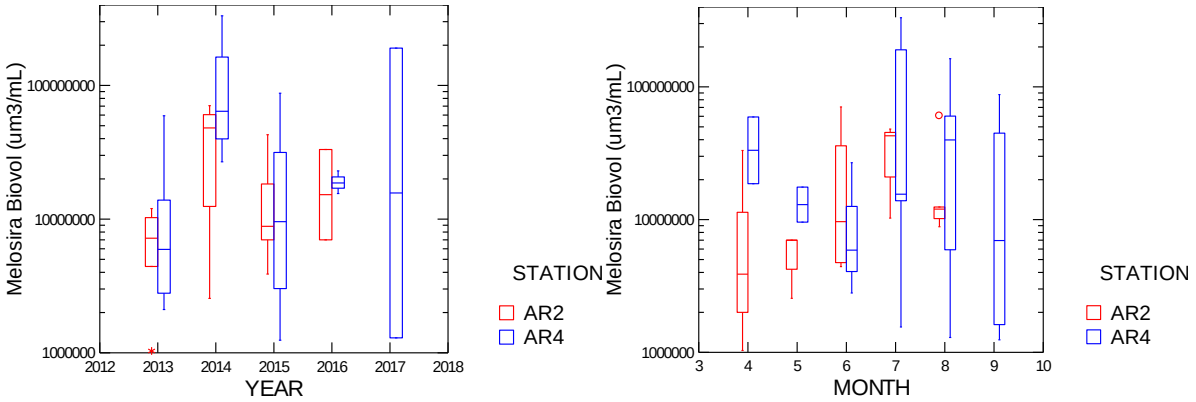

Figure 131. Box plots comparing values of *Melosira* Biovolume among years (left) and by month (right).

An analysis of interannual and seasonal effects also done for selected individual taxa. Median biovolume values of the filamentous diatom *Melosira* showed a clear peak in 2014 at both stations (Figure 131a). *Melosira* also exhibited a clear seasonal pattern of increase from April through July at AR2 (Figure 131b). At AR4 peaks were observed in April and July.

Discoid centric biovolume was high in 2014 and 2917 at AR4 (Figure 132a). At AR2 the year of highest median biovolume was 2013. Seasonal patterns generally indicated that values were relatively high at AR2 in the spring, but declined through August (Figure 132b). At AR4 discoid centrics were less abundant in the spring and increased reaching a peak in mid to late summer.

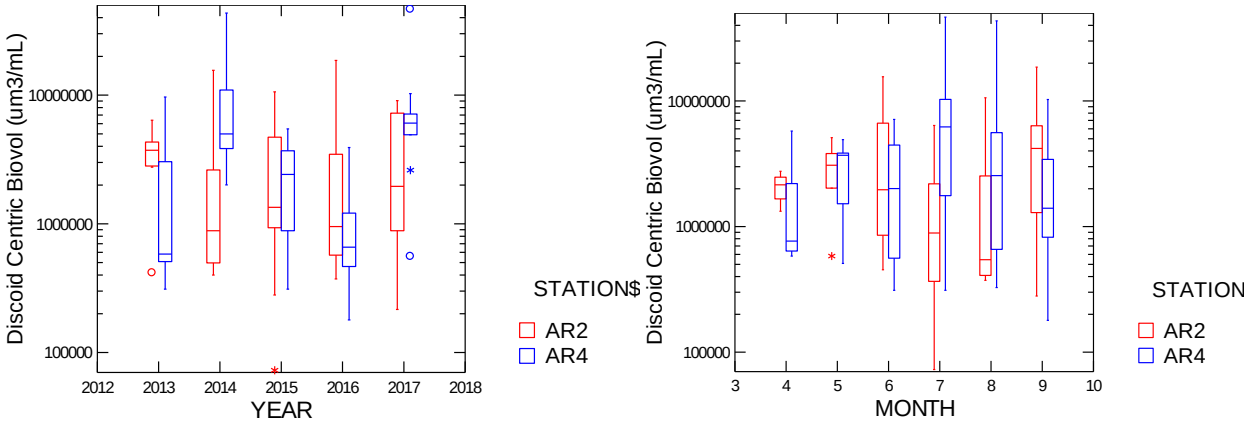

Figure 132. Box plots comparing values of Discoid Centric Diatom Biovolume among years (left) and by month (right).

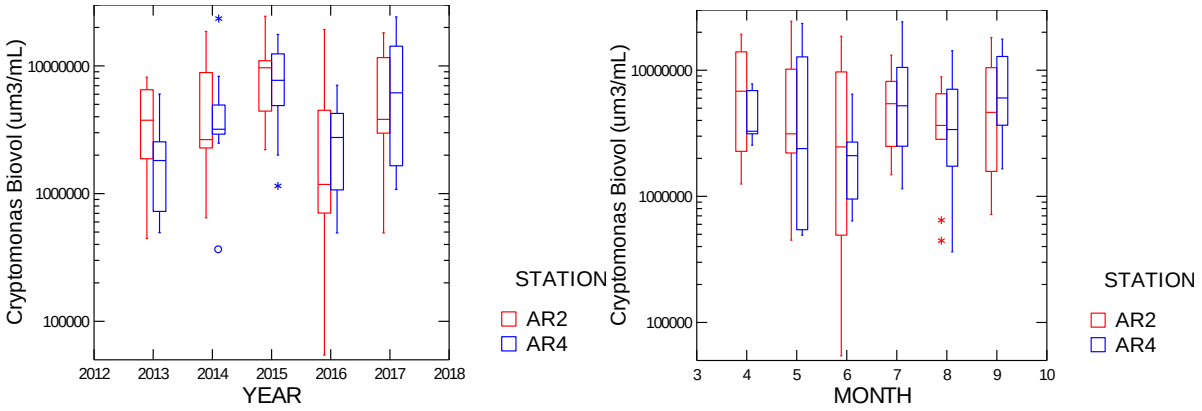

Figure 133. Box plots comparing values of *Cryptomonas* Biovolume among years (left) and by month (right).

Cryptomonas biovolume showed a general increase at both stations over the first three years of study, dropped back down in 2016, and rebounded in 2017 (Figure 133a). The seasonal graph did not show much of a pattern (Figure 133b).

Oscillatoria is the most consistently abundant cyanobacterium in the study area. In 2014 and 2015 it was consistently more abundant at AR4. At both stations peak levels were generally observed in July and August (Figure 134a,b).

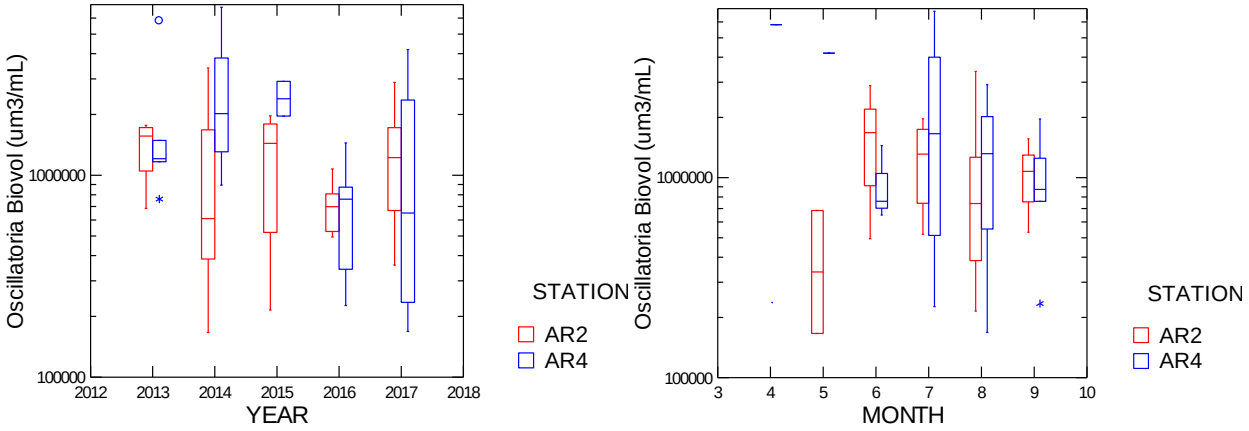

Figure 134. Box plots comparing values of *Oscillatoria* Biovolume among years (left) and by month (right).

E. Zooplankton: Comparison among Years

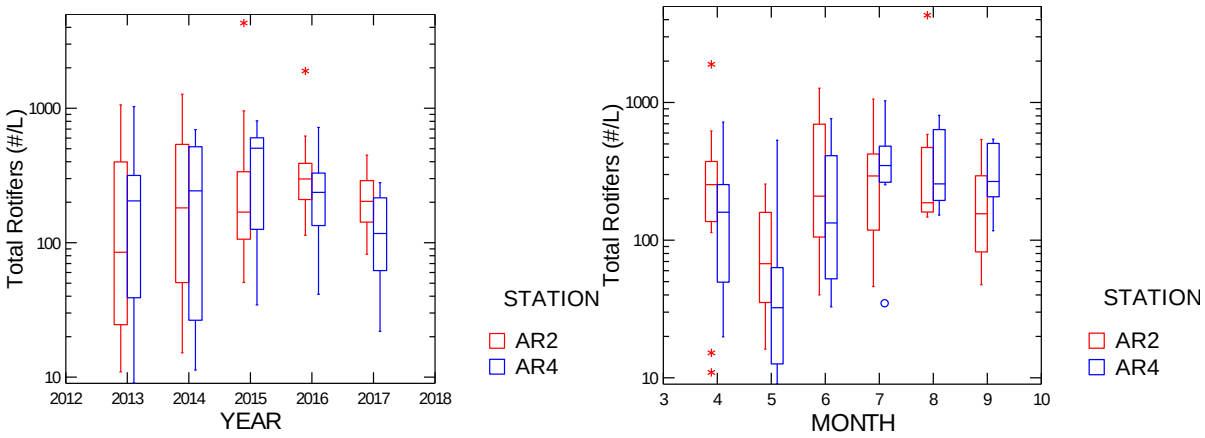

Figure 135. Box plots comparing values of Total Rotifers among years (left) and by month (right).

Median total rotifer density values did not show much of a difference between the two stations, but a trend of change over the years was observed with values increasing for the first three years and declining somewhat in the last 2 years of the study (Figure 135a). A clear seasonal pattern of increase from May through August was found at both stations (Figure 135b).

The common rotifer *Brachionus* (Figure 136a) showed a lot of variability in 2013 at both stations, but has shown less variability since then. The seasonal patterns were similar at the two stations (Figure 136b). Values declined strongly low in May, jumped up in June and July and declined somewhat in August and September.

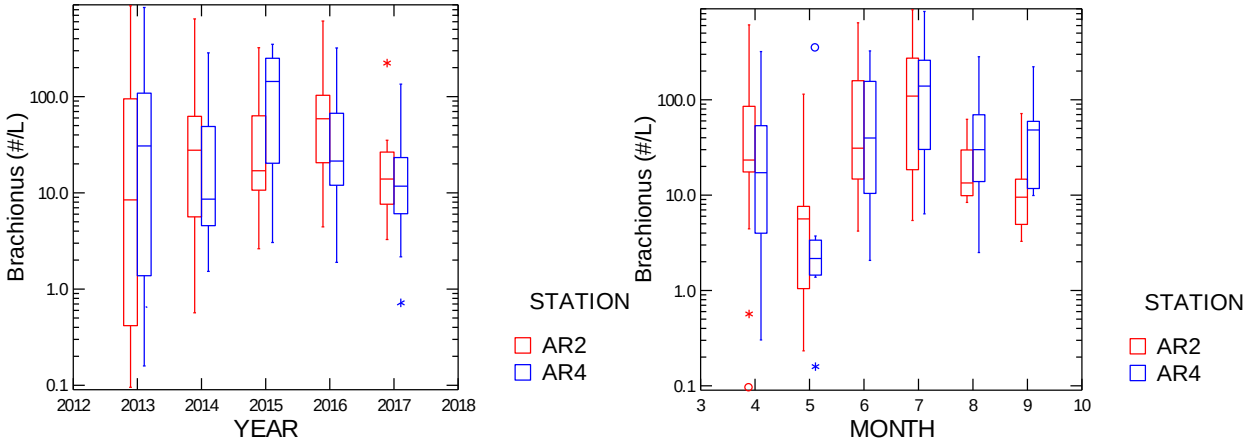

Figure 136. Box plots comparing values of *Brachionus* among years (left) and by month (right).

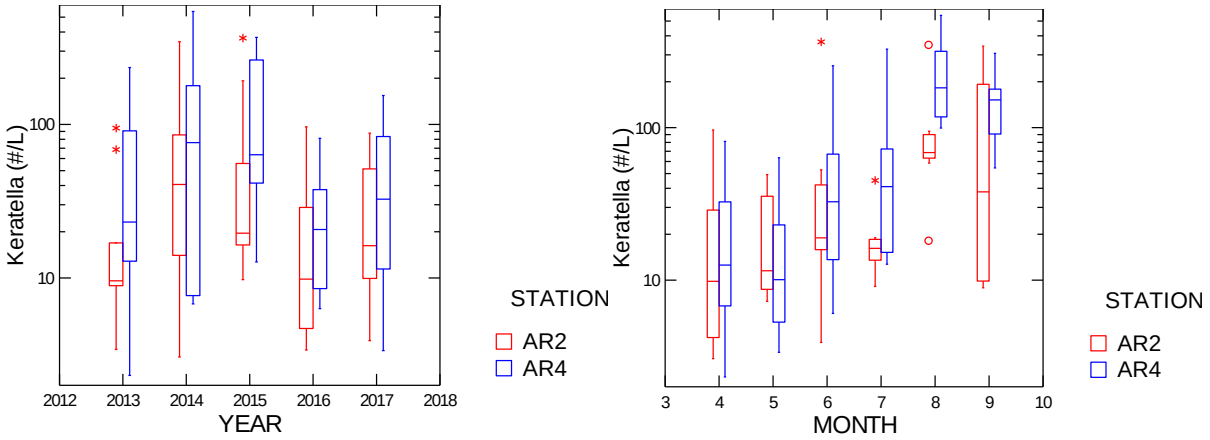

Figure 137. Box plots comparing values of *Keratella* among years (left) and by month (right).

Another common rotifer *Keratella* was clearly more abundant at AR4 than AR2 in all years (Figure 137a). The seasonal pattern was one of fairly consistent increase from spring through late summer at both stations (Figure 137b).

Polyarthra was variable and generally present at lower levels than *Brachionus* or *Keratella*. Few *Polyarthra* were observed at AR4 in 2014, but otherwise there was little difference among years (Figure 138a). Seasonal patterns were variable, but spring values were consistently lower than densities observed later in the year (Figure 138b).

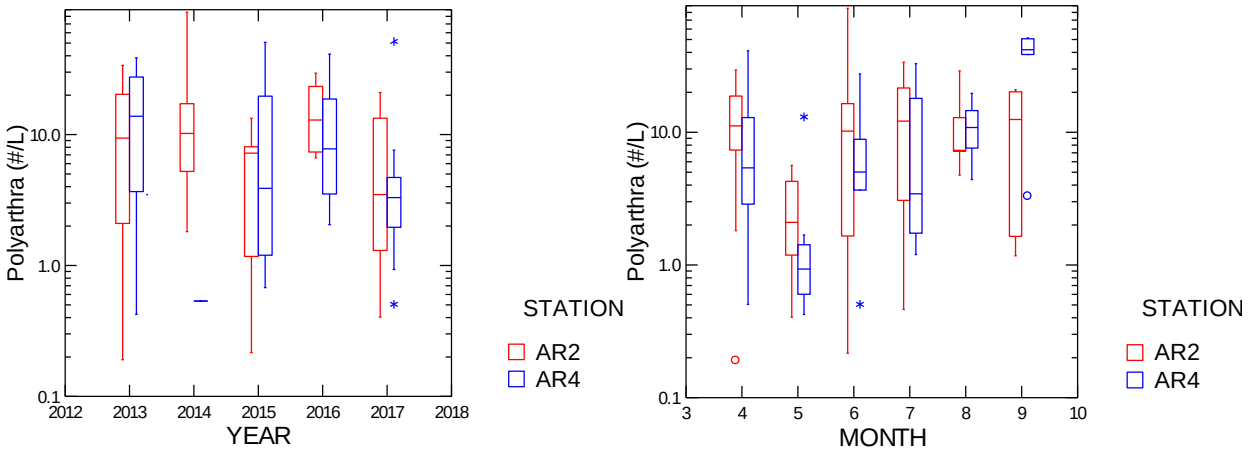

Figure 138. Box plots comparing values of *Polyarthra* among years (left) and by month (right).

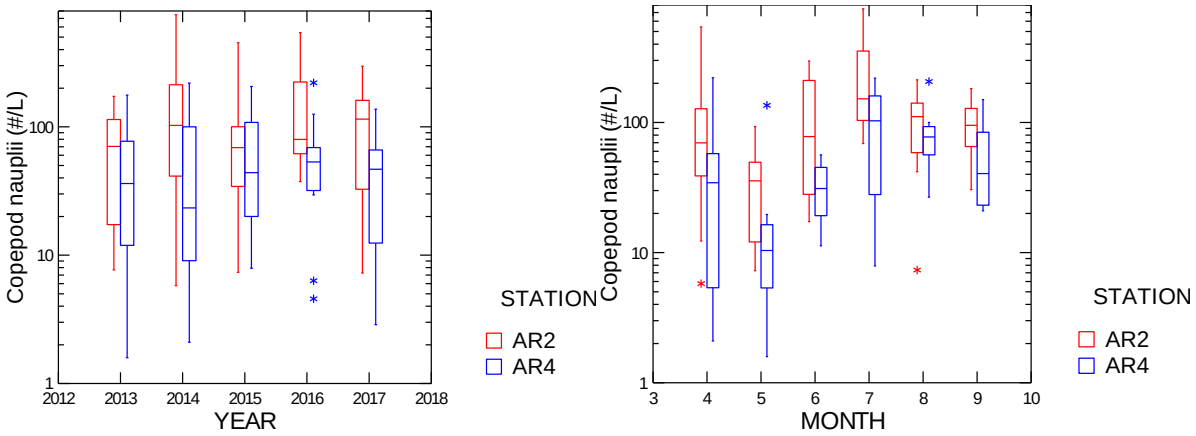

Figure 139. Box plots comparing values of Copepod Nauplii among years (left) and by month (right).

The two taxa on this page are enumerated in the microzooplankton samples because they are small and not quatitatively collected in 202 um nets. However, they are crustaceans and as such are more closely related to the taxa collected in the 202 nets.

Nauplii are the juvenile stages of copepods. As such it is hard to identify them to species since they do not have mature characteristics so they have been lumped for all copepod taxa. Nauplii were consistently higher at AR2 than at AR4, but showed little difference among years (Figure 139a). At both stations a clear seasonal pattern emerged with a steady increase in abundances from May through July followed by a decline in August and September (Figure 139b).

Bosmina is a small cladoceran related to *Daphnia* and *Diaphanosoma* collected in the 202 nets. There was not much overall difference in *Bosmina* levels among the three years, but in each year there was generally higher median densities at AR4 than at AR2 (Figure 140a). A clear seasonal pattern was observed with *Bosmina* increasing steadily from April through July and then stabilizing during August and September (Figure 140b).

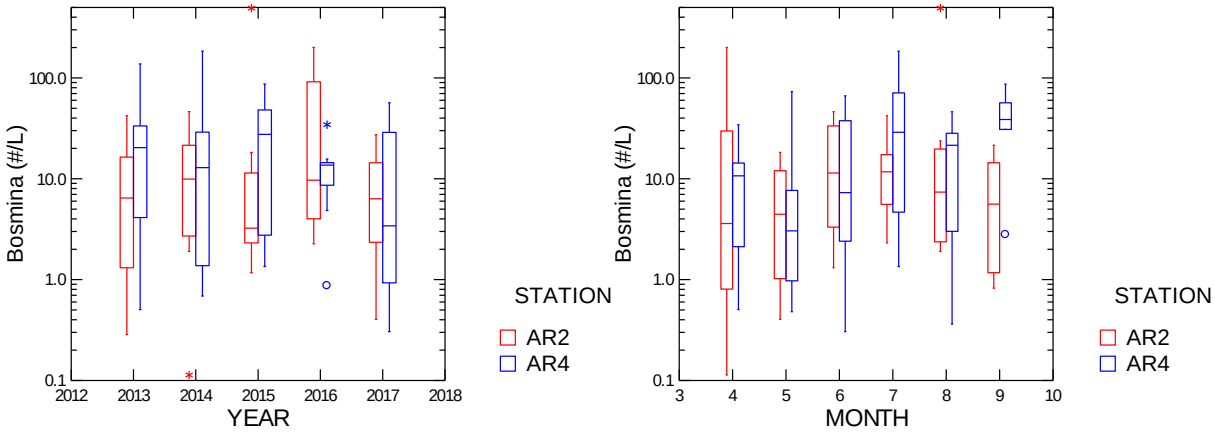

Figure 140. Box plots comparing values of *Bosmina* among years (left) and by month (right).

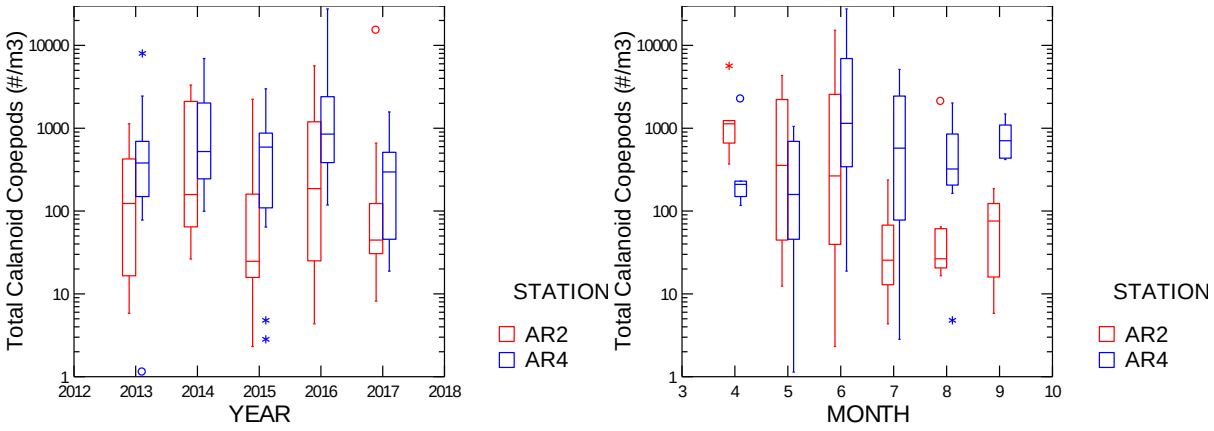

Figure 141. Box plots comparing values of Total Calanoid Copepods among years (left) and by month (right).

Median calanoid copepod densities were similar among the years at AR4 (Figure 141a). At AR4 values were generally lower than at AR2 and were much lower in 2015. Seasonal patterns indicated that AR2 peaked in the April and May and then delcined through September (Figure 141b). Levels at AR4 were gerally highest in June.

Eurytemora is the most common calanoid copepod. Its interannual pattern was quite similar to that observed for total calanoids (Figure 142a) with AR4 clearly higher than AR2 in 2013, 2015, and 2016. Seasonally, it was more abundant at AR2 in April and May and more abundant at AR4 for the remainder of the year (Figure 142b). Highest densities were observed in June at AR4.

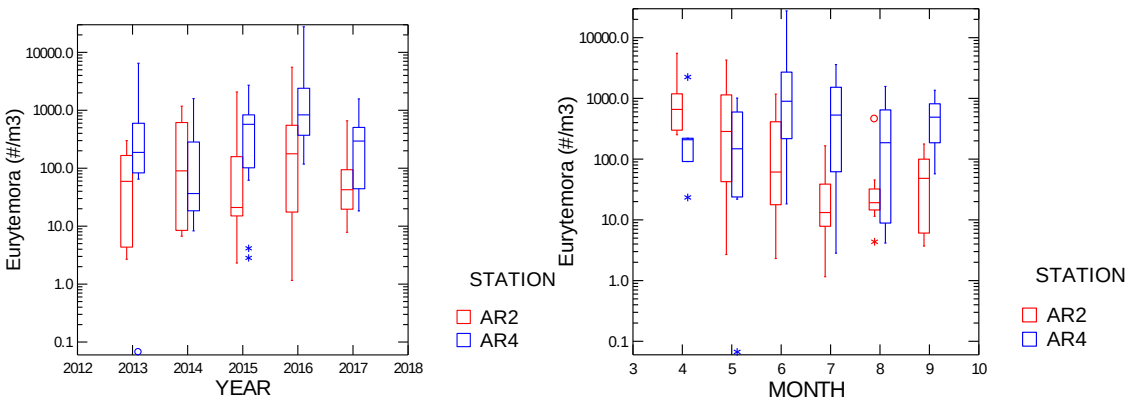

Figure 142. Box plots comparing values of *Eurytemora* among years (left) and by month (right).

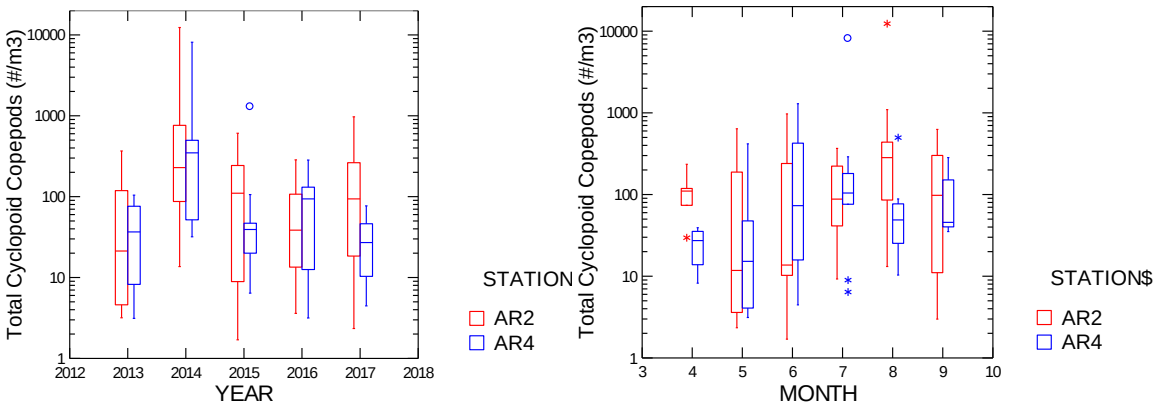

Figure 143. Box plots comparing values of Cyclopoid Copepods among years (left) and by month (right).

Cyclopoid copepods were clearly more abundant in 2014 than in either 2013, 2015 or 2016 at both stations (Figure 143a). Seasonally, levels peaked in June at AR4 and in August at AR2 (Figure 143b).

Mesocyclops is one of the more common cyclopoid copepods. Median values of *Mesocyclops* was lower at AR2 than in previous years, but at AR 4 they were clearly lower in 2014 (Figure 144a). Seasonal patterns in *Mesocyclops* were variable (Figure 144b). The most obvious difference was that AR4 was greater than AR2 in June, they both declined strongly in July, and AR2 was greater than AR4 in August.

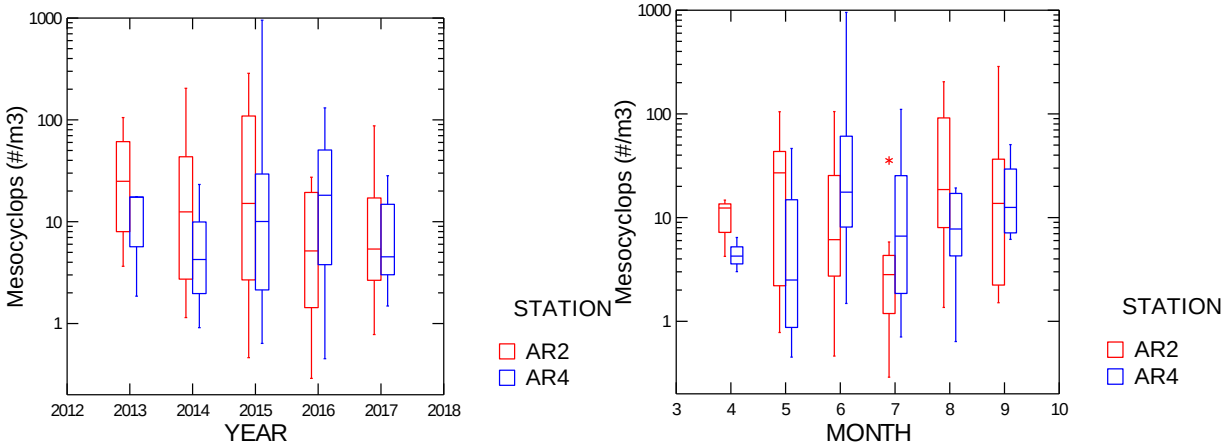

Figure 144. Box plots comparing values of *Mesocyclops* among years (left) and by month (right).

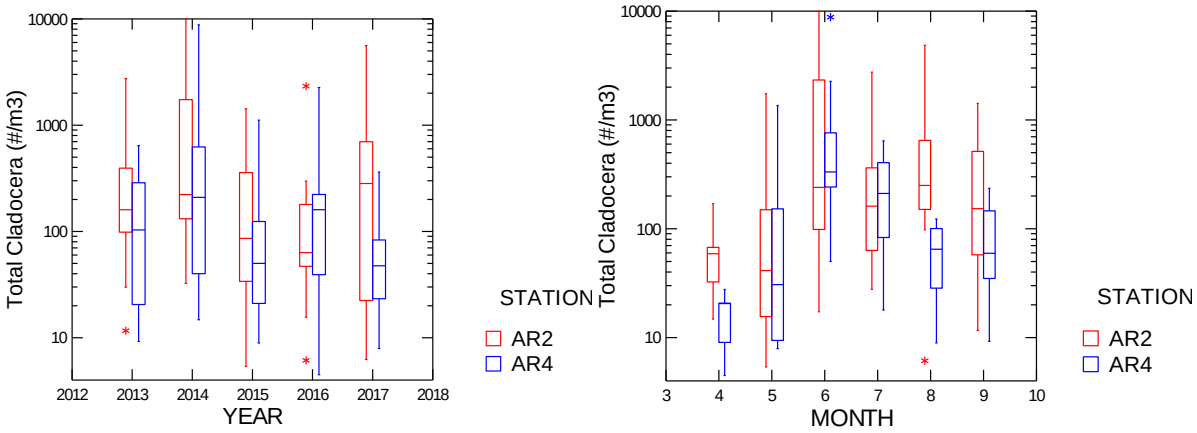

Figure 145. Box plots comparing values of Total Cladocerans among years (left) and by month (right).

Total cladoceran values (excluding *Bosmina*) were clearly lower in 2015 than in the previous two years, but rebounded somewhat in 2016 and 2017 (Figure 145a). A general seasonal pattern was observed with highest values in June (Figure 145b). Values declined quickly in August at AR4, but levels persisted into August at AR2.

Daphnia was found at clearly higher levels in 2014 than in the other three years (Figure 146a). AR2 was clearly greater than AR4 in 2013, but not in the other years. Seasonal patterns consisted of a tendency to higher values in May and Jun than other months (Figure 146b).

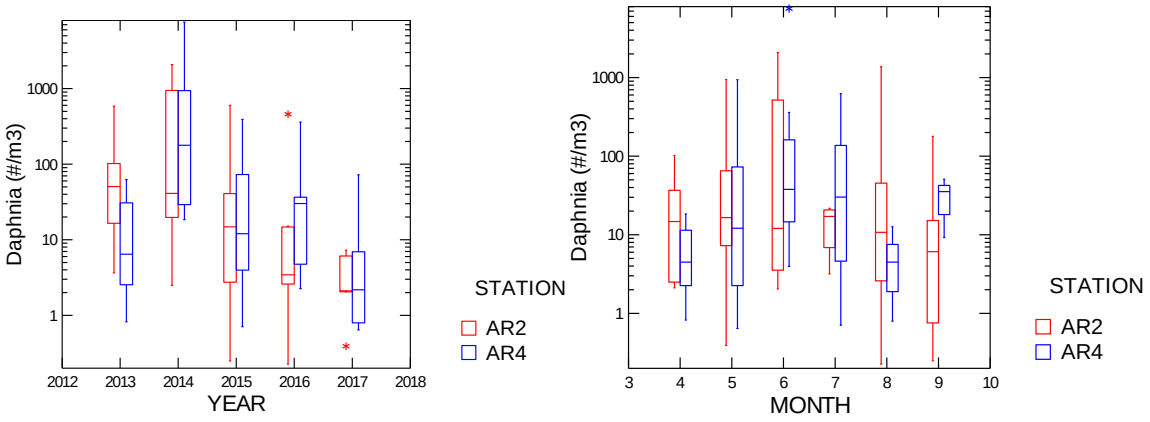

Figure 146. Box plots comparing values of *Daphnia* among years (left) and by month (right).

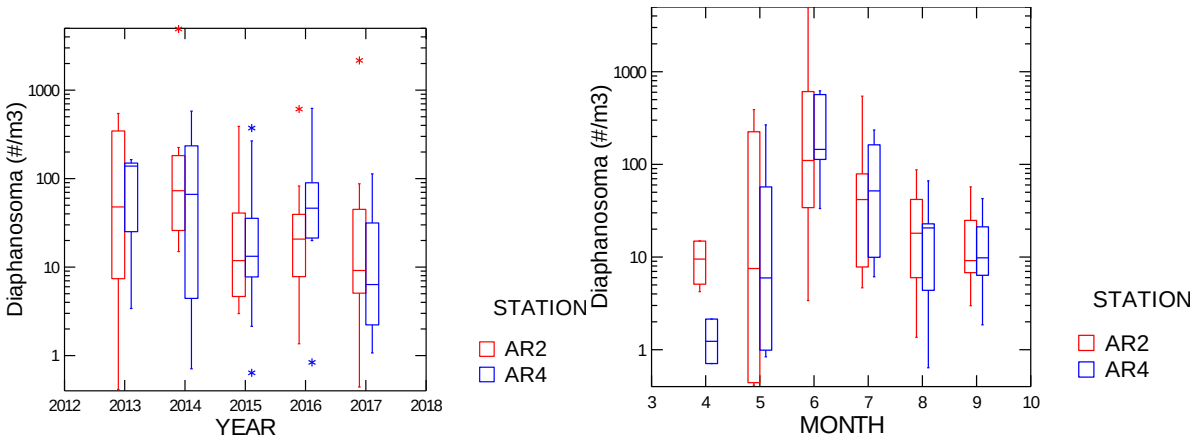

Figure 147. Box plots comparing values of *Diaphanosoma* among years (left) and by month (right).

Diaphanosoma is a very abundant cladoceran in Gunston Cove, but has proven to be less abundant in the Hunting Creek area, although still important. *Diaphanosoma* levels have trended down at both stations (Figure 147a). Seasonal patterns at both stations indicated increasing populations from April to June followed by a steady decline through September (Figure 147b).

Sida was generally less abundant than *Diaphanosoma*, but has maintained its levels over time. It too showed a peak in June at AR4, but has its highest median value in July at AR2.

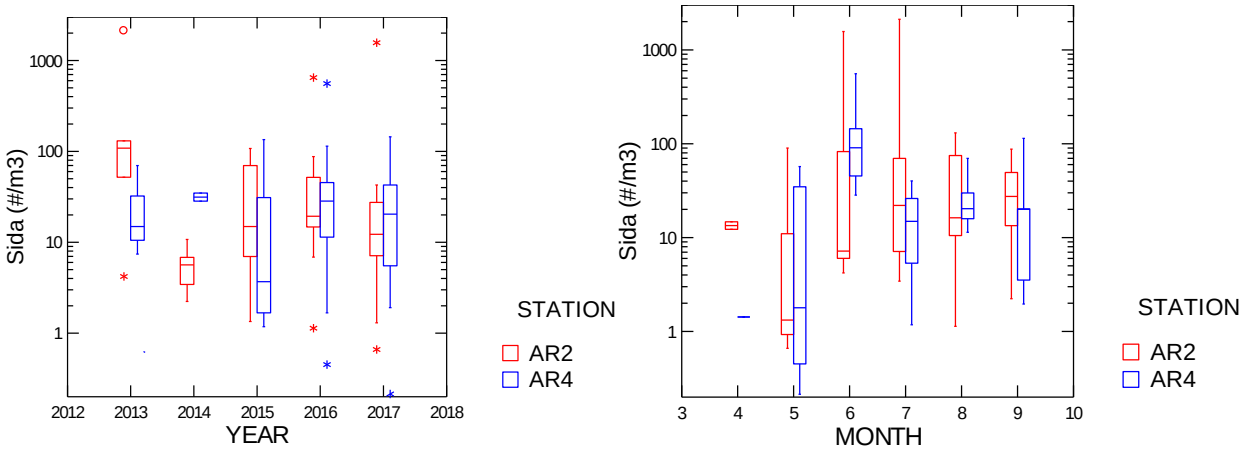

Figure 148. Box plots comparing values of *Sida* among years (left) and by month (right).

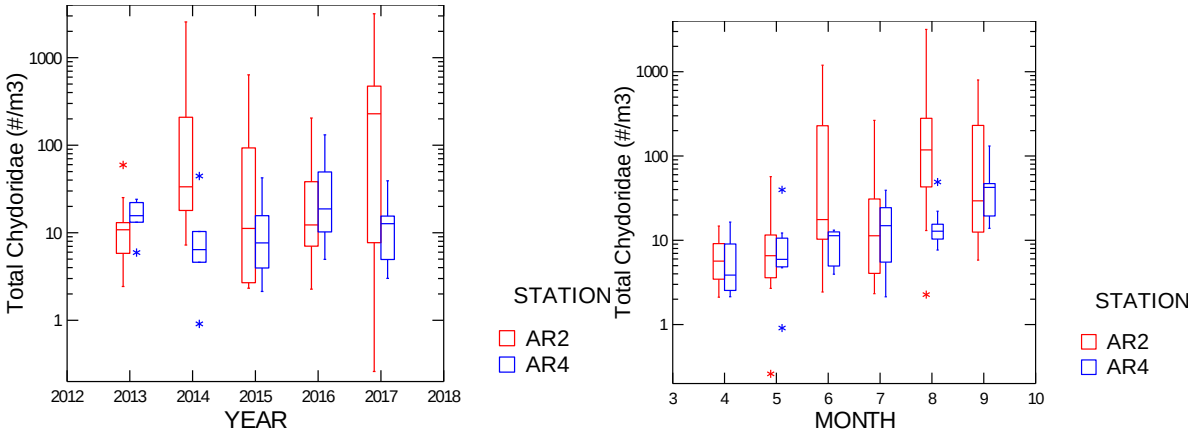

Figure 149. Box plots comparing values of Chydoridae among years (left) and by month (right).

Chydorids have generally been more abundant at AR2 than at AR4 in most years and in June and August (Figure 149a,b). Macrothricids have been found most commonly at AR2 and have been especially abundant in August and September (Figure 150a,b).

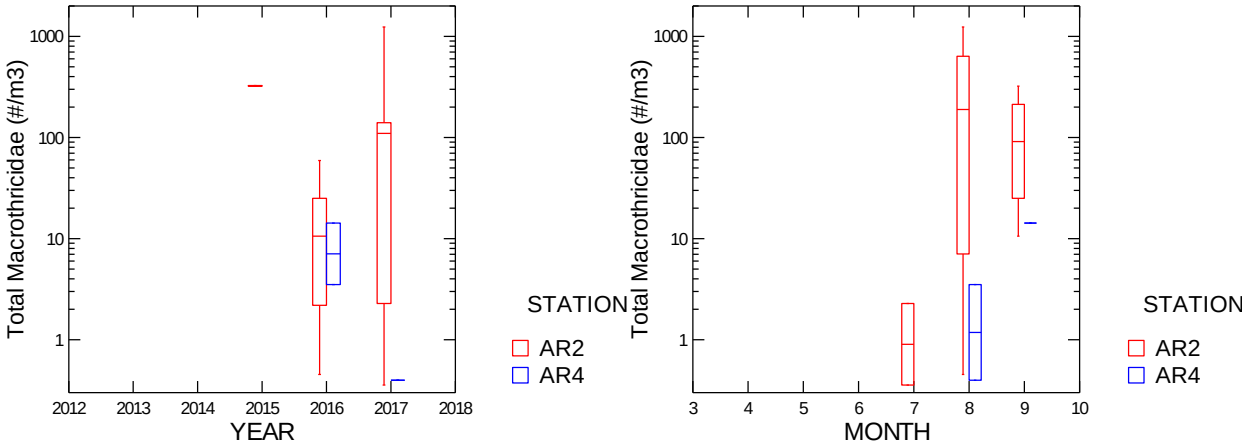

Figure 150. Box plots comparing values of Macrothricidae among years (left) and by month (right).

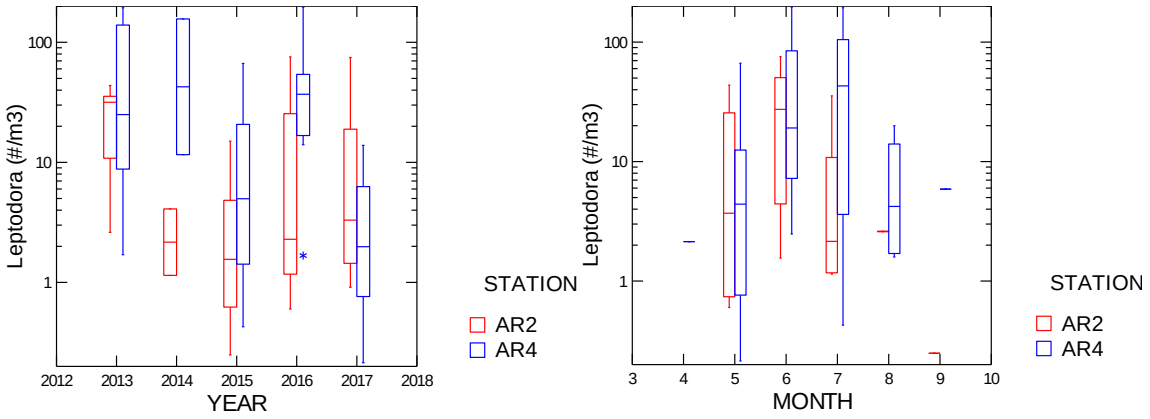

Figure 151. Box plots comparing values of *Leptodora* among years (left) and by month (right).

Leptodora is a large predacious cladoceran which occurs consistently in the study area, but at lower densities. Distinct differences were found between years (Figure 151a). AR4 values were similar in 2013, 2014, and 2016, but distinctly lower in 2017. At AR2 values were highest in 2013. *Leptodora* was found principally in the months May, June and July at both stations, persisting into July and August more strongly at AR2 (Figure 151b).

Total macrozooplankton, those collected in the 202 um net, showed a clear interannual pattern with greatest numbers at both stations in 2014 (Figure 152a). Seasonal patterns were variable (Figure 152b). At AR4 a spring increase ended with a peak in June. Then values declined throughout the summer. The seasonal pattern was variable at AR2.

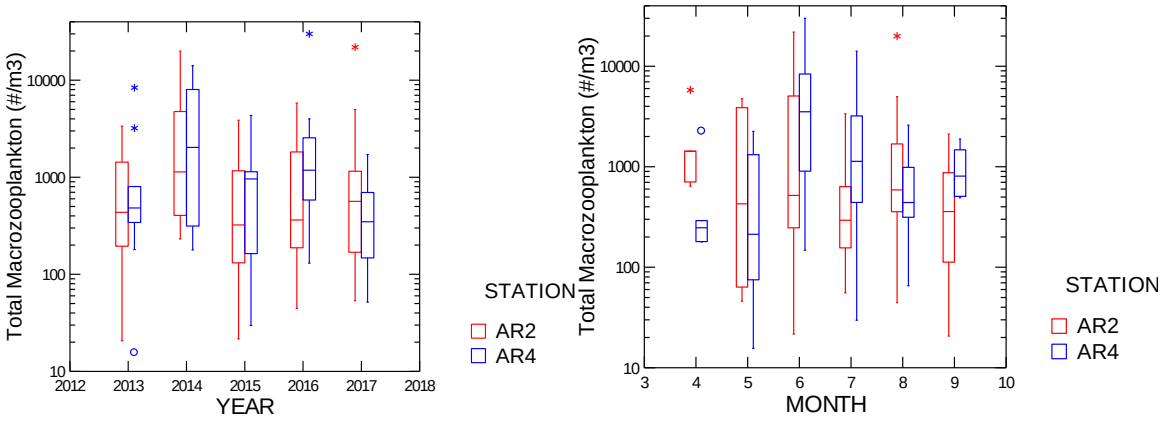

Figure 152. Box plots comparing values of Total Macrozooplankton among years (left) and by month (right).

F. Ichthyoplankton: Comparison among Years

2017 marks the fifth year of our fish collections in Hunting Creek. Both trends and inter-annual variability become apparent when comparing the years of data. In the larval data a high dominance of different species in the herring or shad family (clupeids) are consistently present, and in high densities (Table 19). These include anadromous species of concern such as Blueback Herring and Alewife, for which we also monitor the spawning populations as part of this effort. Overall, larval density was higher in 2017 than 2016, but lower than previous years.

Table 1. Density of larvae collected all years (total # $10m^{-3}$)

Scientific Name	2013	2014	2015	2016	2017
Alosa aestivalis	61.69	200.36	382.05	91.54	205.29
Alosa mediocris	4.80	4.13	12.11	9.63	4.28
Alosa pseudoharengus	139.80	57.70	265.97	78.52	81.75
Alosa sapidissima	0.12	1.32	0.61	1.97	2.80
Alosa species	0.00	18.49	0.00	0.00	0.00
Carassius auratus	56.78	0.89	0.00	0.30	7.02
Carpiodes cyprinus	0.00	0.00	0.00	0.78	0.00
Centrarchidae	0.00	0.00	0.00	0.13	0.00
Clupeid species	422.95	781.67	444.54	175.51	193.31
Cyprinidae	1.14	0.00	0.59	0.00	0.00
Cyprinus carpio	0.00	0.00	0.00	0.00	2.98
Dorosoma cepedianum	438.39	381.85	592.25	221.54	293.50
Eggs	0.16	3.09	2.69	17.80	25.66
Enneacanthus gloriosus	0.00	0.24	0.00	0.00	0.00
Etheostoma olmstedi	0.00	0.00	0.00	0.13	0.00
Fundulus diaphanus	0.00	0.00	0.00	0.00	0.50
Fundulus species	0.14	0.00	0.00	0.20	0.00
Hybognathus regius	0.00	0.00	0.00	0.00	0.50
Lepisosteus osseus	0.00	0.00	0.00	0.00	0.25
Lepomis cyanellus	0.00	0.00	0.00	0.41	0.50
Lepomis gibbosus	0.00	0.00	0.00	1.62	0.99
Lepomis macrochirus	0.00	0.00	0.00	0.00	0.50
Lepomis species	0.60	2.83	0.49	0.00	8.23
Menidia beryllina	2.48	3.32	1.98	20.36	60.78
Menidia species	0.00	0.00	0.00	2.60	0.00
Micropterus dolomieu	0.00	0.00	0.00	0.00	0.25
Morone americana	0.00	5.90	15.93	8.59	17.54

Morone saxatilis	0.00	4.02	0.00	1.09	7.71
Morone species	39.06	43.46	4.32	14.11	3.71
Notemigonus crysoleucas	0.00	0.84	0.00	0.00	0.00
Notropis hudsonius	0.00	0.00	0.00	0.39	2.48
Perca flavescens	38.22	1.41	0.00	0.65	0.50
Strongylura marina	0.00	0.12	0.00	0.00	0.13
Unidentified	11.45	84.35	27.42	34.66	84.23
Total	**1217.80**	**1595.98**	**1750.95**	**682.52**	**1005.38**

G. Adult and Juvenile Fish: Comparison among Years

The total number of adult and juvenile fishes collected in 2017 had the same trend with higher numbers than 2016 but lower than the years before (2013-2015; Table 15).
The SAV beds that have been increasing in cover since the start of the study are a likely contributor to the lower abundances in 2016 and 2017 compared to 2013-2015. It is important to note that the SAV growth obstructs our ability to effectively collect trawl and seine samples, therefore the lower numbers likely do not represent reduced abundances; rather it reflect our reduced ability to collect representative samples. There are clear benefits to the presence of SAV, it for example provides fish habitat and helps improve water clarity. The high amounts of organic matter is representative of a eutrophic system, but a system with higher functionality than a phytoplankton dominated system.
To address the problem of our reduced ability to tow nets, we have added fyke nets to our sampling gear since 2016. The extensive SAV growth makes it highly suitable gear for the location, and total catch with fyke nets actually exceeded that of the trawls in both 2016 and 2017. The fyke nets are likely the most efficient gear to sample thick SAV beds, and we recommend continued use of this gear in our surveys.
In 2017, the clear trend of high abundance and dominance of Banded Killifish (*Fundulus diaphanus*) continues (Figure 153), even while total Banded Killifish abundance is lower than previous years (Table 15). Another consistently abundant species, White Perch (*Morone americana*), while having low abundances in 2016, was present in high abundance again in 2017. Spottail Shiner, which was found in high abundance from 2013-2015 had low abundance both in 2016 and 2017. Some species increased in abundance, such as Goldfish, Bluegill, and Pumpkinseed. The second most abundant species in 2016 (Inland Silverside) was present in relatively high numbers again.
In 2017, 27 different species were collected, which is similar to previous years, and a sign of a healthy diversity. Now that the high abundance of Banded Killifish is reduced, and other species such as sunfishes have increased in abundance, the evenness (distribution of abundance over species) has substantially increased in 2017. The Simpson's Index of Diversity (calculated as $1-(\mathbf{\Sigma}\ (n_i/N)^2)$) was 0.73 in 2013, 0.567 in 2014, 0.55 in 2015, 0.469 in 2016, and 0.834 in 2017 (Figure 154). Note that in the 2016 report the Simpson's index (D) was reported, in which communities with higher diversity or evenness approach zero. In this report we calculated the Simpson's Index of Diversity, which is 1-D. In this index the communities with higher diversity

have higher values (approaching 1) which is more intuitive to interpret. While evenness was reduced each year of sampling before 2017, 2017 shows a high Simpson's Index of Diversity value (Figure 154). Overall, the fish species found in Hunting Creek are characteristic of Potomac River tributaries.

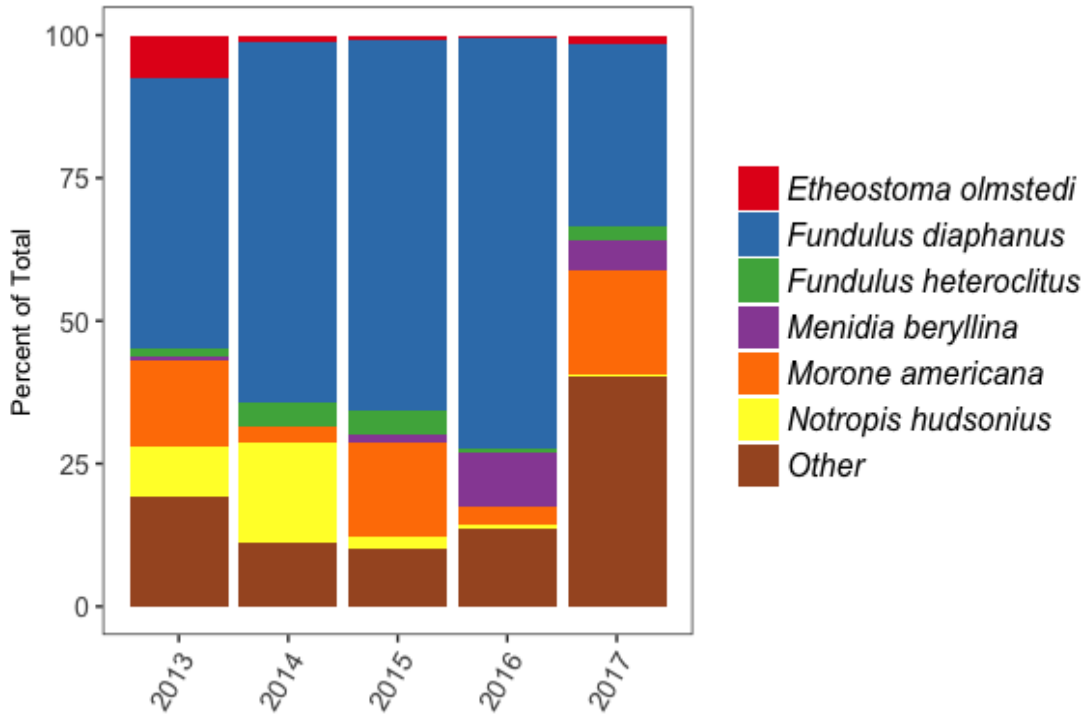

Figure 153. Percentage of total of dominant species collected in all years

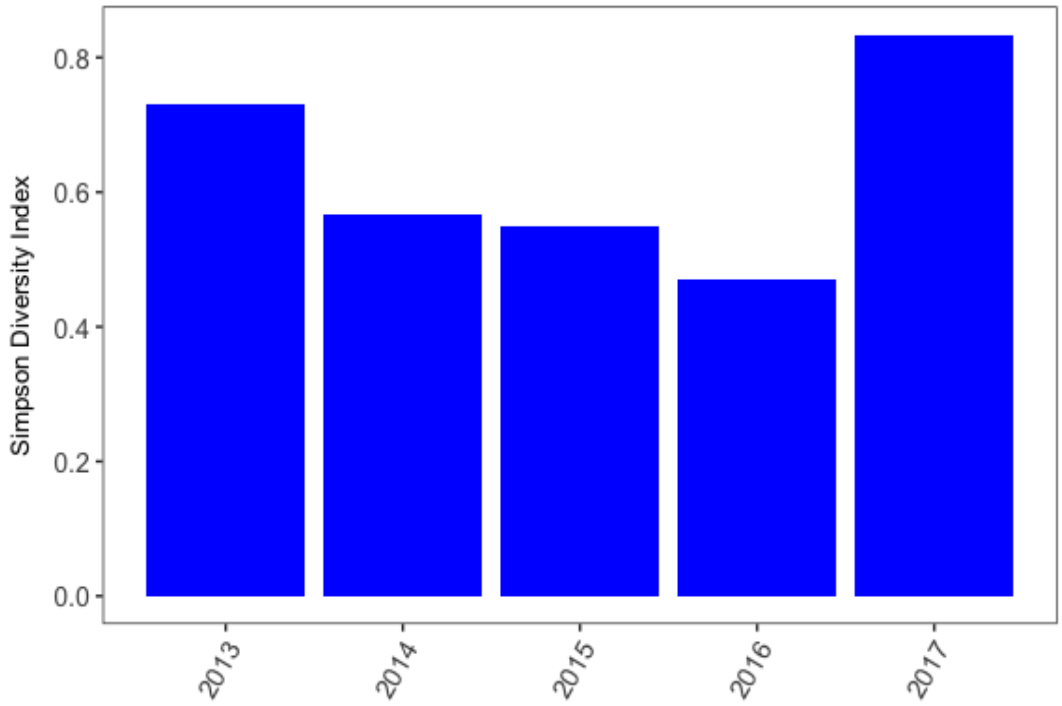

Figure 154. Simpson Diversity Index of fish species collected in Hunting Creek all years.

Table 20. Abundances of adult and juvenile fishes collected all years

Scientific Name	2013	2014	2015	2016	2016 w/ Fyke	2017	2017 w/ Fyke
Alosa aestivalis	16	8	12	29	29	0	0
Alosa pseudoharengus	6	23	28	12	12	0	0
Alosa sapidissima	208	32	163	19	19	2	2
Alosa species	299	8	55	11	12	3	3
Ameiurus catus	0	0	0	1	2	0	0
Ameiurus nebulosus	3	2	3	3	3	2	6
Anchoa mitchilli	69	70	7	0	0	0	0
Anguilla rostrata	1	3	2	0	0	0	0
Carassius auratus	20	39	2	0	12	18	129
Carpiodes cyprinus	9	19	2	0	0	0	0
Cyprinella spiloptera	0	0	1	0	0	0	0

Scientific Name	2013	2014	2015	2016	2016 w/ Fyke	2017	2017 w/ Fyke
Cyprinus carpio	0	3	1	7	16	3	3
Dorosoma cepedianum	5	1	3	0	0	0	0
Enneacanthus gloriosus	0	0	0	0	0	27	53
Etheostoma olmstedi	292	49	39	3	9	33	36
Fundulus diaphanus	1798	2382	2723	1387	1587	690	786
Fundulus heteroclitus	53	152	174	16	16	62	62
Gambusia holbrooki	11	69	19	0	0	1	1
Hybognathus regius	0	6	31	2	4	40	40
Ictalurus furcatus	12	4	4	1	1	6	6
Ictalurus punctatus	0	0	2	0	0	0	0
Lepisosteus osseus	0	0	3	1	1	1	1
Lepomis auritus	0	0	1	2	2	0	0
Lepomis cyanellus	0	0	2	0	0	4	8
Lepomis gibbosus	6	17	11	11	25	39	215
Lepomis macrochirus	12	52	21	8	23	28	227
Lepomis megalotis	0	0	0	0	0	1	1
Lepomis microlophus	6	11	5	2	10	0	0
Lepomis species	5	12	5	27	100	50	198
Menidia beryllina	15	6	73	209	210	114	126
Micropogonias undulatus	1	0	0	0	0	0	0
Micropterus dolomieu	5	5	9	6	6	62	72
Micropterus punctulatus	1	0	0	0	0	0	0
Micropterus salmoides	3	7	0	5	5	2	2
Micropterus species	1	0	0	0	0	0	0
Morone americana	574	107	693	19	67	393	450
Morone saxatilis	2	0	2	1	6	5	9
Morone species	0	1	0	0	0	0	0
Notemigonus crysoleucas	2	3	13	2	2	2	2
Notropis hudsonius	338	666	87	13	18	11	13
Perca flavescens	22	16	7	7	7	1	2
Pomoxis nigromaculatus	0	0	4	0	1	0	0
Strongylura marina	2	4	3	0	0	9	9
Unidentified	2	0	0	0	0	0	0

Scientific Name	2013	2014	2015	2016	2016 w/ Fyke	2017	2017 w/ Fyke
Total	**3798**	**3777**	**4210**	**1804**	**2205**	**1609**	**2463**

H. Submersed Aquatic Vegetation: Comparison among Years

According to annual reports of the Virginia Institute of Marine Science (VIMS) SAV Monitoring Program (http://web.vims.edu/bio/sav/maps.html), virtually the entire surface area of the Hunting Creek embayment has been covered with submersed aquatic vegetation in each of the years of this study (2013-2017). In 2016 and 2017 mapping of species was done in association with the water quality mapping surveys and the results have been reported in the results section of these reports. In 2017 the native SAV species *Ceratophyllum demersum* was substantially more abundant than the exotic species *Hydrilla verticillata* in contrast to 2016 when they had a similar abundance. In future years we plan to collect further data on species composition to allow for trend analysis of species abundances.

I. Benthic Macroinvertebrates: Comparison among Years

River and Embayment Samples

Benthic invertebrate data from the tidal stations indicated that 2017 values and trends were similar to other years. A moderate diversity of organisms were observed at all three tidal stations with flatworms, oligochaetes, and chironomids being most abundant at AR2, bivalves and amphipods most abundant at AR3, and isopods most abundant at AR4. Total abundance was somewhat lower than in previous years of the study.

Table 21. Comparison of Benthic Macroinvertebrate Abundance by Taxonomic Group. 2017 vs. previous years. Turbellaria-flatworms, Oligochaeta-oligochaetes, Hirudinea-leeches, Gastropoda-snails, Bivalva-clams and mussels, Amphipoda-scuds, Isopoda-sow bugs, Chironomidae-midges (mostly larvae).

	AR2		AR3		AR4	
	2013-16 avg	2017	2013-16 avg	2017	2013-16 avg	2017
Turbellaria	1.4	8.6	2.6	4.1	0.2	0.3
Oligochaeta	222.3	67.3	132.5	30.3	70.7	16.9
Hirudinea	0.4	0.4	0.1	0.1	1.1	0.1
Gastropoda	16.4	8.3	61.4	3.8	1.9	0.1
Bivalva	2.9	1.1	1.9	3.2	3.3	2.8
Amphipoda	16.0	14.2	18.9	22.1	13.7	7.4
Isopoda	8.3	0.0	4.3	0.1	4.2	2.6
Chironomidae	33.7	6.1	10.4	1.9	4.8	0.8
Other	2.7	1.5	1.9	0.7	1.2	0.1
Total	303.7	107.5	236.3	66.3	101.1	31.1

Tributary Samples

Tributary benthic samples were collected in 2016 and these data will provide a baseline for assessment of future trends. Overall tributary stations exhibited moderately degraded conditions typical of streams draining urbanized areas such as the Cameron Run watershed. Results for 2017 were similar to 2016. In 2017 we started to calculate metrics and will use those in future years to develop and apply indices of biotic integrity.

LITERATURE CITED

Bigelow, H.B. and W.C.Schroeder. 1953. Fishes of the Gulf of Maine. Fishery bulletin No. 74, Vol. 53. U.S. Government Printing Office. Washinton, D.C. 577 pp.

Carter, V., P.T. Gammon, and N.C. Bartow. 1983. Submersed Aquatic Plants of the Tidal Potomac River. Geological Survey Bulletin 1543. U.S. Geological Survey. 63 pp.

Chesapeake Bay Program. 2006 Ambient water quality criteria for dissolved oxygen, water clarity, and chlorophyll *a* for the Chesapeake Bay and its tidal tributaries. 2006 Addendum. Downloaded from Bay Program website 10/13/2006.

Cummings, H.S., W.C. Purdy, and H.P. Ritter. 1916. Investigations of the pollution and sanitary conditions of the Potomac watershed. Treasury Department, U.S. Public Health Service Hygienic Laboratory Bulletin 104. 231 pp.

Dahlberg, M.D. 1975. Guide to coastal fishes of Georgia and nearby states. University of Georgia Press. Athens, GA 187 pp.

Douglass, R.R. 1999. A Field Guide to Atlantic Coast Fishes: North America (Peterson Field Guides). Houghton Mifflin Harcourt, Boston. 368 pp.

Eddy, S. and J.C. Underhill. 1978. How to know the freshwater fishes. 3rd Ed. W.C. Brown Co. Dubuque, IA. 215 pp.

Froese, R. and D. Pauly (Eds.). 2012. Fish Base. World Wide Web electronic publication. www.fishbase.org, version (04/2012).

Hildebrand and Schroeder. 1928. Fishes of the Chesapeake Bay. U.S. Bureau of Fisheries Bulletin 53, Part 1. Reprinted 1972. T.F.H. Publishing, Inc. Neptune, NJ. 388 pp.

Hogue, J.J, Jr., R.Wallus, and L.K. Kay. 1976. Preliminary guide to the identification of larval fishes in the Tennessee River. Technical Note B19. Tennessee Valley Authority. Knoxville, TN.

Islam, S. 2001. Seasonal dynamics of micro-, nanno-, and picoplankton in the tidal freshwater Potomac River in and around Gunston Cove. Ph.Dissertation. George Mason University. 127 pp.

Jenkins, R.E. and N.M. Burkhead. 1994. The freshwater fishes of Virginia. American Fisheries Society. Washington, DC. 1080 pp.

Jones, P.W., F.D. Martin, and J.D. Hardy, Jr. 1978. Development of fishes of the Mid-Atlantic bight. Volumes I-VI. Fish and Wildlife Service, U.S. Department of the Interior. FWS/OBS-78/12.

Kraus, R.T. and R.C. Jones. 2011. Fish abundances in shoreline habitats and submerged aquatic vegetation in a tidal freshwater embayment of the Potomac River. Environmental Monitoring and Assessment. Online: DOI 10.1007/s10661-011-2192-6.

Kelso, D.W., R.C. Jones, and P.L. deFur. 1985. An ecological study of Gunston Cove - 1984-85. 206 pp.

Lippson, A.J. and R.L. Moran. 1974. Manual for identification of early development stages of fishes of the Potomac River estuary. Power Plant Siting Program, Maryland Department of Natural Resources. PPSP-MP-13.

Loos, J.J., W.S. Woolcott, and N.R. Foster. 1972. An ecologist's guide to the minnows of the freshwater drainage systems of the Chesapeake Bay area. Association of Southeastern Biologists Bulletin 19: 126-138.

Lund, J.W.G., C. Kipling, and E.C. LeCren. 1958. The inverted microscope method of estimation algal numbers and the statistical basis of estimations by counting.

Hydrobiologia 11: 143-170.
Mansueti, A.J. and J.D. Hardy, Jr. 1967. Development of fishes of the Chesapeake Bay region: an atlas of egg, larvae and juvenile stages: Part 1. Natural Resources Institute. University of Maryland. 202 pp.
Merritt, R.W. and K.W. Cummins. 1984. An introduction to the aquatic insects of North America. 2nd edition. Kendall/Hunt Publishing Co., Dubuque, IA. 722 pp.
Pennack, R.W. 1978. Fresh-water invertebrates of the United States. 2nd ed. Wiley-Interscience. New York, NY.
Schloesser, R.W., M.C. Fabrizio, R.J. Latour, G.C. Garman, G.C., B. Greenlee, M. Groves and J. Gartland. 2011. Ecological role of blue catfish in Chesapeake Bay communities and implications for management. American Fisheries Society Symposium 77:369-382.
Scott, W.B. and E.J. Crossman. 1973. Freshwater fishes of Canada. Bulletin 184. Fisheries Research Board of Canada. Ottawa, Canada. 966 pp.
Standard Methods for the Examination of Water and Wastewater. 1980. American Public Health Association, American Waterworks Association, Water Pollution Control Federation. 15th ed. 1134 pp.
Thorp, J.H. and A.P. Covich, eds. 1991. Ecology and classification of North American Freshwater Invertebrates. Academic Press. San Diego, CA. 911 pp.
Wetzel, R.G. 1983. Limnology. 2nd ed. Saunders. 767 pp.
Wetzel, R.G. and G.E. Likens. 1991. Limnological analyses. 2nd ed. Springer-Verlag. 391 pp.

Anadromous Fish Survey of Cameron Run - 2017

Final Report
By

Kim de Mutsert
Assistant Professor, Department of Environmental Science and Policy
Associate Director, Potomac Environmental Research and Education Center
George Mason University

Introduction

The anadromous fishes in the herring family (Clupeidae) live as adults in the coastal ocean, but return to freshwater creeks and rivers to spawn. In the mid-Atlantic region, four species are present: American Shad (*Alosa sapidissima*), Blueback Herring (*Alosa aestivalis*), Alewife (*Alosa pseudoharengus*), and Hickory Shad (*Alosa mediocris*). Two other herring family species are semi-anadromous and spawn in Potomac River tributaries. These are Gizzard Shad (*Dorosoma cepedianum*) and Threadfin Shad (*Dorosoma petenense*). Both are very similar morphologically and ecologically, but only *D. cepedianum* is found as far upriver on the Potomac River watershed as Hunting Creek/Cameron Run. Previous reports describe the history of herring populations in the Potomac River watershed (Jones et al. 2014).

The focus of the Cameron Run fish survey is river herring, the collective name of Blueback Herring and Alewife. River herring populations have declined drastically over their range, spurring conservation efforts since 1970, which have been intensified since 2005 with implementation of moratoria. Identifying all areas used as spawning habitat by Alewife and/or Blueback Herring is an important component of their conservation. Since 1988, George Mason University researchers have focused a monitoring program on the spawning of these species in other tributaries such as Pohick Creek, Accotink Creek, and, less regularly, Dogue Creek. With this study Cameron Run is added, which has not been monitored for presence of river herring or other anadromous species by either George Mason or other fisheries biologists before the start of this study in 2013 (Jim Cummins, pers. comm.). Our 2013 survey provided the first confirmation of Cameron Run as River Herring spawning habitat (Allan Weaver, VDGIF, pers. comm.). Use of Cameron Run by river herring upstream from where the effluent of Alexandria Renew Enterprises enters Cameron Run signifies that the effluent does not deter river herring from using Cameron Run as spawning habitat. In 2014 we moved the collection site approximately 500 m downstream (still above the Alexandria Renew Enterprises effluent), which increased our catches, and allows us to estimate the size of the spawning population. The new location proved successful and will remain the collection site for any subsequent surveys.

Methods

We conducted weekly sampling trips from March 24 to May 25 in 2017. During each trip (when condition allow it) a hoop net was set with wings blocking the complete creek (referred to as

block net) to collect adults swimming upstream, and ichthyoplankton nets were set to collect larvae floating downstream. Cross-section and flow was measured to calculate discharge, and physical parameters were measured using a handheld YSI. In some occasions, water level and flow were too high to complete one or more procedures, Table 1 provides the information on which procedures were completed each sampling day in 2017. The sampling location was chosen to be upstream from the Alex Renew effluent, and downstream of the first dam in Cameron Run (Figure 1).

Table 1. Procedures completed each sampling date

Date	Block net	Plankton nets	Cross-section	YSI
3/24/17	Y	Y	Y	Y
4/1/17	Y	Y	Y	Y
4/7/17	Y	Y	Y	Y
4/14/17	Y	Y	Y	Y
4/20/17	Y	Y	Y	Y
4/27/17	Y	Y	Y	Y
5/4/17	Y	Y	Y	Y
5/11/17	N*	Y	N*	Y
5/18/17	Y	Y	Y	Y
5/25/17	N*	Y **	N*	Y

*Water flow was too high to safely set the block net or cross the creek to conduct a cross-section ** Water was so turbid that the plankton tow was conducted for 10 minutes rather than 20 minutes

Ichthyoplankton was collected by setting two conical plankton net with a mouth diameter of 0.25 m and a square mesh size of 0.333 mm in the stream current for 20 minutes. A mechanical flow meter designed for low velocity measurements was suspended in the net opening and provided estimates of water volume filtered by the net. The number of rotations of the flow meter attached to the net opening was multiplied with a factor of 0.0049 to gain volume filtered (m^3). Larval density (#/$10m^3$) per species was calculated using the following formula:
Larval density (#/$10m^3$) = 10N/(0.0049*(flow meter start reading-flow meter end reading))
Where N is the count of the larvae of one species in one sample.

We collected 2 ichthyoplankton samples per week, and these were spaced out evenly along the stream cross-section. Coincident with plankton samples, we calculated stream discharge rate from measurements of stream cross-section area and current velocity using the following equation:
Depth (m) x Width (m) x Velocity (m/s) = Discharge (m^3/s)
Velocity was measured using a handheld digital flow meter that measures flow in cm/s, which had to be converted to m/s to calculate discharge.

Both depth and current velocity were measured at 12 to 20 locations along the cross-section. At each sampling trip other physical parameters of the creek were recorded as well (water temperature, dissolved oxygen, pH, and conductivity).

The ichthyoplankton samples were preserved in 70% ethanol and transported to the GMU laboratory for identification and enumeration of fish larvae. Identification of larvae was accomplished with multiple taxonomic resources: primarily Lippson & Moran (1974), Jones et

al. (1978), and Walsh et al. (2005). River herring (both species) have semi-demersal eggs (tend to sink to the bottom) that are frequently adhesive. As this situation presents a significant bias, we are not treating egg abundance in the samples as a reliable estimate of egg abundance, and this is not used in population productivity estimates. We estimate total larval production (P) during the period of sampling by multiplying the larval density (m^{-3}) with total discharge (m^3) during the spawning period, which we assume is represented with our sampling period.
The block net was deployed once each week in the morning and retrieved the following morning (see Figure 2). Fish in the block net were identified, enumerated, and measured.

Figure 1. Sampling location Cameron Run.

Since the net was set 24 hours per week for 10 weeks, we approximated total abundance of spawning river herring during the time of collection by extrapolating the mean catch per hour per species during the time the creeks were blocked of over the total collection period as follows:
Average catch/24 hours * 1680 hours = total abundance of spawners
Our total collection period is assumed as a good approximation of the total time of the spawning run of Alewife.

In response to problems with animals tearing holes in our nets in previous sampling experiences, we used a fence device in front of the mouth of the net that significantly reduces this problem. The device effectively excluded wildlife such as otters and turtles, while it has slots that allowed up-running fish to be captured.

Figure 2. Block net deployed in new location in Cameron Run. The hedging is angled downstream in order to funnel up-migrating herring into the opening of the net.

Results and Discussion

During the 10-week sampling period, we caught fourteen adult Alewife, and several non river herring species (Table 2). The abundance of river herring collected in 2017 was similar to previous years, which signifies the consistent use of Cameron Run as spawning ground. The net is set in such a way that fishes need to swim upstream into Cameron Run to be caught in the net, which is a behavior associated with spawning. We did not find adult Blueback Herring specimens in our collections, of which we have only collected 1 in 2014. We also could not positively identify Blueback Herring among the larvae collected, of which we did find some in previous years. Since the spawning populations is small and sampling variability high (for larval density, a small portion of the water column is sampled for 20 minutes per week), sampling over multiple years will provide us with increasingly better estimates of the spawning population of Alewife and Blueback Herring in Cameron Run.

In the ichthyoplankton samples we could positively identify 24 Alewife larvae (Table 3). The few unidentified larvae (10) and especially the unidentified clupeids (6) could potentially include more Alewife larvae and/or larvae of Blueback herring which we have found in previous years. We found 2 Gizzard Shad (*Dorosoma cepedianum*) larvae, which is a clupeid as well, which makes Alewife the most abundant clupeid in the samples. Larvae of other species were present in the samples as well, including Spottail Shiner (*Notropis hudsonius*), a species of darter (*Etheostoma sp.*), Common Carp (*Cyprinus carpio*), inland silverside (*Menidia beryllina*), White Perch or Striped bass (*Morone* sp.), Bluegill (*Lepomis macrochirus*), and Yellow Perch (*Perca flavescens*; Table 3).

Table 2. Adult fishes collected in Cameron Run with block net during weekly sampling from 3/24/17-5/25/17. River herring are indicated by bold font.

Date	Scientific Name	Common Name	Count
3/24/17	*Micropterus salmoides*	Largemouth Bass	1
4/1/17	***Alosa pseudoharengus***	**Alewife**	**4**
4/1/17	*Micropterus salmoides*	Largemouth Bass	1
4/14/17	*Carassius auratus*	Goldfish	1
4/14/17	*Lepomis macrochirus*	Bluegill	1
4/14/17	*Micropterus salmoides*	Largemouth Bass	1
4/20/17	***Alosa pseudoharengus***	**Alewife**	**9**
4/20/17	*Lepomis auritus*	Redbreast Sunfish	1
4/27/17	***Alosa pseudoharengus***	**Alewife**	**1**
4/27/17	*Carassius auratus*	Goldfish	12
4/27/17	*Lepomis macrochirus*	Bluegill	2
4/27/17	*Lepomis megalotis*	Longear Sunfish	2
4/27/17	*Moxostoma macrolepidotum*	Shorthead Redhorse	2

We measured creek discharge and other physical parameters at the same location and times where ichthyoplankton samples were taken, which was about 100 m downstream from the block net (Table 4). Mean creek discharge was much higher compared to last year. Mean discharge in 2017 was 1.12 $m^3 s^{-1}$, ranging from 0.12 $m^3 s^{-1}$ to 3.62 $m^3 s^{-1}$, while mean discharge in 2016 was 0.52 $m^3 s^{-1}$, ranging from 0.16 $m^3 s^{-1}$ to 1.16 $m^3 s^{-1}$. The two dates when the cross-section measurements could not be completed to calculate discharge (5/11 and 5/25), the reason was that discharge was too high; therefore the mean and max in our measurements are an underestimate of field conditions. Water temperature (Temp) was under 10 °C the first sampling day unlike last year, which is too low for river herring spawing. The first sampling date where we found Alewife (larvae) was April 1, when temperature was 10.28 °C. Dissolved oxygen (DO), and pH were in the benign range for occurrence of river herring throughout the sampling period (Table 4).

Table 3. Larvae collected in Cameron Run. Herring larvae (river herring and other clupeids) are in bold. Volume is volume of water sampled, and AveDensity is the average density based on two samples in # $10m^{-3}$.

Date	Scientific Name	Count	Volume	AveDensity
3/24/17	Eggs	4	71.114	0.586
4/1/17	Eggs	2	9.389	1.109
4/14/17	***Alosa pseudoharengus***	**18**	**8.967**	**20.093**
4/14/17	**Clupeid sp.**	**1**	**8.967**	**1.113**
4/14/17	Eggs	14	8.967	15.603
4/14/17	Unidentified	2	8.967	2.225
4/20/17	***Alosa pseudoharengus***	**2**	**0.357**	*****
4/20/17	**Clupeid sp.**	**2**	**0.357**	*****
4/20/17	Eggs	9	0.357	*
4/20/17	*Notropis hudsonius*	1	0.357	*
4/27/17	***Alosa pseudoharengus***	**4**	**17.694**	**2.402**
4/27/17	***Dorosoma cepedianum***	**1**	**17.694**	**1.325**
4/27/17	Eggs	4	17.694	4.335
4/27/17	*Etheostoma* sp.	1	17.694	1.325
4/27/17	*Notropis hudsonius*	2	17.694	1.684
4/7/17	**Clupeid sp.**	**1**	**96.898**	**0.134**
4/7/17	Eggs	467	96.898	47.184
5/4/17	Unidentified	1	0.260	*
5/11/17	**Clupeid sp.**	**2**	**15.024**	**1.150**
5/11/17	*Cyprinus carpio*	1	15.024	0.575
5/11/17	***Dorosoma cepedianum***	**1**	**15.024**	**0.575**
5/11/17	Eggs	49	15.024	32.695
5/11/17	*Menidia beryllina*	1	15.024	0.790
5/11/17	*Morone sp.*	1	15.024	0.790
5/11/17	Unidentified	3	15.024	1.940
5/18/17	Eggs	4	0.397	*
5/25/17	Eggs	31	49.990	6.202
5/25/17	*Lepomis macrochirus*	2	49.990	0.398
5/25/17	*Menidia beryllina*	2	49.990	0.400
5/25/17	*Perca flavescens*	1	49.990	0.201
5/25/17	Unidentified	4	49.990	0.802

*The flow velocity in Cameron Run was too low at this date for the flow meter to function properly; therefore

volume sampled is likely an underestimate, and larval density not calculated.

Table 4. Physical parameters measured or calculated (discharge) at Cameron Run during each sampling week.

Date	Discharge ($m^3 s^{-1}$)	Temp (°C)	SpCond ($mS s^{-1}$)	DO ($mg l^{-1}$)	pH
3/24/17	0.896	7.27	0.737	12.7	7.75
4/1/17	2.759	10.28	0.606	11.21	7.98
4/7/17	3.622	11.08	0.5	10.81	7.45
4/14/17	0.464	18.49	0.603	11.51	7.97
4/20/17	0.560	20.16	0.608	11.04	7.7
4/27/17	0.251	20.53	0.602	9.82	7.32
5/4/17	0.290	19.45	0.633	11.6	7.7
5/11/17	NA	15.4	0.342	10.3	6.87
5/18/17	0.124	25.6	0.4792	13.24	8.52
5/25/17	NA	19.5	0.2891	11.41	8.28

During the sampling period of 10 weeks, the total discharge was estimated to be on the order of 6.8 million cubic meters (Table 5). This is about twice as much as last year. Given the observed mean densities of larvae, the total production of river herring larvae was estimated at approximately 762 thousand for Cameron Run (Table 5). Note that the estimate is based on a small sample (0.00004 % of the total discharge). With 14 adult Alewife collected, and extrapolating over period of the spawning run as explained in the methods, this could mean that the Alewife spawning population in 2017 was the size of 123 individuals (133 last year).

Table 5. Estimation of river herring (alewife and blueback herring) larval production and spawner abundance from Cameron Run during spring 2017

Parameter	CameronRun
Mean discharge ($m^3 s^{-1}$)	1.121
Total discharge, (m^3)	6,778,504.435
Total volume sampled (larvae)(m^3)	270.09
Mean Alosa larvae density (# $10m^{-3}$)	1.125
Total river herring production (# larvae)	762,446.179
Total adult river herring (#)	122.5

Conclusions

After finding that Cameron Run is used as river herring spawning habitat with just one adult river herring and seven larvae in 2013, we were able to confirm this finding by collecting more river herring adults and larvae from 2014-2017 (Figure 3). By moving our sampling site

approximately 500 m downstream in 2014 we have found a better sampling location. Even further downstream Cameron Run becomes too deep and wide for our sampling strategy.

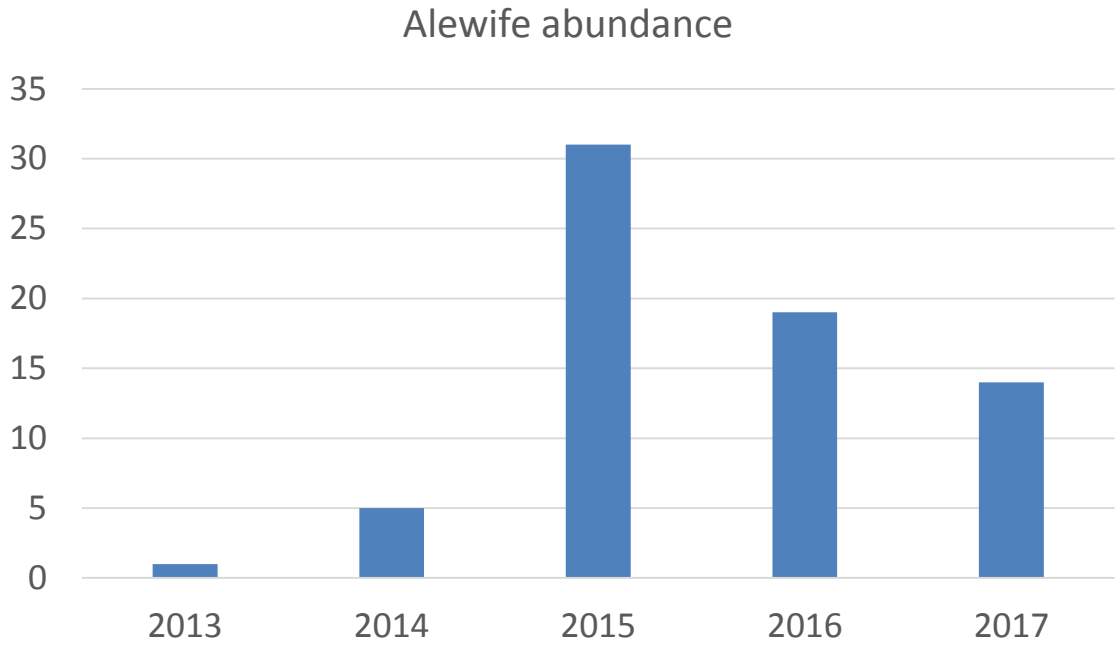

Figure 3. Abundance of Alewife (number of individuals) collected with the block net in each year.

Conclusions

The finding of river herring adults and larvae in an area above the outflow of the Alexandria Renew Enterprises wastewater reclamation facility signifies that the water of Cameron Run is clean enough to use as spawning habitat for these species of concern. These finding will not affect AlexRenew, but will affect the terms of construction permits in and around Cameron Run (i.e. some construction activities may be restricted by the Virginia Department of Game and Inland Fisheries (VDGIF) during the annual spawning period (mid-March to mid-May) of river herring (Allen Weaver, VDGIF, pers. comm.).

Although the current evidence suggests that the importance of Cameron Run may be marginal to Alewife and Blueback Herring populations, it is important to recognize that marginal habitats may sustain fish populations during periods of declining abundance and low recruitment (Kraus and Secor 2005). Due to the moratorium on river herring set in place bay-wide in 2012, annual estimation of spawner abundance should be a continued priority for annual monitoring of this and other Potomac River tributaries. The peak in abundance in 2015 was 3 years after the 2012 moratorium, which is about the time it takes for Alewife to grown to adulthood and return to their spawning grounds. This peak has been seen in other tributaries to the Potomac River as well (Jones and De Mutsert 2016) and could signify the effect of the release from the fishery. This effect was not seen throughout Virginia however (Allen Weaver, VDGIF, pers. comm.), and was not maintained to the same level in the subsequent years (2016 and 2017). Anadromous fishes typically exhibit strong year-class fluctuations, and 2015 could have been a year-class effect as well. Additional years of data collection (at least through 2 generation lengths ~ a decade) should

provide a sufficient understanding of this variability.

Literature Cited

Jones, P. W., F. D. Martin, and J. D. Hardy, Jr. 1978. Development of fishes of the Mid-Atlantic Bight: an atlas of egg, larval, and juvenile stages, volume 1. Acipenseridae through Ictaluridae. U.S. Fish and Wildlife Service, FWS/OBS-78/12.

Jones, R. C., De Mutsert, K., and G. D. Foster. 2014. An Ecological Study of Hunting Creek-2013. Final report to Alexandria Renew Enterprises, Alexandria, VA. 123 p.

Jones, R. C. and De Mutsert, K. 2016. An Ecological Study of Gunston Cove-2015. Final report. Potomac Environmental Research and Education Center, Fairfax, VA.

Kraus, R. T. and D. H. Secor. 2005. Application of the nursery-role hypothesis to an estuarine fish. Marine Ecology Progress Series 290:301-305.

Lippson, A. J., and R. L. Moran. 1974. Manual for the identification of early developmental stages of fishes of the Potomac River estuary. Maryland Department of Natural Resources, Baltimore.

Walsh H.J., L.R Settle, and D.S. Peters. 2005. Early life history of blueback herring and alewife in the lower Roanoke River, North Carolina. Transactions of the American Fisheries Society 134:910-926.

This page left intentionally blank.

Escherichia coli Abundances in Hunting Creek/Cameron Run and Adjacent Potomac River - 2017

Final Report
By

Robert B. Jonas
Associate Professor, Department of Environmental Science and Policy
George Mason University

INTRODUCTION:

Again during 2017, in connection with examination of ecological and chemical parameters, a study of *Escherichia coli* in waters in the areas of Hunting Creek/Cameron Run and adjacent waters of the Potomac River was continued with samples being collected at twelve sites. These consisted of the same sites from which samples were collected in 2016. These included stations AR1, AR2, AR3, AR4, AR10, AR11, AR12, AR13, AR21, AR22, AR23 and AR30. During this sampling period Station AR22 was made inaccessible beginning on out 10 May 2017 sampling date due to large scale construction along the stream bank of Huntington Park and adjacent lands. Therefore no samples were collected at this station after 26 April 2017. Similarly, renovations at Lake Cook (draining and dredging) began during the sampling period. We were unable to collect samples from station AR11 after 09 August 2017. Sediment disturbance at AR11, while we could still sample during the construction and at station AR12 may have affected *E. coli* abundances reported here.

This work provides current microbiological water quality information in these aquatic ecosystems adjacent to and receiving water from the wastewater reclamation facility operated by Alexandria Renew Enterprises (Alex Renew). The research continues to determine if these waters are impaired under the Clean Water Act in terms of their uses as designated by the Commonwealth of Virginia.

The text of the Virginia Water Quality Standards (9 VAC 25-260-10) is as follows:

> *"* All state waters, including wetlands, are designated for the following uses: recreational uses, e.g., swimming and boating; the propagation and growth of a balanced, indigenous population of aquatic life, including game fish, which might reasonably be expected to inhabit them; wildlife; and the production of edible and marketable natural resources, e.g., fish and shellfish." (VSWCB 2011)

Section 9VAC25-260-170 of the Virginia Water Quality Standards (amended as of January 2011) specifies the bacteriological criteria for *E. coli* that apply to primary contact recreational use surface waters:

> "*E.coli* bacteria shall not exceed a monthly geometric mean of 126 CFU/100 ml in freshwater." … "2. Geometric means shall be calculated using all data collected during any calendar month with a minimum of four weekly samples. 3. If there are insufficient data to calculate monthly geometric means in freshwater, no more than 10% of the total samples in the assessment period shall exceed 235 *E.coli* CFU/100 ml . … 5. For beach advisories or closures, a single sample maximum of 235 *E.coli* CFU/100 ml in freshwater … shall apply." (VSWCB 2011b)

Of all of the conditions in rivers and streams which can lead to a listing of "impaired water" the one criterion that, more than any other, results in such a listing is coliform bacteria or *E. coli* abundances (USEPA 2014). Both Hunting Creek and Cameron Run were listed as impaired under the Clean Water Act for exceedances of Virginia's water quality criterion for *E. coli* bacteria (VADEQ, 2012), although the earlier impairment listing of Hunting Creek was based on the then applicable fecal coliform criterion (VADEQ 2010). The fecal coliform criterion was subsequently changed to *E. coli* based on the understanding that this subset of fecal coliforms is more specifically associated with fecal material from humans and other warm-blooded animals. The U.S. EPA (USEPA 2012) recommended and the Commonwealth of Virginia accepted *E. coli* as the better indicator of health risk related to recreational water contact. That is the current microbiological water quality criterion.

Due to this impairment Total Maximum Daily Load allocations for *E. coli* were developed for both of these watersheds in late 2010 (VADEQ 2010). The City of Alexandria is working toward achieving the bacteriological criteria for these waters through a variety of programs including a storm water program, minimizing combined storm water sewer system overflows and eventually eliminating those discharges, reductions in pet waste sources and discovery of illegal discharges. Because the sources of *E. coli* to water systems are many and varied, including wildlife sources which are generally not controlled unless at a nuisance level, continued monitoring of *E. coli* in these waterways is an important aspect of maintaining and improving water quality. The results reported here add to the understanding of the microbiological quality of these systems.

METHODS:

Sampling Regime: Samples were collected on eleven dates from 26 April 2017 to 20 September 2017 (Table EC1). The approach was to sample on a bimonthly basis in May through September with one sample in April. Water samples were collected at twelve stations each time (but see note above regarding AR11 and AR22). Station identifiers and locations are shown in Table EC2 (map of EC sample sites in Appendix A, Figure A1). Samples were collected in clean, steam sterilized (autoclaved), 4 liter, wide-mouth polypropylene bottles. Eight of the stations were approached from the shore and four were sampled from a small, outboard powered research vessel. Of the shore-approached stations AR11 was sampled on the upstream (lake) side of the dam at Lake Cook approximately 10 meters from the shore. In this case only the sample equipment came in contact with the lake water. Stations AR 30, AR21, AR22 and AR23 were sampled from the shore without wading into the stream. At station AR1 samples were collected remotely using a sterilized, 4 liter round, polypropylene wide-mouth bottle fitted with a harness and nylon line. The sample bottle was deployed from atop the George Washington Parkway Bridge over Hunting Creek on the downstream side approximately at mid-span. In all cases the bottles were rinsed twice with sample water and then the final sample was collected. Collection of two shore-approached samples required wading in the streams. At AR12 we waded into the water downstream of the collection site, waited for the current to carry away any disturbed sediment and then collected the sample by submerging the 4 liter bottle upstream of the sample collector. At AR 13 the bottom of the stream at the approach site is paved with concrete. At this site we waded to approximately midstream and to the edge of the concrete paved segment. After waiting for any disturbed sediment to be washed away the sampled was collected

again by submerging the sterile 4 liter bottle in the stream. Boat-approached sites were sampled by submerging the collection bottles over the side of the research vessel.

Immediately after collection, samples were placed in dark, insulated containers and chilled with ice. Samples were returned to the George Mason University (Mason), Fairfax campus where they were processed within about 5 hours of collection.

Analytical Method: Determination of the abundance of *E. coli* followed the EPA Method 1603 (*Escherichia coli* in Water by Membrane Filtration Using Modified membrane-Thermotolerant *Escherichia coli* Agar (Modified mTEC)). This is an EPA-approved method for determining abundance of *E. coli* in fresh water. It is a one-step modification of the EPA Method 1103.1. It is based on *E. coli* production β-Dglucuronidase and the consequent metabolism of 5-bromo-6-chloro-3-indolyl-β-D-glucuronide in the medium to glucuronic acid and a red- or magenta-colored product (USEPA 2009).

Table EC1: Sampling Dates

Date	Date Code for figures
26-Apr-17	20170426
10-May-17	20170510
24-May-17	20170524
07-Jun-17	20170607
21-Jun-17	20170621
05-Jul-17	20170705
20-Jul-17	20170720
09-Aug-17	20170809
23-Aug-17	20170823
06-Sep-17	20170906
20-Sep-17	20170920

Table EC2: Station identifiers, locations and access type.

Station ID	Access Type	Location Description	Latitude	Longitude
AR 1	Shore	Hunting Cr just above GW Parkway Bridge	38º 47.40' N	77º 03.09' W
AR 2	Boat	Northern portion of Hunting Cr.	38º 47.10' N	77º 02.95' W
AR 3	Boat	Southern portion of Hunting Cr.	38º 46.93' N	77º 02.89' W
AR 4	Boat	Potomac River Channel off Hunting Cr.	38º 46.88' N	77º 02.04' W
AR 10	Boat	Potomac River North of Wilson Bridge	38º 47.65' N	77º 02.34' W
AR 11	Shore	Outlet of Lake Cook	38º 48.26' N	77º 05.85' W
AR 12	Shore	Last Riffle of Cameron Run near Beltway crossing	38º 48.11' N	77º 05.07' W
AR 13	Shore	Hoff's Run upstream of Alex renew outfall	38º 48.17' N	77º 03.50' W
AR 21	Shore	South side of Cameron Run downstream from Lake Cook drain	38º 48.19' N	77º 05.73' W
AR 22	Shore	South side of Cameron Run at north end of Fenwick Dr.	38º 47.87' N	77º 04.26' W
AR 23	Shore	South side of Cameron Run across from AlexRenew outfall	38º 47.62' N	77º 03.58' W
AR 30	Shore	Cameron Run upstream near metro rail bridge	38º 48.32' N	77º 06.44' W

For this work mTEC medium (Fisher) was prepared in our laboratory at George Mason University shortly before each sampling trip. The medium was prepared as per package directions, and 5 ml of the molten medium was placed aseptically into sterile, 50 mm Petri dishes with tight fitting lids. Prepared medium was stored at 4°C in the dark until use. Phosphate buffered saline (PBS) was prepared as per Method 1603 and autoclave sterilized. PBS was added to smaller samples (1.0 ml and 10 ml) to make volumes up to at least 20 ml before filtration. This aids in distributing bacteria uniformly across the membrane surface. The PBS was also used for blank controls.

Upon return to the laboratory, samples were processed immediately. Sterile, gridded, 0.45 µm membrane filters were aseptically positioned, grid side up, on the base of a sterile, polycarbonate filter holder, and the filter tower was placed in position on a vacuum flask over the filter and base. Samples were shaken vigorously to assure completely mixing and appropriate volumes (1.0 ml, 10.0 ml, 50.0 ml or 100.0 ml) of sample were added to each of three replicate filter systems. Before adding the two smaller volume aliquots to the filter funnels sufficient PBS was added to make the final volume approximately 20 ml. Samples were then filtered with vacuum (approximately 10 in Hg). Each filter was then removed from the filter holder base aseptically with sterile, blunt-tipped forceps and placed onto the surface of the mTEC agar without trapping any air bubbles beneath the filter. After replacing the Petri dish tops the plates were incubated in a 35°C incubator for 2 ± 0.5 hours. They were then removed, placed in tightly closed double, zipper-locked plastic bags and submerged in a water bath at 44.5°C ± 0.2°C for 22 ± 2 hours. Blank controls consisting of 100 ml of PBS were checked each time samples were processed. Generally no *E. coli* were detected in these blank controls, although occasionally controls had one or two presumptive *E. coli* colonies. The data were not corrected for this low background as it was generally far less than 1 percent of the abundances on

countable plates.

After the water bath incubation, samples were retrieved and observed immediately for typical red or magenta *E. coli* colonies. All Petri dishes (3 volumes x 3 replicates = 9 Petri dishes per sample) were observed. Although only dilutions yielding colony counts between 20 and 80 needed to be enumerated, we generally recorded colonies for each countable dilution. Often, however, when *E. coli* were abundant, the higher volume samples were not countable due to overgrowth. Calculation of final *E. coli* abundances followed the procedures described in Appendix B of the EPA Method 1603 (USEPA 2009). Since there were triplicate analyses of each dilution the colony count per Petri dish was separately converted to *E. coli* abundance per 100 ml and then the triplicates were averaged. If no dilution gave individual counts between 20 and 80 the dilution that resulted in counts nearest to that range were selected and used for the final calculation as described in appendix B of the EPA Method 1603.

RESULTS:

Typical *E. coli* colonies were observed in some dilution in every sample tested. Therefore there is a point estimate of *E. coli* per 100 ml for each. *E. coli* abundances by station are shown in Figures EC1 and EC2 (tabular data is in Appendix A, Table A1). Dates are coded in reverse order for sorting purposes (e.g. 26 April 2017 = 20170426). For clarity only two stations are represented in each "by date" figure (3EC – 8EC), and the station locations and relationships between stations are described in the figure legends.

Since there was no situation in which 4 weekly samples were collected in a calendar month the 235 per 100 ml (more than 10%) criterion is applicable in determining impairment. In contrast to the 2014 situation, when at four of the eight stations sampled in that year (AR11, 10, 3 and 4) thermotolerant *E. coli* abundances never exceeded 235 per 100 ml, in 2017 *E. coli* abundances exceed the 235 per 100ml "impaired water" criterion at all stations sometime during the sampling period as they did in 2015 and 2016. This included all four of the sampled stations (A21, 22, 23 and 30) introduced to the study in 2016 exceeded that criterion most of the time. In 2017 AR1 and AR 30 exceeded the 235 per 100ml level on 10 of the 11 samples throughout the spring and summer whereas in 2016 AR1 samples exceeded that value only 8 of 11 times. This pattern of exceedences of the 235 per 100 ml standard was typical of samples from 2017. Stations 11, 12, 13, 21, 22and 23 all exceeded this criterion in all samples – 11 out of 11 times (except at Station 22 which was sampled only once and Station 11 which was sampled 8 times). Station AR4 in the Potomac River exceeded the criterion on 5 of the 11 sample dates while stations 3 and 2 exceeded the standard 3 and 8 times respectively.

Thermotolerant *E. coli* abundance at Station AR13 (Hoff's Run), which exceeded 235 per 100 ml on all eleven dates from April through the end of September, as it did in 2015 and 2016, averaged 5,061 per 100 ml and had a maximum of over 15,000 per 100 ml on 07 June 2017. The 2015 average *E. coli* at this location was over 4,450 per 100 ml with a maximum value greater than 21,500 on 23 June 2016. These were the highest value found at any station during these three years.

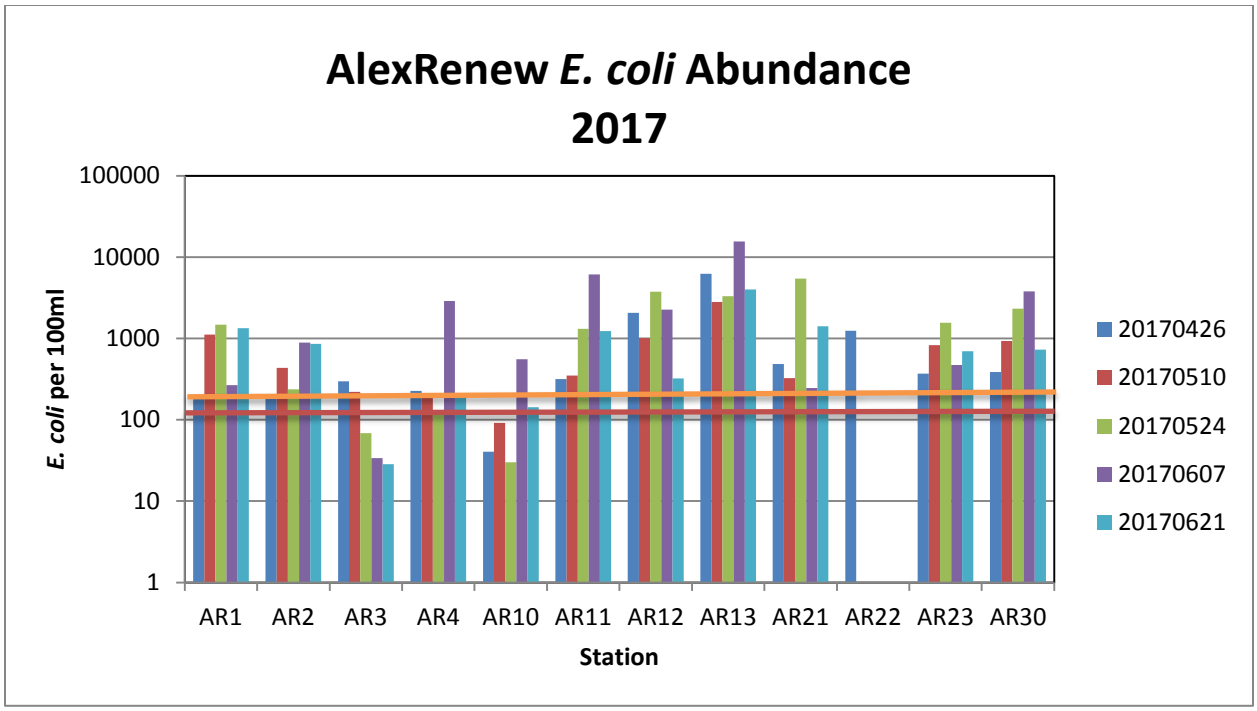

Figure EC1: *E. coli* abundance per 100 ml on 26 Apr, 10 May, 24 May, 07 June and 21 June, 2017 in Cameron Run, Hunting Creek and the adjacent Potomac River. The red horizontal line represents the *E. coli* criterion (126 per 100ml) for the geometric monthly mean allowable abundance, and the orange line represents the criterion (235 per 100ml) for allowable abundance in the absence of four monthly samples.

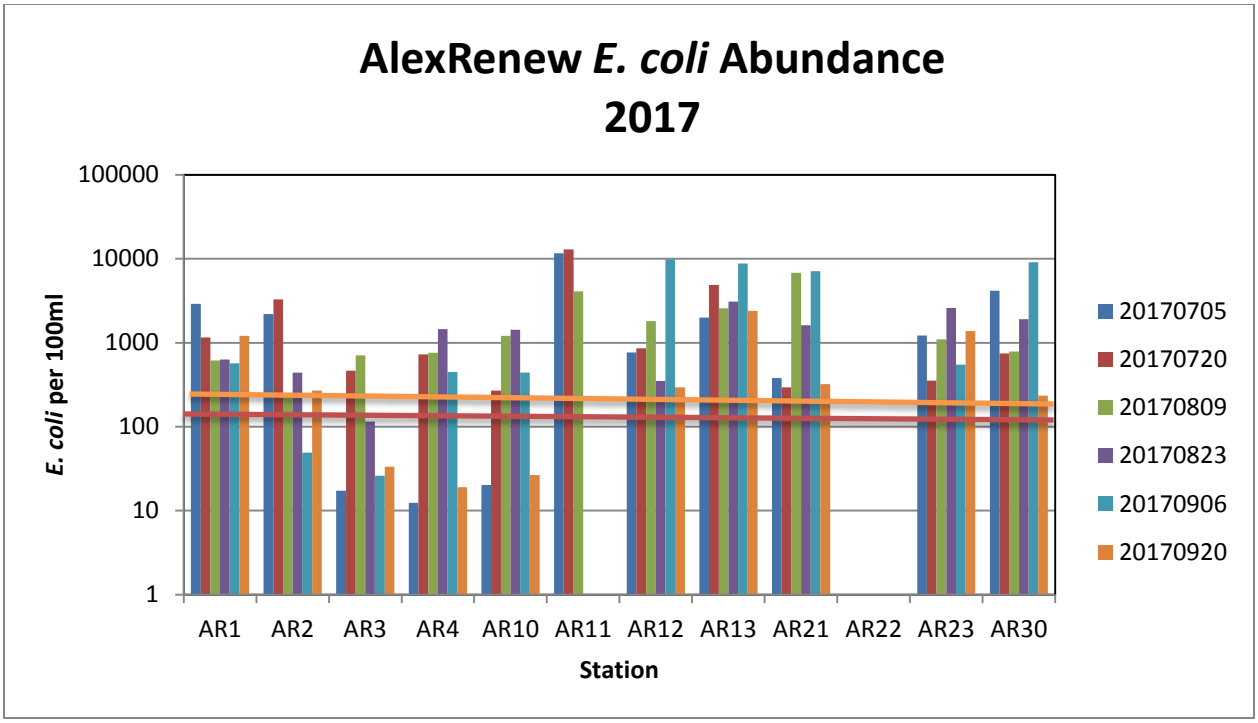

Figure EC2: *E. coli* abundance per 100 ml on 05 July, 20 July, 09 Aug, 23 Aug, 06 Sept and 20 Sept, 2017 in Cameron Run, Hunting Creek and the adjacent Potomac River. The red horizontal line represents the *E. coli* criterion (126 per 100ml) for the geometric monthly mean allowable abundance and the orange line represents the criterion (235 per 100ml) for allowable abundance in the absence of four monthly samples.

In Figures EC3 through EC8, data are arrayed by date with stations displayed by geographic relationships. Figure EC3 shows Hunting Creek at the GW Parkway Bridge (AR1) and the adjacent, nearest off-shore station (AR2). Stations AR3 and AR4 (Figure EC4) are in-shore at the mouth of the Hunting Creek embayment off the Potomac and off-shore Potomac respectively. Figure EC5 displays data from stations AR 10 and 11. AR10 is a Potomac River site upstream of the Wilson Bridge and AR11 is in Lake Cook above Cameron Run. Figure EC6 shows data from AR12, in Cameron Run proper, and AR13 is in Hoff's Run, a tributary of Cameron Run. Newly sampled stations in 2016 and continuing in 2017 are AR21, across Cameron Run from Lake Cook, AR22 across Cameron Run from AR12, AR 23 across Cameron Run from the AlexRenew outfall and AR30 upstream of the Lake Cook drain and near the Cameron Run metro overpass.

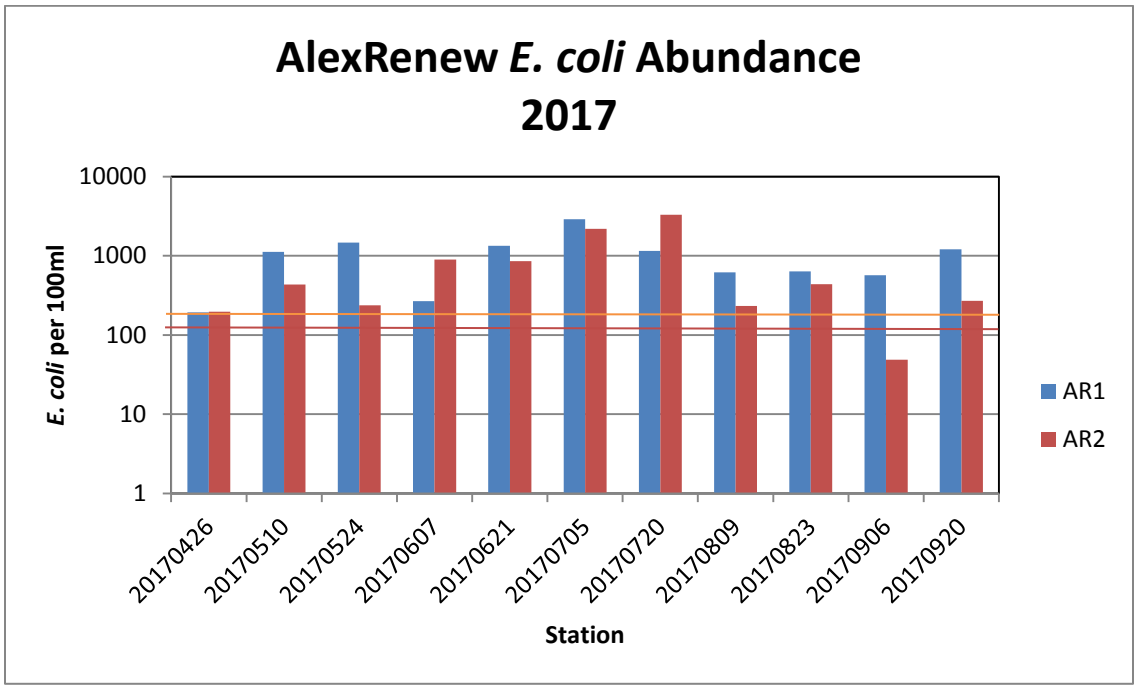

Figure EC3: *E. coli* abundance per 100ml arrayed by date for stations AR1 and AR2. AR1 is located at the mouth of Hunting Creek and AR2 is the next nearest station offshore in the embayment of the Potomac River. *E. coli* criteria are as described above.

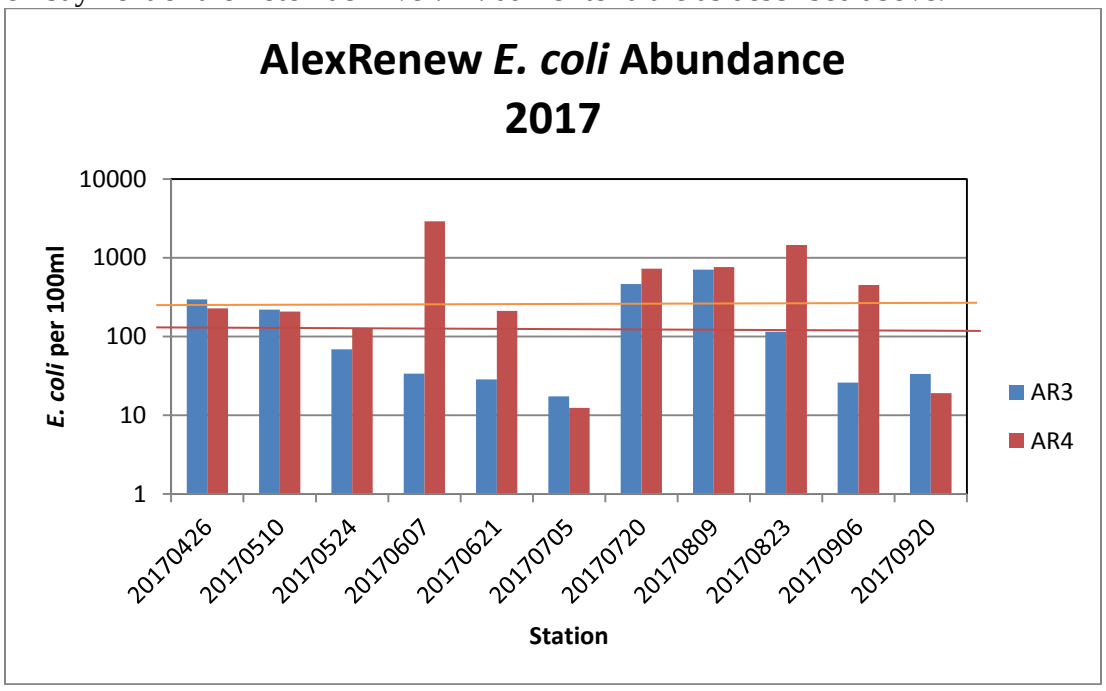

Figure EC4: *E. coli* abundance per 100ml arrayed by date for stations AR3 and AR4. AR4 is an off-shore Potomac station while AR3 is in-shore at the mouth of the Hunting Creek embayment off the Potomac. *E. coli* criteria are as described above.

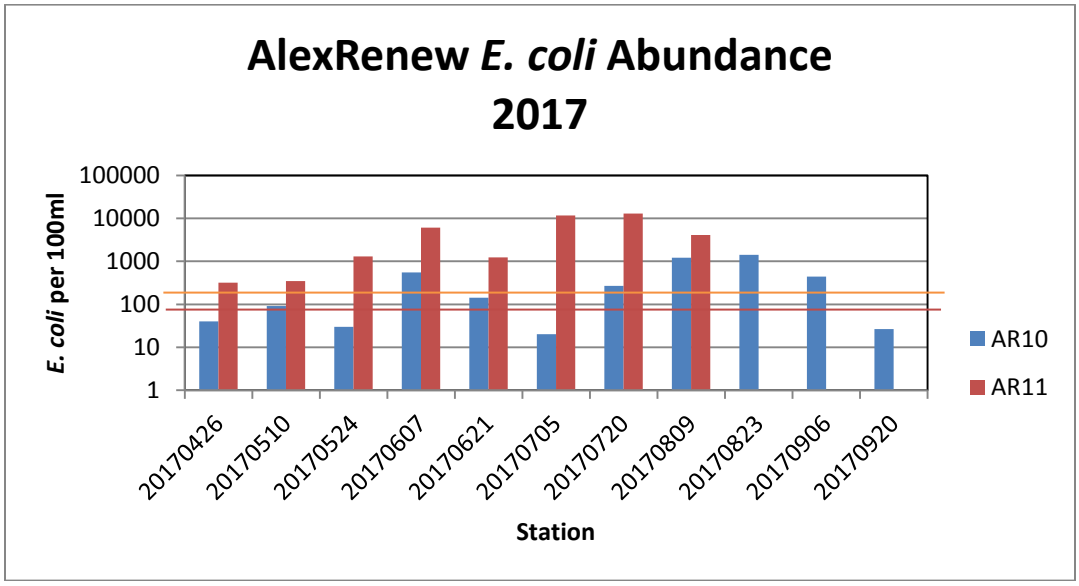

Figure EC5: *E. coli* abundance per 100ml arrayed by date for stations AR10 and AR11. AR10 is a Potomac River station north of the Wilson Bridge. AR11 is above the dam at Lake Cook on a tributary of Cameron Run. AR11 was sampled only 8 times due to draining and dredging of Lake Cook. *E. coli* criteria are as described above.

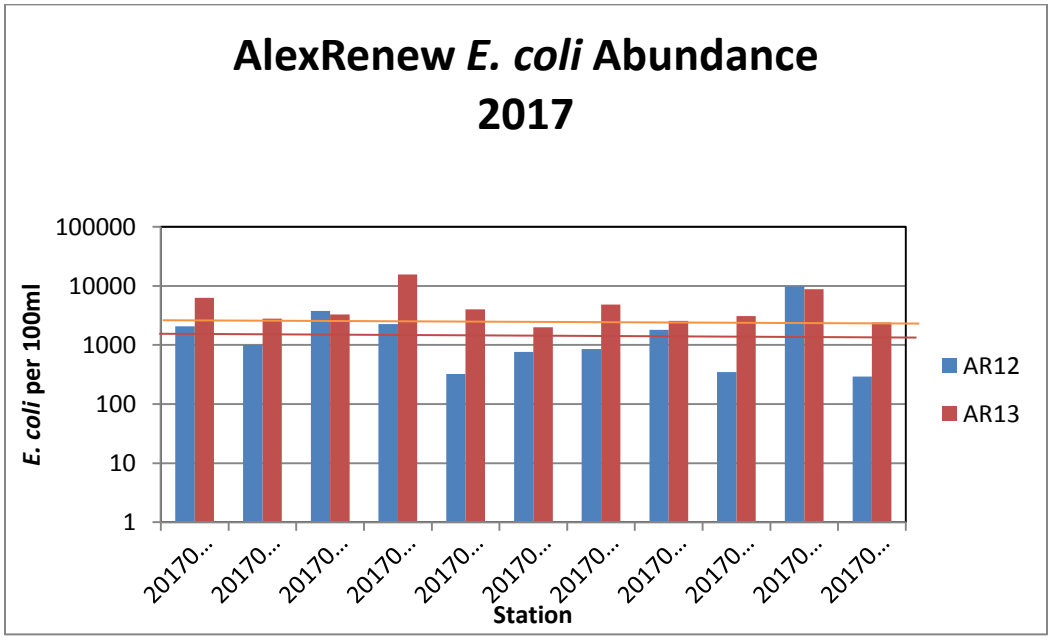

Figure EC6: *E. coli* abundance per 100ml arrayed by date for stations AR12 and AR13. AR12 is a Cameron Run station near Oak Park and AR 13 is located in Hoff's Run upstream from the Alex Renew outfall. *E. coli* criteria are as described above.

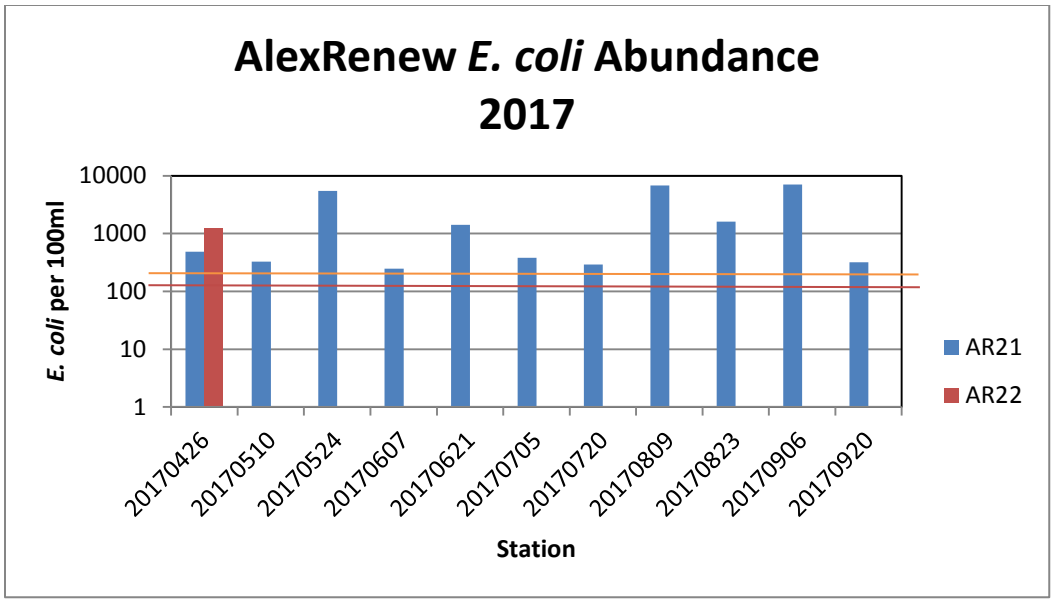

Figure EC7: *E. coli* abundance per 100ml arrayed by date for stations AR21 and 22. AR21 is a Cameron Run station on the south side across Lake Cook and AR22 is also on the south side of Cameron Run across from AR12 at the end of Fenwick Dr. AR22 was sampled only once due to construction along Cameron Run which prohibited approach to the stream bank. *E. coli* criteria are as described above.

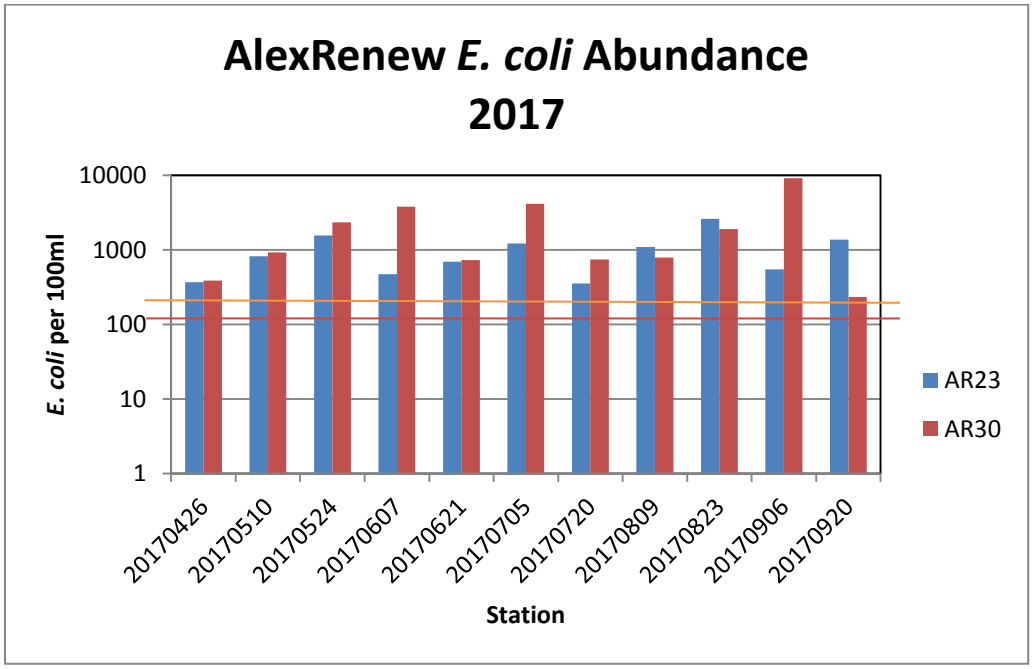

Figure EC8: *E. coli* abundance per 100ml arrayed by date for stations AR23 and AR30. AR23 is a Cameron Run station on the south side across from the AlexRenew outfall, and AR30 is on Cameron Run upstream from Lake Cook near the metro rail overpass. *E. coli* criteria are as described above.

DISCUSSION:

Based on Section 9VAC25-260-170 of the Virginia Water Quality Standards there is insufficient data (less than four samples per calendar month) to apply the geometric mean for freshwater. In that case if we apply the standard that no more than 10% of the samples in the assessment period are to exceed 235 per 100 ml, then all stations exceed that percentage in 2017, as they did in both 2015 and 2016. In 2015 AR4 did not exceed that criterion but it did twice in 2016.

Data has been collected from stations AR1 – AR13 since 2014. Although the 2014 data set is smaller (fewer samples) than those for 2015-2017 we present here a timeline of changes in the percentage of samples that exceeded the 235 per 100 ml standard (Figure EC9).

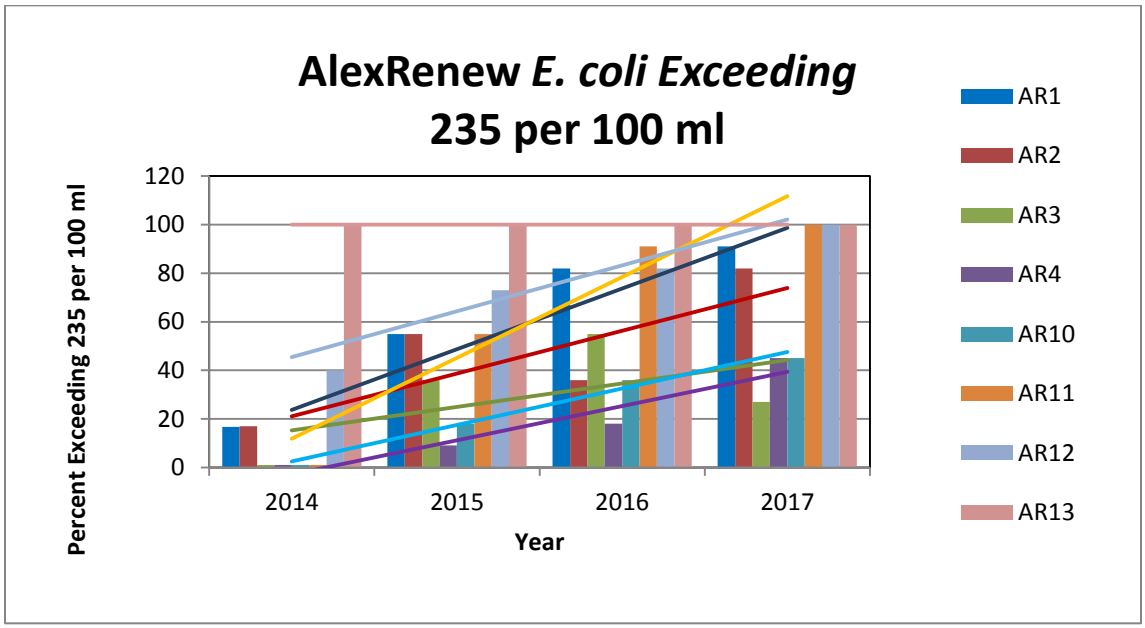

Figure EC9: Percentage of sample event when *E. coli* abundances exceeded 235 per 100 ml for each year of sampling. The set of trend lines (one for each station) indicate increases incidence of E. coli abundances exceeding the 235 per 100 m standard.

Samples were collected 6 times during 2014, whereas in each of the subsequent years samples were collected 11 times. Nevertheless, within this set of sample stations the trend was for increasing exceedances of the 235 per 100 ml standard. The only station were the trend was not positive was AR13 which had *E. coli* abundances above the 235 per 100 ml value every time it was sampled (39 times in total).

CONCLUSION:

The data continue to support a conclusion that the entire area sampled, including the mainstem of the Potomac River (AR4) are impaired for the bacteriological water quality criterion (*E. coli*) content under Section 9VAC25-260-170 of the Virginia Water Quality Standards that applies to primary contact recreational use surface waters. In 2017 even the offshore Potomac River site (AR4) exceeded the 235 per 100ml criterion five time whereas it exceed that value only twice in 2016. More of the stations exceeded the standard in 2017 than in 2016 and there were more in 2016 than 2015. While some of the highest values occurred in June and July there is no clear seasonal trend in the 2017 data. High values occurred at various stations throughout the sample period.

Literature Cited:

U.S. Environmental Protection Agency (USEPA). 2009. Method 1603: *Escherichia coli* (*E. coli*) in Water by Membrane Filtration Using Modified membrane-Thermotolerant *Escherichia coli* Agar (Modified mTEC). Available at: < http://water.epa.gov/scitech/methods/cwa/bioindicators/> search Method 1603, December 2009.

U.S. Environmental Protection Agency (USEPA). 2012. Water: Monitoring & Assessment: 5.11 Fecal Bacteria. Available at: http://water.epa.gov/type/rsl/monitoring/vms511.cfm

U.S. Environmental Protection Agency (USEPA). 2014. National Water Quality Assessment Report, water Quality Assessment and Total Maximum Daily Loads Information. Available at: <http://ofmpub.epa.gov/waters10/attains_index.control>

Virginia Department of Environmental Quality (VADEQ). 2010. Bacteria TMDLs for the Hunting Creek, Cameron Run, and Holmes Run Watersheds. Available at: <deq.state.va.us>

Virginia Department of Environmental Quality (VADEQ). 2012. 2012 Impaired Waters: Category 4 & 5 by Basin and Stream Name, Potomac and Shenandoah River Basins, Cause Group Code: A13R-03-BAC - Cameron Run/Hunting Creek. Available at: <http://www.deq.virginia.gov/Programs/Water/WaterQualityInformationTMDLs/WaterQualityAssessments.aspx>

Virginia. *State Water Control Board* (VSWCB). 2011. 9 VAC 25-260-10 Designation of uses. Virginia Water Quality Standards. Available at: <http://lis.virginia.gov/cgi-bin/legp604.exe?000+reg+9VAC25-260-10>

Virginia. *State Water Control Board* (VSWCB). 2011b. 9 VAC 25-260-170 Bacteria; other recreational waters. Virginia Water Quality Standards. Available at: <http://lis.virginia.gov/cgi-bin/legp604.exe?000+reg+9VAC25-260-170>

APPENDIX A:

Figure A1: Maps of sample sites

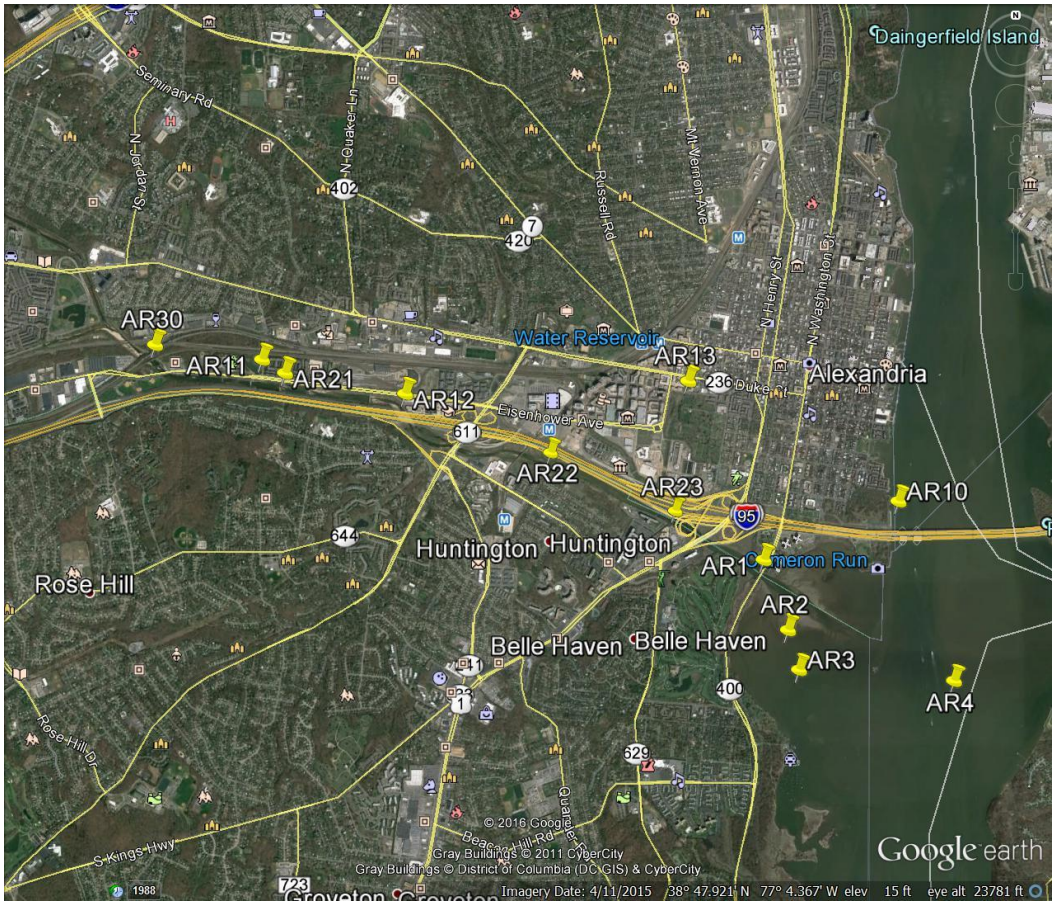

Table A1: *E. coli* abundances, mean of triplicate analyses per sample, seasonal overall means and standard deviations and percent exceedances of criteria.

2017 AlexRenew *Escherichia coli* enumeration

EPA Method 1603

Station	Sample Date	Mean *E. coli* per 100ml	Seasonal Mean *E. coli* per 100ml	Seasonal StndDev *E. coli* per 100ml	Percent exceedances of 126 per 100 ml	Percent exceedances of 235 per 100 ml
	yyyymmdd					
AR1	20170426	193	1043	165	100	91
AR1	20170510	1117				
AR1	20170524	1475				
AR1	20170607	267				

AR1	20170621	1342				
AR1	20170705	2900				
AR1	20170720	1157				
AR1	20170809	617				
AR1	20170823	633				
AR1	20170906	567				
AR1	20170920	1210				
AR2	20170426	197	829	165	91	82
AR2	20170510	435				
AR2	20170524	237				
AR2	20170607	893				
AR2	20170621	860				
AR2	20170705	2200				
AR2	20170720	3300				
AR2	20170809	233				
AR2	20170823	440				
AR2	20170906	49				
AR2	20170920	270				
AR3	20170426	297	183	165	36	27
AR3	20170510	220				
AR3	20170524	69				
AR3	20170607	34				
AR3	20170621	28				
AR3	20170705	17				
AR3	20170720	463				
AR3	20170809	707				
AR3	20170823	115				
AR3	20170906	26				
AR3	20170920	33				
AR4	20170426	227	644	165	82	45
AR4	20170510	207				
AR4	20170524	127				
AR4	20170607	2900				
AR4	20170621	210				
AR4	20170705	12				
AR4	20170720	727				
AR4	20170809	760				
AR4	20170823	1450				
AR4	20170906	450				
AR4	20170920	19				
AR10	20170426	40	387	165	55	45
AR10	20170510	92				
AR10	20170524	30				
AR10	20170607	557				

AR10	20170621	142				
AR10	20170705	20				
AR10	20170720	270				
AR10	20170809	1213				
AR10	20170823	1427				
AR10	20170906	440				
AR10	20170920	27				
AR11	20170426	317	4747	165	100	100
AR11	20170510	350				
AR11	20170524	1312				
AR11	20170607	6100				
AR11	20170621	1233				
AR11	20170705	11600				
AR11	20170720	12967				
AR11	20170809	4100				
AR11	20170823	na				
AR11	20170906	na				
AR11	20170920	na				
AR12	20170426	2067	2125	165	100	100
AR12	20170510	1008				
AR12	20170524	3767				
AR12	20170607	2267				
AR12	20170621	323				
AR12	20170705	763				
AR12	20170720	857				
AR12	20170809	1808				
AR12	20170823	350				
AR12	20170906	9867				
AR12	20170920	293				
AR13	20170426	6267	5061	165	100	100
AR13	20170510	2800				
AR13	20170524	3300				
AR13	20170607	15600				
AR13	20170621	4000				
AR13	20170705	2000				
AR13	20170720	4867				
AR13	20170809	2567				
AR13	20170823	3100				
AR13	20170906	8767				
AR13	20170920	2400				
AR21	20170426	483	2222	165	100	100
AR21	20170510	327				
AR21	20170524	5467				
AR21	20170607	247				

AR21	20170621	1413				
AR21	20170705	380				
AR21	20170720	293				
AR21	20170809	6800				
AR21	20170823	1610				
AR21	20170906	7100				
AR21	20170920	320				
AR22	20170426	1242	1242	165	100	100
AR22	20170510	na				
AR22	20170524	na				
AR22	20170607	na				
AR22	20170621	na				
AR22	20170705	na				
AR22	20170720	na				
AR22	20170809	na				
AR22	20170823	na				
AR22	20170906	na				
AR22	20170920	na				
AR23	20170426	370	1012	165	100	100
AR23	20170510	825				
AR23	20170524	1567				
AR23	20170607	473				
AR23	20170621	697				
AR23	20170705	1222				
AR23	20170720	353				
AR23	20170809	1095				
AR23	20170823	2600				
AR23	20170906	550				
AR23	20170920	1377				
AR30	20170426	387	2285	165	100	91
AR30	20170510	927				
AR30	20170524	2333				
AR30	20170607	3800				
AR30	20170621	727				
AR30	20170705	4167				
AR30	20170720	743				
AR30	20170809	787				
AR30	20170823	1900				
AR30	20170906	9133				
AR30	20170920	233				

Ecological Survey of Micropollutants in Water and Fluvial Sediments from Hunting Creek: Data Summary and 2017 Sampling Results

Final Report
By

Gregory Foster[1,2] and Thomas Huff[3,2]
[1]Department of Chemistry and Biochemistry
[2]Potomac Environmental Research and Education Center
[3]Shared Research Instrumentation Facility
George Mason University

Introduction

There are a wide variety of micropollutants that impact water quality in the Chesapeake Bay watershed. Some micropollutants are regulated through the Clean Water Act (CWA), which includes a list of 65 chemical constituents considered Toxic Pollutants (CWA section 307(a)(1), 40 CFR 401.15). Some of these Toxic Pollutants (e.g., PCBs) have had Total Maximum Daily Loads established in the Potomac River watershed (Haywood and Buchanan 2007) because of extensive historical pollution problems. Other micropollutants such as pharmaceutical chemicals, personal care products and xenoestrogens are unregulated but still pose a potential threat to ecological and environmental health. These emerging chemicals of concern have substantial emissions in the aquatic environment but their sources, fate and risks are not well characterized. As such, there exists a need to determine the sources, fate and risks of these micropollutants in the Potomac River, the second largest tributary of Chesapeake Bay, to assess potential impacts to human and ecological health. Sediment and water collected from Hunting Creek (northern Virginia, USA) in 2017 (May through October) were analyzed for selected emerging micropollutants to characterize their presence, geospatial variability and distribution between water and river bed sediments in a Potomac River tributary receiving wastewater discharge. The present study is a continuation of the 2016 collaboration between the Potomac Environmental Research and Education Center (PEREC) at George Mason University and the Alexandria Renew Enterprises. Hunting Creek is a tidal embayment formed where Cameron Run meets the tidal Potomac River in northern Virginia. Substantial in-stream concentrations of anthropogenically-derived chemicals are expected in the study are due to the dense urban development and wastewater treatment plant discharge compared to the freshwater flow in the stream.[2]

Emerging micropollutants find their way into the aquatic environment primarily through stormwater runoff, agricultural practices and wastewater treatment plant (WTP) discharge or releases. When released into natural waters these chemicals accumulate in organic matter, fine-grained sediments and suspended sediment particles. Because storm runoff and wastewater

discharge represent a sizable fraction of the annual surface water flow in urban regions, these sources are often sufficient to promote in-stream accumulation of micropollutants. Thus, the entire aquatic community may be exposed throughout entire life cycles and across generations to mixtures of biologically-active chemicals in urban areas. To better understand the implications of micropollutants in the Potomac River ecosystem, further ecological baseline investigations are underway since little is known regarding the fate, effects and distribution of emerging micropollutants in the aquatic environment. The 2017 Hunting Creek project was patterned on the long-running Gunston Cove Study, which PEREC has been conducting in partnership with the County of Fairfax Department of Public Works and Environmental Services since 1984.

Study Objectives

Water and fluvial sediments collected in the vicinity of the Hunting Creek embayment of the Potomac River were analyzed for micropollutants associated with urban sources. The objectives of the present investigation were to:

- establish a status and trends list of PPCP analytes that can provide spatial and temporal trend comparisons in PPCP concentrations in Hunting Creek;
- quantify micropollutants in sediments and water in the Hunting Creek region of the Potomac River at parts per trillion concentrations along spatial and temporal scales;
- continue to develop and refine analytical methods that utilize liquid chromatograpy coupled with tandem mass spectrometry as the best method available to measure micropollutants in aquatic matrices;

We report here on methods development to broaden the range of analytes being determined and provide some preliminary results. More results will be available in the final report.

Study Area

Hunting Creek is a tributary embayment of the Potomac River lying 8 km downstream of Washington, DC, immediately south of the city of Alexandria, VA. Hunting Creek exists at the stream confluence of Cameron Run and Hooff Run prior to discharging into the Potomac River. The Cameron Run watershed, the largest of the two sub-sheds, is predominantly urban (95% of residential. Jones Point (Alexandria, VA) forms the northern boundary and Dyke Marsh the southern boundary of Hunting Creek. Alexandria Renew Enterprises WTP is located north of the shoreline of upper Hunting Creek, and discharges an average of 150,000 m^3 of wastewater daily. Riverbed sediments were collected in Hunting Creek for micropollutant analysis. The Hunting Creek sampling grid was divided into four sub-regions based on the location of the Alexandria Renew WTP. The four sub-regions included Cameron Run (upstream zone), upper Hunting Creek (WTP discharge zone), lower Hunting Creek (downstream zone) and the mainstem Potomac River (reference zone).

Included in this year's sampling plan is a reference site, which was selected at Dogue Creek, VA. The Dogue Creek embayment of the Potomac River is south of Hunting Creek by approximately ten miles. Dogue Creek was selected as a reference tributary of the Potomac River because it does not receive direct wastewater discharge.

Sampling

Water Sampling

Five sampling trips were made in Hunting Creek and the Potomac River mainstem in 2017 on 25 May, 25 July, 26 July, 20 September, and 17 October. The Potomac River/Lower Hunting Creek sites were accessed as part of the basic water quality monitoring program, and the Upper Hunting Creek sites were accessed by a flat-hulled jon boat that was carried in from Huntington Park. Sample sites, dates and GPS coordinates are given in Table 1. At each site, three sets of sediment samples and two 20-L water samples were collected. Water was obtained by submerging Cornelius (soda) kegs (Midwest Home Brewing Supplies, Minneapolis, MN) approximately 0.3 m below the surface. The kegs were sealed with an o-ring-lined lid, were stowed and transported to the lab where they were briefly stored at 4 °C prior micropollutant analysis. River water was also collected in 1 L polypropylene bottles for determination of suspended particle concentration.

Table 1. Collections sites, labeling codes and coordinates for 2016 (sediment) and 2017 sampling (water and sediment).

Site	Labeling Code	Sampling Coordinates (DD units)
Cameron Run	CR01	38.79747, -77.06827
	CR02	38.79862, -77.07603
Upper Hunting Creek	UHC01	38.79013, -77.04952
	UHC03	38.79362, -77.05843
Lower Hunting Creek	AR02	38.78022, -77.04812
	AR03	38.78022, -77.04811
	AR04	38.78063, -77.03640
Potomac River	AR10	38.79698, -77.03923
Dogue Creek	DC01	38.69505, -77.11985

Sediment Sampling

Riverbed sediments were obtained using a Petite Ponar grab sampler (Wildco, Saginaw, MI) tethered by rope. Once contained by the Ponar, the sediments were expelled undisturbed as minimally as possible on the boat (or along shoreline) into a stainless-steel tray, where ~10 g of the top 2-4 cm (surficial layer) was placed directly into a cleaned, glass jar, stowed on ice for transport to the laboratory, and stored at -20 °C until chemical analysis. Riverbed sediments were obtained by boat according to the same locations established for water sampling (Table1 and 2) for Cameron Run, lower Hunting Creek, upper Hunting Creek and the Potomac River sites. The sediment collection jars were sealed using a Teflon-lined lid and stored on ice for transportation to the laboratory, whereupon the samples were stored at -20°C until sample processing.

A summary of the samples collected for water and sediment PPCP analysis in 2016 (sediment only) and 2017 is shown in Table 2.

Table 2. Water and sediment sampling summary for the 2016 (sediment only) and 2017 study.

Site	Sampling Dates (Replicate samples)
Sediment Sampling 2016	
CR01	26 July 2016 (3), 17 October 2016
CR02	26 July 2016 (3)
UHC01	26 July 2016 (3)
UHC03	26 July 2016 (3), 17 October 2016
AR02	24 May 2017 (3), 20 July 2017 (3), 6 September 2017 (3)
AR03	24 May 2017 (3), 20 July 2017 (3), 6 September 2017 (3)
AR04	24 May 2017 (3), 20 July 2017 (3), 6 September 2017 (3)
AR10	24 May 2017 (3), 20 July 2017 (3), 6 September 2017 (3)
DC01	-
Water Sampling 2017	
CR01	24 May 2017 (3), 20 July 2017 (3), 6 September 2017 (3)
CR02	24 May 2017 (3), 20 July 2017 (3), 6 September 2017 (3)
UHC01	24 May 2017 (3), 20 July 2017 (3), 6 September 2017 (3)
UHC03	24 May 2017 (3), 20 July 2017 (3), 6 September 2017 (3)
AR02	24 May 2017 (3), 20 July 2017 (3), 6 September 2017 (3)
AR03	24 May 2017 (3), 20 July 2017 (3), 6 September 2017 (3)
AR04	24 May 2017 (3), 20 July 2017 (3), 6 September 2017 (3)
AR10	24 May 2017 (3), 20 July 2017 (3), 6 September 2017 (3)
DC01	13 October 2017 (3)
Sediment Sampling 2017	
CR01	-
CR02	-
UHC01	-
UHC03	-
AR02	24 May 2017 (3), 20 July 2017 (3), 6 September 2017 (3)
AR03	24 May 2017 (3), 20 July 2017 (3), 6 September 2017 (3)
AR04	24 May 2017 (3), 20 July 2017 (3), 6 September 2017 (3)
AR10	24 May 2017 (3), 20 July 2017 (3), 6 September 2017 (3)
DC01	13 October 2017 (3)

Sample Preparation

Water Filtration

In the laboratory, 20-L river water samples were pressure filtered through 150 mm diameter Whatman GF/F 0.7 µm (nominal pore diameter) glass fiber filters to separate particles from water (Fig. 2). Whatman GF/D 2.7 µm prefilters were used to prevent clogging of the 0.7 µm filter. The filters were held in place using a 142 mm filter-holder stand (EMD Millipore,

Billerica, MA). Ultra-high purity gaseous nitrogen was fitted to the inlet ball-lock valve of the keg. The keg's outlet valve was connected to the inlet port of the filter holder. The outlet of the filter holder was connected with tubing that was used to aliquot samples. Nitrogen pressure was held at 40 psi and gas flow was carefully controlled by a needle valve forcing the water through the filter set which collected suspended particles. The filtrate was aliquoted into 1 L amber glass bottles. Nine bottles of filtered water were collected from each keg and stored at 4 °C. The filter set was sealed in an aluminum pouch prior to extraction and micropollutant analysis. The exact volume in each bottle and remaining keg water were measured for total sample volume. The 1 L water samples were vacuum filtered through pre-weighed 47 mm diameter GF/D and GF/F filter sets, air dried and weighed again for determining particle mass per liter (TSM).

Water Extraction

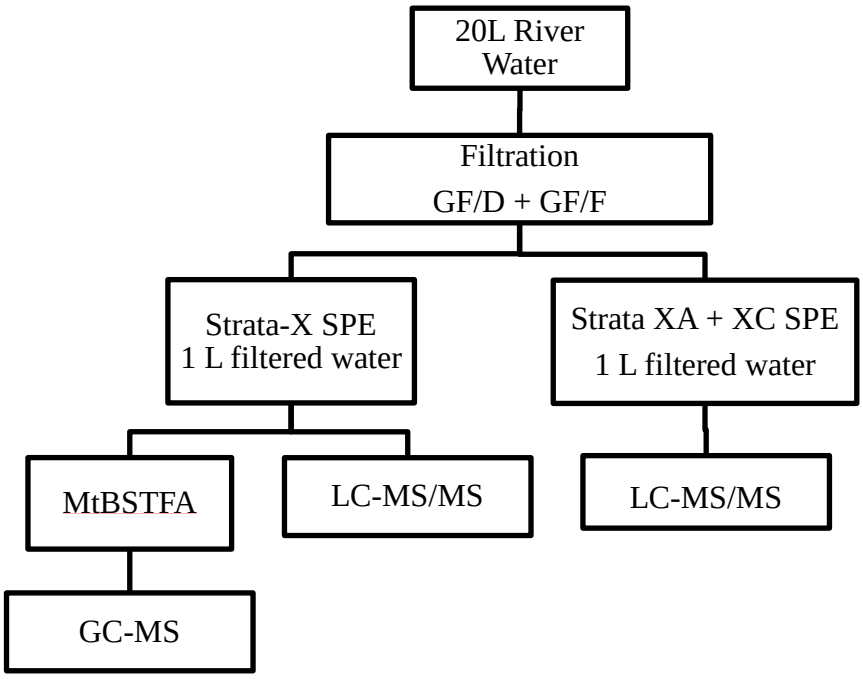

Figure 1. Water analysis method flow chart.

The micropollutants were extracted from filtered water to which surrogate standards were added by using two solid phase extraction (SPE) techniques (Fig. 1). Strata-X SPE cartridges were used for Potomac Science Center (PSC) 5100 series methods. The cartridges were conditioned with 6 mL MTBE, equilibrated with 6 mL MeOH and 6 mL of ultra-high purity water (UHPW; Millipore, Milli-Q). The samples were loaded onto the cartridges using a Supelco vacuum manifold (Sigma-Aldrich, St. Louis, MO) and large volume sample tubing at a rate of 1-2 drops per second. Following extraction, the cartridges were washed with 95:5 UHPW:MeOH and eluted with 6 mL 10:90 MeOH-MTBE into 12 mL deactivated glass centrifuge tubes. The SPE extracts were concentrated by evaporation using a centrivap to 1 mL and quantitatively transferred to a 12 x 32 mm deactivated amber glass autosampler vial with PTFE lined septa for instrumental analysis. A combination SPE method was used for extracting PSC 5200 and 5300 series groups. Strata X-A and X-C cartridges were conditioned with 6 mL of MeOH and equilibrated with 6 mL of UHP water. The cartridges were stacked with X-A on top, and 1 L samples with appropriate surrogate standards (Table 4) were loaded as per above. Following extraction, the cartridges were separated and washed with 2 mL of 95:5 UHP-W:MeOH. The X-C and X-A cartridges were eluted separately with 6 mL of 69:29:2 MeOH:EtOAc: FA and 6 mL of 67.5:27.5:5 MeOH:EtOAc:NH_3. Extracts were combined, and concentrated as per above.

Sediment Sample Extraction

Micropollutants were extracted from sediment using QuEChERS (**Qu**ick-**E**asy-**Ch**eap-**E**ffective-**R**ugged-**S**afe) protocol (Phenomenex, Inc., Torrance, CA, USA). QuEChERS protocol is essentially liquid-solid extraction followed by liquid-liquid extraction followed by sample extract cleanup (Kachhawaha et al. 2017). A methods summary is shown in Fig. 2. The thawed wet sediment was initially centrifuged for 10 minutes at 1500 rpm (Du Pont Sorval RC-5B, New Town, CT) to dewater prior to extraction. An aliquot was reserved for determining percent water. About 1.0 g each of dewatered sediment plus the appropriate surrogate and internal standards were placed in two 50-mL polypropylene centrifuge tube along with 10 mL of ultra-high purity water. Internal standards were added at the beginning to preserve the analyte-to-internal standard ratio prior to analyzing sample aliquots that avoid accidentally obtaining aqueous portions of the bottom phase. One tube was labeled PPCP- and one tube was labeled PPCP+. The tubes were vortexed for 1 min. Then 10 mL of LC-MS grade acetonitrile is added to the slurry followed by vortexing for 1 min. Packets containing 6 g of anhydrous magnesium sulfate and 1.5 g sodium acetate were added to affect a phase separation between water and acetonitrile and to salt out the micropollutants into the organic phase. The mixture was again vortexed. The tubes were then centrifuged for 5 min at 4000 rpm.

The tubes were placed in a -20 °C freezer for 2 hours to aid in obtaining aliquots. An 8-9 mL aliquot was then decanted into a 15-mL polypropylene centrifuge sample clean-up tube containing dispersive solid-phase extraction (dSPE) sorbents to remove matrix interferences. The PPCP+ tube's 8-9 mL aliquot was placed into a tube containing 1.2 g MgSO4 and 0.4 g of primary-secondary amine (PSA) for positively charged micropollutants. The PPCP- tube's 8-9 mL aliquot is placed in a tube containing 1.2 g MgSO4, 0.4 g PSA and 0.4 g C-18 sorbent for negatively charged micropollutants. The tubes were vortexed and centrifuged for 10 min at 3000 rpm. Aliquots of 5 mL were filtered through 0.2 µm PTFE syringe filters into clean 12-mL glass tubes. The volume was reduced to 1 mL in a CentriVap vacuum centrifuge and transferred to 12 x 32 mm deactivated glass autosampler vials for instrumental analysis.

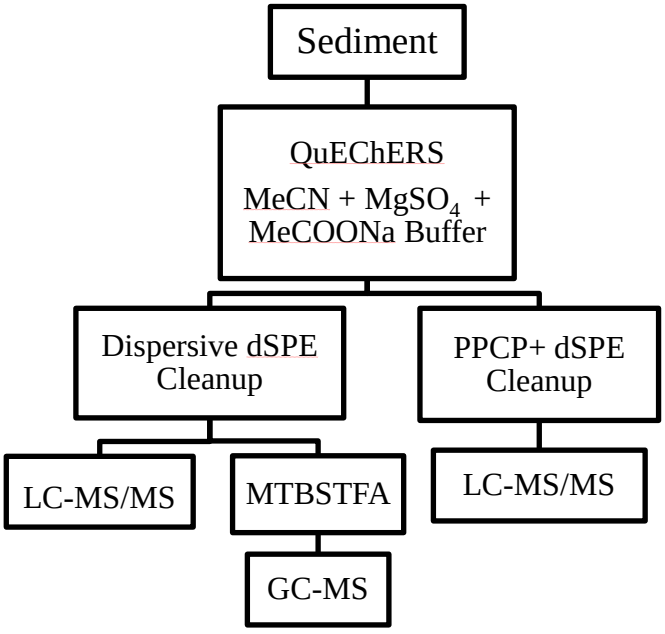

Figure 2. Sediment analysis method flow chart.

Instrumental Analysis

Liquid Chromatography-Tandem Mass Spectrometry (LC-MS/MS) Analysis

Due to their broad range of chemical properties, target micropollutants were placed in numbered

groups sharing similar properties, and instrumental analysis was performed by both LC-MS/MS and GC-MS. LC-MS/MS analysis was performed for less-volatile compounds using a Waters 2695 liquid chromatograph and a Quattro Micro triple quadrupole mass spectrometer with electrospray ionization (Waters Corporation, Milford, MA). The chromatographic separation was performed with either a Restek 3 µm, 2.1 x 150 mm Ultra Biphenyl HPLC column (Restek Corporation, State College, PA) or a 2.1 x 150 mm Atlantis T3 C-18aq column (Waters Corporation, Milford, MA) and a binary mobile-phase gradient with an aqueous phase of UHP-W with 0.1% FA and an organic phase of ACN with 0.1% FA. The mass spectrometer was operated in positive mode (ESI+) for compounds containing amine groups or 3-keto-4-ene cyclohexene groups and negative mode (ESI-) for compounds containing acids or phenol groups. The MS QqQ analyzer was operated in the multiple reaction monitoring (MRM) mode with quantifier and qualifier ion transitions and instrumental operating parameters determined experimentally. Individual solutions containing individual target micropollutants were infused via syringe pump through a t-type connector into the running mobile phase. The mass spectrometer MassLynx version 4.1 software then ran an autotune program that selected an abundant precursor ion and optimized the source cone voltage and then adjusted collision energy to maximize response in product ions derived from the precursor. Selected ion transition pairs provided both a quantifier and a qualifier product ion from which MRM chromatograms are formed.

GC-MS Analysis

GC-MS analyses were performed on an Agilent 7890A series gas chromatograph (Agilent Technologies, Santa Clara, CA) interfaced to an Agilent 5975C ultra-inert mass-selective detector. Instrumental control and data analyses were performed by Agilent MSD ChemStation, version E.02.02, and Agilent MassHunter EnviroQuant version B.07 software, respectively. Instrumental configuration and operating parameters were according to the previous 2014 study with the exception that the autosampler was a customized CTC Analytics CombiPAL (Autosampler Guys, Alexandria, VA) with a refrigerated sample compartment holding the extract vials in the dark at 4 °C.

All extracts were spiked with internal quantitation and surrogate standards (Table 3) prior to derivitization with N-Methyl-N-[(*tert*-butyldimethylsilyl) trifluoroacetamide (MTBSTFA) containing 1% *tert*-butyldimethyl chlorosilane (TBDMS) catalyst. Prior to injection, a 100 µL aliquot of sample extract was transferred to a 300 µL vial insert amended with 50 µL of MTBSTFA and held in a heating block for 30 min at 80 ºC to form *tert*-butyldimethyl silyl derivatives.

Quality Assurance

Background levels of analytes for river water and sediment samples were determined by the analysis of laboratory QA blanks that consisted of ten replicates of 20 L UHPW samples that were processed identically to the samples as described previously. No background levels of analytes were found in any of the laboratory blanks indicating that the glassware, filtration and extraction devices, SPE cartridges and instrument components did not contribute to any of the concentrations reported. Field blanks, which consisted of exposing 20 L of UHP-W to field conditions, also showed that none of the target micropollutant concentrations could be attributed

to field contamination. All calibration curves had regression line R^2 values of 0.995 or higher with a few exceptions noted in the results below. Estimated method detection limits were determined by the standard deviations of ten replicate injections of the low concentration calibration standard multiplied by the student t-test value of 3.250 (9 degrees of freedom and a confidence level of 99%). Method performance was evaluated using QA spikes, which involved spiking DI water (17.8 MΩ) with the entire suite of analytes. The QA spikes were then processed and quantitated as were the regular samples.

Results and Discussion

Data Summary of 2014 and 2015 Surveys

Among the initial goals of the micropollutant sampling program in Hunting Creek has been to characterize the parameters below for pharmaceutical chemicals and personal care products (PPCPs), an important class of micropollutants. The parameters are an attempt to evaluate the presence and amounts of PPCPs in the Hunting Creek aquatic environment, along with important variables such as spatial and temporal variability in water and sediment concentrations. These parameters include

- PPCP chemical composition;
- Spatial PPCP variability within Hunting Creek;
- Temporal PPCP variability (seasonal) in Hunting Creek; and
- Temporal PPCP variability (annual) in Hunting Creek.

PPCPs include a class of micropollutants with >5,000 potential chemical constituents that include prescription drugs, over the counter drugs, cosmetics and commercial household/domestic products. The number of unique chemical constituents increases substantially if transformation products are included for consideration. Thus, the early phase of PPCP monitoring has been to identify the most prominent and relevant PPCPs found in water and riverbed sediments. The rigor and complexity of the chemical analysis of PPCPs in environmental samples allows for including ~50 individual PPCP constituents in a particular analysis method. The initial screening of PPCP has been done by a survey of the literature of PPCPs previously detected in environmental samples, and those known to present a risk to the river ecology, such as the endocrine disrupting chemicals (e.g., estrogens and xenoestrogens). The historical PPCP data for Hunting Creek sampling is summarized below addressing the first two bullet points listed above. The most prominent PPCPs detected in Hunting Creek water and sediment are shown in Table 1. These particular PPCPs represent ~90% by mass of the total PPCPs analyzed in all samples.

Table 3. Most common and abundant PPCPs detected in Hunting Creek water and sediments from 2014 and 2015 sampling.

Acetaminophen	Duloxatine	Progesterone
Bisphenol A	17α-Ethinylestradiol	Sulfamethoxazole
Carbamazepine	Ibuprofen	Testosterone
Clonazepam	Naproxen	Triclosan
Dextromethrophan	4-Nonylphenol	Trimethoprim
Diclofenac	Prednisone	

Spatial variability of PPCPs in water and sediments in Hunting Creek has been evaluated by dividing the sampling stations between four sub-regions within the Hunting Creek stream network based on a spatial position relative to the WTP discharge zone. The four sub-regions included Cameron Run (upstream samples above the discharge zone), upper Hunting Creek (within the direct discharge zone), lower Hunting Creek (downstream samples below the discharge zone) and the Potomac River (reference site outside of Hunting Creek, upstream of the Woodrow Wilson Bridge). Results of the 2014 study are illustrated in Figs. 3-5 for water and sediments, respectively. The concentrations of the ten most abundant PPCPs were added together by sub-region (Σ_{10}PPCP) and compared statistically (ANOVA, 95% level of confidence) to look at large-scale and overall trends. Water concentrations of the PPCPs were not significantly different among the sub-regions in 2014, showing no identifiable spatial trend related to proximity to the WTP discharge point (Fig. 3). Sediment concentrations, however did show significantly different PPCP concentrations, but the significant differences were observed between the lower Hunting Creek and Cameron Run stations (Figs. 4) and not the direct discharge zone. As is typical with the environmental assessment of micropollutants, the variability in PPCP concentrations is in the range of 10-50% RSD, which relates to many factors, such as sediment grain size, organic matter content, transit times, and other factors.

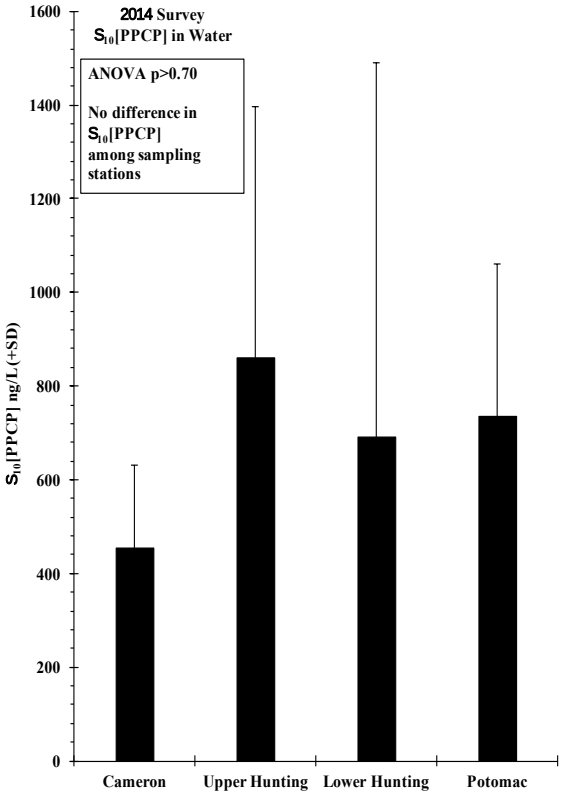

Figure 3. Concentrations of Σ_{10} PPCP in Hunting Creek water samples from 2014 sampling with concentrations grouped within four sub-regions including Cameron Run (Cameron), upper Hunting Creek (Upper Hunting), lower Hunting Creek (Lower Hunting), and the mainstem Potomac River (Potomac).

In the 2015 survey, a modified list of PPCPs were measured relative to 2014, and the spatial profiles of these chemicals in sediments are illustrated in Fig. 6 as the predominant 10 PPCPs, i.e., Σ_{10}PPCP. There appeared to be a discernible declining trend in PPCP concentrations away from the immediate discharge zone (upper Hunting) to the other stations, but the concentrations were not significantly different. Again, no spatial differences could be attributed to Hunting Creek PPCP concentrations in sediment.

The relative abundances of individual Σ_{10}PPCP chemicals in water and sediments from 2014 and 2015 (sediments only) sampling are shown in Figs. 6-8. As the graphs show, the composition of the PPCP mixture differs among the four sub-regions, especially for the upstream Cameron Run stations and downstream Hunting Creek stations relative to the others.

The composition of the Σ_{10}PPCP in water and sediment for the 2014 survey is show in Figs. 6 and 8. In water, the concentrations of 17α-ethinylestradiol and trimethoprim were the greatest (Fig. 6), while is sediment the predominant PPCPs included progesterone, 17α-ethinylestradiol,

testosterone and triclosan (Fig 7). The PPCP composition varied spatially among the sampling stations in sediment than it did for water.

In 2015, a somewhat different group of PPCPs (43 total) were analyzed in sediments, and the predominant PPCPs included prednisone, bisphenol A, clonazepam, diclofenac, naproxen and sulfamethazole (Fig. 8). The corticosteroids and estrogenic steroids seem to be the most abundant PPCPs found to date in Hunting Creek water and sediments as a chemical class of micropollutants. Among the major PPCPs, trimethoprim and 17 α-ethinylestradiol were much more abundant in water, while triclosan was much more abundant in sediment in the 2014 survey.

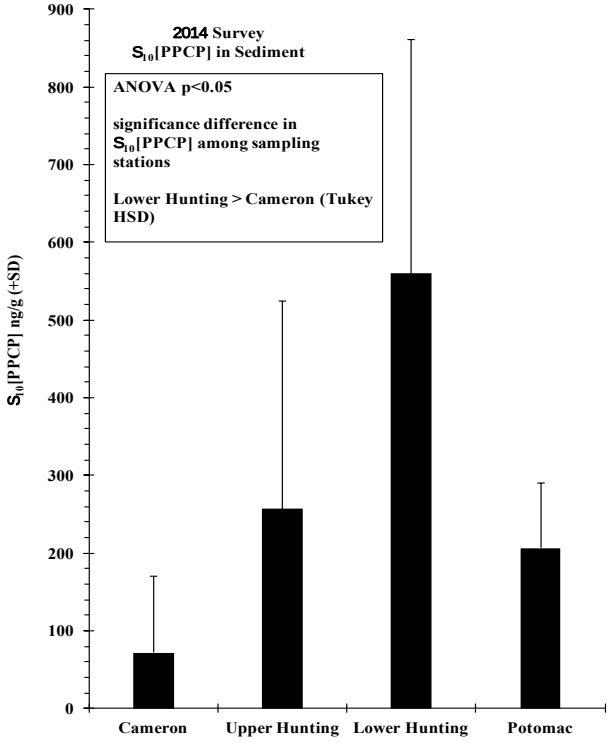

Figure 4. Concentrations of Σ_{10} PPCP in Hunting Creek sediment samples from 2014 sampling with concentrations grouped within four sub-regions including Cameron Run (Cameron), upper Hunting Creek (Upper Hunting), lower Hunting Creek (Lower Hunting), and the mainstem Potomac River

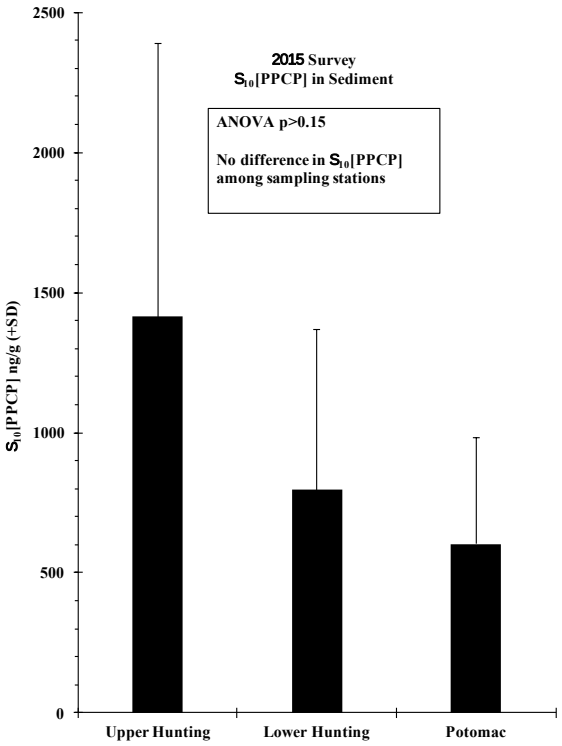

Figure 5. Concentrations of Σ_{10} PPCP in Hunting Creek sediment samples from 2014 sampling with concentrations grouped within four sub-regions including Cameron Run (Cameron), upper Hunting Creek (Upper Hunting), lower Hunting Creek (Lower Hunting), and the mainstem Potomac River

When individual PPCPs were evaluated (Fig. 9), clearly some constituents did vary substantially by site, such as prednisone in sediment (2015 results) even though the Σ_{10}PPCPs did now show substantial site-to-site variability. Prednisone showed a clear downstream gradient from upper Hunting Creek while other PPCPs like bisphenol A showed the opposite trend.

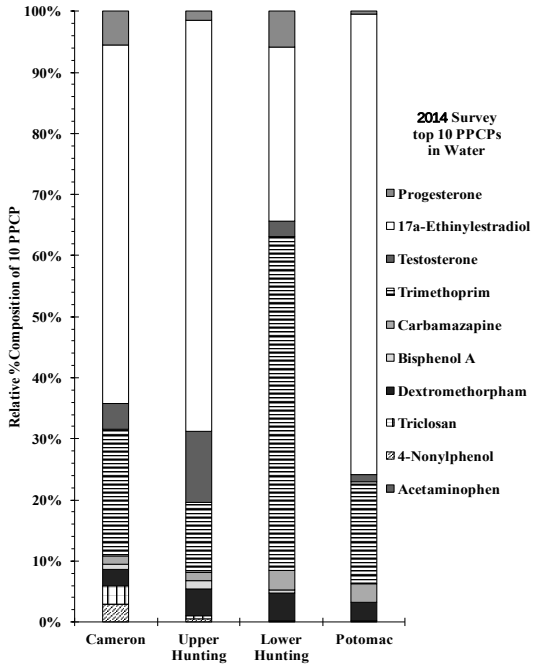

Figure 6. Relative abundance of the Σ_{10}PPCP in water from the 2014 survey.

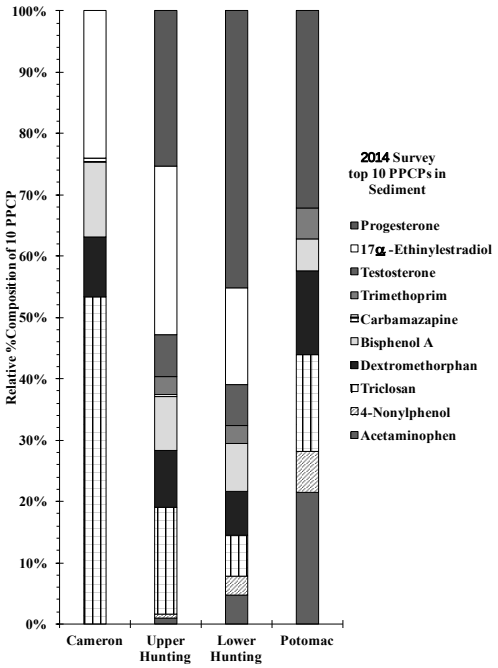

Figure 7. Relative abundance of Σ_{10}PPCP in sediment from 2014 survey.

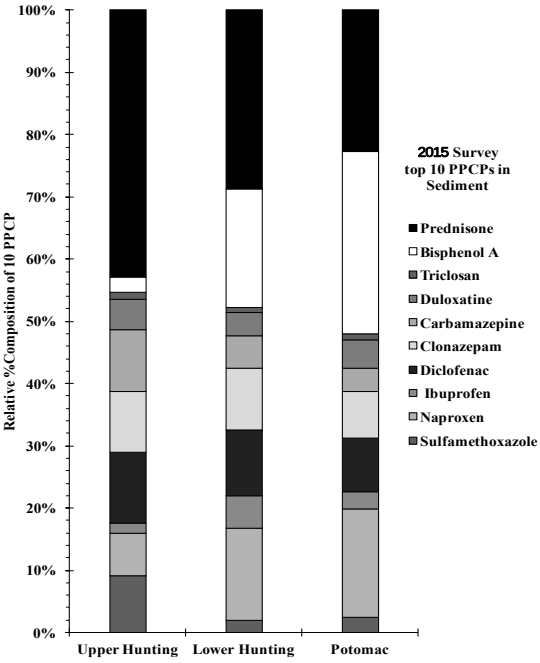

Figure 8. Relative abundance of Σ_{10}PPCP in sediment from the 2015 survey.

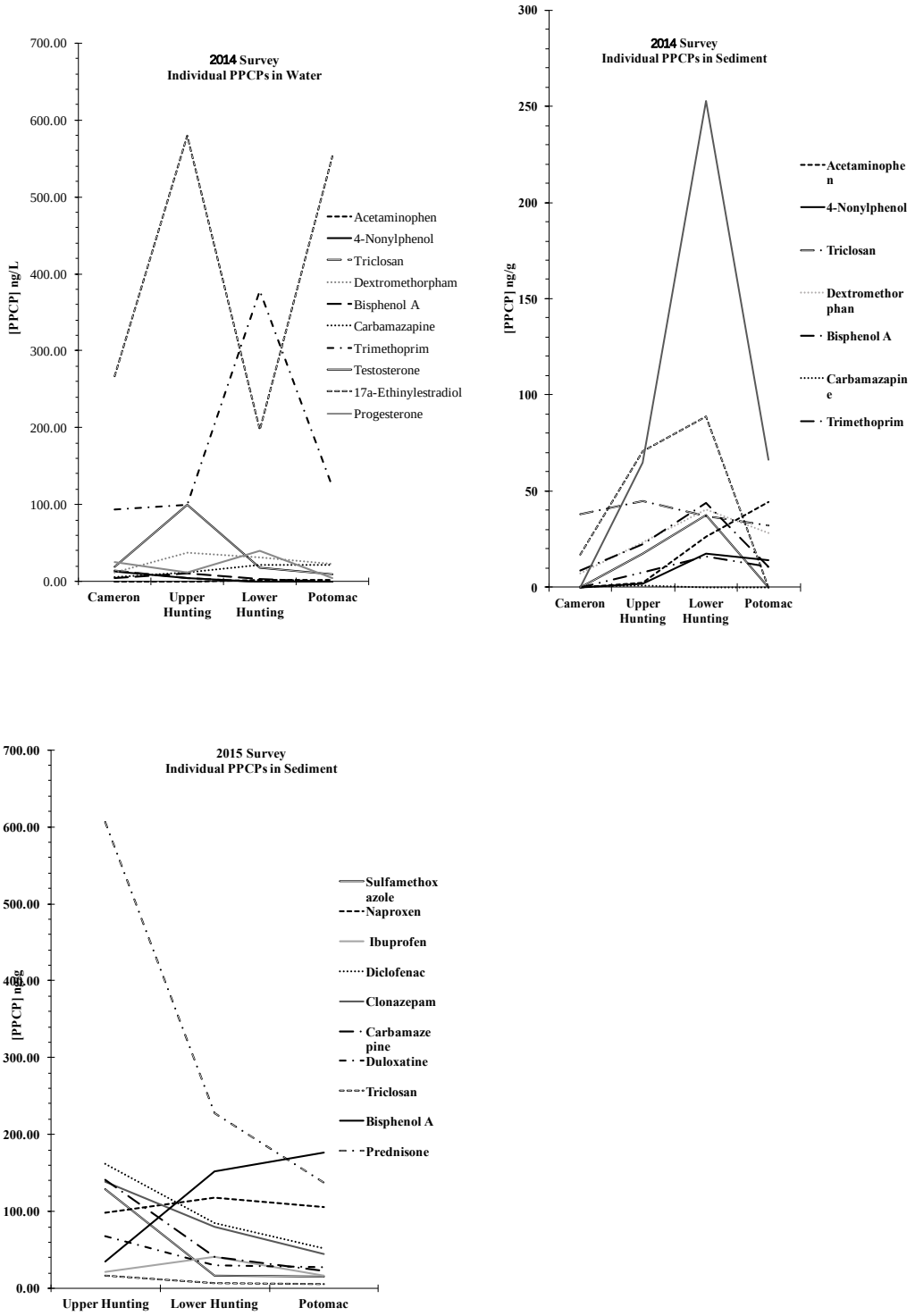

Figure 9. Individual PPCP concentrations by site in 2014 and 2015 surveys.

Results from the 2017 Survey

Currently, results are available for the 2017 sediment survey for antidepressants (22

constituents). PPCPs detected in water (2017 sampling) and sediments (2016 sampling) at Hunting Creek will be provided in a follow up report, along with the remainder of the PPCPs in 2017 sediments. The predominant antidepressants found in Hunting Creek sediments included desmethylvenlafaxine, fluoxetine, norsertraline, sertraline, citalopram, and amitriptyline (Fig. 10). There did appear to be seasonal fluctuation in the relative abundance of some of the antidepressants, especially norsertraline. A very similar profile of similar antidepressants was found in sediments collected from Dogue Creek (our reference site), but the concentrations in Dogue Creek sediments were much less than in Hunting Creek sediments (Fig. 11). Although the composition of antidepressants was constant with location and time of year, the relative abundances differed across all scales.

Quality assurance results included the analysis of laboratory blanks and QA spikes. Laboratory blanks showed no detectable concentrations of the antidepressants (Table 4). The QA spike recoveries varied from 2% (fluoxetine) to 130% (carbamazepine), with an average of 90% for 20 constituents (Fig. 11). Fluoxetine and norsertraline recoveries were not reported because these chemicals were not present in the QA spike.

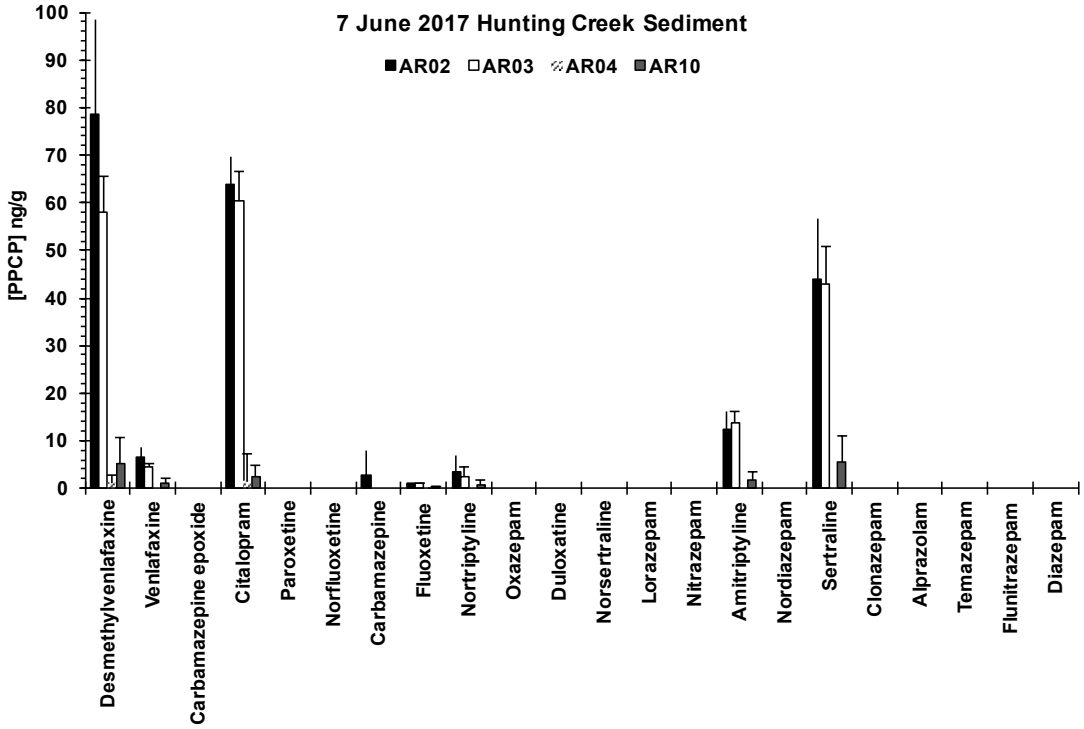
7 June 2017 Hunting Creek Sediment
AR02 AR03 AR04 AR10
[PPCP] ng/g
100
90
80
70
60
50
40
30
20
10
0
Desmethylvenlafaxine
Venlafaxine
Carbamazepine epoxide
Citalopram
Paroxetine
Norfluoxetine
Carbamazepine
Fluoxetine
Nortriptyline
Oxazepam
Duloxatine
Norsertraline
Lorazepam
Nitrazepam
Amitriptyline
Nordiazepam
Sertraline
Clonazepam
Alprazolam
Temazepam
Flunitrazepam
Diazepam

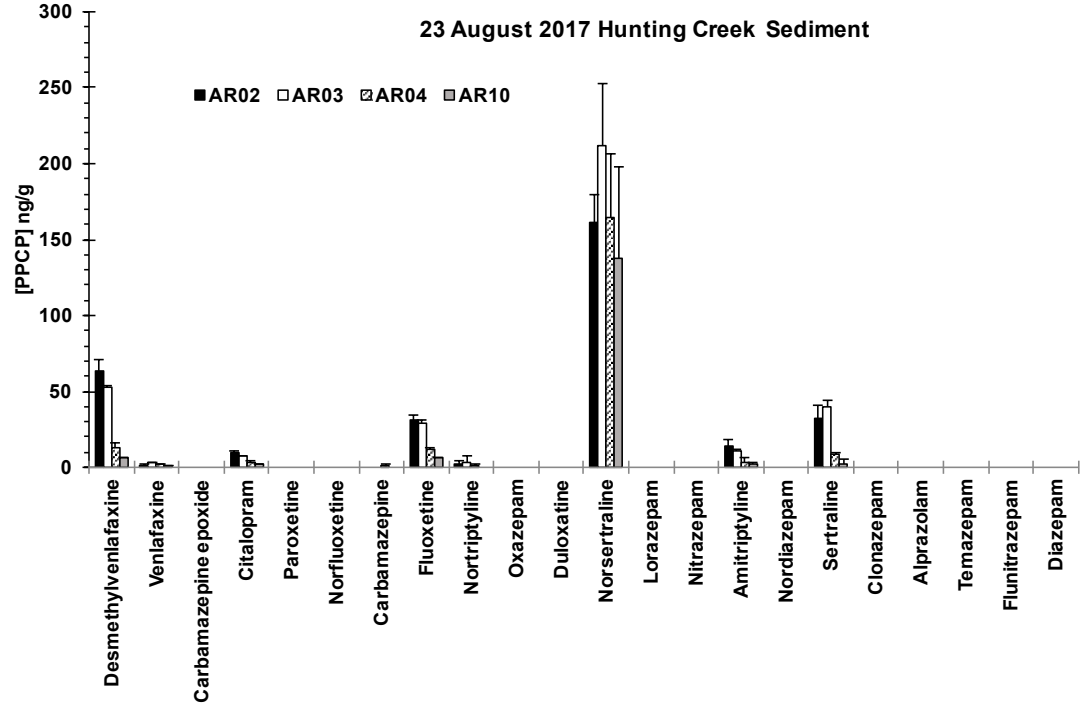
23 August 2017 Hunting Creek Sediment
AR02 AR03 AR04 AR10
[PPCP] ng/g
300
250
200
150
100
50
0
Desmethylvenlafaxine
Venlafaxine
Carbamazepine epoxide
Citalopram
Paroxetine
Norfluoxetine
Carbamazepine
Fluoxetine
Nortriptyline
Oxazepam
Duloxatine
Norsertraline
Lorazepam
Nitrazepam
Amitriptyline
Nordiazepam
Sertraline
Clonazepam
Alprazolam
Temazepam
Flunitrazepam
Diazepam

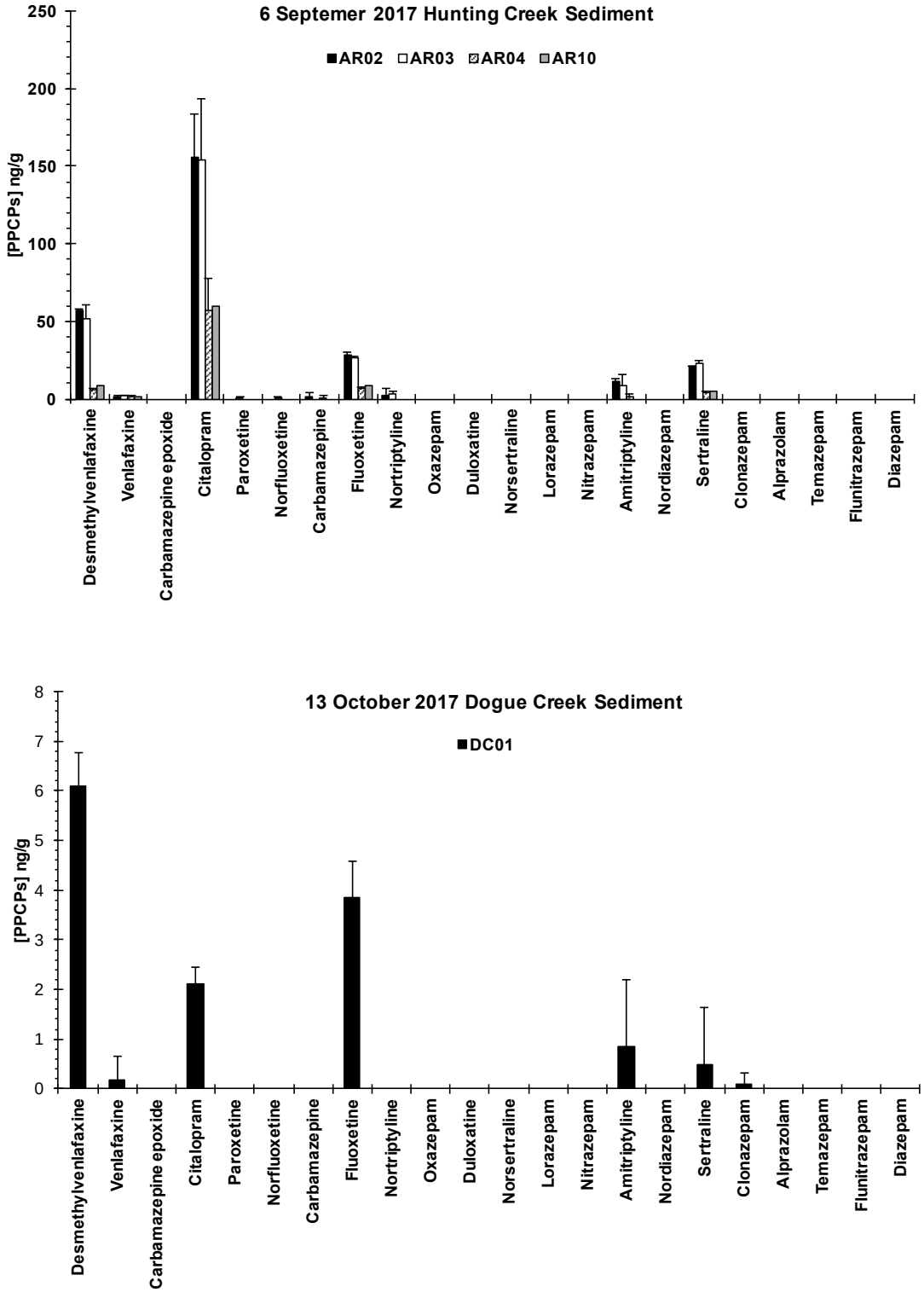

Figure 10. Antidepressant chemicals detected in Hunting Creek and Dogue Creek sediments in the 2017 survey.

Table 3. Laboratory QA blanks.

PPCP	Measured Sediment Blank Concentration (ng/g, N=9)								
	B1	**B2**	**B3**	**B4**	**B5**	**B6**	**B7**	**B8**	**B9**
Desmethylvenlafaxine	<DL	<DL	<DL	<DL	<DL	<DL	<DL	<DL	<DL
Venlafaxine	<DL	<DL	<DL	<DL	<DL	<DL	<DL	<DL	<DL
Carbamazepine epoxide	<DL	<DL	<DL	<DL	<DL	<DL	<DL	<DL	<DL
Citalopram	<DL	<DL	<DL	<DL	<DL	<DL	<DL	<DL	<DL
Paroxetine	<DL	<DL	<DL	<DL	<DL	<DL	<DL	<DL	<DL
Norfluoxetine	<DL	<DL	<DL	<DL	<DL	<DL	<DL	<DL	<DL
Carbamazepine	<DL	<DL	<DL	<DL	<DL	<DL	<DL	<DL	<DL
Fluoxetine	<DL	<DL	<DL	<DL	<DL	<DL	<DL	<DL	<DL
Nortriptyline	<DL	<DL	<DL	<DL	<DL	<DL	<DL	<DL	<DL
Oxazepam	<DL	<DL	<DL	<DL	<DL	<DL	<DL	<DL	<DL
Duloxatine	<DL	<DL	<DL	<DL	<DL	<DL	<DL	<DL	<DL
Norsertraline	<DL	<DL	<DL	<DL	<DL	<DL	<DL	<DL	<DL
Lorazepam	<DL	<DL	<DL	<DL	<DL	<DL	<DL	<DL	<DL
Nitrazepam	<DL	<DL	<DL	<DL	<DL	<DL	<DL	<DL	<DL
Amitriptyline	<DL	<DL	<DL	<DL	<DL	<DL	<DL	<DL	<DL
Nordiazepam	<DL	<DL	<DL	<DL	<DL	<DL	<DL	<DL	<DL
Sertraline	<DL	<DL	<DL	<DL	<DL	<DL	<DL	<DL	<DL
Clonazepam	<DL	<DL	<DL	<DL	<DL	<DL	<DL	<DL	<DL
Alprazolam	<DL	<DL	<DL	<DL	<DL	<DL	<DL	<DL	<DL
Temazepam	<DL	<DL	<DL	<DL	<DL	<DL	<DL	<DL	<DL
Flunitrazepam	<DL	<DL	<DL	<DL	<DL	<DL	<DL	<DL	<DL
Diazepam	<DL	<DL	<DL	<DL	<DL	<DL	<DL	<DL	<DL

<DL = less than analytical detection limit.

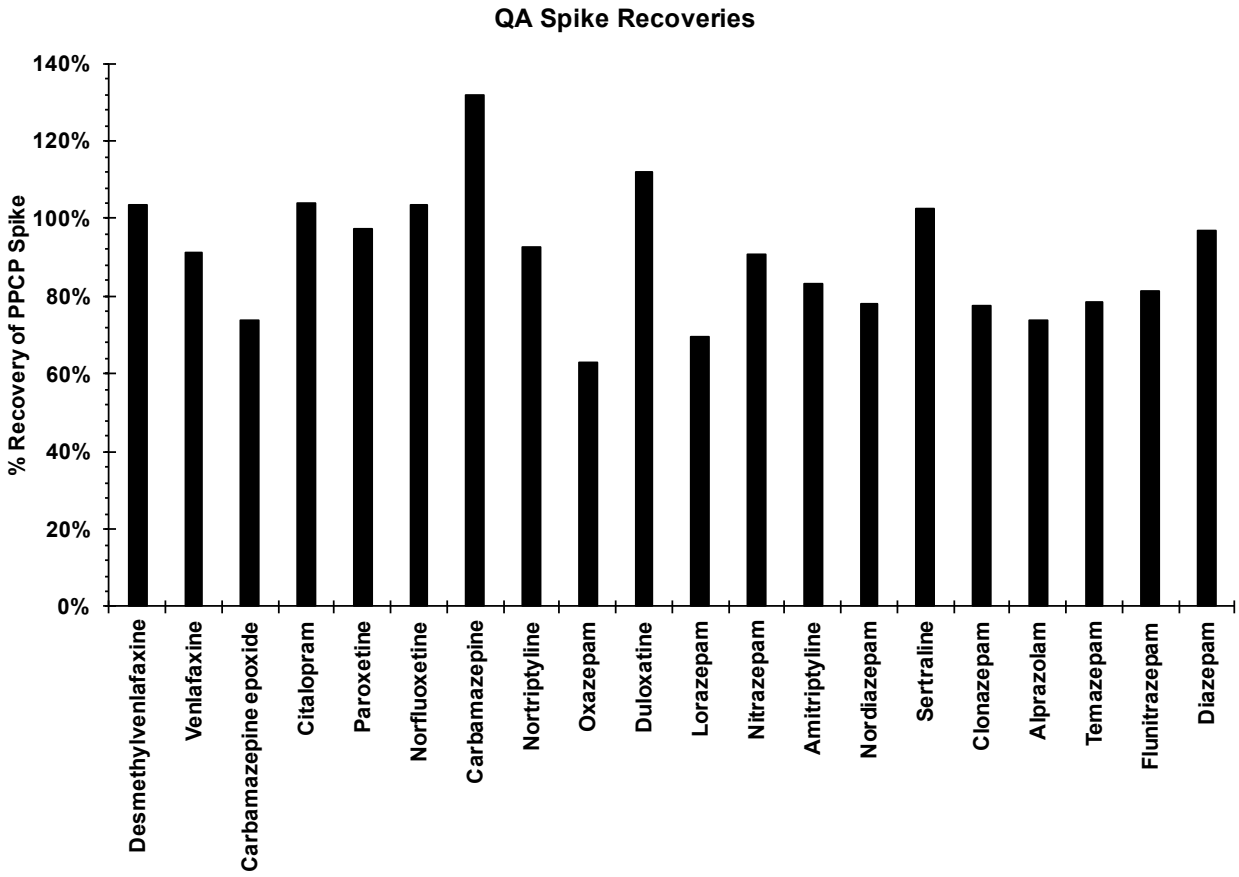

Figure 11. QA spike recoveries.

References

Haywood C, Buchanan C 2007: Total maximum daily loads of polychlorinated biphenyls (PCBs) for tidal portions of the Potomac and Anacostia rivers in the District of Columbia, Maryland and Virginia, Interstate Commission on the Potomac River Basin, Rockville, MD

Kachhawaha AS, Nagarnaik PM, Jadhav M, Pudale A, Labhasetwar PK, Banerjee K (2017): Optimization of a Modified QuEChERS Method for Multiresidue Analysis of Pharmaceuticals and Personal Care Products in Sewage and Surface Water by LC-MS/MS. J. AOAC Int. 100, 592-597